Reactions of unsaturated hydrocarbons catalysed by transition metal compounds

Peter Richard Ellis

Reactions of Unsaturated Hydrocarbons Catalysed by Transition Metal Compounds

Volume One

Peter Richard Ellis

Submitted for examination for Degree of Doctor of Philosophy

University of Durham

Department of Chemistry

1998

If you can keep your head when all about you
Are losing theirs and blaming it on you,
If you can trust yourself when all men doubt you
But make allowance for their doubting too;
If you can wait and not be tired of waiting,
Or being lied about don't deal in lies,
Or being hated don't give way to hating,
And yet don't look too good, nor talk too wise:

If you can dream – and not make dreams your master;
If you can think – and not make thoughts your aim,
If you can meet with Triumph and Disaster
And treat those two imposters just the same;
If you can bear to hear the truth you've spoken
Twisted by knaves to make a trap for fools
Or watch the things you gave your life to, broken,
And stoop and build 'em up with worn out tools;

If you can make one heap of all your winnings
And risk it on one turn of pitch-and-toss
And lose, and start again at your beginnings
And never breathe a word about your loss
If you can force your heart and nerve and sinew
To serve your turn long after they are gone,
And so hold on when there is nothing in you
Except the Will which says to them: 'Hold on!'

If you can talk with crowds and keep your virtue,
Or walk with Kings – nor lose the common touch,
If neither foes nor loving friends can hurt you,
If all men count with you, but none too much:
If you can fill the unforgiving minute
With sixty seconds' worth of distance run,
Yours is the Earth and everything that's in it,
And – what is more – you'll be a man, my son!

Rudyard Kipling

Acknowledgements

I would like to thanks all the people who have contributed to this thesis: Drs. D.S. Yufit, A.S. Batsanov, J.W. Yao and C.W. Lehmann, Messrs. M. Leech, A. Mackinnon and S. Borwick for crystallographic data, Miss J. Magee for help with synthetic work and the staff of Kvaerner Process Technology, especially Mr. S.W. Colley, for help in setting up and running the catalytic testwork.

Thanks are also due to Dr. Mel Kilner for his help and encouragement, and to the people who have been lucky enough to share a lab with me: Simon Crabtree, Graham Robertson, Nicky Moore, David Bryant and Derek Tyers.

I would like to acknowledge my gratitude to EPSRC and KPT for CASE award funding.

Finally, I must thank my friends and family for their support during the last three years.

Abbreviations Used

Ac	acyl, $COCH_3$
AcO	acetate, CO_2CH_3
Ar	any aromatic group
br	broad (IR and nmr)
CI	chemical ionisation (MS)
COD	cycloocta-1,5-diene
d	doublet (nmr)
dd	doublet of doublets (nmr)
ddd	doublet of doublet of doublets (nmr)
dt	doublet of triplets (nmr)
δ_C	^{13}C nmr chemical shift
δ_F	^{19}F nmr chemical shift
δ_H	^{1}H nmr chemical shift
δ_P	^{31}P nmr chemical shift
DIOP	2,2-dimethyl-4,5-bis(diphenylphosphinomethyl)-1,3-dioxalane
DMF	N,N-dimethylformamide
dppa	N,N'-bis(diphenylphosphino)amine
dppb	1,4-bis(diphenylphosphino)butane
dppe	1,2-bis(diphenylphosphino)ethane
dppipen	N,N'-bis(diphenylphosphino)-N,N'-di-*iso*-propylethylenediamine
dppippn	N,N'-bis(diphenylphosphino)-N,N'-di-*iso*-propylethylenediamine
dppm	bis(diphenylphosphino)methane
dppma	N,N'-bis(diphenylphosphino)methylamine
dppmen	N,N'-bis(diphenylphosphino)-N,N'-dimethylethylenediamine
dppmpn	N,N'-bis(diphenylphosphino)-N,N'-dimethylpropylenediamine
dppp	1,3-bis(diphenylphosphino)propane
dpppen	N,N'-bis(diphenylphosphino)-N,N'-diphenylethylenediamine
dpppip	N,N'-bis(diphenylphosphino)piperazine
dpptben	N,N'-bis(diphenylphosphino)-N,N'-di-*tert*-butylethylenediamine
ee	enantiomeric excess – the yield of one enantiomer over another in an enantioselective reaction.

EI	electron ionisation (MS)
eq	equivalents
Et	ethyl, CH_2CH_3
FAB	fast atom bombardment (MS)
fac	facial isomer (of an octahedral complex)
GC	gas chromatography
GC-MS	gas chromatography - mass spectrometry
^{i}Pr	*iso*-propyl, $CH(CH_3)_2$
IR	infrared (spectroscopy)
KPT	Kvaerner Process Technology
L	a two-electron donor ligand, especially a phosphine
m	moderate intensity (IR)
Me	methyl, CH_3
MS	mass spectrometry
NBD	norbornadiene (bicyclo[2.2.1]hepta-2,5-diene)
NOBA	3-nitrobenzyl alcohol
nmr	nuclear magnetic resonance (spectroscopy)
Ph	phenyl, C_6H_5
ppm	parts per million
psi	pounds per square inch (of pressure)
psig	pounds per square inch of pressure as read on a pressure gauge
R	any organic group
s	strong (IR)
	singlet (nmr)
sh	shoulder (IR)
t	triplet (nmr)
^{t}Bu	*tert*-butyl, $C(CH_3)_3$
THF	tetrahydrofuran
ν	stretching frequency (IR)
vs	very strong (IR)
vw	very weak (IR)
w	weak (IR)
wt. %	weight percent

Abstract

Two separate areas of catalysis have been investigated.

A range of different heterogeneous catalysts for the isomerisation of *ortho*-xylene have been prepared and evaluated. These included commercially-available samples, supported metal catalysts and zirconia-based catalysts. The greatest activity was seen for the former, which was found also to be active for a number of related reactions.

Zirconia-based catalysts, in particular sulphated zirconia, gave significant activity. It was possible to prepare a catalyst to give 9.5% conversion of *ortho*-xylene per gram of catalyst with good selectivity to the *meta* isomer. The catalyst was prepared in two ways, either by the action of ammonium sulphate on "zirconium hydroxide", a hydrated zirconia precursor, or by precipitation from a sulphuric acid-containing solution of zirconium (IV) propoxide. The factors in the synthesis procedure which affect the catalytic performance of the catalyst were investigated. These included choice of reagents, preparative method and calcination procedure. This information was used to prepare an 'idealised' catalyst, which showed activity for a number of reactions of commercial interest.

A range of different aminophosphine complexes based on the reaction of a N,N'-substituted diamine with chlorodiphenylphosphine have been prepared for subsequent study as ligands in complexes active in homogeneous catalysis. Palladium and platinum complexes of the type [(diaminodiphosphine)MCl_2] have also been prepared and characterised. A number of x-ray diffraction analyses have been performed, which along with other data has allowed the solid state and solution structures to be discussed. The relative reactivities of the ligands have been determined by reactions with manganese pentacarbonyl bromide and also with palladium dichloride complexes. This depends largely on the steric requirements of the ligand in question.

The potential of these ligands in catalysis has been evaluated by the performance of their platinum dichloride complexes in the tin (II)-promoted hydroformylation of styrene, and their palladium acetate complexes for the methoxycarbonylation of ethene.

Contents

Chapter One: The Production of *Para* - Xylene

1.1 Why *Para*-Xylene?

The demand for *para*-xylene production is linked to the production of polyesters. The use of mixed xylenes, which contains the three xylene isomers plus ethylbenzene and originates from catalytic reforming of naphtha, is an economically attractive route to *para*-xylene. This is oxidised to terephthalic acid, which in turn is co-polymerised with a suitable diol to form polyesters, as summarised in Scheme 1.1.

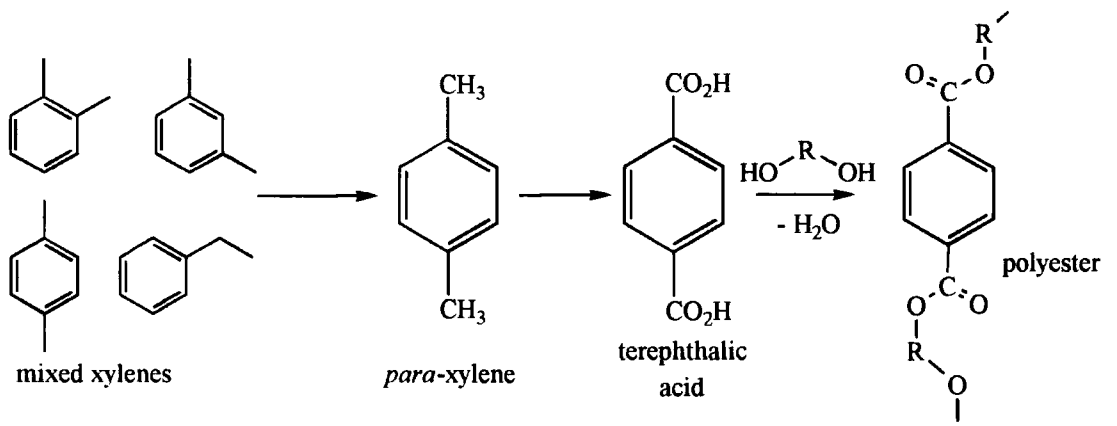

Scheme 1.1: The Production of Polyester

The separation of a mixture of xylene isomers is difficult due to the closeness of their boiling points [1]. Ethylbenzene may be removed by distillation with some difficulty, but the advances in the alkylation of benzene mean that this is often not economically worthwhile. Relevant physical data are shown in Table 1.1.

Table 1.1 Physical Properties of the Xylene Isomers

Compound	Boiling Point / °C	Melting Point / °C
Ortho-Xylene	144.41	-25.182
Meta-Xylene	139.12	-47.872
Para-Xylene	138.37	+13.263
Ethylbenzene	136.19	-94.975

Differences in melting point mean that fractional crystallisation is often used to separate the isomers, as discussed below.

The use of *para*-xylene in the production of polyester keeps its market value high. The major use of the other isomers is oxidation to *iso*-phthalic acid or phthalic anhydride for *meta*- and *ortho*-xylene respectively which are used as chemical intermediates. The value of ethylbenzene is also kept high, as dehydrogenation to styrene for polystyrene manufacture is its major use. The relative prices as at 27th July, 1998 are shown in Table 1.2 [2].

Table 1.2: Prices of Feedstocks for *Para*-Xylene Production

Compound	Price	Cost for 10 l	Type of Cost
Benzene	\$0.75 per US gallon	\$1.703	free on-board†
Methanol	\$0.245 per US gallon	\$0.556	free on-board at producing point
Ethylbenzene	\$0.2545 per pound	\$4.860	free on-board
Toluene	\$0.68 per US gallon	\$1.544	spot price
Ortho-Xylene	\$0.14 per pound	\$2.714	works
Meta-Xylene	\$0.65 per pound	\$12.372	free on-board high purity
Para-Xylene	\$0.1575 per pound	\$2.987	delivered
Mixed Xylenes	\$0.65 per US gallon	\$1.476	spot price

The price quoted for *meta*-xylene may be artificially high as it is for 'high-purity' compound. Table 1.2 does, however, show the financial benefit of converting mixed xylenes or toluene into *para*-xylene. This has led to expansion of production capacity by many producers [3].

1.2 Routes to *Para*-Xylene

The production of *para*-xylene has been achieved by two methods - separation of the isomer from a mixture, followed by re-isomerisation of the remaining mixture, or by

† Free on-board shows that a tax regarding the shipping of the compound is paid by the vendor.

chemical synthesis from a number of different starting materials. These two areas will be considered separately.

1.2.1 Separation of *Para*-Xylene

As mentioned above, the closeness of the boiling points of the xylene isomers makes separation by distillation, which is often the method of choice for liquid mixtures, practically impossible. However, the freezing point of *para*-xylene is more than thirty degrees higher than the nearest isomer (Table 1.1) and so fractional crystallisation has been used with some success. Crystallisation of *para*-xylene from a mixture of xylenes takes place below -4°C, due to the its solubility in the mixture of other isomers, and above -68°C where the other isomers will also start to crystallise. It is performed in scraped chiller units, with either direct or indirect cooling by a gas such as carbon dioxide or ethene. The efficiency of this process is closely related to the size of crystals produced and so their ease of separation from the mother liquor. It is limited to a maximum value of 70% due to the solubility of *para*-xylene in the other isomers, loss of small crystals into the mother liquor and the heat generated by mechanical work melting the crystals. *Para*-xylene crystals are usually separated from the mixture by centrifuge. Two such steps will give *para*-xylene of >99% purity [1].

A technology which rivals crystallisation is the selective adsorption of *para*-xylene using a zeolite. The pore size of a zeolite is selected to be such that it adsorbs *para*-xylene in preference to the other isomers in the mixture. This is then removed by a desorbent such as *para*-diethylbenzene or toluene which can be separated from *para*-xylene by a one-step distillation. This kind of process is often run in conjunction with a xylene isomerisation unit, with the unreacted xylenes being re-isomerised before passing across the zeolite for a second time. The efficiency of this process is greater than for crystallisation processes.

Other methods of separating the xylene isomers have focused on selective complexation with systems such as HF - BF_3 [4]. These tend to complex the *meta*-isomer preferentially as it is the most basic (accepts a proton most readily) [5]. Nickel- or cobalt-based "Werner Complexes" also complex one of *meta*- or *para*-xylene selectively

[6-10], whilst α-cyclodextrin complexes *para*-xylene selectively [11]. Both employ host-guest type chemistry to achieve selective binding. Carbon tetrachloride, carbon tetrabromide and trichloroethanal [12] all form selective 1:1 complexes with *para*-xylene.

1.2.2 Chemical Production of *Para*-Xylenes

Chemical production of *para*-xylene can be done in a number of ways and using a number of feedstocks. Which process is chosen depends largely on the relative value of the starting material compared to the products as discussed above. Acid catalysed rearrangements and disproportionation reactions of aromatic compounds have been extensively studied and used industrially for this purpose.

Possibly the most studied of this class of reactions is xylene isomerisation, which has been found to be catalysed by acidic catalysts of both Lewis and Brønsted types [13]. Industrially, it is a Lewis acid such as silica-alumina which is used to isomerise xylenes, although other catalysts such as aluminium halides have also been studied. The isomerisation is therefore related to Friedel-Crafts alkylations and acylations, as both involve electrophilic reactions [14]. The mechanism of this reaction has been shown [15] to be a series of 1,2-methyl shifts around the ring. This means that direct isomerisation of *ortho*-xylene to *para*-xylene does not occur. For substituents other than methyl groups this is not necessarily the case [5]. The mechanism has been variously reported as involving one or both of σ- and π-bound intermediates. These are shown in Fig. 1.1.

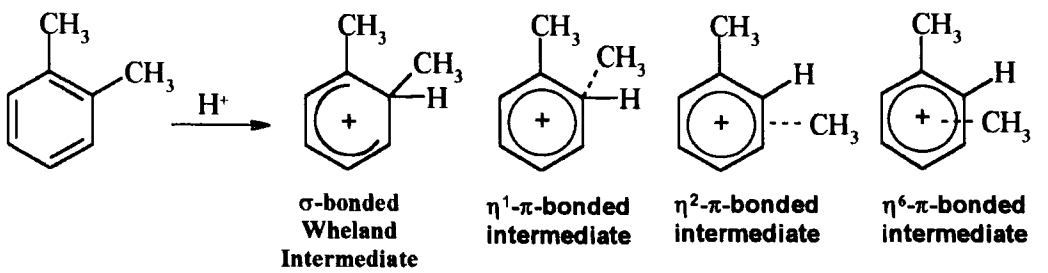

Fig. 1.1: Intermediates in Xylene Isomerisation

Recently, calculations have been performed on the stability of these intermediates [16]. These have suggested that the σ-complex is more stable than any of the π-complexes, which will collapse to a σ-complex without crossing any energy barrier. The η^2-π-complex was postulated as being the intermediate between two σ-complexes, as would be observed during xylene isomerisation. The η^6-intermediate was not expected to form, which is in contrast to reactions found in transition metal complexes, for example, and this was ascribed to the coordinatively unsaturated nature of the methyl cation. It has also been reported that the isomerisation of *para*-xylene to *meta*-xylene is approximately 1.7 times faster than the conversion of *ortho*-xylene to *meta*-xylene. This reflects the relative ease of protonation of the related σ-complexes, and their transition to *meta*-xylene. The *meta*-isomer is the most easily protonated of all three xylene isomers. This is because greater hyperconjugation occurs as stabilisation using both methyl groups is possible, as shown in Scheme 1.2.

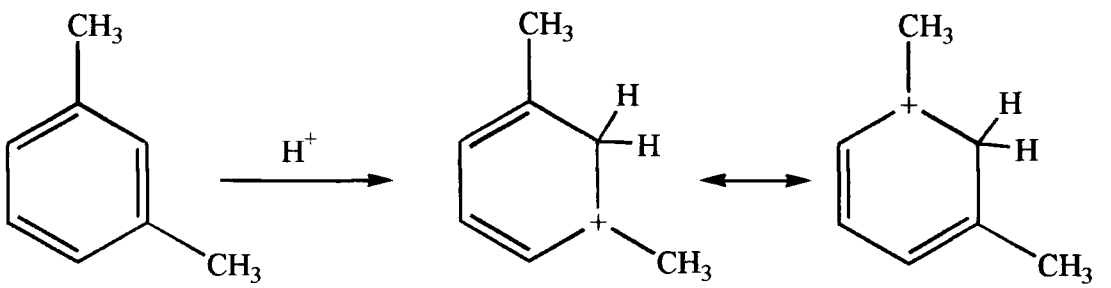

Scheme 1.2: Protonation of *Meta*-Xylene

Another factor which comes into play is the relief of steric interactions in *ortho*-xylene on protonation. The formation of an sp^3-hybridised carbon as part of the ring means that the two methyl groups can move further away from each other. The impact of this is that *ortho*-xylene is easier to protonate than *para*-xylene.

Disproportionation reactions, such as the disproportionation of xylenes to give trimethylbenzenes and toluene are also catalysed by acid catalysts. However, this is not seen so frequently for methyl group-bearing compounds, such as toluene or the xylenes, as for other aromatics with bulkier substituents, such as ethylbenzene or *tert*-butylbenzene. This is related to the relative instability of the primary methyl carbocation -

tertiary carbocations can delocalise the charge more effectively, and their increased stability makes them easier to transfer to another ring during disproportionation. In zeolite catalysts, a bimolecular disproportionation - transalkylation mechanism has been found to operate in the isomerisation of xylenes [17]. This is shown in Scheme 1.3.

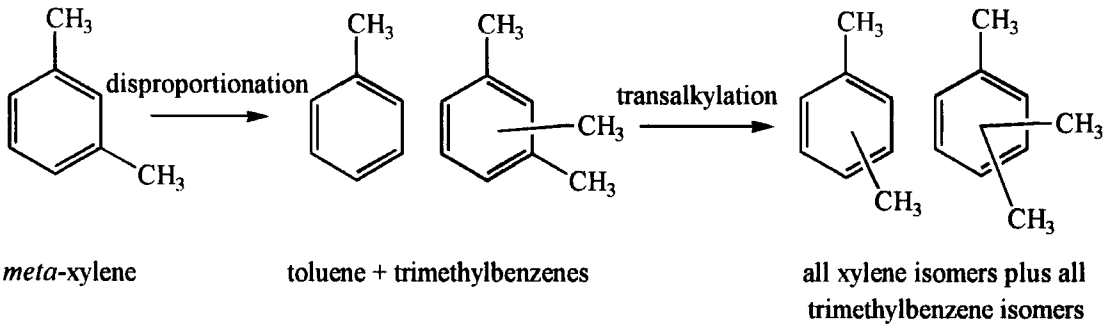

Scheme 1.3: Isomerisation of *Meta*-Xylene by Disproportionation - Transalkylation

One related reaction which deserves mention in the context of the use of sulphated zirconia catalysts for xylene isomerisation is the Jacobsen reaction [5]. This involves co-ordination of a sulphonic acid group to the aromatic ring, which provokes a rearrangement. The reaction is of most synthetic use in the rearrangement of 1,2,4,5-tetramethylbenzene, as shown in Scheme 1.4. For other systems a mixture of products is likely.

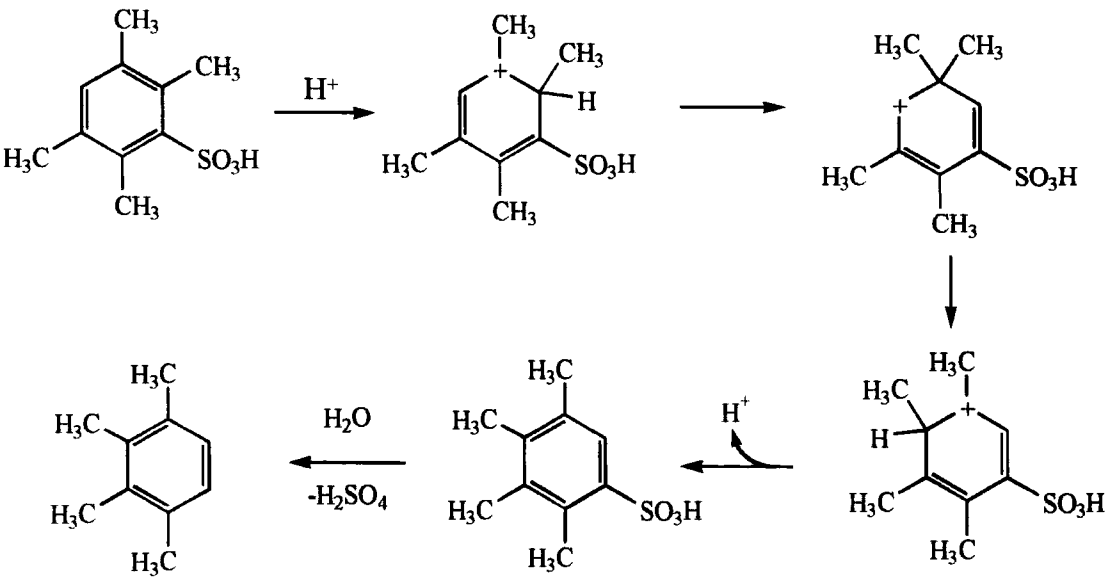

Scheme 1.4: The Jacobsen Reaction

Sulphated aromatics, such as the starting material for the Jacobsen reaction in Scheme 1.4, may be prepared by standing the relevant aromatic in sulphuric acid.

Industrially, the catalysts used for xylene isomerisation are usually alumina - silica catalysts. These catalysts are active at high temperatures, but are prone to developing a deactivating layer of coke. This can be removed by burning in air, and the catalysts themselves are sufficiently resilient to withstand this, even though the process needs repeating approximately every 3 - 30 days.

A more sophisticated catalyst contains a small amount of platinum, usually around ½wt.% [18]. This provides the catalyst with hydrogenation activity, and so it can interconvert between xylenes and ethylbenzene by means of saturated intermediates such as dimethylcyclohexane, ethylcyclohexane and trimethylcyclopentane. This is useful as ethylbenzene is present in the feedstock to levels of around 20% and can build up as a diluent in the system if it is not converted. Traditional xylene isomerisation processes often remove ethylbenzene by distillation. Zeolite catalysts have also been successfully studied for xylene isomerisation [13].

Another well - studied process is the disproportionation of toluene to give xylenes and benzene. Again the economics of the process vary depending on the relative value of xylenes, toluene and benzene. It is possible to perform this reaction with selectivity to the *para*-isomer by means of modified zeolite catalysts. Using a zeolite catalyst, the shape - selective reactions which produce *para*-xylene only occur inside its pore structure where geometry is restricted. Reactions on the catalyst outer surface are not selective, and can reduce *para*-selectivity dramatically. Two strategies have been used to gain selectivity: firstly, reduction of the pore volume of the zeolite using various compounds of magnesium, phosphorus and boron, which further restricts the pore volume and hence increases selectivity to the smaller *para*-xylene. This also occurs when a layer of coke builds up on the catalyst surface [20]. The second approach uses an inert compound such as a silicon-containing polymer to deactivate the catalyst surface and so eliminate the non-selective reactions [21]. Strong acid sites appear to be necessary for toluene disproportionation [22], and the external sites can be amongst the most active for this [23]. The mechanism of the reaction has been found to involve diphenylmethane-type

intermediates, and to proceed by a carbocation chain mechanism [24], as shown in Scheme 1.5.

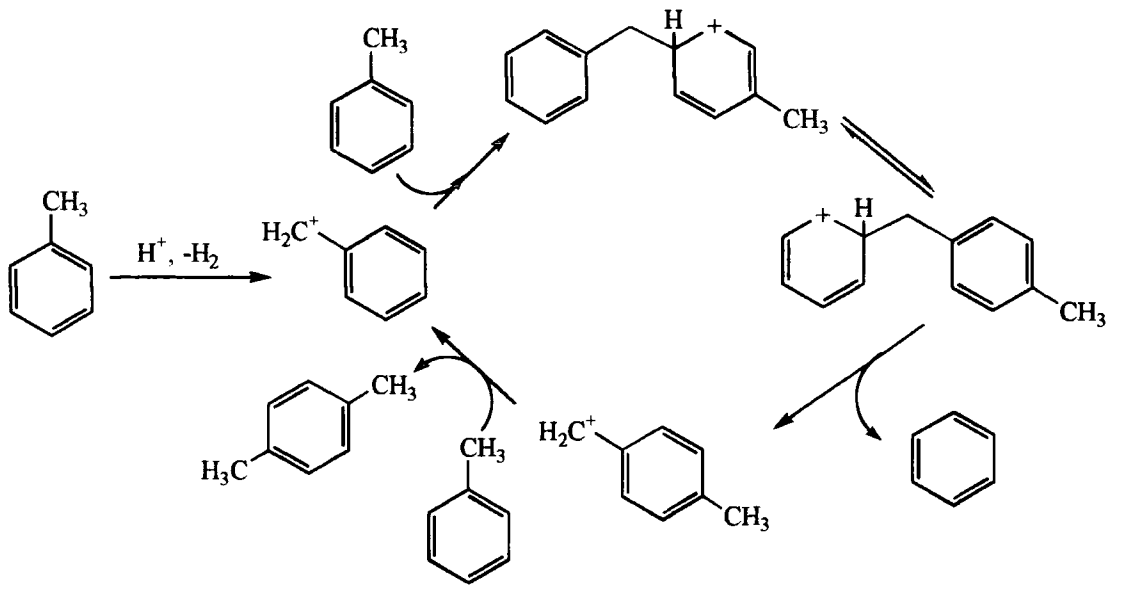

Scheme 1.5: Mechanism of Toluene Disproportionation

It is this chemistry which lies at the heart of Mobil's Selective Toluene Disproportionation Process [25]. This uses a modified zeolite catalyst and produces a mixed xylene product which has 70-80% selectivity to *para*-xylene.

The reaction of toluene and methanol to give xylenes and water has also been investigated. This uses similar modified zeolites to those discussed above for toluene disproportionation [26]. A zirconia-based catalyst has also been used [27]. The reaction produces tri- and tetra-methylbenzenes by second and third reactions, although this can be controlled by careful choice of catalyst. Good selectivity to *para*-xylene has also been seen, using a catalyst with the surface sites deactivated.

1.3 Alternative Routes to Terephthalic Acid

The production of terephthalic acid is the major use of *para*-xylene, and so there is good reason to investigate the direct synthesis of terephthalic acid from the feedstocks usually used for the manufacture of *para*-xylene, such as toluene or benzene. One route which appears very attractive is the carbonylation or carboxylation of aromatic substrates. This

would be of particular interest with toluene as it is a cheap feedstock. This reaction was first performed in 1888 when benzene was converted to benzoic acid by reaction with carbon dioxide [28]. Since then, similar reactions have been catalysed by palladium (II) salts such as palladium acetate [29, 30]. The reaction appears to proceed with good yield, although a second compound is used to reoxidise the palladium, and this is consumed during the reaction. Examples of this second compound are *tert*-butyl peroxide, sodium nitrate and copper (II) acetate. Alternative examples use carbon monoxide instead of carbon dioxide [31], or use an electrocatalytic process [32]. This is an interesting prospect, although it is unlikely to be commercially viable whilst a consumable oxidant is required. Processes using oxygen or even air in this capacity would be better candidates for commercialisation.

A second route to terephthalic acid is the Henkel process. This is a rearrangement or disproportionation process used for the synthesis of aromatic carboxylates as their alkali metal salts, as shown in Scheme 1.6.

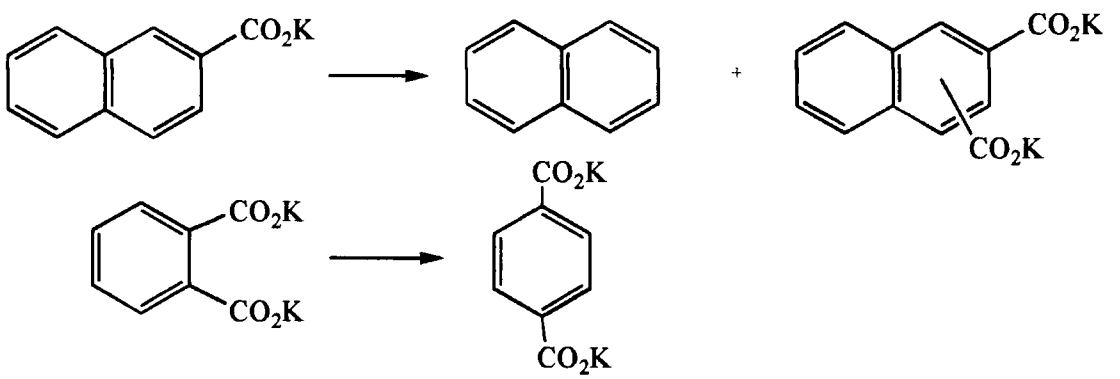

Scheme 1.6. Examples of the Henkel Reaction

Catalysts for this process have typically been cadmium salts [33, 34], although more recently less toxic zinc salts have been successfully used in their place [35]. A blanket of carbon dioxide is maintained during the reaction and pressures above atmospheric pressure are usually used. One disadvantage regarding the commercialisation of this process is the high reaction temperature, which is typically 400°C - 450°C. The use of alkali metal salts may also be a problem, unless they could be reclaimed.

1.4 Superacids

The acidity of compounds which are classified as superacids is often not measurable on the pH scale, as they are not aqueous systems. This makes the concept of the hydrogen ion concentration or H_3O^+ ion concentration of little use. Instead, the Hammett parameter, H_o, is used to measure acidity [36]. This is defined as

$$H_o = pK_{BH+} - \log([BH^+] / [B])$$

where BH^+ is the superacid in question, and it dissociates into a conjugate base B and a proton H^+. The value of H_o for 100% sulphuric acid, -11.93 [37], is often taken as something of a benchmark in superacidity, with systems having a lower (more negative) H_o value being said to be superacidic. In this region, aromatic nitro compounds are used as indicators of acidity.

The most simple superacids, and indeed the first systems studied, are liquids or solutions. If acidity can be defined as the ability of a compound to donate a proton, then the more stable the counterion to the proton, the more favoured is dissociation and so the easier donation becomes. The easier the donation, the stronger is the acidity. It was this rationale that led to the first superacidic systems such as H_2SO_4 - SO_3 [37], HF - SbF_5 [38] or HF - BF_3 [39]. These rely on the stability of polysulphate, hexafluoroantimonate and tetrafluoroborate anions respectively. These systems have been used as catalysts for organic reactions such as those of chlorinated compounds [40], including dehydrogenation of organic substrates using CCl_3^+ as a hydride acceptor [41]. Carbonylation of methane [42], protonation of benzene [43], synthesis of aromatic sulphoxides [44] and many other electrophilic reactions [45] have been investigated. The reactions of alkanes have been extensively studied [46, 47]. Fluorosulphuric acid has been used in the synthesis of gold carbonyl cations. The combination of fluorosulphuric acid and gold (III) fluorosulphate was found to be a novel superacid system [48].

Formylation of benzene, toluene and other aromatic hydrocarbons using carbon monoxide are reactions of interest in the context of the preparation of terephthalic acid.

These reactions have been performed using CF_3SO_3H - HF - BF_3 or CF_3SO_3H - SbF_5 superacid systems [49]. This reaction is shown in Scheme 1.7.

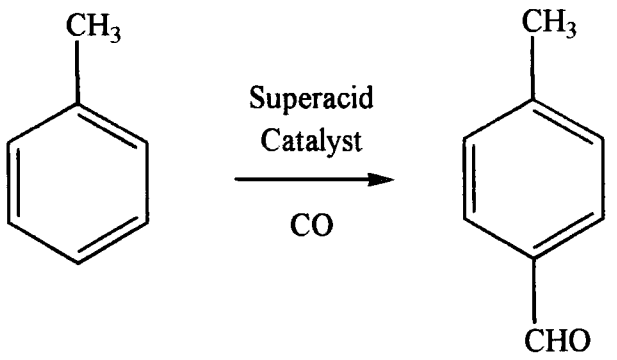

Scheme 1.7: Formylation of Toluene

Para-selectivity of greater than ninety per cent was observed using mild conditions - atmospheric pressure and room temperature.

A second type of superacid is fluorinated alkanesulphonic acids, the classic example of this being trifluoromethanesulphonic acid ("triflic acid"). Again the acidity of this compound is based on the stability of the corresponding triflate anion, $CF_3SO_3^-$. These and related systems have been used as catalysts for organic reactions such as aromatic condensations [50-52], nitrations [53] and silylations [54]. They can be extremely hygroscopic, which presents some handling difficulties [55].

There is a strong interest in the development of solid superacids [56, 57] for industrial applications, as they are less susceptible to leaching and easier to handle than conventional systems based on, for example, HF or SO_3. It is possible to prepare supported analogues of the liquid systems described above, such as SbF_5 supported on graphite or metal oxides [58], which have been reported to be active catalysts for disproportionation of alkylbenzenes [59] and isomerisation reactions of butane respectively. A different type of solid superacid was prepared by the reaction of aluminium trichloride with a cation exchange resin. This was used as an esterification catalyst, and was found to be superior to the parent ion-exchange resin [60]. In another attempt to aid separation of products and catalyst, superacidic molten salt media have been prepared and used [61]. These consisted of Me_3SOBr, HBr and either $AlCl_3$ or

$AlBr_3$, and are molten to well below room temperature. They were found to be strong enough acids to protonate a range of aromatic substrates, including *meta*-xylene and toluene.

Other compounds have been found to be solid superacids. Certain zeolites have been reported as having superacidic sites within their structures [62], formed by interactions of their Lewis and Brønsted acid sites. The hydroxyl (OH) and Al-O groups present could interact in the same way as, for example, HF and SbF_5. However, a study of the zeolite ZSM-20 found that although it possessed strong acidity through its strong Brønsted acid sites, it did not contain any superacid sites [63]. Zeolites have aroused some commercial interest as strong acid catalysts [64].

Some heteropolyacids [65, 66] have also been reported as being superacids. These are compounds formed by condensation of tungstate or molybdate anions in acidic solution, either in the presence or absence of heteroatoms. Heteropolyacids containing a wide range of heteroatoms have been prepared and studied, although the most frequently encountered are phosphorus and silicon (from phosphate and silicate respectively). The structures of these compounds are the focus of much attention: they are very diverse, and constructed from octahedral MO_6 units. They have received attention industrially as catalysts for dehydration and oxidation processes [67].

The polymer Nafion, a registered trademark of Du Pont, has become the subject of much interest as a superacidic catalyst [58]. It contains the fully fluorinated carbon backbone with pendant sulphonic acid groups shown in Fig. 1.2.

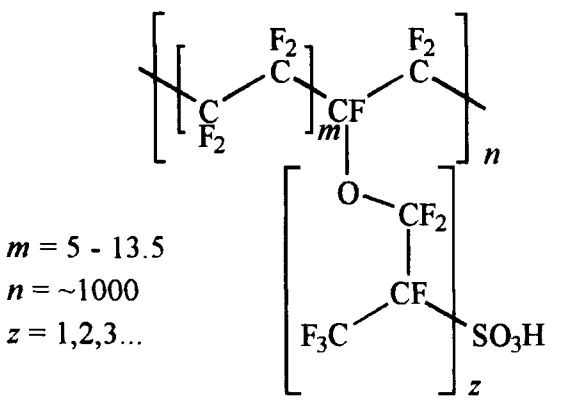

Fig 1.2: The Structure of Nafion®

Nafion can be prepared by the copolymerisation of tetrafluoroethene and a suitable sulphonic acid-containing perfluoroalkene monomer. Nafion has been found to have an H_o value of between -11 and -13, making it a superacid [58]. The catalysis of many reactions using Nafion has been investigated [68], including many rearrangements and condensations. Of particular interest is its performance in the isomerisation of xylenes, disproportionation of toluene and condensation of toluene with methanol. Activity for xylene isomerisation and toluene disproportionation has been reported at 160°C, and the rate of xylene conversion at 193°C is $5x10^{-5}$ mol per minute per gram of catalyst. In a typical isomerisation reaction, benzene, toluene, the three xylene isomers and the three trimethylbenzene isomers would be observed, indicating that other processes such as disproportionation of xylenes are occurring. The reaction of toluene with methanol [69] gave a 14.3% yield of xylenes at 209°C. The ratio of isomers was 32:29:39 *ortho* : *meta* : *para*. Deactivation of the catalyst was seen when dimethyl ether was used as the methylating agent due to esterification of the sulphonic acid groups of Nafion. This was not a problem when methanol was used as the water formed as a by-product during the reaction suppressed the esterification reaction.

It is also possible to prepare 'functionalised' Nafion by cation exchange methods. Some of these compounds have been used as catalysts [58].

A different kind of superacid is produced by the sulphation of metal oxides. Of these, sulphated zirconia has attracted the most attention [70]. It has been determined that the active zirconia is the tetragonal crystalline form. Under normal conditions, this is not stable at room temperature, with the monoclinic form being preferred. Tetragonal zirconia becomes the most stable form above 1000°C and below 2300°C. At temperatures higher than these the cubic form is the most stable [71].

The preparation of tetragonal zirconia as a metastable species at room temperature has been found to be possible by precipitation of a zirconium salt by hydrolysis. The compounds typically chosen as precursors are zirconium (IV) alkoxides [72-76] or halides [77]. The precipitation is catalysed by the addition of a small amount of acid. The solid produced is collected by filtration, and washed to remove any impurities. This is particularly the case when using the chloride precursor as the presence of chloride ions can affect the catalyst activity. A silver nitrate test of the washings is often used to

determine the presence of chloride or other halide ions. The solid obtained is an amorphous precursor, referred to as "zirconium hydroxide", which by calcination at temperatures above 410°C may be crystallised into the tetragonal form [75]. The metastable tetragonal form of zirconia is stabilised by the addition of sulphate [78]. This can be added to the amorphous precursor or to the precipitation, usually either as sulphuric acid or ammonium sulphate. This then allows calcination at higher temperatures - up to 700°C - without the transformation into the inactive monoclinic form [79, 80]. A process for large scale production of sulphated zirconia catalyst has been reported in the patent literature [81].

The nature of the active sites on sulphated zirconia catalysts is a matter for debate [82-85]. It has been determined that the catalyst possesses both Lewis and Brønsted acidity, and that different preparations give different ratios or even different types of these sites. The origin of Brønsted acidity is thought to come from hydroxyl groups, either directly bonded to zirconium or bound to sulphur in a manner reminiscent of sulphuric acid. It is the presence of these hydroxyl groups that allows the addition of sulphate into the "zirconium hydroxide" precursor by condensation during the calcination. Indeed, in the absence of sulphate, tetragonal zirconia does not possess Brønsted acidity [86]. The presence or absence of water in the structure is crucial in determining the extent and nature of activity [87-90]. Extensive dehydration of the compound has been shown to reduce Brønsted acidity considerably, and increase Lewis acidity. This reinforces the argument that Brønsted acidity is due to hydroxyl groups. The Lewis acidity is thought to be due to the presence of 'bare' Zr^{4+} or Zr^{3+} ions in the lattice which can accept electron density. They disappear on the addition of water - presumably water can co-ordinate to such a strong Lewis acid site [70]. A number of studies have proposed structures similar to those shown in Fig. 1.3.

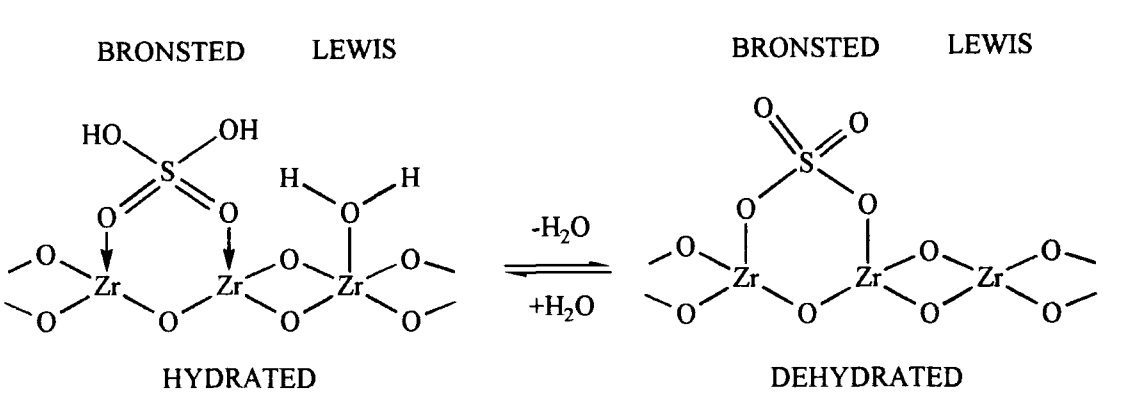

Fig. 1.3: Possible Active Sites on Sulphated Zirconia

The addition of dopants to sulphated zirconia can modify its properties. Addition of a small amount (< 10wt.%) of lanthanum oxide, yttrium oxide, magnesium oxide or calcium oxide has been reported as being beneficial to the stability of the tetragonal zirconia and increases the catalyst's surface area [91-93]. The addition of platinum to the system also increases the catalyst activity and stability, and can add a hydrogenation function to the catalyst [94, 95]. The effect of adding rhenium or titanium compounds has also been examined [77], although their catalytic performance has not been investigated. Sulphated zirconia catalysts doped with a 2:1 ratio of iron to manganese have been found to be active for reactions of ethane [96] and *n*-butane [97]. Sulphated zirconia doped with iron and magnesium is being developed for industrial applications, and is reported to be the most active non-halide superacid available [98]. The doping of a zirconia catalyst with tungstate ions provides an extremely active catalyst, which has been the subject of patents for NO reduction, ring opening and alkylation processes, including the alkylation of toluene with methanol [27, 99-103].

The reaction of sulphated zirconia with benzene has been studied. This is of interest as an aromatic system, and so is relevant to the isomerisation of xylenes. The first reaction of benzene at a sulphated zirconia has been reported to be a one electron oxidation to give a radical cation [104]. These then react to give coupling products such as diphenylmethane, biphenyl and phenylcyclohexane and oxidation products, such as phenol. The latter originate from esterification of the surface hydroxyl groups. Some alkylbenzenes were also produced [105]. The conversion of benzene to carbon dioxide and coke by sulphated zirconia has also been reported [106]. Evolution of sulphur

dioxide and oxygen was also seen, indication that sulphur (VI) at the catalyst surface had been reduced to sulphur (IV) during the reaction.

Sulphated zirconia catalysts have been use in a number of different catalytic reactions. The most frequently studied is the isomerisation of butane, for which sulphated zirconia has been shown to be active at room temperature [107]. Other reactions in which sulphated zirconia catalysts have been used include esterification [106], acylation and dehydration [108].

The concept of sulphating a metal hydroxide to produce a superacid has been extended to metals other than zirconium. Titanium dioxide and hafnium dioxide have both been sulphated to produce acidic catalysts [58, 109]. Extending the group four - group fourteen analogy, tin dioxide has been sulphated and used as both a catalyst and a sensor for toxic gases such as carbon monoxide [110]. Iron oxide and alumina have also been sulphated to give catalysts [111, 112]. These have been used for a similar range of reactions as sulphated zirconia catalysts - for example, for dehydration reactions such as the esterification of ethanoic acid with an alcohol or the dehydration of methanol to dimethyl ether, conversion of *n*-butane to *iso*-butane and the reduction of NO to N_2 using NH_3 as the reductant.

Sulphated zirconia catalysts are looked upon as highly active, environmentally benign catalysts which present a very real alternative to current strong acid catalysts such as the HF - SbF_5 system.

1.5 Concluding Remark

The production of *para*-xylene is a worthwhile exercise, provided a suitable catalyst can be found to convert a low-cost feedstock such as mixed xylenes or toluene with adequate selectivity. Given that the processes starting from either mixed xylenes, toluene or benzene are likely to be acid catalysed, superacid catalysts may fit the profile. From the literature surveyed, there is precedent for their use in catalysis of similar aromatic reactions.

1.6 References

1. D.L. Rawnsley, "Xylenes and Ethylbenzene" in "The Kirk-Othmer Dictionary of Chemical Technology", 3rd Edn., Vol. 24, pp.710-44.
2. *Chemical Market Reporter*, 1998, **254**(4), 21-31.
3. For example: *(a) Chemical Market Reporter*, 18th October, 1993, p.4. *Catalyst Review Newsletter*, November 1993, p.5. *(b) Chemical Week*, 23rd March, 1994, p.48. *Catalyst Review Newsletter*, April 1994, p.3. *(c) European Chemical News*, 21st March, 1994, p.42. *Catalyst Review Newsletter*, April 1994, p.2. *(d) Catalyst Review Newsletter*, August 1994, p.3. *Japan Chemical Week*, 28th July, 1994, p.3. *(e) Catalyst Review Newsletter*, August 1994, p.2. *European Chemical News*, 8th August 1994, p.2. *(f) Chemical Market Reporter*, 8th August 1994, p.3. *Catalyst Review Newsletter*, August 1994, p.1. *(g) Catalyst Review Newsletter*, December 1994, p.1. *European Chemical News*, 21st November 1994, p.26. *Oil Gas J.*, 21st November, 1994, p.38. *(h) Japan Chemical Week*, 11th January 1995, p.10. *Catalyst Review Newsletter*, February 1995, p.5.
4. *Hydrocarbon Processing*, November 1969, pp.244-5.
5. H.J. Shine, "Aromatic Rearrangements", Elsevier, 1967, pp.1-32, and references therein.
6. W.D. Schaeffer and J.D. Woolins, United States Patent 2798103 (1957). *Chemical Abstracts*, 1958, **52**, 2086*g*.
7. W.D. Schaeffer and J.D. Wordie, United States Patent 2591104 (1960). *Chemical Abstracts*, 1961, **55**, 2092*i*.
8. W.D. Schaeffer and W.S. Dorsey, United States Patent 2798102 (1957). *Chemical Abstracts*, 1958, **52**, 2086*f*.
9. W.D. Schaeffer, United States Patent 2798891 (1957). *Chemical Abstracts*, 1958, **52**, 2086*i*.
10. W.D. Schaeffer, United States Patent 2798069 (1957). *Chemical Abstracts*, 1958, **52**, 2088*e*.
11. W.K.T. Gleim, R.C. Wackher and F.C. Ramquist, United States Patent 3465055 (1969). *Chemical Abstracts*, 1969, **71**, 127053*r*.
12. C.J. Egan and R.V. Luthy, *Ind. Eng. Chem.*, 1955, **47**, 250-7.

13. D.L.H. Williams, "Aromatic Rearrangements" in "Comprehensive Chemical Kinetics", C.H. Bamford and C.F.H. Tipper (eds), Vol. 12, Elsevier Publishing Company, 1972, pp. 433-86.

14. L.M. Harwood, "Polar Rearrangements", Oxford University Press, 1992, pp.69-81.

15. R.H. Allen and L.D. Yats, *J. Am. Chem. Soc.*, 1959, **81**, 5289-92.

16. P.C. Miklis, R. Ditchfield and T.A. Spencer, *J. Am. Chem. Soc.*, 1998, **120**, 10482-9.

17. S. Morin, N.S. Gnep and M. Guisnet, *J. Catal.*, 1996, **159**, 296-304.

18. *Catalyst Review Newsletter*, March 1995, pp.10-14.

19. E. Benazzi, S. De Tavernier, P. Beccat, J.F. Joly, C. Nédez, A. Choplin and J.M. Basset, *Chemtech*, 1994, **October**, 13-8.

20. P. Beltrame, P.L. Beltrame, P. Carniti, L. Forni and G. Zuretti, *Zeolites*, 1985, **5**, 400-5.

21. W.W. Kaeding, C. Chu, L.B. Young and S.A. Butter, *J. Catal.*, 1981, **69**, 392-8.

22. N.R. Mesham, S.G. Hegde and S.B. Kulkarni, *Zeolites*, 1986, **6**, 434-8.

23. P. Beltrame, P.L. Beltrame, P. Carniti, G. Zuretti, G. Leofanti, E. Moretti and M. Padovan, *Zeolites*, 1987, 7, 418-22.

24. Y. Xiong, P.G. Rodewald and C.D. Chang, *J. Am. Chem. Soc.*, 1995, **117**, 9427-31.

25. *Catalyst Review Newsletter*, March 1995, pp.6-9.

26. W.W. Kaeding, C. Chu, L.B. Young, B. Weinstein and S.A. Butter, *J. Catal.*, 1981, **67**, 159-74.

27. C.D. Chang, F.T. DiGuiseppi and S. Han, United States Patent 5563310 (1996).

28. C. Friedel and J.-M. Crafts, *Ann. Chim. (Paris)*, 1888, **6**, 441, quoted in P. Braunstein, D. Matt and D. Nobel, *Chem. Rev.*, 1988, **88**, 747-64.

29. Y. Taniguchi, Y. Yamaka, K. Nakata, K. Takaki and Y. Fujiwara, *Chem. Lett.*, 1995, 345-6.

30. H. Sugimoto, I. Kawata, H. Taniguchi and Y. Fujiwara, *J. Organomet. Chem.*, 1984, **266**, C44-C46.

31. R. Ugo and A. Chiesa, *J. Chem. Soc., Perkin Trans. 1*, 1987, 2625-9.

32. C. Amatore, A. Jutand, F. Khalil and M.F. Nielsen, *J. Am. Chem. Soc.*, 1992, **114**, 7076-85.

33. E. McNelis, *J. Org. Chem.*, 1965, **30**, 1209-13.

34. B. Raecke and H. Schirp, *Org. Synth. Coll. Vol. 5*, 1973, 813-6.

35. K. Fujishiro and S. Mitamura, *Bull. Chem. Soc. Jpn.*, 1989, **62**, 786-90.

36. L.P. Hammett and A.J. Deyrup, *J. Am. Chem. Soc.*, 1932, **54**, 2721-39.

37. R.J. Gillespie and T.E. Peel, *Adv. Phys. Org. Chem.*, 1971, **9**, 1-24.

38. D. Fărcasiu, S.L. Fisk, M.T. Melchior and K.D. Rose, *J. Org. Chem.*, 1982, **47**, 453-7.

39. D. Fărcasiu and D. Hâncu, *J. Chem. Soc., Farad. Trans.*, 1997, **93**, 2161-5.

40. R. Minkwitz and D. Konikowski, *Z. Anorg. Allgem. Chem.*, 1995, **621**, 2055-60.

41. A. Martin, M.-P. Jouannetand and J.-C. Jacquisy, *Tetrahedron Lett.*, 1996, **37**, 7731-4.

42. A. Bagno, J. Bukala and G.A. Olah, *J. Org. Chem.*, 1990, **55**, 4284-9.

43. G.A. Olah, K. Laali, G. Adler, R.J. Spear, R. Schlosberg and J.A. Olah, *J. Org. Chem.*, 1985, **50**, 1306-9.

44. K.K. Laali and D.S. Nagvekar, *J. Org. Chem.*, 1991, **56**, 1867-74.

45. K.K. Laali, J.E. Gano, C.W. Gunlach IV and D. Lenoir, *J. Chem. Soc., Perkin Trans. 2*, 1994, 2169-73.

46. P.-L. Fabre, J. Devynck and B. Trémillon, *Chem. Rev.*, 1982, **82**, 591-614.

47. M.D. Heagy, Q. Wang, G.A. Olah and G.K.S. Prakash, *J. Org. Chem.*, 1995, **60**, 7531-4.

48. H. Willner and F. Aubke, *Inorg. Chem.*, 1990, **29**, 2195-200.

49. G.A. Olah, K. Laali and O. Farooq, *J. Org. Chem.*, 1985, **50**, 1483-6.

50. D.A. Klumpp, K.Y. Yeung, G.K.S. Prakash and G.A. Olah, *J. Org. Chem.*, 1998, **63**, 4481-4.

51. D.A. Klumpp, K.Y. Yeung, G.K.S. Prakash and G.A. Olah, *Synlett*, 1998, 918-21.

52. G.A. Olah, G. Rasul, C. York and G.K.S. Prakash, *J. Am. Chem. Soc.*, 1995, **117**, 11211-4.

53. G.A. Olah, A. Orlinkov, A.B. Oxyzoglov and G.K.S. Prakash, *J. Org. Chem.*, 1995, **60**, 7348-50.

54. A.P. Davis and M. Jaspars, *J. Chem. Soc., Chem. Commun.*, 1990, 1176-8.

55. W.L.F. Armarego and D.D. Perrin, "Purification of Laboratory Chemicals", 4th Edn., 1996, Reed Elsevier, p.55.

56. M. Misono and T. Okuhara, *Chemtech*, 1993, **November**, 23-9.

57. T. Yamaguchi, *Appl. Catal.*, 1990, **61**, 1-25.

58. K. Arata, *Appl. Catal.*, 1990, **37**, 165-211.

59. K. Laali and J. Sommer, *Nouv. J. Chim.*, 1981, **5**, 469-71, quoted in ref. 40.

60. H. Yang, B. Li and Y. Fang, *Synth. Commun.*, 1994, **24**, 3269-75.

61. M. Ma and K.E. Johnson, *J. Am. Chem. Soc.*, 1995, **117**, 1508-13.

62. C. Mirodatos and D. Barthomeuf, *J. Chem. Soc., Chem. Commun.*, 1981, 39-40.

63. H. Kosslick, H. Berndt, H.D. Lanh, A. Martin, H. Miessner, V.A. Tuan and J. Jänchen, *J. Chem. Soc., Farad. Trans.*, 1994, **90**, 2837-44.

64. K.M. Mackay, R.A. Mackay and W. Henderson, "Introduction to Modern Inorganic Chemistry", 5th Edn., Blackie Academic and Professional, 1996, pp.266-8.

65. N.N. Greenwood and A. Earnshaw, "Chemistry of the Elements", 2nd Edn., Reed Elsevier, 1997, pp.1014-6.

66. *Catalyst Review Newsletter*, July 1994, p.5. *Chemical Week*, 7th June, 1994, pp.94-6.

67. For example: (a) J.F. Knifton, United States Patent 5349110 (1994). *Chemical Abstracts*, 1995, **122**, 30956*w*. (b) N. Mizuno, M. Tateishi and M. Iwamoto, *J. Chem. Soc., Chem. Commun.*, 1994, 1411-2.

68. G.A. Olah, P.S. Iyer and G.K.S. Prakash, *Synthesis*, 1986, 513-31.

69. J. Kaspi, D.D. Montgomery and G.A. Olah, *J. Org. Chem.*, 1978, **43**, 3147-50.

70. B.H. Davis, R.A. Keogh and R. Srinivasan, *Catal. Today*, 1994, **20**, 219-56.

71. S.-M. Ho, *Mat. Sci. Eng.*, 1982, **54**, 23-29.

72. H.-C. Wang and K.-L. Lin, *Mat. Sci. Eng.*, 1991, **A136**, 171-8.

73. A. Ayral, T. Assih, M. Abenoza, J. Phalippou, A. Lecomte and A. Dauger, *J. Mat. Sci.*, 1990, **25**, 1268-74.

74. B.E. Yoldas, *J. Mat. Sci.*, 1986, **21**, 1080-6.

75. H.-C. Wang and K.-L. Lin, *J. Mat. Sci.*, 1991, 2501-6.

76. K.-L. Lin and H.-C. Wang, *J. Mat. Sci.*, 1988, **23**, 3666-70.

77. M. Valigi, A. Cimino, D. Gazzoli and G. Minelli, *Solid State Ionics*, 1989, **32/33**, 698-705.

78. F.-C. Wu and S.-C. Yu, *J. Mat. Sci.*, 1990, **25**, 970-6.

79. R.A. Comelli, C.R. Vera and J.M. Parera, *J. Catal.*, 1995, **151**, 96-101.

80. C. Morterra, G. Cerrato, F. Pinna and M. Signoretto, *J. Catal.*, 1995, **157**, 109-23.

81. *Japan Chemical Week*, 14th July 1994, p.3. *Catalyst Review Newsletter*, August 1994, p.4.

82. L.M. Kustov, V.B. Kazansky, F. Figueras and D. Tichit, *J. Catal.*, 1994, **150**, 143-9.

83. R.L. White, E.C. Sikabwe, M.A. Coelho and D.E. Resasco, *J. Catal.*, 1995, **157**, 755-8.

84. F.R. Chen, G. Coudurier, J.-F. Joly and J.C. Verdrine, *J. Catal.*, 1993, **143**, 616-26.

85. F.R. Chen, G. Coudurier, J.-F. Joly and J.C. Verdrine, *Symposium on Alkylation, Aromatisation, Oligomerisation and Isomerisation of Short Chain Hydrocarbons over Heterogeneous Catalysts*, American Chemical Society, Division of Petroleum Chemistry, New York City Meeting, August 1991, pp.878-86.

86. C. Morterra, G. Cerrato, V. Bolis, S. Di Ciero and M. Signoretto, *J. Chem. Soc. Farad. Trans.*, 1997, **93**, 1179-84.

87. C. Morterra, G. Cerrato, F. Pinna and M. Signoretto, *J. Phys. Chem.*, 1994, **98**, 12373-81.

88. C. Morterra, G. Cerrato, F. Pinna, M. Signoretto and G. Strukul, *J. Catal.*, 1994, **149**, 181-8.

89. V. Bolis, G. Magnacca, G. Cerrato and C. Morterra, *Langmuir*, 1997, **13**, 888-94.

90. F. Babou, B. Bigot and P. Sautet, *J. Phys. Chem.*, 1993, **97**, 11501-9.

91. F.-C. Wu and S.-C. Yu, *J. Crystal Growth*, 1989, **96**, 96-100.

92. K.S. Chan, G.K. Chuah and S. Jaenicke, *J. Mat. Sci. Lett.*, 1994, **13**, 1579-81.

93. C. Morterra, G. Cerrato, L. Ferroni and L. Montanaro, *Mater. Chem. Phys.*, 1994, **37**, 243-57.

94. M. Signoretto, F. Pinna, G. Strukul, P. Chies, G. Cerrato, S. Di Ciero and C. Morterra, *J. Catal.*, 1997, **167**, 522-32.

95. C. Morterra, G. Cerrato, S. Di Ciero, M. Signoreto, F. Pinna and G. Strukul, *J. Catal.*, 1997, **167**, 172-83.

96. T.-C. Cheung and B.C. Gates, *Chem. Commun.*, 1996, 1937-8.

97. T.-C. Cheung, J.L. D'Itsi and B.C. Gates, *J. Catal.*, 1995, **151**, 464-6.

98. *European Chemical News*, 2nd November 1992, p.31.

99. C.D. Chang, J.G. Santiesteban and D.L. Stern, United States Patent 5345026 (1994).

100. C.D. Chang, J.G. Santiesteban, D.S. Shihabi and S.A. Stevenson, Unites States Patent 5401478 (1995).

101. C.D. Chang, R.D. Bastian, S. Han and J.G. Santiesteban, United States Patent 5382731 (1995).

102. C.D. Chang, S. Han, J.G. Santiesteban, M.M. Wu and Y. Xiong, United States Patent 5516954 (1996).

103. D.K. Kuhn, United States Patent 5396011 (1995).

104. A. Ghenciu and D. Fărcasiu, *J. Mol. Catal. A*, 1996, **109**, 273-83.

105. A. Ghenciu and D. Fărcasiu, *Chem. Commun.*, 1996, 169-70.

106. G.D. Yadav and P.H. Mehta, *Ind. Eng. Chem. Res.*, 1994, **33**, 2198-208.

107. M. Hino, S. Kobayashi and K. Arata, *J. Am. Chem. Soc.*, 1979, **101**, 6439-41.

108. P. Moles, *Speciality Chemicals*, 1992, **Nov/Dec**, 382-8.

109. J.P. Chen and R.T. Young, *J. Catal.*, 1993, **139**, 277-88.

110. A. Keshavaraja, B.S. Jayasuri, A.V. Ramaswamy and K. Vijayamohanan, *Sensors & Actuators*, 1995, **B23**, 75-81.

111. K. Arata and M. Hino, *Bull. Chem. Soc. Jpn.*, 1980, **53**, 446-9.

112. M. Waqif, J. Bachelier, O. Saur and J.-C. Lavalley, *J. Mol. Catal.*, 1992, **72**, 127-38.

Chapter Two: Preliminary Investigations into Xylene Isomerisation

2.1 Introduction

This chapter describes a number of experiments in which the aim is to convert *ortho*-xylene to the other xylene isomers, especially para-xylene which is commercially the most valuable isomer. The catalysts considered come from a number of sources. Some were synthesised with this purpose in mind, others were commercial or developmental samples supplied by catalyst manufacturers. These catalysts are compared to each other and the reasons for their activity discussed.

2.1.1 Zirconia Catalysts

Following reports [1,2] of activity of zirconia catalysts for isomerisation processes, a range of zirconia catalysts was prepared. Some were metal doped, as some metals, notably platinum [3,4], had been reported as giving extra activity or stability to zirconia catalysts. Others were doped with sulphate, to achieve the superacidic properties assigned to sulphated zirconia [5,6]. Phosphate was added to some catalysts to give a comparison to sulphate [7].

2.1.2 Supported Metal Catalysts

Transition metal catalysts have long been known to interact with aromatic systems [8]. They can do this in a number of ways, the most frequently-observed being via the aromatic π-electrons, as observed in compounds such as $(C_6H_6)Cr(CO)_3$ [9], and as a single electron σ-bound ligand, such as a metal aryl complex [10]. Silver has been observed to bind to aromatic rings in a number of different fashions [23]. By choosing metals that bind in different fashions - chromium, silver and palladium - it was hoped to be able to exploit these different modes of co-ordination to activate the ring towards isomerisation reactions.

Silver and palladium have been shown [11,12] to act in a synergistic fashion in some reactions, and it was hoped that this metal combination could lead to some enhancement of reactivity. Using a very small amount of palladium compared to silver was reported to give a novel surface species with greater activity than a one-to-one mixture [13], and this was also investigated.

A variety of inorganic supports were used, giving a range of environments for the metals, with the aim of promoting different, and possibly unusual, effects.

2.1.3 Commercial Samples

These were used for two reasons - to 'prove' the reactor system, and to give a benchmark against which future reactions could be evaluated. They were not prepared especially for this reaction, but were either standard laboratory chemicals (molecular sieve, alumina) or were supplied by a catalyst manufacturer.

2.2 Experimental

2.2.1 Synthesis of Zirconia Catalysts

2.2.1.1 Synthesis of Zirconia

A mixture of n-propanol (200ml), concentrated nitric acid (4ml) and distilled water was added dropwise, overnight, to a solution of zirconium tetra-n-propoxide (70wt.% solution in n-propanol, 32g) in n-propanol (50ml). This gave a pale yellow solution with a small amount of gel formation. A further 30ml of distilled water was added, followed by 400ml of concentrated aqueous ammonia, which was added dropwise overnight and precipitated the gel from solution. The solution was filtered, and the solid obtained dried in air for 24 hours. A portion was calcined at 600°C for three hours, giving a pale green powder. Other portions were used in further syntheses.

2.2.1.2 Synthesis of Pt-Zirconia

Platinum dichloride (0.22g, 0.83 mmol) was dissolved in concentrated hydrochloric acid by heating. To this was added the zirconia as synthesised in 2.2.1.1 above (3.04g).

This gave a suspension, which was heated to dryness at 150°C and the resulting solid calcined at 600°C for three hours giving a black powder.

In a second synthesis, $Pt(OH)_2$, used in place of $PtCl_2$, was prepared [14] by dissolving potassium hydroxide (0.17g, 3.0 mmol) in water, and heating the solution to 85°C. $PtCl_2$ (0.8g, 3.0 mmol) was added slowly, forming a black precipitate. More water was added to the reaction, and the black slurry formed was removed by filtration using a filterstick and dried either in air or under vacuum. This gave 0.60g of a black solid (87.1% yield).

A portion of $Pt(OH)_2$ (0.2g, 0.87mmol) was placed with zirconia synthesised in 2.2.1.1 above (4.0g) in a pestle and mortar and ground together. The resulting light grey powder was calcined at 600°C for three hours giving a darker grey powder.

2.2.1.3 Synthesis of Al-SO_4^{2-}-Zirconia

Aluminium sulphate (0.31g, 2.5 mmol) was placed into a pestle and mortar with zirconia, synthesised in 2.2.1.1 above, (1.00g) and ground together for five minutes. This was calcined at 600°C for three hours to give a white solid.

2.2.1.4 Synthesis of Ni-SO_4^{2-}-Zirconia

Nickel sulphate (0.24g, 1.6 mmol) was placed in a pestle and mortar with zirconia, synthesised as in 2.2.1.1 above, (1.00g) and ground together for five minutes. This was then calcined at 600°C for three hours to give a pale green/grey solid.

2.2.1.5 Synthesis of Pt-SO_4^{2-}-Zirconia

Ammonium sulphate (0.27g, 2.4 mmol) was placed in a pestle and mortar with Pt-zirconia as synthesised in 2.2.1.2 above, and these were ground together for five minutes. The resulting mixture was heated to 150°C for two hours, then calcined at 600°C for three hours giving a black powder.

2.2.1.6 Synthesis of Al-Zirconia

Aluminium trichloride (0.26g, 1.9 mmol) was dissolved in diethylether (20ml). To this was added zirconia as synthesised in 2.2.1.1 above (1.00g). The resulting suspension

was stirred for 45 minutes, and the solvent removed *in vacuo*, giving an off-white powder. On calcination at 600°C for three hours, this gave a grey powder.

2.2.1.7 Synthesis of PO_4^{3-}-Zirconia

Phosphoric acid (85% in water, 1ml) was added to zirconia as synthesised in 2.2.1.1 above (1.00g) and stirred for 5 minutes, before being dried at 150°C. This was then calcined at 600°C for three hours to give a white solid.

In a second synthesis, $(NH_4)_2HPO_4$ (0.21g, 1.6 mmol) was ground with "zirconium hydroxide" in a pestle and mortar. The resulting light grey powder was calcined at 600°C for three hours, giving a grey powder.

2.2.1.8 Synthesis of Pt-PO_4^{3-}-Zirconia

Phosphoric acid (85% in water, 1ml) was added to Pt-zirconia as synthesised in 2.2.1.2 above (1.00g) and stirred for 5 minutes before being dried at 150°C. This was then calcined at 600°C for three hours to give a grey-brown powder.

2.2.1.9 Synthesis of Ni-Zirconia

Nickel dichloride hexahydrate (0.22g, 0.93 mmol) was dissolved in 20ml water. To this was added zirconia as synthesised in 2.2.1.1 above, giving a pale green suspension. This was heated to 150°C for two hours, when dryness had been reached. This was then calcined at 600°C for three hours to give a brown-grey powder.

In a second synthesis, $NiCl_2.6H_2O$ (0.22g, 0.93 mmol) was dissolved in water by stirring, to give a green solution. To this was added "zirconium hydroxide" (1.00g), giving a pale green suspension. This was allowed to stir for 90 minutes, then was taken to dryness at 180-220°C under vacuum. This gave an orange-pink solid, which was calcined at 600°C for three hours, giving a brown powder.

In a third synthesis, $NiCl_2.6H_2O$ (0.44g, 1.9 mmol) was dissolved in the minimum amount of water (5ml). To this was added "zirconium hydroxide" (2.00g) giving a green - white suspension, which was stirred for twenty minutes, before being heated to dryness

at 150°C in air. This gave a pale yellow powder, which was calcined at 600°C for three hours, giving a grey powder.

In a fourth synthesis, $Ni(OH)_2$ (0.49g, 5.3 mmol) and "zirconium hydroxide" (10.04g) were ground together in a pestle and mortar. This gave a white - green powder, which was heated to 600°C for 5½ hours, giving a pale grey powder.

2.2.1.10 Synthesis of Cr-Zirconia

Chromium trioxide (0.58g, 5.8 mmol) was suspended in diethyl ether (25ml) by heating to the reflux temperature. After it had been cooled to room temperature, "zirconium hydroxide" (15.0g) was added and the resulting suspension stirred for one hour. The solvent was removed under vacuum giving a yellow - green powder. Calcination at 600°C for three hours gave a yellow - grey powder.

2.2.1.11 Synthesis of Cr-SO_4^{2-}-Zirconia

Cr-zirconia (5.0g), as synthesised in 2.2.1.10 above, and ammonium sulphate (0.14g, 1.1 mmol) were ground together in a pestle and mortar. The resulting green powder was calcined at 600°C for three hours giving a green/grey powder.

2.2.1.12 Synthesis of SO_4^{2-}-Zirconia (Sulphated Zirconia) by Grinding

Ammonium sulphate (0.21g, 1.6 mmol) and zirconia, as synthesised in 2.2.1.1 above, were placed together in a pestle and mortar and ground together for five minutes. This was calcined at 600°C for three hours to give an off-white powder.

2.2.1.13 Synthesis of Sulphated Zirconia by Precipitation

To a solution of zirconium tetra-n-propoxide (70wt.% in n-propanol, 32.0g) in n-propanol (55ml) was added a mixture of n-propanol (185ml), distilled water (3.2ml), concentrated sulphuric acid (2ml) and concentrated nitric acid (2ml). This was added dropwise over a period of approximately eight hours. This gave a greyish suspension containing some gel. A further 200ml of water was added, giving a white gel. Excess ammonia was then added, causing solid to precipitate, and the mixture was allowed to settle overnight into two layers. The solid was removed by filtration and dried under vacuum for six hours at 110°C. It was calcined at 600°C for three hours before use.

2.2.2 Synthesis of Supported Metal Catalysts

2.2.2.1 Preparation of Supports

Samples of alumina (5.00g), magnesium oxide (5.04g), silica (5.00g), titanium dioxide (5.20g) and "zirconium hydroxide" (5.09g) were calcined separately at 600°C for three hours, then cooled to room temperature and stored in a desiccator prior to testing for catalytic activity. The following masses of calcined products were obtained: alumina, 4.95g; magnesium oxide, 4.63g; silica, 4.26g; titanium dioxide, 5.13g; "zirconium hydroxide", 3.82g. All the calcined compounds were white powders.

2.2.2.2 Preparation of Supported Silver Catalysts

Commercial samples of 2 wt. % silver supported on magnesium oxide, silica, titanium dioxide and zirconia were supplied by KPT. Samples were calcined at 600°C for three hours as described in Table 2.1.

Table 2.1: Calcination of Supported Metal Catalysts

Catalyst	Appearance before calcination	Mass Calcined / g	Appearance after calcination	Mass Resulting / g
Ag on MgO	Coarse Grey Powder	5.17g	Coarse Light Brown Powder	3.96g
Ag on SiO_2	Olive Green Powder	5.06g	Yellow - Green Powder	4.97g
Ag on TiO_2	Grey Powder	5.14g	Off-White Powder	5.12g
Ag on ZrO_2	Black Powder	5.00g	Coarse Grey Powder	4.97g

Silver on alumina was prepared separately. Silver nitrate (0.66g, 3.9 mmol) was dissolved in a mixture of distilled water (3ml) and diethylether (80ml). Alumina (20.0g) was added, and the resulting suspension allowed to stir overnight. The solvent was removed under reduced pressure, giving 21.01g of an off-white solid. This was calcined

at 600°C for three hours, and allowed to cool to room temperature, giving 19.95g of a grey - brown powder.

2.2.2.3 Synthesis of Supported Palladium Catalysts

To a solution of palladium acetate (0.21g, 0.94 mmol) in acetone (10ml) was added the desired support. The resulting suspension was allowed to stir for three hours, then the solvent was removed under reduced pressure. The residue was calcined at 600°C for three hours. Further details of individual preparations are given in Table 2.2.

Table 2.2: Preparation of Supported Palladium Catalysts

Support (mass)	Dried Product Colour (mass)	Calcined Product Colour (mass)
Alumina (5.1g)	Cream - Beige (5.11g)	Dark brown (5.10g)
Magnesium oxide (5.4g)	Beige (5.39g)	Brown (5.00g)
Silica (5.0g)	Pale beige (5.28)	Brown (4.46g)
Titanium dioxide (5.0g)	Off - white (5.19g)	Brown (5.02g)
"Zirconium hydroxide" (5.0g)	Orange - beige (4.56g)	Brown (3.58g)

2.2.2.4 Synthesis of Supported Chromium Catalysts

To a suspension of chromium trioxide (0.20g, 2.0 mmol) in diethylether (12 - 20ml) was added the desired support. The resulting suspension was allowed to stir overnight, after which time the solvent was removed under reduced pressure. The residue was calcined for three hours at 600°C. Details of individual preparations are given in Table 2.3.

Table 2.3: Preparation of Supported Chromium Catalysts

Support (mass)	Colour of Dried Product (mass)	Colour of Calcined Product (mass)
Alumina (5.0g)	Light brown (4.93g)	Grey (4.78g)
Magnesium oxide (5.2g)	Light brown (5.19g)	Green (4.79g)
Silica (5.2g)	Off - white (5.23g)	Green (4.62g)
Titanium dioxide (5.0g)	Light grey (4.66g)	Off - white (4.85g)
"Zirconium hydroxide" (5.0g)	Yellow (5.11g)	Yellow - Green (3.84g)

2.2.2.5 Synthesis of Supported Chromium - Silver Catalysts

To a solution of chromium trioxide (0.20g, 2.0 mmol) in acetone (7 ml) was added 5g of supported silver catalyst (2 wt.% Ag on MgO, SiO_2, TiO_2 or ZrO_2) to give a suspension. This was allowed to stir for one hour, before the solvent was removed in vacuo, giving a solid. This was calcined at 600°C for three hours. Descriptions and masses of the products are given in Table 2.4.

Table 2.4: Description of Supported Chromium-Silver Catalysts

Support	MgO	SiO_2	TiO_2	ZrO_2
Colour of Suspension	Black	Grey - Brown	Dark Red - Black	Black
Colour of Dried Solid	Brown	Brown	Brown-Grey	Grey
Mass of Dried Solid	5.1g	5.1g	5.3g	5.2g
Colour of Calcined Solid	Yellow	Yellow	Grey	Red
Mass of Calcined Solid	3.59g	4.79g	4.89g	5.06g

In a separate preparation, chromium trioxide (0.19g, 1.9 mmol) was dissolved in methanol (25ml) in an exothermic process, and the silver - alumina catalyst (2 wt.% Ag, 5.0g) added. The suspension was stirred for three hours, then the methanol removed under reduced pressure. This gave 5.14g of a light brown solid, which became 4.81g of a light brown powder after being calcined at 600°C for three hours.

2.2.2.6 Synthesis of Palladium - Silver Supported Catalysts

Two types of palladium - silver catalyst were prepared, one with a 1:1 ratio of palladium to silver, and one with a 1:10000 ratio of palladium to silver.

2.2.2.6.1 Synthesis of 1:1 Palladium - Silver Supported Catalysts

To a solution of palladium acetate (0.21g, 0.94 mmol) in methanol (6ml) was added 5g of a supported silver catalyst (2 wt.% silver on MgO, SiO_2, TiO_2 or ZrO_2).

This gave a suspension which was stirred for one hour, after which time the methanol was removed under reduced pressure. This gave a dried solid, which was calcined at 600°C for three hours. The descriptions of these catalysts are given in Table 2.5.

Table 2.5: Description of Supported 1:1 Palladium - Silver Catalysts

Support	Al_2O_3	MgO	SiO_2	TiO_2	ZrO_2
Colour of Dried Compound	Light Brown	Black	Green-Grey	Grey	Black
Mass of Dried Compound	5.2g	4.8g	4.7g	4.8g	4.8g
Colour of Calcined Compound	Dark Brown - Grey	Black	Black	Light Brown	Grey
Mass of Calcined Compound	5.1g	3.6g	4.4g	4.7g	4.8g

2.2.2.6.2 Synthesis of 1:10000 Palladium - Silver Catalysts

To a solution of palladium acetate (2mg, 8.9 μmol) in acetone (20ml) was added a portion of a supported silver catalyst (2 wt.% Ag on Al_2O_3, MgO, SiO_2, TiO_2 or ZrO_2, 5g). The resulting suspension was allowed to stir for two hours, and then the solvent was removed under reduced pressure. This gave the dried product, which was then calcined at 600°C for three hours. Descriptions of the catalysts are given in Table 2.6.

Table 2.6: Descriptions of 1:10000 Palladium - Silver Catalysts

Support	Al_2O_3	MgO	SiO_2	TiO_2	ZrO_2
Colour of Dried Solid	Light Brown	Grey	Green	Grey	Dark Grey
Mass of Dried Solid	4.9g	5.0g	4.9g	4.9g	4.9g
Colour of Calcined Solid	Light Brown	Grey	Green - Yellow	Yellow - Green	Light Grey
Mass of Calcined Solid	4.4g	4.0g	4.8g	4.8g	4.8g

2.2.3 Commercial Samples

The following commercial samples were investigated for activity in the isomerisation of *ortho*-xylene:

Molecular Sieve Type 13X. The catalyst was supplied (BDH) as 0.1" pellets. Its composition is that of an aluminium sodium silicate, with pore sizes of approximately 10Å [15].

Alumina Spheres. These were supplied by United Catalysts, Inc., and were heated to 220°C for two hours before use.

Commercial Zeolite EX - 1720. This was supplied under a non-analysis agreement by the catalyst manufacturer Süd-Chemie. It was described as "Zeolite, Na form" and "synthetic aluminosilicate".

Developmental Catalyst T - 2581. This was also supplied by Süd-Chemie under a non-analysis agreement. It was described as "aluminium oxide on a mordenite carrier" and contained nickel.

2.2.4 Experimental Procedure

Experiments were performed as described in Section 3.2.2 and using the apparatus shown in figure 3.2.

2.3 Results

Selected results from this section are presented in graphical form in Appendix 2.1, and full data are presented in Appendix 2.2.

2.3.1 Zirconia Catalysts

2.3.1.1 Undoped Zirconia

Undoped zirconia was not active for *ortho*-xylene isomerisation, whether prepared from zirconium tetra-n-propoxide or "zirconium hydroxide".

2.3.1.2 Sulphated Zirconia

Sulphated zirconia prepared from zirconium tetra-n-propoxide showed little activity in this instance. This is in contrast to results reported in later chapters.

Sulphated zirconia prepared from "zirconium hydroxide" was active, and details of this are given in Figs. A2.1 and A2.2 (Appendix 2.1). Activity is by far the greatest at lower temperatures, the maximum conversion being seen below 300°C. The major products are xylene isomers. At higher temperatures activity is seen to fall away.

2.3.1.3 Phosphated Zirconia

This compound was not active for *ortho*-xylene isomerisation.

2.3.1.4 Platinum-doped Zirconia

No activity was observed for *ortho*-xylene isomerisation for compounds prepared from either platinum hydroxide or platinum chloride.

2.3.1.5 Platinum-doped Sulphated Zirconia

The isomerisation of *ortho*-xylene was studied on this catalyst between 200°C and 475°C (figs. A2.3 and A2.4, Appendix 2.1). Activity was greatest at 200°C, with *ortho*-xylene conversion being approximately 0.5%. Above this temperature, activity seems to decline quickly, although conversions are of the levels of impurities in the feedstock so it is difficult to be certain. However, the yield of trimethylbenzenes falls to zero, suggesting that disproportionation activity has disappeared (trimethylbenzenes are not present in the feedstock).

2.3.1.6 Platinum-doped Phosphated Zirconia

No activity for *ortho*-xylene isomerisation was observed with this compound.

2.3.1.7 Aluminium-doped Zirconia

The activity of aluminium-doped zirconia was evaluated between 250°C and 470°C (Figs. A2.5 and A2.6, Appendix 2.1). Conversion of *ortho*-xylene was low, the greatest conversion being approximately 0.3% at 470°C. The major product at this temperature was toluene, although there was no corresponding increase in the yield of trimethylbenzenes, as would be expected for a disproportionation reaction.

2.3.1.8 Aluminium-doped Sulphated Zirconia

The activity of aluminium-doped sulphated zirconia prepared from zirconium tetra-*n*-propoxide, as described in section 2.2.1.1 above, is greatest at low temperature. At 250°C, the conversion is approximately 0.5%, and the products largely comprise the other xylene isomers and toluene. At higher temperatures, the activity drops away, although some activity is seen at 425°C (Figs. A2.7 and A2.8, Appendix 2.1). Here the *ortho*-xylene conversion is nearer 0.3%, and the concentration of non-xylene products is greater than at low temperature. However, the major products are still the other xylene isomers and toluene. The selectivity of the catalyst to either xylenes or toluene is lower at high temperature.

A second sample of aluminium doped sulphated zirconia was prepared using "zirconium hydroxide". This was also found to be active for the isomerisation of *ortho*-xylene (Figs. A2.9 and A2.10, Appendix 2.1). Again, the activity was greatest at lower temperatures, with xylene isomers being the major products. At higher temperatures toluene is produced, possibly by dealkylation or disproportionation.

2.3.1.9 Nickel-doped Zirconia

Nickel-doped zirconia catalysts prepared from nickel dichloride showed little or no activity towards *ortho*-xylene isomerisation (Figs. A2.11 and A2.12, Appendix 2.1). Unlike many of the catalysts examined here, there was no initial activity at low temperatures, the only activity being seen at 400°C, although this has dropped away by 445°C. The major product detected at 400°C was toluene by a large margin. The maximum conversion of *ortho*-xylene was approximately 0.8%.

A different picture was seen using catalysts prepared from nickel hydroxide (Figs. A2.13 and A2.14, Appendix 2.1). Activity was seen at lower temperatures, between 300°C and 350°C, but drops away both below 300°C and above 400°C. No xylenes were produced (the 0.1% seen being residual in the feedstock) but toluene and benzene were seen, suggesting dealkylation or disproportionation activity.

2.3.1.10 Nickel-doped Sulphated Zirconia

There was a large maximum in activity for the isomerisation of *ortho*-xylene over nickel-doped sulphated zirconia at 360°C (Figs. A2.15 and A2.16, Appendix 2.1). Unlike many of the other catalysts, there was little or no activity at lower temperatures, but a large conversion - 0.6% - of which the major product was the other xylene isomers with 63.5% selectivity. There was a maximum in toluene production at 400°C and one in trimethylbenzene production at 250°C.

2.3.1.11 Chromium-doped Zirconia

No activity for reactions with *ortho*-xylene was observed with this catalyst.

2.3.1.12 Chromium-doped Sulphated Zirconia

The activity of this material was exclusively at higher temperatures (>350°C). It was different to many of the compounds investigated in that the major products at this temperature were xylenes, representing isomerisation activity, rather than toluene or benzene, representing dealkylation. At lower temperatures the catalyst was inactive (Figs. A2.17 and A2.18, Appendix 2.1).

2.3.2 Supported Metal Catalysts

None of the supported metal catalysts prepared showed activity for *ortho*-xylene isomerisation in the temperature range investigated (200°C to 500°C). The carbon content of the catalysts was investigated, and all the catalysts had gained in carbon during the reaction. The catalysts were investigated using hydrogen as a flow gas to try and reduce this. This did have the effect of reducing the coking - as shown in Fig. 2.1 - but there was no increase in activity.

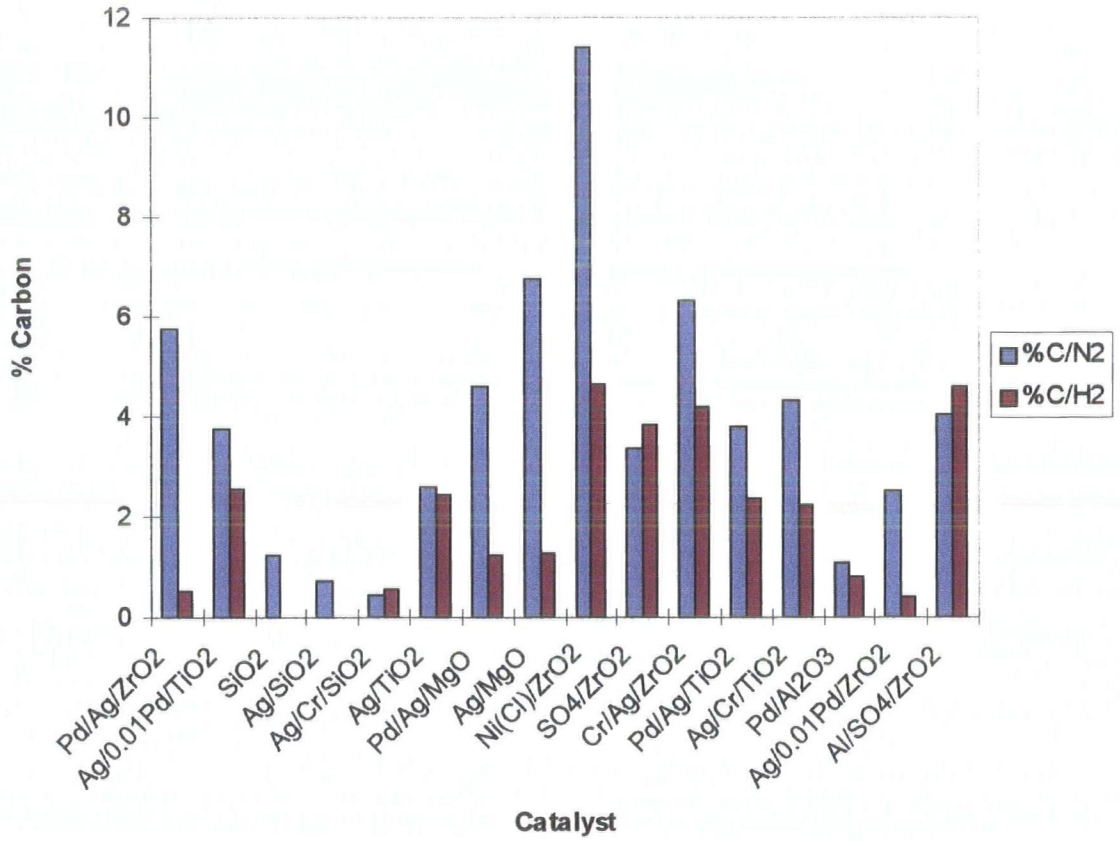

Fig. 2.1: Carbon Content of Catalyst Samples run using Nitrogen or Hydrogen as Flow Gas

2.3.3 Commercial Samples

The molecular sieve was investigated at temperatures in the region of 400°C. No activity for *ortho*-xylene isomerisation was seen; all the liquid products were ortho-xylene. The alumina spheres were investigated at a range of temperatures from 200°C to 470°C. Again, no conversion of *ortho*-xylene to other products was observed.

The catalysts EX-1720 and T-2581 were more active. Using EX-1720, slight conversion of ortho-xylene was seen from 250°C (Fig. A2.19, Appendix 2.1). This reached a plateau value of approximately 75% conversion at and above 350°C. By far the major product was *meta*-xylene (50%) although *para*-xylene (20%) was also formed. The ratio of *meta* to *para* isomer was approximately 5:2.

Catalyst T-2581 was also active for *ortho*-xylene isomerisation, although in a different way to EX-1720 (Fig. A2.20, Appendix 2.1). The *ortho*-xylene conversion at 250°C was almost zero, but the activity increased to a maximum conversion (50%) at 350°C. This dropped away on further heating, conversion being ca. 30% at 450°C. The major product again was *meta*-xylene (35% at 350°C) but some *para*-xylene was also produced. The ratio of *meta* to *para* was 5:1.

The same charge of catalyst T-2581 was re-used after being allowed to stand overnight. The flow gas was changed from 100% nitrogen to 10% hydrogen - 90% nitrogen. The activity profile had changed - there was no isomerisation activity, just a small conversion (ca. 15%) at 450°C (Fig A2.21, Appendix 2.1).

The reactions of other aromatic feedstocks relevant to xylene isomerisation were investigated using catalyst EX-1720. Activity was found for processes other than *ortho*-xylene isomerisation.

Mixed xylenes were investigated as this would be the feedstock used industrially. The composition of the starting material was determined by GC and is given in Table 2.7.

Table 2.7: Composition of Mixed Xylene Feedstock

Compound	Content / %
Meta - Xylene	72.7
Ortho - Xylene	5.7
Para - Xylene	0.3
Ethylbenzene	20.2
Toluene	1.0
Benzene	nil
Others	0.1

The catalyst converts *meta*-xylene to *ortho*- and *para*-xylene over the range of temperatures investigated (Fig. A2.23, Appendix 2.1). At lower temperatures a yield of toluene is seen, suggesting that disproportionation of xylene is occurring. At higher

temperatures, the catalyst 'cracks' ethylbenzene to form benzene, which is seen in these results, and ethene, which is not seen in this liquid analysis.

Disproportionation of toluene is a recognised method of producing xylenes [16] and is even used commercially [17]. Catalyst EX-1720 was investigated for reactions of toluene (Fig. A2.24, Appendix 2.1). Conversion of toluene was low (less than five percent at all temperatures investigated), and benzene was the major product. This suggests that dealkylation occurs at higher temperatures.

The reaction of toluene and methanol to give xylene and water has also been proposed as a viable method of producing xylenes [18]. This reaction was therefore investigated using catalyst EX-1720 (Fig A2.25, Appendix 2.1). The catalyst only becomes active above 250°C, when it makes *ortho*-, *meta*-, and *para*-xylene in approximately a 1:3:1 ratio. The reaction will also go further, with two substitutions on the ring giving rise to a significant yield of trimethylbenzenes.

Ethylbenzene reactions are a concern in xylene isomerisation, since mixed xylenes - the feedstock used commercially - can contain around 20% ethylbenzene. A typical isomerisation catalyst would 'crack' this to give benzene and ethene; however, the isomerisation of ethylbenzene to xylenes would clearly be of interest.

Cracking was seen when ethylbenzene was passed over catalyst EX-1720, and benzene was the major product, particularly at higher temperatures (Fig A2.26, Appendix 2.1). At lower temperatures, benzene was also produced, along with diethylbenzene isomers. This implies a disproportionation mechanism. Little or no xylene was seen at any temperature.

2.4 Discussion

2.4.1 Zirconia Catalysts

The majority of the zirconia catalysts investigated - all except the undoped, chromium-doped, phosphate-doped, platinum-doped and platinum and phosphate-doped

samples - showed activity for conversion of *ortho*-xylene to other products. At a typical value of around one percent, the conversion was not large. The major products were usually xylenes at lower temperatures and toluene and benzene at higher temperatures.

It is possible that two different reactions are occurring with these catalysts. At higher temperatures, the products being toluene, benzene and trimethylbenzenes suggest dealkylation and disproportionation activity, whilst at low temperatures isomerisation is predominant, giving *meta*- and *para*- xylene. These reactions are shown in Scheme 2.1.

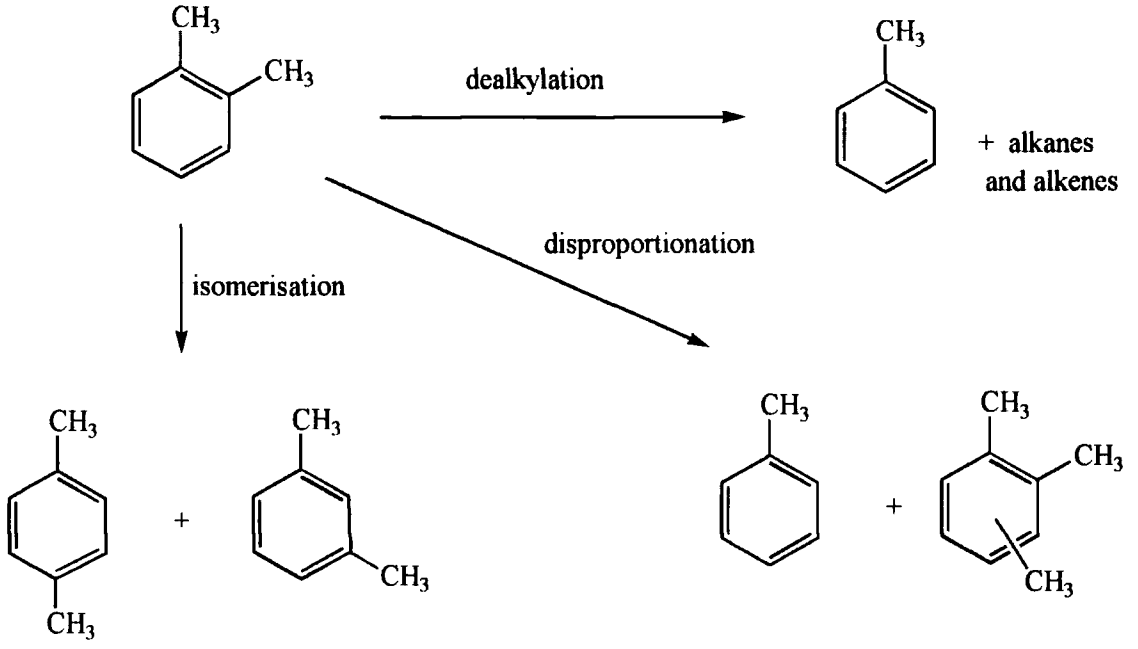

Scheme 2.1: Reactions of *Ortho*-Xylene

The temperature profile of the reactions is of interest. At lower temperatures (below 350°C), the production of xylenes suggests that xylene isomerisation is occurring. However, above 400°C, toluene and sometimes benzene are seen as the dominant products, indicating that a dealkylation pathway is operating. The by-products of the dealkylation reaction might include alkanes and alkenes, but since only the liquid products were monitored these were not observed. The activity of the catalysts is summarised in Table 2.8.

Table 2.8: Reactivity Profiles of Zirconia Catalysts

Catalyst	Lower Temperature		Higher Temperature	
	Products	**Range / °C**	**Products**	**Range / °C**
Sulphated Zirconia	xylenes	250-400	none	-
Platinum-doped Sulphated Zirconia	xylenes	200-250	none	-
Aluminium-doped Zirconia	none	-	toluene	>400
Aluminium-doped Sulphated Zirconia	xylenes	250-350	none	-
Nickel Chloride-doped Zirconia	none	-	toluene	400
Nickel Hydroxide-doped Zirconia	toluene	300-350	none	-
Nickel-doped Sulphated Zirconia	xylenes	300-400	none	-
Chromium-doped Sulphated Zirconia	none	-	xylenes toluene	>450

From these data it is seen that these catalysts possess more than one type of activity. The low temperature activity is seen in the catalysts containing sulphate (with the exception of chromium-doped sulphated zirconia), and this leads to the conclusion that this activity is linked to the presence of sulphate in the catalyst. Sulphated zirconia has been reported as being both a Brönsted and a Lewis acid [19,20] and it is possible that the different types of site gives rise to different activity at different temperatures. This is summarised in Schemes 2.2 and 2.3.

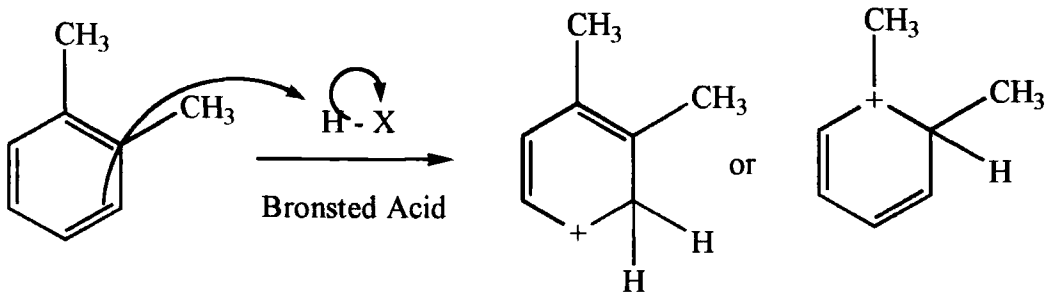

Scheme 2.2: Reaction of a Brønsted Acid with *Ortho*-Xylene

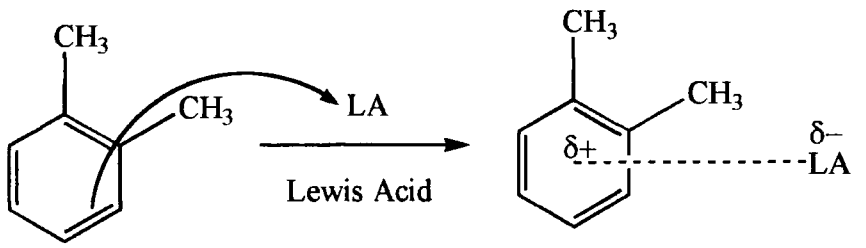

Scheme 2.3: Reaction of a Lewis Acid with *Ortho*-Xylene

It would seem that low temperature activity - and so activity for *ortho*-xylene isomerisation - is related to the presence of sulphate anions and hence to Brönsted acidity. It is also possible that the higher temperature activity for dealkylation reactions is related to Lewis acidity. This is backed up by the observation that zirconia doped with aluminium trichloride - which is known to function as a Lewis acid [20, 21] in its interactions with aromatic systems - shows this high-temperature activity.

The zirconia catalysts were all found to gain a black carbon layer (coke) during use. This could be due to deposition of a polyaromatic species on the catalyst surface, as shown in Scheme 2.4. The interaction of a molecule of *ortho*-xylene with the catalyst activates it towards attack by nucleophiles, and a second molecule of *ortho*-xylene can perform that nucleophilic function. The resulting species is also cationic, and so is susceptible to further reaction. This will give a layer of coke across the catalyst surface. This mechanism has been seen on sulphated zirconia catalysts using benzene as a reagent [1(a)]

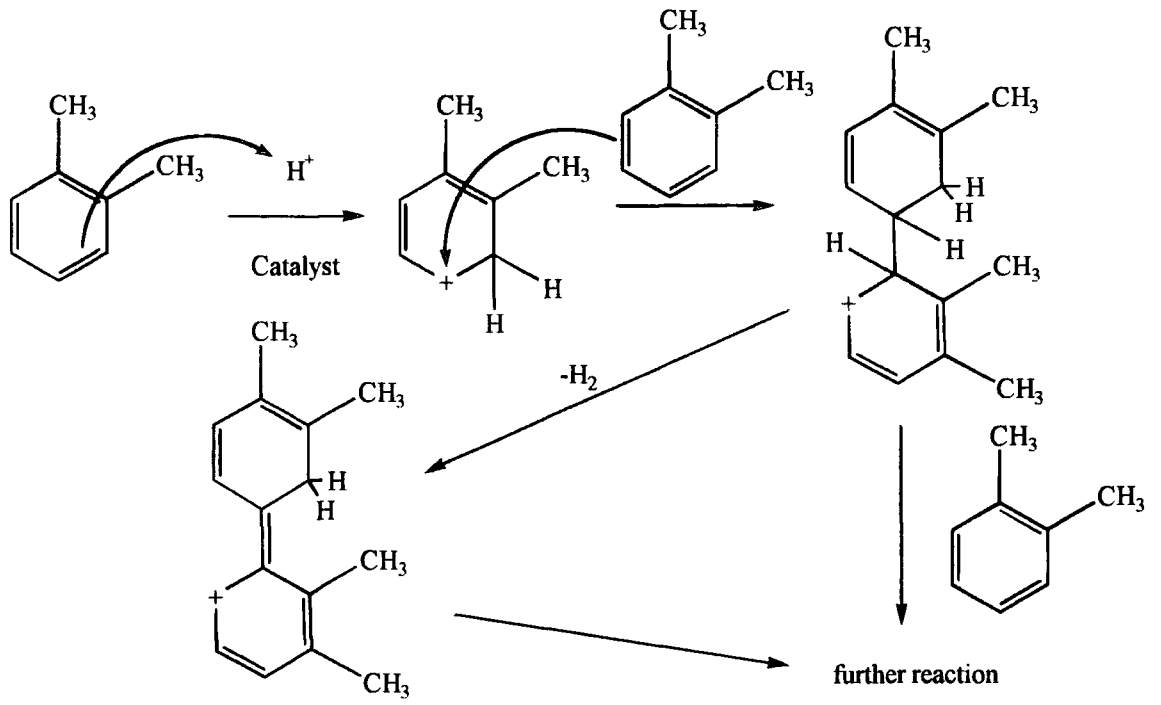

Scheme 2.4: Formation of Coke at the Catalyst Surface

It has been reported that the development of a layer of coke at the catalyst surface deactivates zeolite catalysts to aromatic reactions [18]. This could also be the case here, although it is not known whether the coke forms at high or low temperatures, and whether it is a function of time on-stream.

2.4.2 Supported Metal Catalysts

Despite not being active for *ortho*-xylene isomerisation, all the supported metal catalysts were found to develop a layer of coke at the surface (see Fig. 2.1). This could be the reason for their inactivity - any active sites which catalysts possess are covered by the layer of coke. Running the reaction using hydrogen as the carrier gas decreased the level of coking in most cases. This is thought to suppress the equilibrium shown in Scheme 2.5.

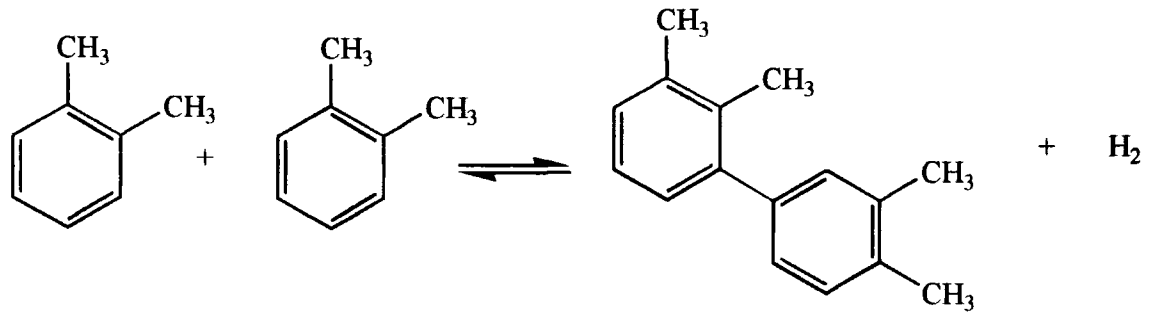

Scheme 2.5: Coking Reaction

It is interesting to notice the colour of the supported chromium catalysts prepared in section 2.2.2.4 above. Different colours are produced by chromium in different oxidation states [24] and it is seen that different supports stabilise different coloured chromium species, as shown in Table 2.9.

Table 2.9: The Colour of Supported Chromium Catalysts

Support	Colour	Chromium Oxidation State	Related Chromium Oxide Species
Alumina Titanium oxide	Grey	zero	metallic chromium
Magnesium oxide Silica	Green	+3	Cr_2O_3
"Zirconium hydroxide"	Yellow - Green	+3	Cr_2O_3
Silver on magnesium oxide, silica or alumina	Brown	+4	CrO_2

2.4.3 Commercial Catalysts

The samples of molecular sieve and alumina spheres used were inactive. This is perhaps unsurprising given that they are laboratory chemicals rather than catalysts.

The commercial catalyst samples showed very different activities for *ortho*-xylene isomerisation. Again different reactions were catalysed at different temperatures. For zeolite catalyst EX-1720, xylene isomerisation dominating at 350°C and xylene disproportionation and dealkylation steadily increasing at higher temperatures. Below

350° no activity at all was seen. For aluminium oxide T-2851, there was a maximum in activity at 350°C, and this was for xylene isomerisation. Both catalysts tended to convert the *ortho*-xylene to *meta*-xylene, with relatively little *para*-xylene being produced. The difference in activity profile is related to differences in active site, and the way in which they change at increasing temperature.

Other reactions were studied using the zeolite catalyst EX-1720. The reaction of a mixed xylenes feedstock showed that, under these conditions, *meta*- xylene was converted to *ortho*- and *para*- xylene, giving an isomer ratio *ortho* : *meta* : *para* = 1:2:1. The initial composition of the feedstock was approximately *ortho* : *meta* : *para* = 6 : 73 : 0, as shown in Table 2.7. It is interesting that ethylbenzene is also converted over the catalyst, although the yields of benzene would imply a cracking mechanism as shown in Scheme 2.6. It is possible that ethylene was also produced, but this was not seen as only the liquid products were analysed.

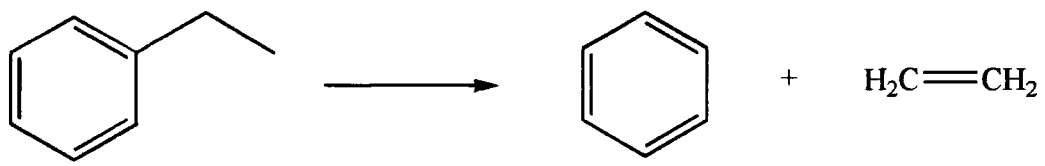

Scheme 2.6: Cracking of Ethylbenzene

When toluene was used as a feedstock, disproportionation activity was observed at temperatures above 300°C, giving benzene and xylenes. As the yield of benzene is greater than that of toluene, some dealkylation is also implied. This is shown in Scheme 2.7. At temperatures below 350°C no activity was seen.

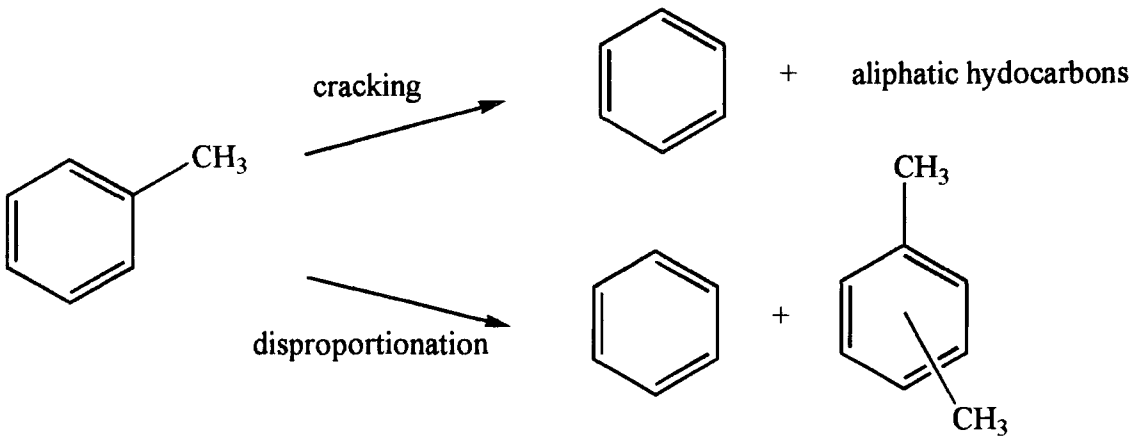

Scheme 2.7: Reactions of Toluene

The reaction of toluene with methanol took place at temperatures from 300°C. The major products were xylenes, which were produced in a ratio of approximately *ortho* : *meta* : *para* = 1:2:1. A large amount of the trimethylbenzene isomers was detected. This indicates that a second addition of methanol may take place.

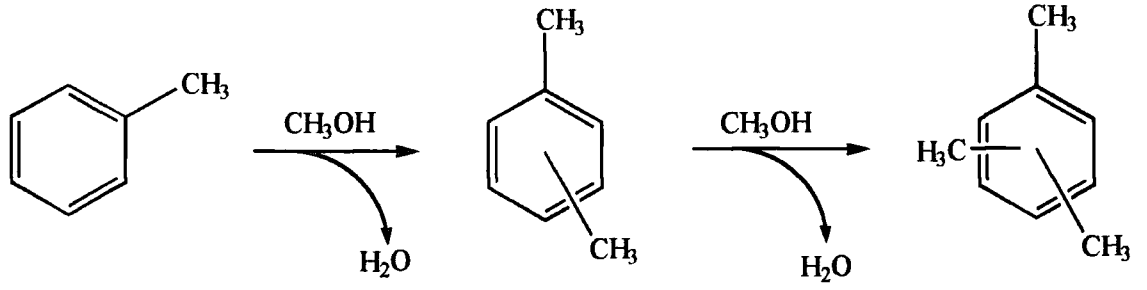

Scheme 2.8: Reactions of Toluene with Methanol

The elimination of water as a reaction by-product was also observed, although the quantity was not measured.

The reactions of ethylbenzene were also studied. Cracking was detected at all temperatures, plus a smaller amount of disproportionation to give the diethylbenzene isomers. However, conversion to xylenes was disappointingly small.

The zeolite catalyst EX-1720 appears to be most active at 350°C and above. At 350°, it has been shown that *ortho*-xylene isomerises to the other xylene isomers with

reasonable selectivity. However, at higher temperatures disproportionation and cracking reactions also occur, which decrease the selectivity to the desired product. The nature of the agreement with the catalyst supplier made it impossible to take this work further.

2.5 Summary

The isomerisation of *ortho*-xylene and related reactions have been studied over two commercial catalysts - EX-1720, a synthetic aluminosilicate, and T-2851, which is a nickel - containing supported alumina. The former catalyst was markedly the most active, and converted *ortho*-xylene to *meta*- and *para*-xylene isomers at 350°C, giving a final product ratio of approximately *ortho* : *meta* : *para* = 1:2:1, with ca. 75% conversion of the feedstock. At higher temperatures, however, dealkylation and disproportionation reactions gave benzene, toluene and trimethylbenzenes as by-products. Catalyst T-2851 also showed greatest activity for isomerisation of *ortho*-xylene to the other xylene isomers at 350°C; however, activity dropped away above and below this temperature.

Catalyst EX-1720 was also found to be active for the disproportionation of toluene to benzene and xylenes, the reaction of toluene and methanol to form xylenes and trimethylbenzenes, and the cracking of ethylbenzene to form benzene and (presumably) ethene. In a sample of mixed xylenes, *meta*-xylene, the major component, was isomerised to *ortho*- and *para*-xylene isomers.

A range of supported silver, chromium, palladium and silver - palladium catalysts was prepared. No activity was observed for *ortho*-xylene isomerisation, possibly due to the build up of coke on the catalyst surface, which was reduced by changing the carrier gas from nitrogen to hydrogen.

A number of zirconia catalysts were prepared, and many of these were found to show activity for the isomerisation of *ortho*-xylene at temperatures below 350°C. The greatest activity was shown by sulphated zirconia prepared from zirconium hydroxide and ammonium sulphate. This shows great promise, and will be examined further in the following chapter. At higher temperatures these catalysts also showed activity for disproportionation and dealkylation of the *ortho*-xylene feedstock.

2.6 References

1. (a) F.R. Chen, G. Coudurier, J.-F. Joly and J.C. Vedrine, *J. Catal.*, 1993, **143**, 616-26. (b) P. Moles, *Speciality Chemicals*, 1992, 362-8.
2. F.R. Chen, G. Coudurier, J.-F. Joly and J.C. Vedrine, *Symposium on Alkylation, Aromatisation, Oligomerisation and Isomerisation of Short Chain Hydrocarbons over Heterogeneous Catalysts*, American Chemical Society Meeting, New York, 1991, Division of Petroleum Chemistry, pp. 878-86.
3. B.H. Davis, R.A. Keogh and R. Srinivasan, *Catal. Today*, 1994, **20**, 219-56.
4. M. Hino and K. Arata, *Catal. Lett.*, 1995, **30**, 25-30.
5. M. Hino, S. Kobayashi and K. Arata, *J. Am. Chem. Soc.*, 1979, **101**, 6439.
6. L.M. Kustov, V.B. Kazansky, F. Figueras and D. Tichit, *J. Catal.*, 1994, **150**, 143-9.
7. K.M. Parida and P.K. Pattnayak, *J. Colloid Interface Sci.*, 1996, **182**, 381-7.
8. R.H. Crabtree, "The Organometallic Chemistry of the Transition Elements", John Wiley and Sons, 1988, pp. 112-4, 359-63.
9. For example: (a) B. Nicholls and M.C. Whitting, *J. Chem. Soc.*, 1959, 551-6. (b) S. Top and G. Jaouen, *J. Organomet. Chem.*, 1979, **182**, 381.
10. A.N. Vedernikov, A.I. Kuramshin and B.N. Solomonov, *J. Chem. Soc., Chem. Commun.*, 1994, 121-2.
11. B.M. Trost and J.M.D. Fortunak, *Organometallics*, 1982, **1**, 7-13.
12. A. El Hamdaoui and G. Bergeret, J. Masardier, M. Primet and A. Renonprez, *J. Catal.*, 1994, **148**, 47-55.
13. R.W. McCabe and P.J. Mitchell, *J. Catal.*, 1987, **103**, 419-25.
14. N.V. Sidgwick, "Elements and Their Compounds", Oxford University Press, 1950, p. 1581.
15. BDH Laboratory Supplies Catalogue, 1996, p. **2**-348.
16. P. Beltrame, P.L. Beltrame, P. Carniti, G. Zuretti, G. Leofanti, E. Moretti and M. Padovan, *Zeolites*, 1987, **7**, 418-22.
17. *Catalyst Review Newsletter*, 1995, **March**, 6-9.
18. W.W. Kaeding, C. Chu, L.B. Young, B. Weinstein and S.A. Butter, *J. Catal.*, 1981, **67**, 159-174.
20. X. Song and A. Sayari, *Chemtech*, 1995, **August**, 27-35.

21. K. Wade and A.J. Banister, "Aluminium, Gallium, Indium and Thallium" in "Comprehensive Inorganic Chemistry", Vol. 1, J.C. Bailar, H.J. Emetêus, R. Nyholm and A.F. Trotman-Dickerson (eds), Pergamon Press, 1973, pp. 1019-28.

22. N.N. Greenwood and K. Wade, "Coordination Compounds of Aluminium and Gallium Halides" in "Friedel-Crafts and Related Reactions", Vol. 1, G.A. Olah (ed), Interscience, 1963, pp. 569-83.

23. A.S. Batsanov, S.P. Crabtree, J.A.K. Howard, C.W. Lehmann and M. Kilner, *J. Organomet. Chem.*, 1998, **550**, 59-61.

24. N.N. Greenwood and A. Earnshaw, "Chemistry of the Elements", Pergamon Press, 1984, pp. 1171-3.

Chapter Three : Development of Sulphated Zirconia Catalysts

3.1 Introduction

This chapter builds on the initial experience of the activity of sulphated zirconia catalysts towards *ortho*-xylene isomerisation. The aim of the work is to investigate how the method of synthesis of a catalyst affects its performance. A number of factors were investigated involving the type and quantity of reagents, synthesis and calcination procedures and the storage and treatment of catalysts prior to use. The desired outcome of these experiments is to be able to design an 'idealised' catalyst based on knowledge of what makes the best catalyst.

3.2 Experimental

3.2.1 Synthesis of Catalysts

3.2.1.1 Synthesis of 'Standard' Sulphated Zirconia

"Zirconium hydroxide" (5.0g) and ammonium sulphate (0.34g, 2.6 mmol, 5 wt.%) were ground together in a pestle and mortar. The resulting mixture was then calcined at 600°C for three hours. The rate of heating to 600°C was approximately 70 °C min^{-1}, and the rate of cooling to room temperature was approximately 3°C min^{-1}. The sample was stored in a desiccator until required, and activated at 150°C prior to use.

3.2.1.2 Synthesis of Catalysts with Varied Heating Rates

The catalyst samples were synthesised by the standard procedure, but the rate of heating to 600°C was varied from 1°C min^{-1} to 76°C min^{-1}.

3.2.1.3 Synthesis of Catalysts with Varied Cooling Rates

The catalyst samples were synthesised by the standard procedure, but the rate of cooling from 600°C to room temperature was varied from 0.1°C min^{-1} to 4°C min^{-1}.

3.2.1.4 Synthesis of Samples Calcined at Different Temperatures

The samples were prepared according to the procedure given in 3.2.1.1. The temperature at which different samples were calcined was varied between 300°C and 1200°C in 100°C steps. The rates of heating and cooling were unchanged, and all samples were calcined for three hours.

3.2.1.5 Synthesis of Samples Heated for Different Lengths of Time

These samples were prepared by the standard route. They were all calcined at 600°C, but for different lengths of time: none (sample heated to 600°C then immediately started cooling), 10 minutes, 1 hour, 2 hours, 6 hours, 12 hours. The rates of heating and cooling were kept constant throughout.

3.2.1.6 Synthesis of Samples Prepared to Evaluate the Effect of Different Storage and Activation Procedures

The samples were prepared and calcined according to the standard procedure outlined in 3.2.1.1 above. They differ in how they had been treated after calcination. All samples were cooled once calcination was complete, then some were stored in a desiccator and some were activated at 150°C in air before they were used. Details of the treatments afforded to different samples are given in Table 3.1.

Table 3.1: Storage and Activation of Catalysts

Sample	Treatment
A	Stored in a desiccator until required. Activated at 150°C in air prior to use.
B	Not stored in a desiccator or activated.
C	Stored in a desiccator until required. Not activated.
D	Transferred to a desiccator whilst still hot (150°C). Activated at 150°C prior to use.
E	Calcined (600°C, 3 hours) immediately prior to use.

3.2.1.7 Synthesis of Samples Containing Different Sources of Sulphur

3.2.1.7.1 Solid Ammonium Sulphate as Dopant

This sample was prepared according to the standard procedure given in section 3.2.1.1.

3.2.1.7.2 Aqueous Ammonium Sulphate Solution as Dopant

Ammonium sulphate (0.34g, 2.6 mmol) was dissolved in distilled water (15ml) to give a clear solution. "Zirconium hydroxide" (5.0g) was added to give a white suspension which was allowed to stir for one hour, then heated to 110°C until all the water had evaporated. The white solid thus obtained was calcined according to the standard procedure.

3.2.1.7.3 Sulphuric Acid as Dopant

Concentrated sulphuric acid (0.26g) was dissolved in distilled water (10ml) to give a clear solution. To this was added "zirconium hydroxide" (5.0g), giving a white suspension which was allowed to stir for 100 minutes and then heated to dryness at 110°C. The resulting white solid was calcined according to the usual procedure.

3.2.1.7.4 Elemental Sulphur as Dopant

Sulphur (flowers of sulphur, 0.09g, 2.8 mmol) was ground with "zirconium hydroxide" (5.0g) in a pestle and mortar to give a yellow powder. This was calcined in the standard fashion.

3.2.1.8 Synthesis of Samples Containing Different Sources of Zirconium

3.2.1.8.1 Samples Prepared From "Zirconium Hydroxide"

These were prepared by the method given in 3.2.1.7 above.

3.2.1.8.2 Samples Prepared From Zirconium (IV) Oxide

These were prepared by the method given in 3.2.1.7 above. "Zirconium hydroxide" was replaced by an equivalent mass of zirconium (IV) oxide.

3.2.1.8.3 Samples Prepared From Zirconium Propoxide

3.2.1.8.3.1 Standard Precipitation

Zirconium propoxide ($[Zr(OCH_2CH_2CH_3)_4]$ 70wt.% solution in *n*-propanol, 20.0g) was dissolved in a further 50ml *n*-propanol. To this was added a mixture of *n*-propanol (100ml), distilled water (2.5ml), concentrated nitric acid (1.25ml) and concentrated sulphuric acid (1.25ml) dropwise over a period of one hour. This gave a white precipitate almost immediately on addition. A further 125ml of distilled water was added dropwise, followed by 125ml concentrated aqueous ammonia. The final pH of the solution was pH 11. The resulting precipitated solution was allowed to stand for 72 hours before being filtered through filter paper. The white solid collected was dried at 110°C for eight hours. It was then calcined according to the standard procedure.

3.2.1.8.3.2 Precipitation Containing Surfactant

A surfactant, "Aerosol OT" (dioctylsulphosuccinic acid, 1.93g, 4.6 mmol), the structure of which is shown in Fig. 3.1, was dissolved in *n*-propanol (50ml) by stirring. To this was added zirconium propoxide ($[Zr(OCH_2CH_2CH_3)_4]$, 70wt.% solution in n-propanol, 20.0g) in one portion, followed by a mixture of *n*-propanol (100ml), distilled water (2.5ml), concentrated nitric acid (1.5ml) and concentrated sulphuric acid (1ml). This mixture was added dropwise overnight. Precipitation began immediately on the addition of the first drops of the mixture. A portion of distilled water (125ml) was added dropwise, followed by the dropwise addition of 300ml concentrated aqueous ammonia. The resulting solution was allowed to stand overnight before being filtered through a filter paper and air-dried overnight. It was heated to 110°C for six hours before being calcined according to the usual procedure.

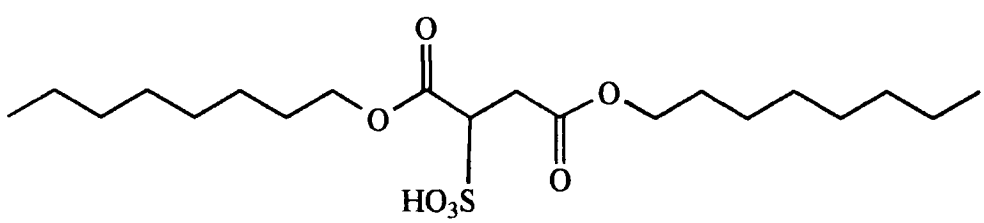

Fig. 3.1: The Structure of Aerosol OT Surfactant

3.2.1.8.3.3 Slow Precipitation

This experiment was an attempt to precipitate the product slowly to control particle size. Zirconium propoxide ($[Zr(OCH_2CH_2CH_3)_4]$, 70wt.% solution in *n*-propanol, 20.0g) was dissolved in *n*-propanol (200ml). To this was added a mixture of *n*-propanol (125ml), distilled water (2.5ml), concentrated sulphuric acid (1.25ml) and concentrated nitric acid (1.25ml) dropwise overnight. This did not give a precipitate. A further portion of distilled water (100ml) was added dropwise over an eight hour period giving an opaque, gelatinous solution. To this was added three portions of a mixture of concentrated aqueous ammonia (75ml) and distilled water (75ml), followed by two 75ml portions of concentrated aqueous ammonia. The suspension produced was allowed to stand overnight, then filtered by passing it through a filter paper. The solid obtained was air-dried for two days, then dried further by heating to 110°C overnight. The sample was calcined by the usual procedure.

3.2.1.9 Synthesis of Catalysts with Other Dopants Replacing Sulphate

The catalyst samples were synthesised according to the standard procedure. The level of doping was kept at 5 wt.%, and a range of dopants were used, as shown in Table 3.2. The additives were either ammonium salts, which will lose ammonia on calcination, or oxides. Alkali metal salts and metal chlorides were not used due to the risk of contamination by metal or chloride ions.

Table 3.2: Amount of Dopants added to "Zirconium Hydroxide"

Dopant	Additive	Amount Added
SO_4^{2-}	$(NH_4)_2SO_4$	0.34g
PO_4^{3-}	$(NH_4)_2HPO_4$	0.34g
Y_2O_3	Y_2O_3	0.25g
MgO	MgO	0.25g
CaO	CaO	0.25g
La_2O_3	La_2O_3	0.25g
MoO_4^{2-}	$(NH_4)_2MoO_4$	0.31g
CrO_3	CrO_3	0.25g
WO_4^{2-}	$(NH_4)_{10}W_{12}O_{41}.5H_2O$	0.29g
VO_3^-	NH_4VO_3	0.30g

3.2.1.10 Synthesis of Samples Containing Different Concentrations of Sulphate

The samples were prepared according to the general procedure outlined in 3.2.1.1 above. The difference is the concentration of sulphate in each sample, which was varied from 0.5wt.% to 30wt.%. Calcination was using the standard technique.

3.2.1.11 Synthesis of Samples Containing Different Supports

Samples of sulphated metal oxides and related compounds were prepared by grinding ammonium sulphate (where appropriate) and a metal compound together in a pestle and mortar, followed by calcination at 600°C for three hours. Details of the catalysts prepared are given in Table 3.3. Nickel sulphate and iron (III) sulphate were calcined without the addition of any further sulphate.

Table 3.3: Preparation of Sulphated Metal Compounds

Support	Mass / g	Mass of Ammonium Sulphate added / g (wt.%)	Colour of Compound
Al_2O_3	5	0.35 (5)	white
Cr_2O_3	5	0.36 (5)	green
MgO	5	0.34 (5)	white
$Ni(OH)_2$	5	0.35 (5)	black
$NiSO_4$	5	0 (0)	green
SiO_2	2.4	0.19 (5)	white
SnO_2	5	0.36 (5)	white
TiO_2	5	0.35 (5)	white
"ZrOH"	5	0.36 (5)	white
Y_2O_3	5	0.35 (5)	white
Nb_2O_5	5	0.36 (5)	cream
Pr_2O_3	2	0.16 (5)	black
RuO_2	2	0.16 (5)	black
OsO_2	5	0.34 (5)	black
Fe_2O_3	5	0.34 (5)	red / brown
$Fe_2(SO_4)_3$	5	0 (0)	red / brown

3.2.1.12 Synthesis of Samples Prepared with Different Amounts of Grinding

These samples were prepared and calcined using the standard procedure outlined in 3.2.1.1 above. The ammonium sulphate and "zirconium hydroxide" were ground together for different amounts of time (10 seconds, one minute, five minutes). Also, a sample was prepared where no grinding had taken place although the components had been well mixed.

3.2.2 Experimental Procedure

Testwork was carried out with a reactor system designed, built and used at the KPT research laboratories in Stockton-on-Tees. It is shown in Fig. 3.2. The reactor was assembled using 1/8" piping unless otherwise stated. Between the cylinder and the T-piece the piping is made from stainless steel, as was the larger piping within the heated section. Other piping was made from teflon to give flexibility. Flow gas (nitrogen, hydrogen, or a pre-mixed blend of hydrogen in nitrogen) was supplied from a small cylinder through a cylinder head (230 bar, B.I.G.) and regulated by a mass flow controller (0.6 litres of gas per hour, Brooks). Liquid feed was supplied from a reservoir with a burette connected in parallel to measure flow rate. It was then passed through a pump (0-100ml/min, LDC/Milton Ray Constametric III metering pump), and mixed with the feed gas at a T-piece. This mixture was passed through a pre-heater consisting of ¼" stainless steel piping surrounded by a heating tape (Isotape) and insulated by glass fibre tape. The temperature was measured and controlled by a thermostat (KPT in-house design). Between the pre-heater and the reactor is a pressure gauge (0-10 bar; 0-140lbf/in^2, Boss). The reactor was a ca. 40cm length of ½" stainless steel piping with a ½" Swagelok connector at each end, allowing the reactors to be removed from the system. Two such reactors were used, allowing one to be packed and dried in the oven whilst the other one was in use. The top half of the reactor was heated by a furnace (0-1200W, 0-1000°F, Autoclave Engineers) which was insulated by a length of glass wool above and asbestos covered with foil below. The temperature was measured at the top (thermostat, TES 1310 type K) and bottom (thermostat, KPT in-house design) of the catalyst bed and varied using a rotary-type controller (Rotary Regavolt, The British Electrical Resistance Co. Ltd.). Liquid products were caught in a dropping funnel and samples were taken from here at the end of each run. Gases were then bubbled through

sodium hydroxide solution to remove H_2S and through an acetone - solid carbon dioxide trap to remove volatiles in the gas stream before being vented outside the laboratory.

The procedure for a typical experiment would be as follows: The reactor was loaded with a plug of glass wool, onto which was weighed between one and two grams of catalyst, followed by a second plug of glass wool on top. This was stored in an oven at 150°C until required (at least sixty minutes). The reactor was attached into the system using the Swagelok couplings described above, and fastened tightly to avoid leakage of xylene vapours. The insulation was put in place above and below the reactor. Firstly the gas flow was turned on, and flow noted in the H_2S scrubber (which also served as a bubbler). Secondly, the preheater and furnace were switched on and allowed to warm up. Finally, when both had reached temperatures above 150°C - the boiling point of *ortho*-xylene being 145°C - the feed was switched on. Once the feed was flowing steadily into the catchpot, the experiment was commenced.

The intention at the start of an experiment was to perform five runs at temperatures between 250°C and 500°C, nominally 250-300°C, 300-350°C, 350-400°C, 400-450°C and 450-500°C. although this was not strictly adhered to. In most cases five or six runs were performed at different temperatures on the same sample of catalyst. The temperature of the catalyst bed was increased by increasing the furnace temperature between runs.

For each experiment, the catalyst type and weight of catalyst in the reactor, the liquid feed type and flow rate, the gas feed type and flow rate and the preheater temperature were recorded.

For each run, the start time, setting of the controller to the furnace (in % of input volts), the pressure in the reactor (in gauge psi), the initial and final temperatures of the catalyst bed top and bottom, the mass of liquid products in the catchpot and the finishing time were recorded. Many of these parameters were standardised so that direct comparisons between catalysts could be made.

After the experiment had finished, the feed, preheater and furnace were switched off and the insulation on the reactor removed to allow the system to cool down. Once the feed had stopped flowing into the catchpot, the gas flow was stopped and the reactor removed. The catalyst and glass wool were transferred to a sample vial. The inside of the reactor was swept clean with a piece of tissue before being loaded with catalyst for the next experiment.

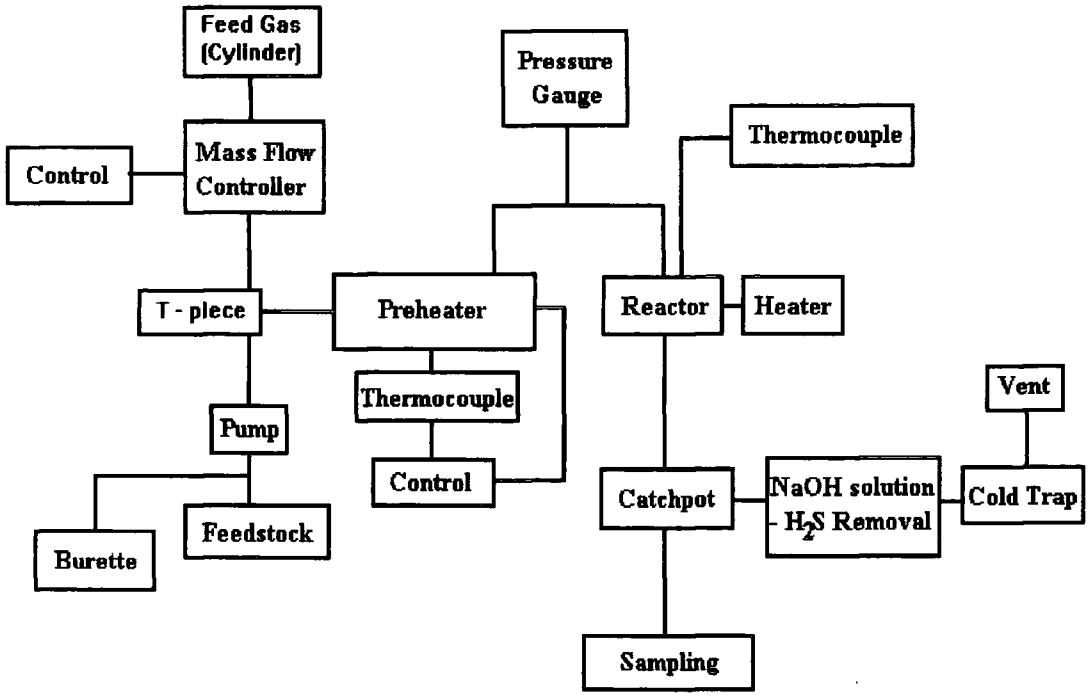

Fig. 3.2: Schematic Diagram of the Flow Reactor Used

3.3 Results

These results are presented in graphical form in Appendix 3.1. Raw Data are presented in Appendix 3.2.

3.3.1 Variation in the Rate of Heating

Catalysts with heating rates of 1 - 76 °C min^{-1} were produced for evaluation. All catalysts behaved in the usual manner for a sulphated zirconia catalyst - that is, they had a maximum of activity at low temperature, which quickly dropped off as the temperature of reaction increased (Figs. A3.1 and A3.2, Appendix 3.1) The catalysts were all

selective to the production of *meta*-xylene. Selectivity to *meta*-xylene was typically 60 - 75% at the temperature giving greatest conversion, and the ratio of *meta*-: *para*- xylene was between 8:1 and 12:1. Conversion of *ortho*-xylene to toluene and the other xylene isomers was 3 - 5%; this level dropped away as the rate of heating increased. This information is summarised in Table 3.4.

Table 3.4: Activity of Catalysts with Varied Heating Rates

Heating Rate / °C min^{-1}	**Reaction Temperature for Greatest Activity / °C**	**Selectivity to *Meta*-Xylene at this Temperature / %**	***Meta*:*Para* Ratio at this Temperature**	**Conversion of *Ortho*-Xylene at this Temperature / %**
1	246	68.4	8.8:1	4.7
50	232	73.3	8.8:1	5.2
60	220	71.4	8.7:1	3.1
70	206	70.3	8.7:1	4.8
76	235	62.5	6.7:1	2.5

Reasonable selectivity to xylene isomerisation was seen, although small yields of toluene suggest a small amount of dealkylation or disproportionation at low and high temperature. No benzene production was observed.

3.3.2 Variation in the Rate of Cooling

Again these catalysts behaved in a manner typical of sulphated zirconias (Figs. A3.3 and A3.4, Appendix 3.1). The greatest activity was seen at low temperatures (200 - 300°C) and this fell away markedly as the reaction temperature was raised. A small amount of toluene was produced using these catalysts, but no benzene was seen. The selectivity to *meta*-xylene was generally good, being greater than 90% in some cases. This information is summarised in Table 3.5.

Table 3.5: Performance of Catalysts Prepared with Varied Cooling Rates

Cooling Rate / °C min^{-1}	Temperature for Maximum Activity / °C	*Ortho*-Xylene conversion at this Temperature / %	*Meta*-Xylene Selectivity at this Temperature / %	*Meta*:*Para* isomer ratio at this Temperature
0.1	214	4.7	74.5	10.0:1
0.3	253	8.5	89.3	15.0:1
0.5	243	8.1	94.5	17.3:1
0.8	242	8.8	89.6	8.6:1
1.0	290	5.0	85.7	9.0:1
2.0	281	5.0	85.7	9.0:1
2.2	287	3.4	85.0	7.7:1
3.0	269	3.3	83.3	8.3:1
4.0	280	5.8	83.3	10.3:1

The activity and selectivity of the catalyst drop away for catalysts with higher cooling rates. The exceptions to this are the catalysts with cooling rates of 0.1 and 4.0°C min^{-1}.

3.3.3 Variation in the Calcination Temperature

Catalysts calcined at a range of temperatures from 300°C to 1200°C with 100°C intervals were examined (Figs. A3.5 and A3.6, Appendix 3.1). The catalysts calcined at 300°C and 400°C were active for xylene isomerisation, but markedly less so than those calcined at 500°C and 600°C. Above 600°C the activity began to decrease, and catalysts calcined at above 800°C showed no activity at all. The catalysts all showed good selectivity to xylene products with greatest activity at lower temperatures.

3.3.4 Variation in the Calcination Period

All the catalysts considered in this study are active for the conversion of *ortho*-xylene to *meta*- and *para*- xylene (Figs. A3.7 and A3.8, Appendix 3.1). The activity is greatest for the catalyst calcined for two hours, and drops away noticeably for

calcination periods longer than three hours. The catalysts are again selective to *meta*-xylene production, selectivity being in the range 75-85%, with the catalyst calcined for two hours having a selectivity to *meta*-xylene of 91.9% at its most active temperature. Very little *para*-xylene is produced at this temperature by this catalyst - the estimated ratio of *meta*- to *para*-xylene is greater than 20:1. These data are summarised in Table 3.6.

Table 3.6: Effect of Calcination Period on Catalyst Activity and Selectivity

Heating Period / minutes	Most Active Temperature / °C	*Ortho*-xylene Conversion at this Temperature / %	*Meta*-xylene Selectivity at this Temperature / %	*Meta*:*Para* Ratio at this Temperature
0	223	7.5	84.0	12.6
10	241	6.0	81.7	12.3
60	250	4.9	79.6	13.0
120	239	7.4	91.9	est. >20
180	275	7.4	70.3	7.4
360	316	3.9	76.9	10.0
720	246	3.5	77.1	13.5

3.3.5 Evaluation of Different Storage and Activation Procedures

The catalysts prepared with different activation or storage parameters were all active catalysts for the isomerisation of *ortho*-xylene at low temperatures (Figs. A3.9 and A3.10, Appendix 3.1). Selectivity was again to the production of *meta*-xylene. The catalyst stored in a desiccator and activated at 150°C before use was the most active of those studied. The catalyst calcined 'in situ' was less active than the other catalysts.

3.3.6 Evaluation of Different Sources of Sulphur and Zirconium

All the sources of sulphur tested were active as part of a catalyst ground with "zirconium hydroxide" (Figs. A3.11 and A3.12, Appendix 3.1). However, elemental sulphur gave a markedly less active catalyst than either ammonium sulphate or sulphuric

acid. Of those, sulphuric acid gave a slightly more active catalyst. Ammonium sulphate gave a more active catalyst when added as a solid rather than a solution.

The source of zirconium was rather more critical. Both zirconium hydroxide and precipitated zirconium propoxide gave active catalysts, but compounds based on zirconium dioxide gave no catalysis at all (Figs. A3.11 and A3.12, Appendix 3.1). The most active catalyst was based on a compound obtained by a slow precipitation of zirconium propoxide. The addition of a surfactant to control the particle size resulted in a marked drop in activity.

The catalysts which were active were all selective to *meta*-xylene product. The overall selectivity to this isomer was typically 70-80%, and the ratio of *meta* to *para*-xylene in the range 5:1 to 35:1, although typically around 10:1.

3.3.7 Variation in the Concentration of Sulphate

Catalysts prepared with varied amounts of sulphate present were active for *ortho*-xylene isomerisation (Figs. A3.11 and A3.12, Appendix 3.1). The activity and selectivity did not appear to have any direct relationship with the sulphate content. This information is summarised in Table 3.7.

Table 3.7: Performance of Catalysts Prepared with Varied Sulphate Contents

Sulphate Content / wt.%	Temperature for Maximum Activity / °C	Conversion at this Temperature / %	Xylene Selectivity at this Temperature / %
0.5	495	0.75	96.0
1	390	6.16	97.6
2	253	1.38	93.5
5	261	5.47	96.3
7	266	6.65	97.1
10	248	5.41	95.7
20	251	0.33	97.0
30	280	7.01	96.1

The greatest activity and selectivity was seen for a catalyst containing 7 wt.% sulphate.

3.3.8 Replacement of Sulphate Anion

Catalysts with the sulphate ion replaced by another species were active for the conversion of *ortho*-xylene to other products. In all cases they were more active than sulphated zirconia (Figs A3.15 and A3.16, Appendix 3.1). However, they showed poor selectivity to xylenes and to aromatic compounds generally, producing a wide range of compounds as shown by the GC analysis.

3.3.9 Evaluation of Different Supports for the Sulphate Anion

The majority of catalysts examined were inactive for xylene isomerisation. The exception was sulphated zirconia, which performed in the manner reported earlier. Sulphated ruthenium dioxide produced small amounts of benzene, toluene and xylenes at all temperatures studied, but the conversions were always much less than 0.1%.

3.3.10 Variation in the Time Spent Grinding Ammonium Sulphate and "Zirconium Hydroxide"

The catalysts prepared with different lengths of time spent grinding ammonium sulphate and "zirconium hydroxide" all showed the same activity (Figs. A3.17 and A3.18, Appendix 3.1). Conversion was modest at around 4%, and selectivity to the *meta* isomer was in the region of 70%. Little difference was seen on changing the amount of grinding.

3.4 Discussion

The sulphated zirconia catalysts prepared are selective to *meta*-xylene products. This would imply a stepwise transfer of the methyl group, which requires one step to

give *meta*-xylene but two steps to give *para*-xylene. Also formation of *meta*-xylene from *para*-xylene is favoured with a stepwise mechanism.

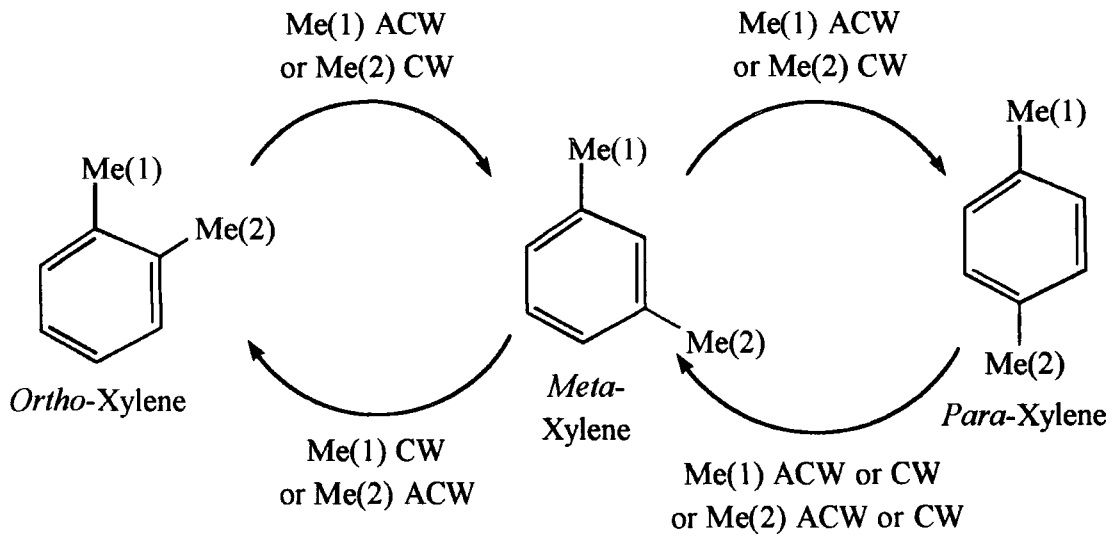

Scheme 3.1: Stepwise Mechanism for Xylene Isomerisation[†]

This idea is supported by the findings of Allen and Yats [1], who determined that the direct interconversion of *ortho*-and *para*-xylene was not seen for liquid-phase isomerisation using aluminium trichloride. The intramolecular nature of the reaction is confirmed by the small amounts of disproportionation seen - toluene and trimethylbenzenes would be formed in much larger amounts if a methyl group was completely removed from its aromatic ring. A speculative mechanism for the isomerisation of *ortho*-xylene to *meta*-xylene might resemble the one below. Intramolecular 1,2-alkyl shifts are allowed for aromatic systems as the electrophile - in this case H^+ or CH_3^+ - can interact with the π-electrons of the ring [2].

[†]ACW = anti-clockwise. CW = clockwise.

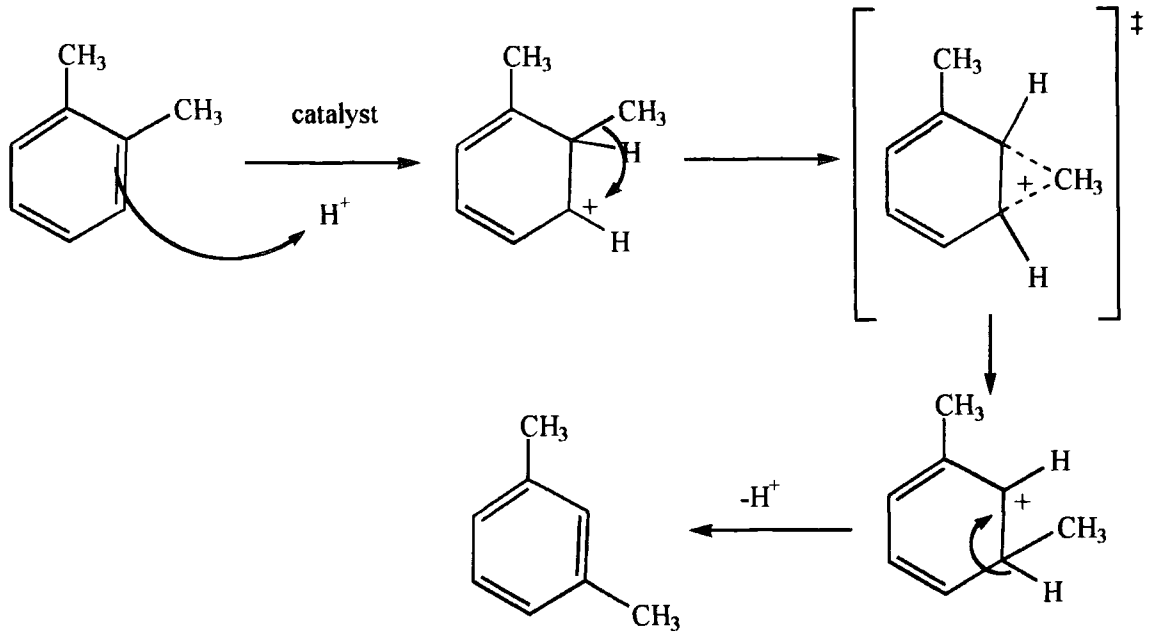

Scheme 3.2: Speculative Mechanism for a Stepwise Isomerisation of Xylenes

At higher temperatures, greater activity for disproportionation of xylenes to toluene and trimethylbenzenes is seen. This implies that carbon - carbon bond fission occurs at elevated temperatures.

3.4.1 Catalyst Prepared with Varied Heating Rates

This study concerned the rate of heating to the calcination temperature (600°C) rather than the calcination temperature itself. The rate of temperature increase has an effect on the length of time spent heating, as a catalyst heated to the calcination temperature more slowly will be heated for longer.

It was found that increasing the rate of heating from 1°C per minute to 50°C per minute had little effect on the catalyst selectivity or activity. Rate increases above that could be detrimental to both activity and selectivity.

It is known that crystallisation of sulphated zirconias starts from approximately 435°C [3, 4]. A slower temperature rise through this region could be beneficial to the quality of crystals produced, their size or some other morphological feature, giving a more active catalyst. Alternatively, the longer time spent heating contributes to the heating period, which affects the nature of the catalyst produced (see below). This does

not explain why a catalyst heated at 50°C min^{-1} should behave in a similar fashion to one calcined at 1°C min^{-1}. It is possible that the slower crystallisation (beneficial) and prolonged calcination (detrimental) effects combine to give a maximum activity located at a heating rate between 1 and 50°C min^{-1}.

The trend seen in these data is not easy to explain. It is possible that other factors outweigh heating rate in determining the catalytic activity of a sulphated zirconia. The most active and selective catalyst was produced with a heating rate of 50°C min^{-1}.

3.4.2 Catalysts Prepared with Varied Cooling Rates

It has been found that catalysts prepared with cooling rates slower than 1.0°C min^{-1} are more active and selective than those cooled more quickly. This could be due to a slow cooling aiding the crystallisation process, and so giving a more active catalyst. Alternatively, it could favour crystallisation into the catalytically active tetragonal form.

An anomaly in this is that the catalyst prepared with a cooling rate of 0.1°C min^{-1} is less active than other catalysts prepared with cooling rates lower than 1.0°C min^{-1}. This could be due to a drying effect - cooling from 600°C to room temperature at 0.1°C min^{-1} takes 100 hours! This is, of course, three times as long as for the next sample, which was cooled at 0.3°C min^{-1}, and so the difference between the two would be noticeable.

Considering the selectivity and activity of the catalysts produced here, the best catalyst is produced by a cooling rate of 0.3°C min^{-1}.

3.4.3 Catalysts Calcined at Different Temperatures

The most active catalysts were those calcined between 500 and 700°C. They had their greatest activity at the lowest temperatures studied, whereas less active catalysts had a maximum in their activity - temperature profile. This is shown in Fig. 3.3.

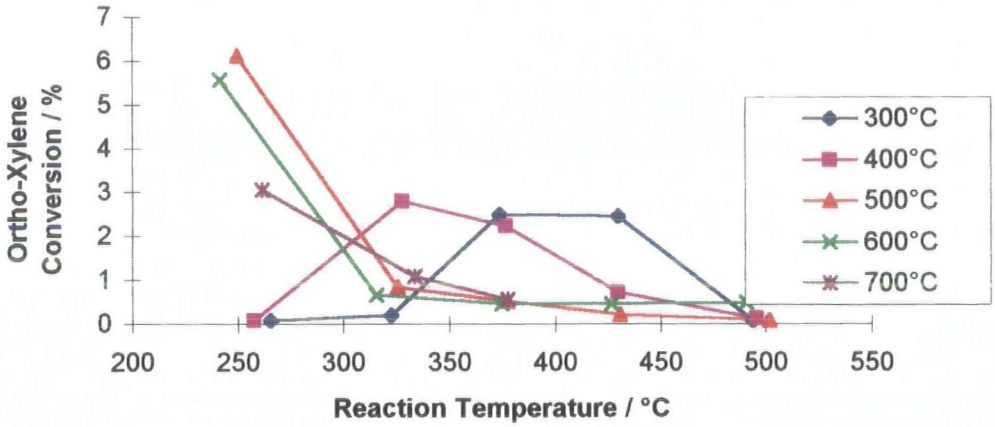

Fig. 3.3: Activity of Catalysts Calcined at Different Temperatures

The calcination temperature has been found to determine the activity of a sulphated zirconia by influencing its crystal type. The active form of a zirconia catalyst is the tetragonal form [5], which is usually only stable above 1000°C [6]. Below this temperature, the most stable form is monoclinic. Calcination of a sample of zirconia prepared by precipitation of a zirconium alkoxide would usually give an amorphous zirconium oxide which becomes tetragonal on heating above its crystallisation temperature, which is in the region of 420°C [7]. When the temperature is increased above 600°C, this prompts a change in crystal type to monoclinic. This has been reported as being inactive for catalytic reactions such as *n*-butane isomerisation: the work reported here is in agreement with that finding. The addition of sulphate ions has been reported to stabilise tetragonal zirconia, and to delay the onset of the change to monoclinic to a higher temperature [3]. This is only a limited effect and there is still a point where stabilised tetragonal zirconia will change into the monoclinic form. It is thought that certain surface sites are responsible for promoting the crystal change, and that these are blocked by the addition of sulphate [8].

These ideas are mirrored in the results presented here. The catalysts calcined below 500°C are only moderately active, and have a different activity profile to catalysts calcined at 500 - 700°C, which are more active. This could be because they are amorphous phase zirconia, which has been reported to resemble the tetragonal form [8] and so may show some catalytic activity. Samples calcined above 700°C have been seen

to exhibit minimal catalytic activity. These will have been converted to the monoclinic form by calcination at an elevated temperature.

The most active and selective catalysts were produced by calcination at 500°C or 600°C.

3.4.4 Catalysts Calcined for Different Periods of Time

The most striking trend seen in this study is that the activity of catalysts calcined for longer than three hours shows a marked decrease. This could be due to a decrease in residual water. Water has been proposed by a number of authors as being critical to the activity of a sulphated zirconia catalyst. In modest amounts, it has been found to promote Brønsted acidity, either as a Zr-OH or S-OH moiety [9]. This has been confirmed by a theoretical study [10]. However, greater amounts of hydration have been found to decrease the Brønsted acidity to zero [11]. The other acidity possessed by a sulphated zirconia is Lewis acidity, and this is enhanced by drying the catalyst [11]. This acidity originates from coordinatively unsaturated Zr^{4+} ions at the catalyst surface, which are blocked by water rendering them inactive. A long calcination time could result in extensive dehydration, making the resulting catalyst a better Lewis acid and a poorer Brønsted acid. This would change the activity profile, as is seen to occur.

The greatest activity and selectivity of these catalysts is seen when using the catalyst calcined for two hours. This may represent a compromise between the level of Lewis and Brønsted acid sites. The catalyst prepared with no dwell time at 600°C is as active, but has a lower selectivity to xylene products.

3.4.5 Catalysts Activated and Stored in Different Ways

The storage and activation procedures used were seen to affect the activity of the sulphated zirconia catalysts produced. Storing the catalyst in a desiccator appears to have a beneficial effect, but activating at 150°C prior to use has only a small effect. It could be that in the environment of the tube reactor, water is not lost during drying, but drying in the open air before packing at 150°C would be more beneficial.

The catalyst calcined in situ was seen to be less active than the other catalysts. This could be due to an inability to lose gases such as ammonia and sulphur oxides during the calcination step.

The most active catalyst was that stored in a desiccator and activated at 150°C before being used.

3.4.6 Catalysts Prepared with Different Sources of Zirconium and Sulphur

Catalysts prepared from zirconium dioxide were found to be inactive. This is because they are the monoclinic crystal form, which does not produce an active catalyst [12]. It is zirconium hydroxide which must be sulphated to give activity. This may be because it is able to incorporate sulphuric acid (or sulphate) into its structure with loss of water [13].

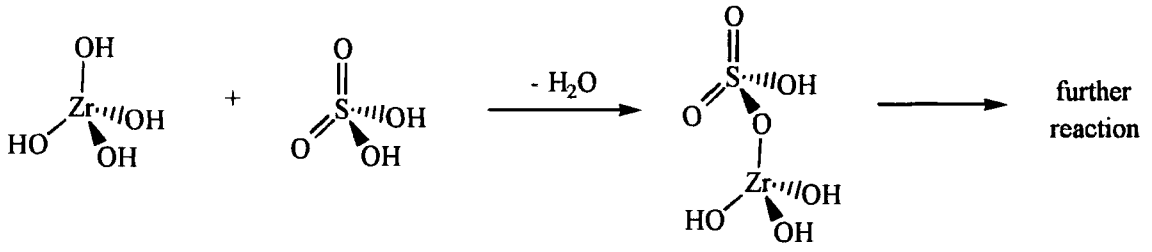

Scheme 3.3: Reaction of "Zirconium Hydroxide" with Sulphuric Acid

Precipitated samples could be more active than samples made using pre-formed "zirconium hydroxide" because they are freshly prepared, and so will have more Zr-OH groups. As a catalyst ages these are lost through dehydration, rendering the catalyst unable to take up sulphate efficiently.

The use of a surfactant to control the precipitation proved to be disadvantageous. This was possibly because the sulphur it contained was not in the correct form to be catalytically active. The use of elemental analysis showed that there was a similar amount of sulphur present to other catalysts prepared by precipitation of zirconium propoxide.

It has been reported that the source of sulphur is not important in gaining catalytic activity in a sulphated zirconia, as long as it is in oxidation state +6 [14]. This could be the problem in using elemental sulphur to introduce sulphate into the system - it is not entirely oxidised to a +6 oxidation state, and activity is not maximised. The use of sulphuric acid or ammonium sulphate would clearly provide an advantage here. The routes used for incorporation of sulphur into "zirconium hydroxide" are shown in Table 3.8.

Table 3.8: Levels of Incorporation of Sulphur into Sulphated Zirconia Catalysts

Dopant	Amount of Sulphur Added / wt.%	Amount Incorporated / wt.%	Maximum *Ortho*-Xylene Conversion / % per g of catalyst
$(NH_4)_2SO_4$ (solid)	1.6	0.63	6.82
$(NH_4)_2SO_4$ (solution)	1.6	1.14	4.14
H_2SO_4	1.7	1.03	8.27
Sulphur	1.8	0.63	2.91

It is seen from these data that the level of sulphur added and the amount actually incorporated into the catalyst are not the same. This implies that some sulphur is lost during the calcination step, possibly as H_2S, SO_2 or SO_3 gas. The catalytic activity of these catalysts does not vary linearly with the sulphur content, which suggests that not all the sulphur in the catalyst is active [14]. Some may be in a different oxidation state, or it may be co-ordinated to a different zirconium environment to the active sulphate in the catalyst.

Ammonium sulphate and sulphuric acid give approximately equal activities. This is in agreement with a report that they give identical surface species on zirconia catalysts [15]. However, it was also reported that more sulphate is lost during the calcination step when using sulphuric acid than ammonium sulphate. This is not necessarily borne out by this study, as shown in Table 3.8.

The most active and selective catalyst in this study was produced by slow precipitation of "zirconium hydroxide" containing sulphuric acid.

3.4.7 Catalysts Containing Different Concentrations of Sulphate

The majority of the catalysts prepared with varied sulphate concentrations have their maximum in xylene isomerisation activity at low temperature. This is something which has been seen throughout this study. The activity is generally of the order of 5 - 7% *ortho*-xylene isomerisation, although this is also a function of factors unrelated to the synthesis, such as residence time of the feedstock on the catalyst, and hence flow rate, bed size and so forth. The selectivity to xylene isomerisation is generally good, and typically the maximum selectivity and activity come together at low temperature. The by-products observed were toluene and benzene, which suggests the presence of dealkylation and disproportionation reaction pathways. In some cases, benzene was seen without toluene, which is unusual as both these reactions would be considered to proceed in a stepwise fashion. The benzene could be a contaminant from a previous experiment as it was observed at low temperature (the start of an experiment).

It is seen from the results shown in section 3.3.7 above, and in appendix 3.1, that the relationship between the concentration of sulphate added to a sample and its catalytic activity is not a linear one. The role of sulphate is to stabilise the tetragonal form of zirconia [3] which is believed to be the catalytically active form [16]. It is possible that at low concentrations of sulphate there is insufficient to stabilise this form during calcination, and so the activity would be lost. This could apply to zirconia doped with 0.5 wt.% sulphate. It has also been reported that sulphate concentration affects the amount of tetragonal zirconia in a catalyst, although not in a linear fashion [3]. The formation of zirconium sulphate, $Zr(SO_4)_2$, is also reported at higher sulphate concentrations. High concentrations of sulphate have been found to be required for Brønsted acidity, with only Lewis acid sites being found at lower concentrations [17, 18]. The nature of the sulphate species on the catalyst surface has also been found to depend on the degree of sulphation [19]. Other authors have found that the amount of sulphate present has only a small effect on catalytic activity, and that other factors dominate it [12]. This could be an explanation of the anomalous behaviour of the samples containing 2 wt.% and 20 wt.% sulphate: a small change in another parameter could give rise to a large difference in catalytic activity.

The catalyst which gives the best performance in terms of activity and selectivity contains 7 wt.% sulphate.

3.4.8 Catalysts with Sulphate Replaced by Another Compound

A number of zirconia catalysts with dopants other than sulphate ions have been investigated in the literature. Many reports focus on platinum doped zirconia or sulphated zirconia as this is reported to give extra stability to a zirconia catalyst [20]. Other group-eight transition metals have been investigated as dopants for sulphated zirconia, and found to give highly active acid catalysts in the isomerisation of butane to 2-methylpropane [21].

Phosphated zirconia has been prepared from zirconium hydroxide and phosphoric acid [22]. This has been found to be an acidic solid, although its acidity is less than that of sulphated zirconia. The amount of phosphate added affects the number and type of acid sites found, and also stabilises the tetragonal phase of zirconia up to 800°C. It is thought that polyphosphate species are formed on the zirconia surface by loss of water during the calcination step. Zirconium phosphate ($Zr(HPO_4)_2 \cdot H_2O$) has also been investigated as a catalyst [23]. When exchanged with divalent first-row transition metal ions, activity is seen for the oxidation of propene to aldehydes.

The phosphated zirconia prepared in this study showed some activity for the conversion of *ortho*-xylene, implying that it has also stabilised the tetragonal phase of zirconia. This has implications for the role of sulphate in a sulphated zirconia - it must play a part in the catalytic activity and is not merely a template for a particular surface geometry, since phosphate and sulphate dopants give different activity profiles. Stabilisation of the tetragonal phase of zirconia is not the sole requirement. The phosphated zirconia studied was found to convert *ortho*-xylene to ethylbenzene with 34% selectivity. This is presumably by a dealkylation - recombination route, such as described in Scheme 3.4.

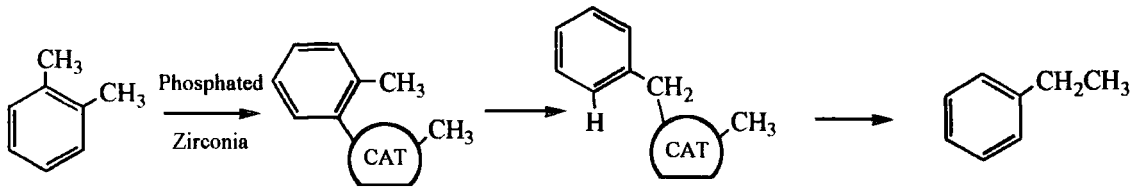

Scheme 3.4: Speculative Route for Conversion of *Ortho*-Xylene to Ethylbenzene

This could be a unimolecular or bimolecular pathway - the methyl group may or may not return to its original ring.

The addition of yttrium, magnesium or calcium oxides to zirconium hydroxide has been found to stabilise either the cubic or tetragonal phase of sulphated zirconia [4]. The doping metal was found to be present as its sulphate in the compound. Yttrium oxide has been reported to stabilise the tetragonal [24] and cubic [25] phases of zirconia, whilst the addition of lanthanum oxide has been reported to increase the catalyst surface area [26,27]. A sulphated zirconia catalyst containing magnesium and iron has been reported to be active for the isomerisation of butane [28].

The yttrium oxide, magnesium oxide, calcium oxide and lanthanum oxide doped zirconias prepared in this study were all active for *ortho*-xylene isomerisation. The conversion of *ortho*-xylene was better than sulphated zirconia, although the selectivity to xylene products was poor (8-9%). It is possible that the metal oxides are better at stabilising the active crystal phase of zirconia, but the Brønsted acidity created by the presence of sulphate anions gives selective activity to isomerisation. It is worth noting that metal-doped systems are active at higher temperatures. The dependence of catalytic activity on the presence of both Lewis and Brønsted acidity has been postulated before [12]. Lewis acidity could be provided by coordinatively unsaturated zirconium ions at the catalyst surface.

Zirconias containing group-six transition metal oxyanions, especially tungstate[‡], have been reported as being active catalysts for alkylation of aromatic compounds with either alkenes or alcohols [29-32], ring opening of cyclic hydrocarbons such as cycloalkanes or aromatics to give alkanes [33,34] and selective reduction of nitrogen

[‡] Note added in proof: A full paper on the use of tungstate-doped zirconia for xylene isomerisation has been published: D.G. Barton, S.L. Soled, G.D. Meitzner, G.A. Fuentes, E. Iglesia, *J. Catal.*, 1999, **181**, 57-72.

oxides to nitrogen [35]. Molybdate doped systems have been reported to stabilise tetragonal zirconia in a similar fashion to sulphate but to a higher temperature [26].

The catalysts containing chromium oxide, molybdate, vanadate and tungstate were all active for conversion of *ortho*-xylene, although selectivity to xylenes was low in all cases (less than 20%). This could be the ring opening process described in the patent literature [33,34] as the majority of products were not identified. The activity seen implies that an active form of zirconia has been produced in these compounds, although it could be that to obtain similar low-temperature activity to a sulphated zirconia, enhanced Brønsted acidity is required.

Replacing sulphate ions with a different dopant can give catalysts of greater activity. However, in view of the selectivity of these catalysts, sulphate remains the best dopant for zirconia to give activity for *ortho*-xylene isomerisation.

3.4.9 Catalysts Containing Different Supports

No activity was seen for compounds prepared using different supports for sulphate. This is in contrast to reported activity for sulphated oxides of iron [36], titanium, aluminium, tin, silicon and bismuth [37,38]. The difference is that the compounds prepared in these literature reports began with aqueous solutions of catalyst precursors such as metal nitrates or chlorides, which were precipitated by addition of ammonia and water giving a metal hydroxide. This was dried and then sulphated by an aqueous solution of ammonium sulphate. The situation is analogous to that with zirconium - pre-formed oxides (such as ZrO_2) show no catalytic activity, presumably due to an inability to react with sulphate during calcination. Preparations conducted using hydroxides of other metals may yield catalysts which show activity for xylene isomerisation.

3.4.10 Catalysts Prepared with Different Amounts of Grinding

The amount of time spent grinding ammonium sulphate and "zirconium hydroxide" together does not greatly affect the catalytic activity. The only requirement for activity is good mixing of the reagents. However, a small amount of grinding does give a slight rise

in the activity. This could be due to crushing of ammonium sulphate crystals, giving a greater surface area to react with the "zirconium hydroxide".

3.5 Conclusions

In this chapter, the effects of changing variables in the synthesis of a sulphated zirconia catalyst on its catalytic performance have been assessed. The trends seen are often complex, due to the different types of catalytically active site that are produced on the catalyst. The activity of these catalysts is thought to involve both Brønsted and Lewis acid sites. The catalysts produced are all selective to the *meta* isomer of xylene, which suggests a stepwise 1,2-alkyl shift of a methyl group around the benzene ring. This is supported by the low yields of toluene and benzene seen, and also by literature reports.

The most active catalyst is given by

- a sample prepared using a metal hydroxide rather than a metal oxide.
- a sample made by slow hydrolysis of zirconium propoxide.
- a sample containing sulphate as dopant.
- a sample with sulphate added as sulphuric acid.
- a sulphate content of 7 wt.%.
- calcination at 500°C or 600°C.
- a heating rate of 50°C min^{-1}.
- a cooling rate of 0.3°C min^{-1}.
- a calcination period of 2 hours.

This information will be used to produce a catalyst for studies of the isomerisation of *ortho*-xylene, reported in Chapter 4.

3.6 References

1. R.H. Allen and L.D. Yats, *J. Am. Chem. Soc.*, 1959, **81**, 5289-92.
2. L.M. Harwood, "Polar Rearrangements", Oxford University Press, 1992, pp. 69-73.
3. F.-C. Wu and S.-C. Yu, *J. Mat. Sci.*, 1990, **25**, 970-6.
4. F.-C. Wu and S.-C. Yu, *J. Crystal Growth*, 1989, **96**, 96-100.

5. F.R. Chen, G. Coudurier, J.-F. Joly and J.C. Vedrine, *Symposium on Alkylation, Aromatisation, Oligomerisation and Isomerisation of Short Chain Hydrocarbons over Heterogeneous Catalysts*, American Chemical Society, New York City, August 1991, pp. 878-886.

6. S.M. Ho, *Mat. Sci. Eng.*, 1982, **54**, 23-9.

7. H.-C. Wang and K.-L. Lin, *J. Mat. Sci.*, 1991, **26**, 2501-6.

8. R. Srinivasan, T.R. Watkins, C.R. Hubbard and B.H. Davis, *Chem. Mater.*, 1995, **7**, 725-30 and references therein.

9. C. Morterra and G. Cerrato, *J. Phys. Chem.*, 1994, **98**, 12373-81.

10. F. Babou, B. Bigot and P. Sautet, *J. Phys. Chem.*, 1993, **97**, 11501-9.

11. C. Morterra, G. Cerrato, F. Pinna, M. Signoretto and G. Strukul, *J. Catal.*, 1994, **149**, 181-8.

12. F.R. Chen, G. Coudurier, J.-F. Joly and J.C. Vedrine, *J. Catal.*, 1993, **143**, 616-26.

13. B.H. Davis, R.A. Keogh and R. Srinivasan, *Catal. Today*, 1994, **20**, 219-56.

14. C. Morterra, G. Cerrato, F. Pinna and M. Signoretto, *J. Catal.*, 1995, **157**, 109-23.

15. C. Sarzanini, G. Sachero, F. Pinna, M. Signoretto, G. Cerrato and C. Morterra, *Mater. Chem.*, 1995, **5**, 353-60.

16. R.A. Comelli, C.R. Vera and J.M. Parera, *J. Catal.*, 1995, **151**, 96-101.

17. C. Morterra, G. Cerrato and V. Bolis, *Catal. Today*, 1993, **17**, 505, quoted in ref. 2.

18. P. Nascimento, C. Akratopoulou, M. Oszagyan, G. Coudurier, C. Travers, J.-F. Joly and J.C. Verdine in "New Frontiers in Catalysis", L. Guczi et al (eds), Elsevier, 1993, pp.1185-97, quoted in ref. 5.

19. C. Sarzanini, G. Sacchero, F. Pinna, M. Signoretto, G. Cerrato and C. Morterra, *J. Mater. Chem.*, 1995, **5**, 353-60.

20. R. Srinivasan, R.A. Keogh, A. Ghenciu, D. Farcasiu and B.H. Davis, *J. Catal.*, 1996, **158**, 502-10.

21. M. Hino and K. Arata, *Catal. Lett.*, 1995, **30**, 25-30.

22. K.M. Parida and P.K. Pattnayak, *J. Colloid Interf. Sci.*, 1996, **182**, 381-7.

23. M. Iwamoto, Y. Nomura and S. Kagawa, *J. Catal.*, 1981, **69**, 234-7.

24. C. Morterra, G. Cerrato, L. Ferroni and L. Montanaro, *Mater. Chem. Phys.*, 1994, **37**, 243-57.

25. R.G. Silver, C.J. Hou and J.G. Ekerdt, *J. Catal.*, 1989, **118**, 400-16.

26. P. Afanasiev, C. Geantet and M. Breysse, *J. Mater. Chem.*, 1994, **4**, 1653-7.

27. S. Chan, G.K. Chuah and S. Jaenicke, *J. Mat. Sci. Lett.*, 1994, **13**, 1579-81.

28. *European Chemical News*, 2nd November, 1992, p.31.

29. C.D. Chang, J.C.-Y. Cheng, S. Han, J.G. Santiesteban, D.E. Walsh, M.M. Wu and Y. Xiong, International Patent Application WO 95/07874 (1995). *Chem. Abs.*, 1995, **123**, 12345*n*.

30. C.D. Chang, F.T. DiGuiseppi and S. Han, United States Patent 5563310 (1996).

31. C.D. Chang, S. Han, J.G. Santiesteban, M.M. Wu and Y. Xiong, United States Patent 5516954 (1996).

32. D.K. Kuhn, United States Patent 5396011 (1995).

33. C.D. Chang, R.D. Bastian, S. Han and J.G. Santiesteban, United States Patent 5382731 (1995).

34. C.D. Chang, J.G. Santiesteban and D.L. Stern, United States Patent 5345026 (1994).

35. C.D. Chang, J.G. Santiesteban, D.S. Shihabi and S.A. Stevenson, United States Patent 5401478 (1995).

36. T. Yamaguchi, T. Jin and K. Tanabe, *J. Phys. Chem.*, 1986, **90**, 3148-52.

37. T. Jin, T. Yamaguchi and K. Tanabe, *J. Phys. Chem.*, 1986, **90**, 4794-6.

38. T. Yamaguchi, *Appl. Catal.*, 1990, **61**, 1-25.

Chapter Four : Synthesis and Catalytic Performance of an 'Exploratory' Catalyst

4.1 Introduction

The work described in this chapter builds on the conclusions of chapter three. Having answered the questions regarding the link between synthesis procedure and catalyst performance, the aim is to put this into practice by synthesising an 'exploratory' catalyst, for characterisation in terms of its catalytic performance with a range of feedstocks.

4.2 Experimental

4.2.1 Synthesis of Sulphated Zirconia Catalysts

This preparation is based on the results of the experiments described in chapter three. One change which should be mentioned is the omission of nitric acid from the precipitation, as the concentration of sulphuric acid was increased to increase the sulphate content of the final product.

A mixture of n-propanol (125ml), concentrated sulphuric acid (3.5ml) and distilled water (2.5ml) was added to a solution of $[Zr(O^nPr)_4]$ (70wt.% solution in n-propanol, 20.0g) in n-propanol (200ml) dropwise over a period of approximately twelve hours, giving the solution a yellowish tint. Distilled water (125ml) was then added dropwise over a period of eight hours, causing the immediate formation of a white suspension. A white solid separated on the dropwise addition of a mixture of concentrated aqueous ammonia (75ml) and distilled water (75ml) over a period of approximately eight hours. Typically two or three such portions were required to precipitate the compound completely. After precipitation, the compound was allowed to stand for twenty-four hours. It was found that this made the compound more solid-like and less gelatinous, and so more easy to handle. After this time it was removed by filtration through a filter paper

and allowed to air-dry for approximately eight hours. The resulting white solid was transferred to a 100ml beaker and heated in air to 110°C for approximately eight hours to remove all water, ammonia and n-propanol. The catalyst was then ready for calcination.

A small sample of the catalyst (approximately 1 - 2g, or 5mm depth in the calcination vessel) was charged into a quartz calcination boat and loaded into the furnace. It was heated to 550°C at a rate of 50°C per minute and held at 550°C for two hours, before being allowed to cool to room temperature at a rate of 0.3°C per minute. The catalyst was then stored in a desiccator until required.

Four such preparations were performed, and the catalyst produced combined, with a small portion of each held back for testing. This produced an "averaged" catalyst which was then used in testwork.

4.2.2 Preparation of Commercial Samples

4.2.2.1 Commercial Sulphated Zirconias

Two types of "zirconium hydroxide" were supplied by MEL Chemicals. The difference between them was the size of the particles. A portion of each was weighed, and was ground with ammonium sulphate before being calcined at 600°C for three hours. The samples were then cooled slowly to room temperature, and stored in a desiccator before being used. Details of the preparations are given in Table 4.1.

Table 4.1: Preparation of Sulphated Zirconia from Commercial Samples

	MELCAT X20631/01	MELCAT X20632/03
Particle Size of "Zirconium Hydroxide"	0.01μm	0.03μm
Mass of "Zirconium Hydroxide"	3.3g	5.1g
Mass of Ammonium Sulphate	0.23g	0.34g
Mass Before Calcination	2.9g	3.0g
Mass of Product	2.1g	2.1g
Description of Product	white powder	white powder

4.2.2.2 Commercial Zirconia Catalysts

Samples of "lanthanum hydroxide - doped zirconium hydroxide" and "sicilic acid - doped zirconium hydroxide" were also supplied by MEL Chemicals. A 2.6g portion of each was calcined for three hours at 600°C giving a beige powder and a white powder respectively.

4.2.3 Reactor Details

The reactor was assembled and used as detailed in Section 3.2.2 and Figure 3.2. The system is constructed from stainless steel piping, generally 1/8" diameter. The piping between the pump and the T-piece, the T-piece and the pre-heater, the reactor and the catchpot, the catchpot and the scrubber, cold trap and vent are all 1/8" teflon piping to give flexibility to the system. The reactor was assembled inside a fume cupboard to eliminate the problem of dangerous gases being released into the open lab.

4.3 Results

4.3.1 Reaction with Different Feedstocks

The reactions of a number of different feedstocks catalysed by a sulphated zirconia catalyst were investigated. The results of these are presented below, and full data are

found in Appendix 4.1. Experiments reported in Section 4.3.1 were conducted using the 'averaged' catalyst synthesised as described in Section 4.2.1 above.

4.3.1.1 Reaction with *Ortho*-Xylene

Ortho-xylene was used as the test feedstock for the catalysts under investigation. The small amounts of *meta*- and *para*-xylene produced can be resolved easily from the *ortho*-xylene feedstock by GC analysis, as the retention times are markedly different. The closeness of the retention times of *meta*- and *para*- xylene mean that if one of these peaks is very large, as would be the case if either is used as the feedstock, the peak for the other isomer cannot be observed as it is underneath the feedstock peak. The reaction of the 'averaged' catalyst with *ortho*-xylene gave somewhat disappointing results. The expected conversion at low temperature was not seen, and only toluene was produced below 250°C. Above this temperature small amounts of *meta*-xylene were produced, but no *para*-xylene was detected. The maximum conversion of *ortho*-xylene was approximately 0.5%.

4.3.1.2 Reaction with *Meta*-Xylene

The isomerisation of *meta*-xylene using the 'averaged' catalyst is expected to yield *ortho*- and *para*- xylenes in approximately equal amounts since the isomerisation proceeds by a stepwise mechanism. This is in contrast to isomerisation of either of the other two isomers: for example, interconversion of *ortho*- to *para*- xylene proceeds *via* the *meta*-isomer [1]. Conversion of *meta*-xylene to *ortho*-xylene was seen, although the *para*-xylene produced could not be resolved by GC methods from the large *meta*-xylene peak. The production of toluene and a small amount of 1,3,5-trimethylbenzene was observed, indicative of xylene disproportionation. However, the yield of toluene was greater than that of 1,3,5-trimethylbenzene. The maximum conversion of *meta*-xylene to all products was between 1% and 1.5%.

4.3.1.3 Reaction with *Para*-Xylene

The isomerisation of *para*-xylene using the 'averaged' catalyst produced very small quantities of *ortho*-xylene. The *meta*-isomer peak was not resolved from the much larger starting material peak. A small amount of toluene was produced, although no trimethylbenzene isomers were seen. The maximum conversion of *para*-xylene to all products was in the region of 0.5-1.0%.

4.3.1.4 Reaction with Mixed Xylenes

Reaction of mixed xylenes is of particular interest since it is this feedstock which would be used commercially. The effect of the 'averaged' sulphated zirconia catalyst on the isomer distribution was low, with changes being in the region of 0.2% on average. Again the *meta*- and *para*- isomers were not resolved. At lower temperatures (< 350°C) yields of *ortho*-xylene and ethylbenzene were increased at the expense of *meta*- and *para*-xylene. Above this temperature other products appeared at the expense of the ethylbenzene peak. The concentration of toluene remained approximately constant, and a small amount of 1,2,4-trimethylbenzene was seen.

4.3.1.5 Reaction with Ethylbenzene

The reaction of ethylbenzene over the 'averaged' sulphated zirconia catalyst gave small amounts of xylene isomers and toluene as products. This was confirmed using GC-MS analysis. The conversion remained low (0.2-0.3%). Conversion was greater at high temperatures (>450°C) although the selectivity to xylene products at this temperature was low.

4.3.1.6 Reaction with Toluene

Reaction of toluene over the 'averaged' sulphated zirconia catalyst gave a mixture of products - *ortho*-, *meta*- and *para*-xylene as well as some ethylbenzene at higher temperatures. However, the expected peak for benzene was not seen. The conversion was low, being greatest at higher temperature and having a maximum value of approximately 0.5%.

4.3.1.7 Reaction with Toluene - Methanol

The reaction of a toluene and methanol mixture produced all three of the xylene isomers, with *ortho*-xylene being the major product at all temperatures. A small amount of ethylbenzene was also formed. Conversion was better here than in most cases at 1-2%, and it also increased with increasing temperature.

4.3.1.8 Reaction with Methyl Methanoate

The reaction of methyl methanoate (methyl formate) with an acid or base catalyst has been reported to result in decomposition to carbon monoxide and methanol by decarbonylation [2,3]. This technology is of interest as a source of high purity carbon monoxide. Reaction of methyl methanoate over the 'averaged' sulphated zirconia catalyst did indeed produce methanol and carbon monoxide, with conversion increasing to 5% at higher temperatures (250°C). Dimethyl ether was also seen as a by product from methanol dehydration.

4.3.1.9 Reaction with Ethyl Ethanoate

A number of reactions were detected when ethyl ethanoate (ethyl acetate) is used as a feedstock over the 'averaged' sulphated zirconia catalyst. The expected reaction was the cracking of the ester to give two C_2 units, with compounds such as ethanol and ethanal (acetaldehyde) being produced. However, the production of C_4-based compounds such as 1-butanol and butyl ethanoate (butyl acetate) and, more surprisingly, C_3-based compounds such as acetone were also observed. Conversions were low, rising to a maximum value of 0.8% at high temperatures (450°C). The distribution of products is shown in Fig. 4.1.

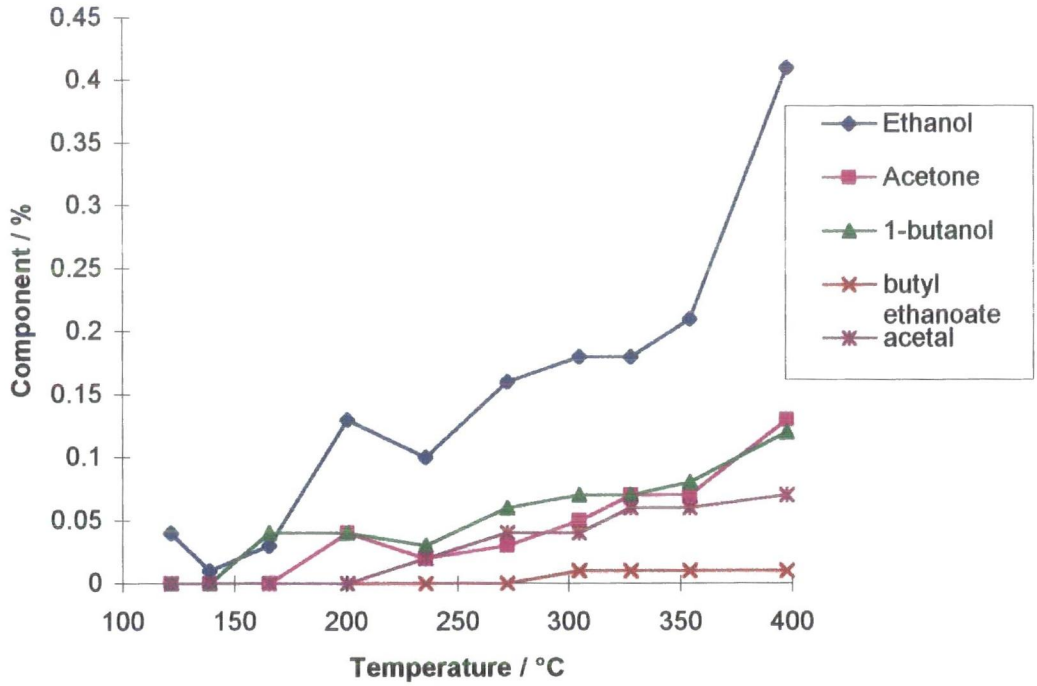

Fig. 4.1: Reaction of Ethyl Ethanoate over 'Averaged' Sulphated Zirconia Catalyst[†]

4.3.2 Reactions of Different Samples of Sulphated Zirconia

The 'averaged' sample of sulphated zirconia was prepared by mixing of equal amounts of sulphated zirconias from different preparations. Samples of the original unmixed sulphated zirconias were evaluated for the isomerisation of *ortho*-xylene to gauge the effect of mixing them together. Very little conversion was seen with any of the catalysts. In one case the catalyst was diluted with alumina particles (anti-bumping granules) to help the feed flow across the catalyst bed. The anti-bumping granules were also evaluated to see their effect on the catalysis, and no activity was seen. One of the catalysts was slightly active at temperatures below 300°C, although the conversion detected was never more than 0.5%.

4.3.3 Lifetime of a Sulphated Zirconia Catalyst

One question which is important to commercial use of sulphated zirconia catalysts is whether the deactivation seen during testing is due to the high exposure temperature,

[†] Acetal = 1,1-diethoxyethane.

rather than a function of time on-stream. To investigate this, a sample of the 'averaged' sulphated zirconia catalyst was used to catalyse *ortho*-xylene isomerisation at approximately 200°C for six hours. The products seen were both *meta*- and *para*-xylene, in contrast to the results presented in section 4.3.1.1 above. This is shown in Fig. 4.2.

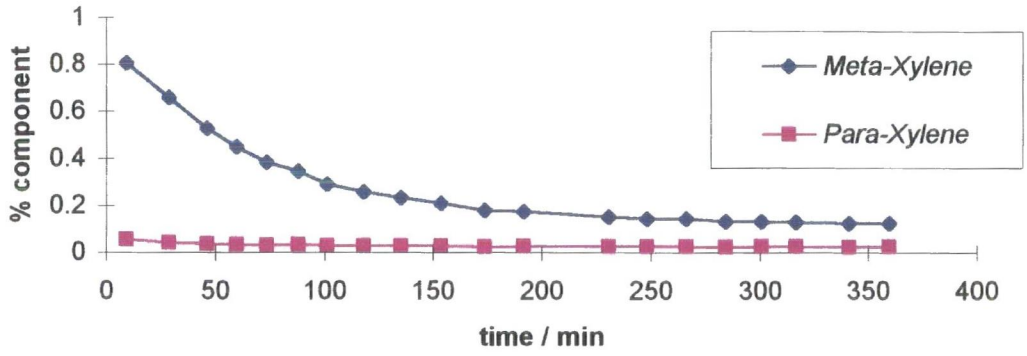

Fig. 4.2: Activity of a Sulphated Zirconia Catalyst over Time

Fig. 4.2 shows that the catalyst deactivates slowly over time, and that the *meta* to *para* ratio also decreases from approximately 14 : 1 to close to 5 : 1.

4.3.4 Performance of Commercial Catalyst

Four different commercially - available catalysts were tested. No activity was seen for zirconia catalysts doped with either lanthanum hydroxide or silicic acid. In contrast to this, catalysts based on zirconium hydroxide doped with ammonium sulphate did show some activity. Activity was by far the greatest at low temperatures (<250°C), where products were *meta*- and *para*-xylene. These catalysts differ in their particle size. The catalyst with the smaller particle size (0.01μm) showed the greatest activity, and also the greatest *meta* to *para* ratio. Small amounts of trimethylbenzenes were produced as by-products, and some ethylbenzene was also seen. In contrast, the larger particle size (0.03μm) was less active, but greater yields of trimethylbenzenes and toluene were seen, suggesting a greater activity for xylene disproportionation, especially above 400°C.

4.4 Discussion

Considering the results reported in the previous chapter, the low activity shown by the 'exploratory' catalyst is a little disappointing. This could be a consequence of the impact of one factor in the synthesis on another factor in the synthesis. For example, the alterations made to the calcination procedure all lead to the catalyst being calcined less - a lower temperature (550°C rather than 600°C) and a shorter calcination time (two rather than three hours) - although the slower rate of cooling does in some way compensate for this. The cumulative effect of these changes to the calcination procedure could change the nature of the catalyst and so its catalytic performance. Another reason for the low activity could be the elimination of nitric acid from the precipitation step. The nitric acid was omitted to keep the level of acidity constant as the concentration of sulphuric acid had been increased to increase the sulphate content of the catalyst. The nitric acid may act as a catalyst for the hydrolysis step, and so its omission may affect the catalyst's chemical nature, leading to a less active catalyst.

The product distribution seen when using the various xylene isomers as feedstocks are all in agreement with the operation of a stepwise transfer of methyl groups [1]. This is summarised in Table 4.2.

Table 4.2: Products from Xylene Isomerisation Reactions

Feedstock	*Ortho*-Xylene	*Meta*-Xylene	*Para*-Xylene
Ortho-Xylene	-	0.8%	0.05%
Meta-Xylene	0.8%	-	nd‡
Para-Xylene	0.1%	nd‡	-

It is found that the products from the isomerisation of *ortho*-xylene gives much more *meta*-xylene than *para*-xylene. This is because the isomerisation from *ortho*- to *para*-xylene takes two sequential methyl group shifts, whereas the isomerisation of *ortho*- to *meta*- xylene takes just one. The *ortho*- to *meta*- isomerisation needs to occur before *para*-xylene production is possible. In a similar way, more *ortho*-xylene is

‡ nd = not determined due to the proximity of the much larger feedstock GC peak.

produced in the isomerisation of *meta*-xylene (one methyl group shift) than in the isomerisation of *para*-xylene (two methyl group shifts required).

The experiment run at an active temperature of approximately 200°C for an extended length of time showed that the 'averaged' sulphated zirconia catalyst steadily deactivates. This could be due to loss of sulphur (sulphate), or a gradual transition from the tetragonal to monoclinic zirconia, which was found to be inactive (see chapter three) in agreement with previous results [4]. The presence of sulphate stabilises the active tetragonal form [4] and so loss of sulphate may cause the transition to the inactive monoclinic form.

Reactions of ethylbenzene over the 'averaged' sulphated zirconia catalyst are of interest as ethylbenzene is present in significant quantities in mixed xylenes. In the present study, a small yield of ethylbenzene has been noted using *ortho*-xylene as a feedstock. Also, during the reaction performed using mixed xylenes as the feedstock, the level of ethylbenzene was seen to vary from its initial value of 20.2%. This implies that there is a route between ethylbenzene and xylenes using this catalyst. A speculative mechanism for this process is presented in Scheme 4.1.

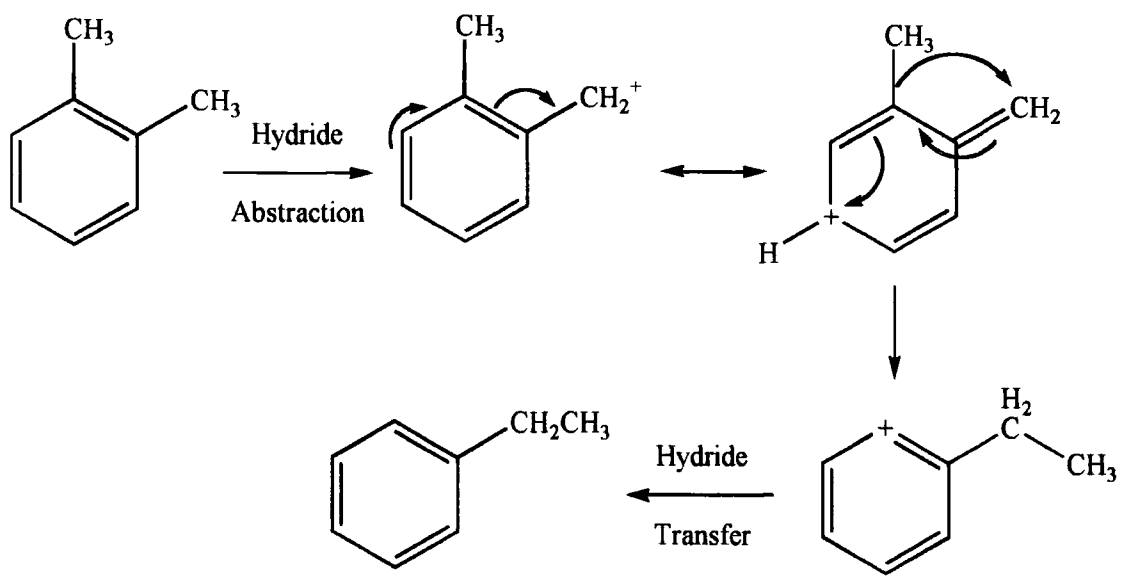

Scheme 4.1: Speculative Mechanism for the Conversion of *Ortho*-Xylene to Ethylbenzene

This mechanism is speculated on the basis of comparisons with other aromatic reactions [5] such as Fries or reverse Fries rearrangement [5, 6]. Although these involve heteroatom-containing species (specifically oxygen), the concept of transfer of one ring substituent onto another is relevant.

In the reaction of toluene, disproportionation activity was expected, as disproportionation of xylenes to give toluene and trimethylbenzenes has been observed before for these catalysts. However, despite the formation of all three xylene isomers, no benzene was produced as expected for toluene disproportionation. It is possible that the aromatic ring is destroyed during the reaction as the reaction of benzene over sulphated zirconia to form coke and carbon dioxide has been reported [7].

Reactions of toluene with methanol showed some selectivity to production of the *ortho*-isomer, indicating a preference for reaction at the *ortho* position. This could be related to the known *ortho*, *para* directing effect of a methyl group during electrophilic reactions [5], although the *para* isomer is not produced in the same quantities. However, it is possible that a combination of steric effects favouring the *para* product, and the presence of two *ortho* positions (one either side of the methyl group on toluene) statistically favouring the *ortho* position give the product ratios seen.

The reactions of methyl methanoate are of interest as a possible source of high purity carbon monoxide. The decarbonylation of methyl methanoate was indeed catalysed by sulphated zirconia catalysts, and dehydration of the product methanol was also seen. The proposed reaction scheme is shown in Scheme 4.2.

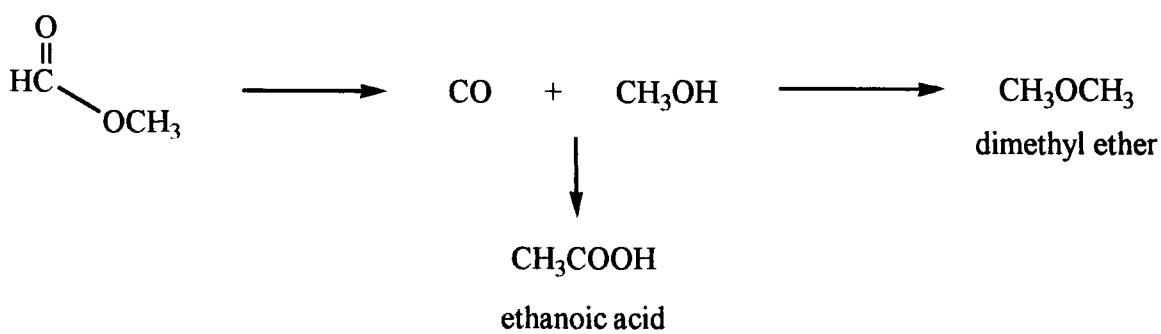

Scheme 4.2: Reactions of Methyl Methanoate

A related reaction which is also industrially relevant is the carbonylation of methanol to give ethanoic acid, which can also be considered to be a rearrangement of methyl formate [2]. The production of ethanoic acid was not observed over this catalyst.

The reaction of ethyl ethanoate over the sulphated zirconia catalyst gave some unexpected products.

The presence of hydrogen in the system, which was used as the flow gas, allows the catalyst to show hydrogenation activity. The hydrogenation of an ester gives two molecules of alcohol. In the case of ethyl ethanoate, hydrogenation produces two molecules of ethanol, as shown in Scheme 4.3.

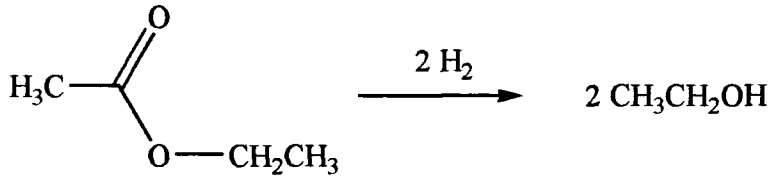

Scheme 4.3: Hydrogenation of Ethyl Ethanoate

Ethanal (acetaldehyde) can also be produced in this hydrogenation reaction. In the presence of ethanol, however, it is trapped as the corresponding acetal, 1,1-diethoxyethane, shown to be present by GC-MS. The hemi-acetal, 1-ethoxyethanol, was not observed, due to a fast condensation with a second molecule of ethanol. Acetal formation in the presence of acidic catalysts is a well-documented reaction [8].

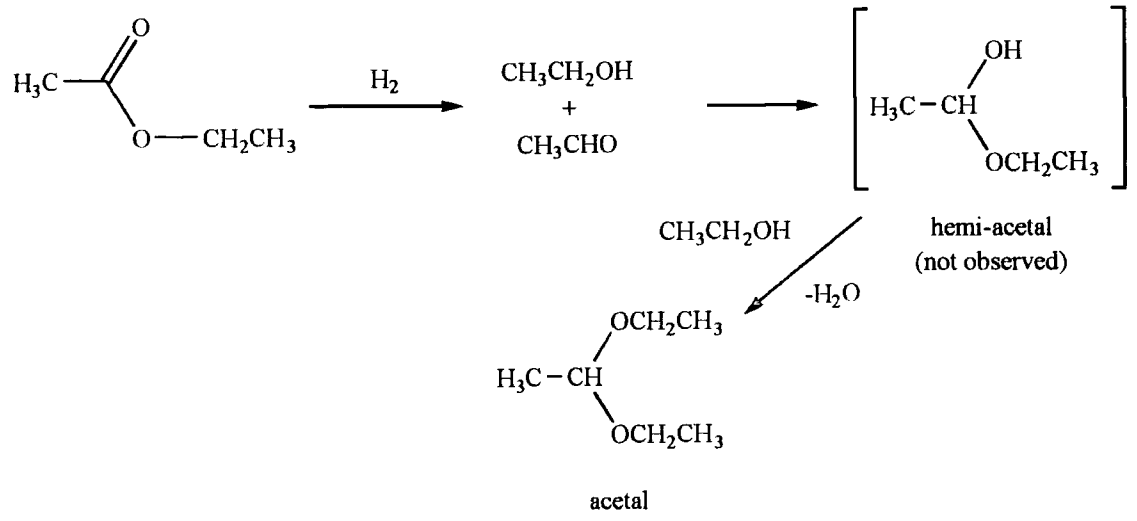

Scheme 4.4: Acetal Formation

Hydrogenation of organic compounds using a sulphated zirconia catalyst is unusual, although not unknown. Hydrogenation of 2-methylpropene occurs at temperatures as low as 60°C [9], and the removal of sulphate from sulphated zirconia has been proposed to proceed by successive hydrogenation, until hydrogen sulphide is lost from the catalyst [10]. The use of a hydrogen atmosphere to reduce coke deposition on the catalyst surface has been reported by a number of authors [11]. The hydrogenation activity of a sulphated zirconia can be enhanced by the addition of platinum [10]. The presence of hydrogenation activity is reinforced by the observation of the reduction of hexadec-7-enic acid (oleic acid) to 1-hexadecanol.

One other common reaction which can produce ethanol from ethyl ethanoate is hydrolysis [12]. In the absence of water hydrolysis cannot occur, and so cannot be the initial route to the formation of ethanol. Some water is liberated in other reactions (such as those shown in Schemes 4.4 and 4.6) so hydrolysis may play a part at a later stage. The presence of water has been reported to enhance the Brønsted acidity of a sulphated zirconia [13].

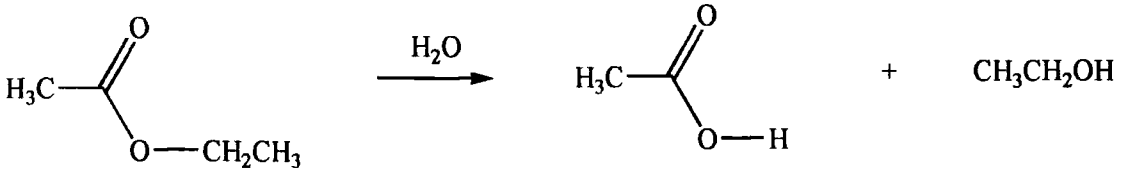

Scheme 4.5: Hydrolysis of Ethyl Ethanoate

The formation of butanol could occur by dehydration of two molecules of ethanol. Other products of dehydration include diethylether, which was not observed with certainty by either GC or GC-MS analysis. However, it is possible that diethylether would co-elute with the water and ethanol peaks. A second product could be ethene, which would be lost to the system with other volatile compounds.

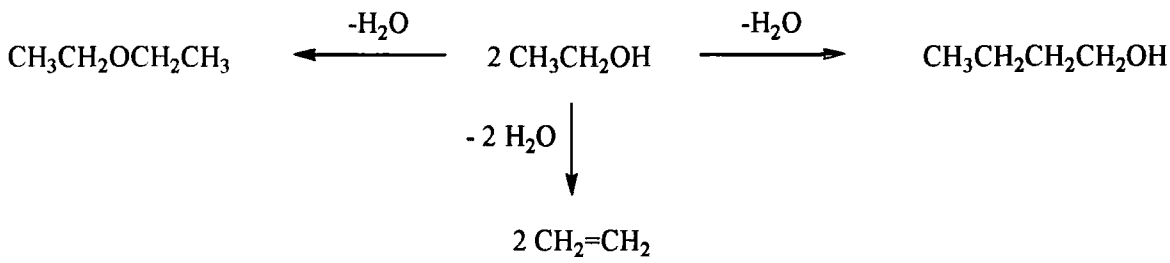

Scheme 4.6: Dehydration of Ethanol

The pyrolysis of ethyl ethanoate would also give ethene, as well as ethanoic acid [14]. The reaction is believed to proceed *via* β-hydride elimination.

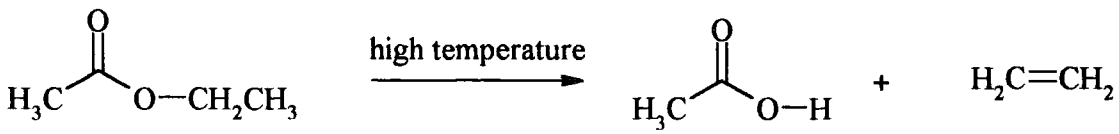

Scheme 4.7: Pyrolysis of Ethyl Ethanoate

The dehydration of ethanol to form butanol is catalysed by metal oxide catalysts, especially those of groups 2 and 12 [14]. Butyl ethanoate can be formed by the transesterification reaction of butanol with ethyl ethanoate [12]. Sulphated zirconia has been shown to be an active catalyst for esterification reactions [15].

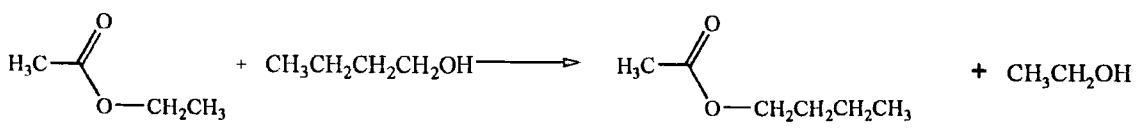

Scheme 4.8: Transesterification of Ethyl Ethanoate with Butanol

Some three-carbon compounds (such as acetone) were formed during the reaction. This implies that carbon - carbon bond fission has taken place. For example, breaking the carbon - oxygen single bond in ethyl ethanoate would give an acetyl (CH_3CO) fragment, which could combine with a methyl group to form acetone as shown in Scheme 4.9.

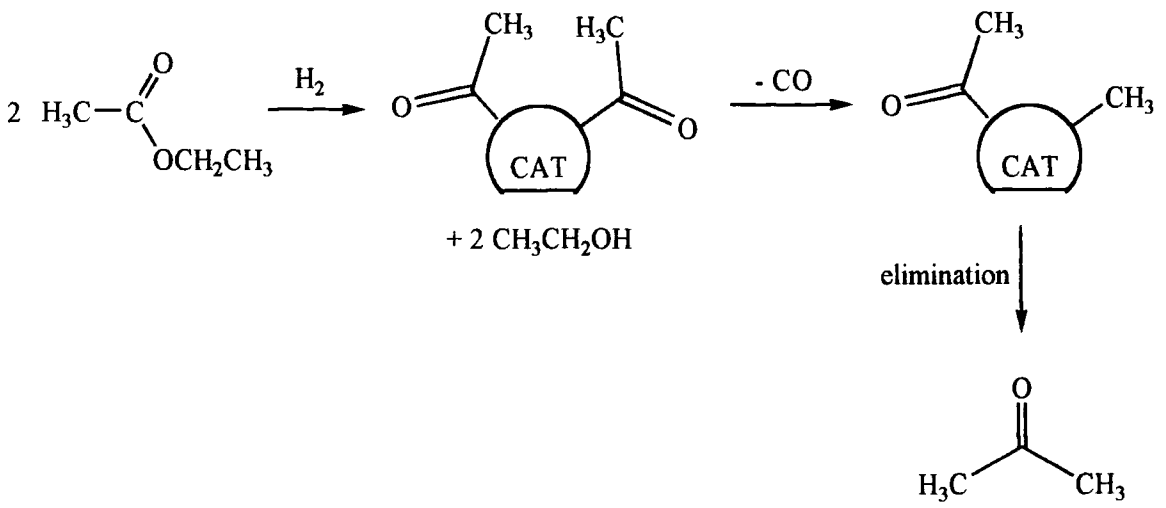

Scheme 4.9: Speculative Route for the Formation of Acetone from Ethyl Ethanoate

Two commercial samples of "zirconium hydroxide" were sulphated using ammonium sulphate, calcined at 600°C and evaluated as catalysts. Both these catalysts were active for the isomerisation of *ortho*-xylene, more active than the other catalysts described in this chapter, although less active than catalysts reported elsewhere in this thesis. The only difference between these commercial catalysts was their particle size. The smaller particle size must give a greater surface area to the sample, and so greater reactivity. This could be as a consequence of a higher surface sulphate content, or faster reaction with reagent molecules. The other commercial samples investigated, "zirconium hydroxide" doped with either silicic acid or lanthanum hydroxide, were not active for the isomerisation of *ortho*-xylene.

4.5 Conclusions

An 'exploratory' catalyst was prepared using the conclusions drawn from the development work discussed in chapter three. This was less active than many of the

catalysts discussed earlier. The reason for this lies either in the omission of nitric acid from the precipitation step, or in changes made to the calcination procedure.

Activity was seen for reactions of the xylene isomers. The yields of the different isomers as products were consistent with the observation of no direct interconversion of the *ortho*- and *para*-isomers, and that isomerisation occurs *via* a 1,2-shift of a methyl group [1]. Interconversion of the xylene isomers with ethylbenzene was also observed. Xylene isomers could also be produced by reaction of toluene, either with or without the addition of methanol. However, the formation of benzene was never observed, possibly due to degradation of the ring.

The decarbonylation of methyl methanoate was catalysed by this catalyst, giving methanol and carbon monoxide. Some of the methanol reacted further to form dimethyl ether by dehydration. Reactions of ethyl ethanoate were also studied, and included hydrogenation, dehydration and the formation of acetals by condensation of ethanal with ethanol. Some three-carbon compounds, for example acetone, were also produced. The reaction of oleic acid to form 1-hexadecanol confirms the hydrogenation activity of the catalyst.

Although the catalyst prepared was less active than some studied previously, the reactivity trends observed here have been used to investigate the sulphated zirconia catalyst.

4.6 References

1. R.H. Allen and L.D. Yats, *J. Am. Chem. Soc.*, 1959, **81**, 5289-92.
2. M. Röper, *Erdöl und Kohle-Erdgas-Petrochemie vereinigt mit Brennstoff-Chemie*, 1984, **37**, 506-11.
3. K. Samo, Y. Yamamoto and S. Horie, European Patent Application EP 57090 (1982). *Chem. Abs.*, 1982, **97**, 165496*g*.
4. For example, C. Morterra, G. Cerrato, F. Pinna and M. Signoretto, *J. Catal.*, 1995, **157**, 109-123.
5. L.M. Harwood, "Polar Rearrangements", Oxford University Press, 1992, pp. 69-81.

6. D.L.H. Williams, "Aromatic Rearrangements", in C.H. Bamford and C.F.H. Tipper (eds), "Comprehensive Chemical Kinetics", Vol. 12, Elsevier Publishing Company, 1972, pp. 433-86.

7. R. Srinivasan, R.A. Keogh, A. Ghenciu, D. Fărcasiu and B.H. Davis, *J. Catal.*, 1996, **158**, 502-10.

8. J.E. McMurry, "Organic Chemistry", Brooks/Cole Publishing, 1992, pp.730-3.

9. F. Garin, D. Andriamasinovo, A. Abdulsamad and J. Sommer, *J. Catal.*, 1991, **131**, 199-203.

10. M. Signoretto, F. Pinna, G. Strukul, P. Chies, G. Cerrato, S. Di Ciero and C. Morterra, *J. Catal.*, 1997, **167**, 522-32.

11. For example, P. Moles, *Speciality Chemicals*, 1992, **Nov/Dec**, 382-8.

12. J. March, "Advanced Organic Chemistry", 4th Edn., John Wiley & Sons, 1992.

13. C. Morterra and G. Cerrato, *J. Phys. Chem.*, 1993, **97**, 11501-9.

14. R. Taylor, "Pyrolysis of Acids and their Derivatives" in S. Patai (ed), "The Chemistry of Functional Groups Supplement B: The Chemistry of Acid Derivatives", John Wiley and Sons, 1979, pp.860-914.

15. G.D. Yadav and P.H. Mehta, *Ind. Eng. Chem. Res.*, 1994, **33**, 2198-2208.

Chapter Five: Summary of Xylene Isomerisation Work

A number of compounds have been studied as catalysts for the isomerisation of xylenes, mostly using *ortho*-xylene as a feedstock. Experimental data are presented in Appendices 2.2, 3.2 and 4.1. The first compounds were commercially - supplied catalysts. One was a "synthetic aluminosilicate zeolite", whilst the other was "nickel - containing aluminium oxide on a mordenite carrier". The former catalyst showed the greatest activity towards *ortho*-xylene isomerisation, and had its maximum activity around 350°C. It was also shown to be active for the disproportionation of toluene to xylenes and benzene, the reaction of toluene with methanol, and reactions of ethylbenzene. Selectivity was generally to the *meta*-isomer, except with ethylbenzene as the feedstock, where disproportionation to benzene and diethylbenzenes was the dominant process. Isomerisation of a sample of mixed xylenes was also promoted by this catalyst. In all the processes investigated, activity was greatest at or above 350°C. The nature of the agreement with the catalyst supplier made any further work with these catalysts impossible.

The isomerisation of *ortho*-xylene was also studied using a series of supported silver, palladium and chromium catalysts. Although the deposition of coke was seen in almost all cases, no isomerisation activity was reported.

A number of doped zirconia catalysts were investigated for the same reaction. A small amount of activity was seen for many of these catalysts, but the most active catalyst was found to be a sulphated zirconia. Once this activity had been confirmed, development work was commenced to link catalytic performance with steps in the catalyst synthesis procedure, and as a result to be able to produce a better catalyst. It was found that compounds based on "zirconium hydroxide" gave good activity, whilst those based on pre-formed zirconium dioxide gave no activity at all. This is in agreement with literature results [1], and relates to the crystal form of the zirconia catalyst, the monoclinic form is the most stable at room temperature, and up to 900°C, although it is the least catalytically active. However, a metastable tetragonal phase can be prepared by calcination of an amorphous "zirconium hydroxide" precursor, and this is stabilised to

approximately 700°C by the addition of sulphate groups [2]. None of the other sulphated metal oxides studied showed activity, and it is possible that the solution to the problem may be the same as found with zirconium dioxide - hydroxide groups are needed in the compound to react with the sulphate by elimination of water. The presence of too few hydroxide groups in the precursor gives poor sulphate incorporation and low activity. The use of freshly - precipitated "zirconium hydroxide" prepared from zirconium propoxide gave the best catalysts. This could be due to the larger number of hydroxide groups available.

The effect of using different sources of sulphur was also considered. It was found that the best source of sulphur was sulphuric acid, but ammonium sulphate, either as a solid or an aqueous solution, gave catalysts of almost equal activity. Elemental sulphur gave much poorer catalysis suggesting that the sulphur needs to be present in the +6 oxidation state to be effective [3]. Other dopants were considered which had been reported to give stability or activity to zirconia or sulphated zirconia catalysts. None of these was able to match the selectivity to xylene isomerisation offered by a sulphated zirconia catalyst, although some transition - metal oxide doped samples gave much greater activity. The amount of sulphate added to a catalyst did not have a linear effect on the catalytic activity observed, the most active catalyst having a sulphate content of 7 wt.%.

The steps of the calcination process were also considered. The heating rate, cooling rate, calcination temperature and length of heating period were found to be inter -dependant and so the trends were not easily understood. Heating to temperatures above 700°C caused the tetragonal to monoclinic phase transformation to occur, giving inactive catalysts. Otherwise, the heating procedure appears to have effects on the level of hydration seen in the catalyst. For efficient Brønsted acidity, a level of hydration is required, whilst Lewis acidity is enhanced by anhydrous conditions [4]. Whilst no clear trends were evident in the calcination procedures, the best catalysts were given by a catalyst calcined between 500°C and 600°C, heated to this temperature at a rate of 50°C min^{-1}, held there for two hours, and then cooled to room temperature at a rate of 0.3°C min^{-1}. The storage of the catalyst after this was also investigated, and found not to have a great effect on the catalytic performance of a catalyst sample.

It was found to be possible to prepare a catalyst which gave 9.5% conversion of *ortho*-xylene per gram of catalyst, with good selectivity to *meta*-xylene.

Information gained from the experiments described above was used to synthesise an 'exploratory' catalyst. This turned out to be considerably less active than many of its predecessors in the isomerisation of *ortho*-xylene. This is either due to the replacement of nitric acid with sulphuric acid affecting the precipitation or the nature of the precipitated product in some way, or changes to the calcination procedure having a synergistic effect and producing unintended effects on the catalyst. The lifetime of this catalyst was investigated, and activity was found to decrease exponentially over time. This could be caused by loss of sulphate or a slow change to the inactive monoclinic form of zirconia.

The 'exploratory' catalyst was tested for some aromatic reactions apart from the isomerisation of *ortho*-xylene. The relative yields of the xylene isomers from the reactions of *meta*- or *para*-xylene over the catalyst imply that a stepwise mechanism of 1,2-methyl shifts is in operation. This has been proposed in the literature, and is thought to operate when using the majority of catalysts [5-7]. The reaction of toluene was found to give xylenes, although no benzene was detected, whilst the reaction of toluene and methanol gave larger yields of the xylene isomers. The reaction of ethylbenzene gave small yields of xylenes, which is of interest due to their presence in the mixed xylenes feedstock used commercially.

Other acid - catalysed reactions were studied over the catalyst. Methyl methanoate was decarbonylated to give methanol and carbon monoxide. In a side - reaction, methanol was also dehydrated to give dimethyl ether. A number of reactions of ethyl ethanoate in the presence of hydrogen as the flow gas were detected, including hydrogenation, dehydration and acetal formation. The major product was ethanol, although conversion was low. In a separate reaction, oleic acid was hydrogenated to 1-hexadecanol. The possession of hydrogenation activity by a sulphated zirconia is uncommon, but has been reported for the hydrogenation of 2-methylpropene [8].

The application of this catalyst system to *ortho*-xylene isomerisation has been studied, and its utility demonstrated. Good conversions - the maximum obtained being approximately 9.5% conversion per gram of catalyst used - have been demonstrated at temperatures much lower than those currently used (250°C compared with typically 400-500°C) in a single pass reactor in a bed whose size was limited due to the catalyst being a powder and so causing pressure to build up in the system. This low temperature activity could be developed by changes in catalyst morphology and reactor design which would allow longer residence times to be used. Despite questions over its long - term stability, the low environmental impact compared to liquid systems means that this is a catalyst which merits further study.

References

1. F.R. Chen, G. Cordurier, J.-F. Joly and J.C. Vedrine, *J. Catal.*, 1993, **143**, 616-26.
2. R. Srinivasan, T.R. Watkins, C.R. Hubbard and B.H. Davis, *Chem. Mater.*, 1995, **7**, 725-30.
3. C. Morterra, G. Cerrato, F. Pinna and M. Signoretto, *J. Catal.*, 1995, **157**, 109-23.
4. C. Morterra, G. Cerrato, F. Pinna, M. Signoretto and G. Strukul, *J. Catal.*, 1994, **149**, 181-8.
5. R.H. Allen and L.D. Yats, *J. Am. Chem. Soc.*, 1959, **81**, 5289-92.
6. D.L.H. Williams, "Aromatic Rearrangements", in C.H. Bamford and C.F.H. Tipper, "Comprehensive Chemical Kinetics", Elsevier Publishing Company, 1972, pp.433-86.
7. H.J. Shine, "Aromatic Rearrangements", Elsevier Publishing Company, 1967, pp.1-12.
8. F. Garin, D. Andriamasinovo, A. Abdulsamad and J. Sommer, *J. Catal.*, 1991, **131**, 199-203.

Chapter Six: Applications of Aminophosphines in Synthesis and Catalysis

6.1 Introduction

The use of phosphine ligands in synthesis and catalysis is widespread. They are valued for their ability to control the electronic properties of a metal centre, and so be able to tailor its reactivity. Tertiary phosphine ligands are one of the few types of ligand where this kind of tuning is possible, and so the search for different kinds to give more active and more selective catalysts has been intensive. The properties of phosphines which make them valuable in catalysis are discussed below.

6.2 Phosphine Ligands in Synthesis

A phosphine ligand is typically a three co-ordinate, three valent system, which can bind to a metal using its lone pair of electrons. However, phosphines can also accept electron density back from a metal by π-donation from a metal d - orbital to the phosphine P - C antibonding (σ^*) orbital [1]. This is shown in Fig. 6.1.

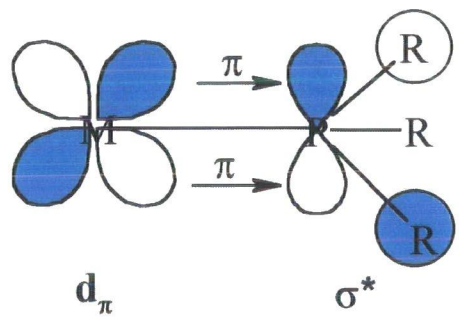

Fig. 6.1: Illustration of π-Bonding Between a Transition Metal and a Phosphine Ligand

The degree to which this backbonding can take place is controlled by the substituents on the phosphorus atom, and so the relative stability of the σ^* orbital. A

more electronegative substituent lowers the energy level of this orbital, and so makes the phosphine a better π-acceptor.

A scheme for measuring the donor - acceptor properties of a phosphine ligand was proposed by Tolman [2], who used the carbonyl stretching frequency of a [(phosphine)$Ni(CO)_3$] complex to determine the relative electronic properties of a range of phosphines and related ligands. He found that electronegative substituents on the phosphine ligand gave rise to a higher A_1 carbonyl stretching frequency, and so a lower electron density at nickel. However, it was not possible to separate this effect into the ligands' π-acceptor and σ-donor properties. This is discussed further in chapter eight.

Variations in the size and shape of ligands can also be of interest to the chemist. A good example of this is the use of bulky ligands to shield a co-ordinatively or electronically unsaturated metal centre from attack by nucleophilic reagents [1]. Tolman [3] devised a method of assessing the bulk of a phosphine ligand by use of the cone angle. This was defined as being the angle between two straight lines drawn from the metal centre to which the phosphine is bound along its outside edges with the substituents folded back as much as possible. The cone angle of a ligand can be assessed by making space-filling molecular models and measuring the relevant angle. This is shown schematically in Fig. 6.2.

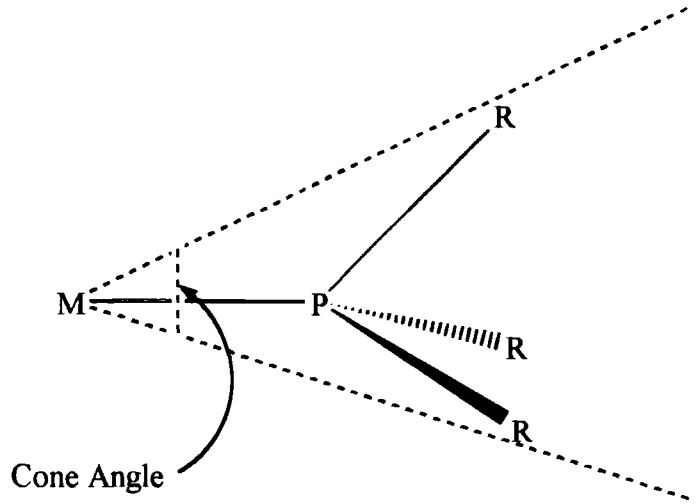

Fig. 6.2: The Cone Angle

In the case of polydentate ligands, the 'bite angle' is usually quoted rather than the cone angle. In the case of diphosphines this is the phosphorus - metal phosphorus bond angle, and is usually determined experimentally from diffraction studies, although it can again be calculated by molecular modelling.

It is a combination of these steric and electronic factors which can be used to determine the reactivity of a transition metal phosphine complex.

Reactions undergone by phosphine ligands typically involve the lone pair, and many involve oxidising the phosphorus atom from oxidation state +3 to +5. Examples of this are reactions with oxygen or sulphur, giving the phosphine oxide and sulphide respectively. This is shown in Scheme 6.1.

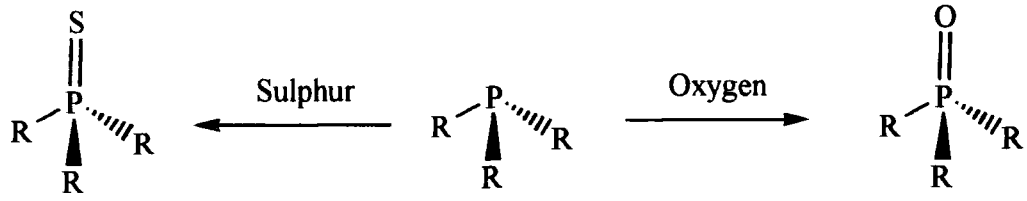

Scheme 6.1: Reaction of a Phosphine Ligand with Oxygen or Sulphur

These compounds are also used as ligands, but donation is through the oxygen or sulphur atom [4] as the phosphorus lone pair is used in intramolecular bonding.

Phosphine ligands bind strongly to transition metal centres, and can displace most kinds of ligands, as in the preparation of [(phosphine)$Ni(CO)_3$] by reaction of the appropriate phosphine with [$Ni(CO)_4$] [2]. This ability of phosphines to substitute other neutral ligands such as benzonitrile, norbornadiene or cyclooctadiene is utilised in the synthesis of transition metal complexes.

The tuning of the properties of a phosphine ligand by changing its substituents has found a great deal of applications in synthesis. Bulky phosphine ligands can be used to protect reactive metal species, such as low oxidation states [5] or metal - metal bonding by discouraging the attack of other reagents. Smaller phosphine ligands can stabilise

metal complexes by binding to vacant co-ordination sites unavailable to larger donors. This stabilisation can often make complexes easier to isolate.

The characterisation of phosphorus containing compounds can involve many methods available to the research chemist - infrared, ^{1}H and ^{13}C nmr spectroscopy, mass spectrometry, and X-ray crystallography for example - but one technique which deserves a special mention is ^{31}P nmr. The nuclear properties and abundance of ^{31}P (natural abundance = 100%, I = ½ [6]) make it especially suitable for nmr studies, and highly informative spectra can be obtained within a few minutes. Coupling to nmr-active metals such as rhodium or platinum gives further information on the bonding of the phosphine ligands.

6.3 Phosphine Ligands in Catalysis

The range of steric and electronic properties available to tertiary phosphine ligands make them ideal ligands for catalysis. Changes in the phosphine bound to a metal complex give marked changes in catalyst activity. A classic example of this is the hydroformylation reaction. Since the initial work of Osborn, Wilkinson and co-workers [7], which used triphenylphosphine ligands, many different ligands have been tested for the same reaction. Replacement of one or more phenyl rings with a different organic group has been discussed [8], as has the use of chelating diphosphines [9]. Water soluble phosphines [10] and phosphine-containing polymer supports have also been used [11, 12] to aid separation of the catalyst from the products. The use of phosphites over phosphines has been found to increase catalyst stability [13], and selectivity in the case of cyclic phosphites [14, 15]. Hence changes in the nature of the tertiary phosphine ligand gives catalysts with different properties suitable for different situations.

The ability to design the shape of phosphine ligands has been applied in the field of asymmetric catalysis. Here the steric interaction between the catalytic complex and a reagent molecule favours the production of one stereoisomer over another. In the field of asymmetric catalysis, this has involved chiral ligands such as those shown in Fig. 6.3, which have been used for asymmetric hydroformylation [16-19].

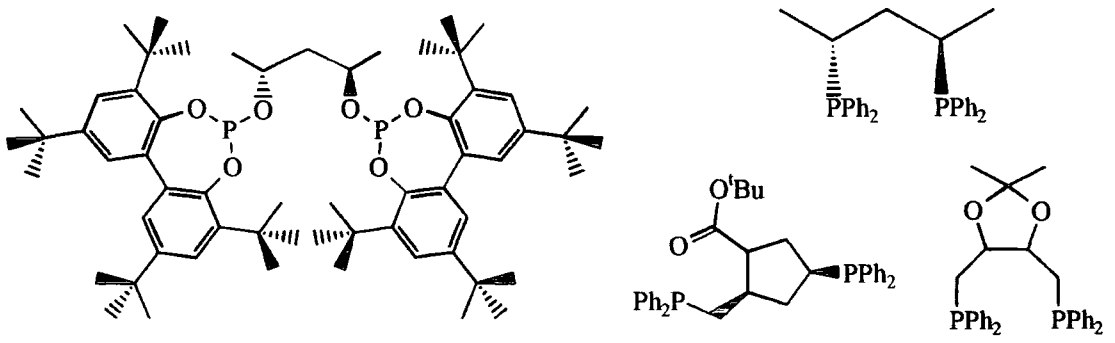

Fig. 6.3: Examples of Chiral Ligands used in Asymmetric Hydroformylation

6.4 Phosphites: Uses in Synthesis and Catalysis

Phosphite ligands, $P(OR)_3$, bear a close relationship to aminophosphines, represented $P(NR_2)_3$, and can be considered as heteroatom-containing analogues of common tertiary phosphines. They can be synthesised by the reaction of PCl_3 with alcohols [20], although a base such as triethylamine or pyridine is needed to remove the hydrogen chloride produced by the elimination reaction. This is shown in Scheme 6.2.

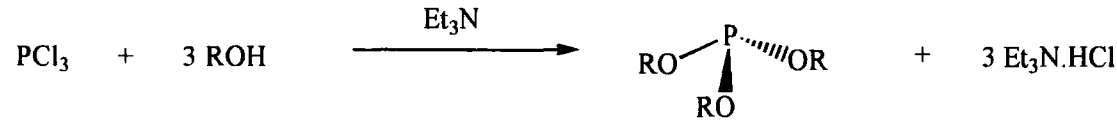

Scheme 6.2: Synthesis of Phosphites

The removal of hydrogen chloride from the reaction is critical, since tertiary phosphites react with it to give the alkyl chloride and a phosphorus hydroxy species. This is not the case for aromatic substituents, which are more stable than their aliphatic counterparts.

Alternative syntheses involve the action of an alcohol on phosphorus oxides, which is particularly applicable to the reaction of methanol with P_4O_9, or alkoxide exchange, which is the reaction of a trialkylphosphite with an alcohol and is catalysed by the metal alkoxide corresponding to the alcohol.

Many of the reactions of trialkyl- or triarylphosphites mirror those of the corresponding phosphine. Phosphites are known to be strong acceptors of sulphur and oxygen, even desulphurising organic thiols and removing oxygen from organic compounds.

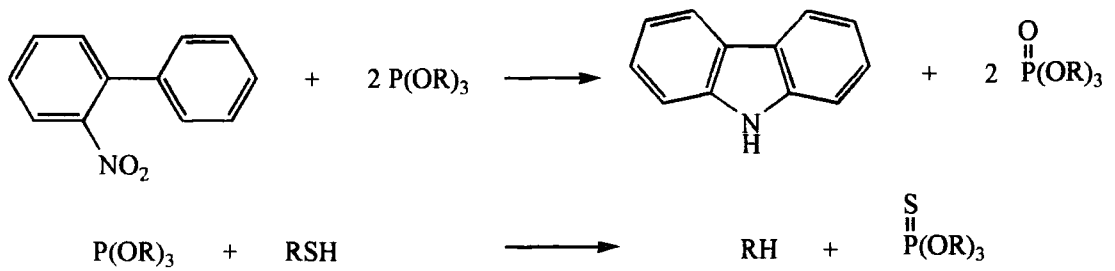

Scheme 6.3: Reactions of Tertiary Phosphites

Another important reaction undergone by tertiary phosphites is the Arbuzov rearrangement [21]. This is a rearrangement to the related phosphorus (V) oxide as shown in Scheme 6.4.

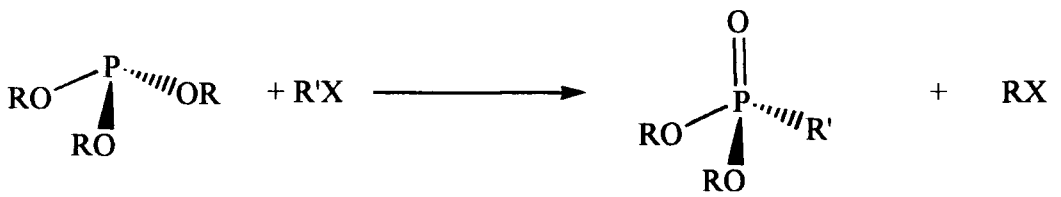

Scheme 6.4: The Abrizov Rearrangement

A related rearrangement has been found to occur at co-ordinated phosphites, and is promoted by heating. When co-ordinated, phosphites are also susceptible to hydrolysis to yield the parent alcohol, and an oxidised phosphorus species. Cyclometallation of an aryl group attached to the phosphite is also seen, as it is with the analogous phosphine ligands [22].

Preparation of transition metal phosphite complexes uses the same methods as for phosphine complexes. These include such methods as direct reaction with the metal, or

displacement of a weakly co-ordinated ligand. A wide variety of complexes of the transition elements is reported, mirroring that of the tertiary phosphines [22].

A phosphite ligand is reported as being a better π-electron acceptor than the related tertiary phosphine [1, 20]. However, the σ-donor properties depend more on the substituent at oxygen, and they are generally weaker electron donors than the corresponding phosphine. Triphenylphosphite is a worse σ-donor than PF_3 [20].

The complexes of phosphites are increasingly being used in catalysis. They have been used in hydroformylation and asymmetric hydroformylation as mentioned above. Chiral diphosphites have been used in the asymmetric hydrogenation of keto-esters [23]. This study relates to compounds discussed below. Other recent uses of phosphites in catalysis are given in Table 6.1. This information is not intended to be comprehensive, but more to give a flavour of the range of processes where phosphites have been employed. A key to the more complex ligands used is presented in Fig. 6.4. These ligands can be synthesised by a stepwise reaction with a diol, before being condensed with another alcohol as shown in Scheme 6.5.

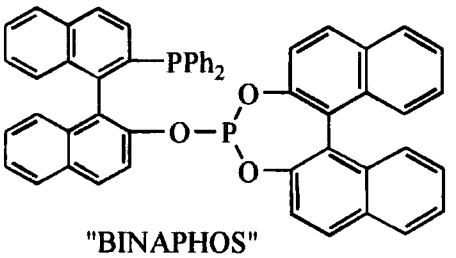

"BINAPHOS"

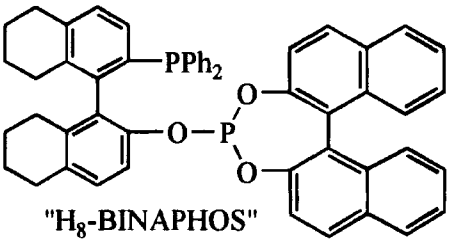

"H_8-BINAPHOS"

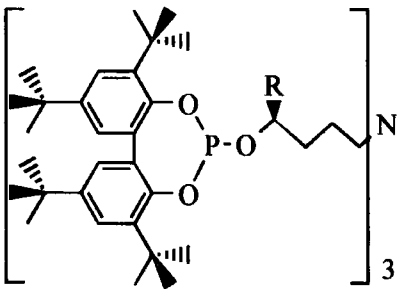

Ligand A

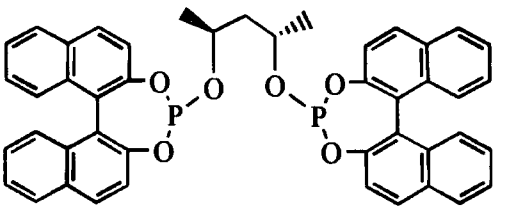

Ligand B

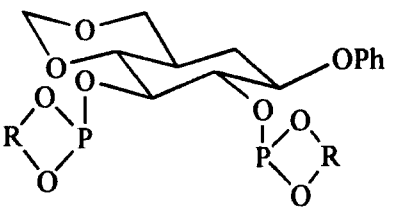

R = aryl, alkyl

Ligand C

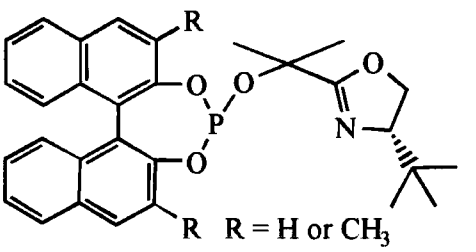

R = H or CH_3

Ligand D

Fig. 6.4: Bulky Phosphite Ligands Used in Catalysis

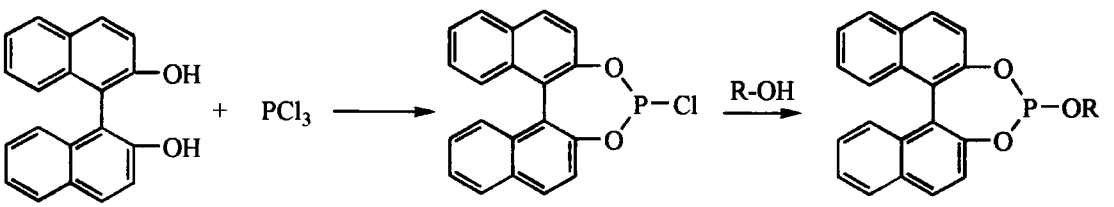

Scheme 6.5: Synthesis of a Bulky Phosphite Ligand

Table 6.1: Examples of Tertiary Phosphite Ligands in Catalysis

Process	Phosphite	Metal	Reagents	Products	Conversion	Selectivity	Notes	Ref
Co-polymerisation	BINAPHOS H_8-BINAPHOS	Pd	propene CO	polyketone	yields up to 2.9%	isotactic polyketone	H_8-BINAPHOS is the better ligand	[24]
	BINAPHOS	Pd	propene CO	polyketone	68% in 4 days at -25°C	> 95% ee isotacticity observed		[25]
Hydrosilylation	Ligand A	dimeric Rh complex	$PhCOCH_3$	$PhCH(OH)CH_3$	up to 67%	up to 81%	Process uses bulky phosphites	[26]
	$P(OAr)_3$	Pd	alkyne $HSiCl_3$	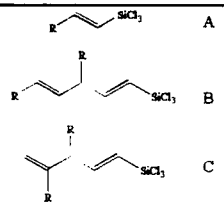 A B C	100% in 14 - 45 h	selectivity usually to B	ratio of isomers linked to phosphite cone angle	[27]
Hydrogenation	$P(OAr)_3$	Ir	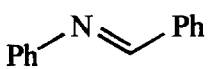	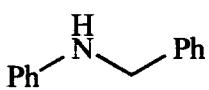	up to 99.6% in 1 h	-	Bulky groups needed on Ar to give activity	[28]

Hydroformyl-ation	Ligand B	Pt / Sn	styrene CO, H_2	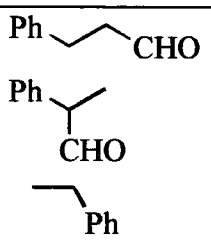	up to 100% in 2h at 60°C	up to 91% ee, n/iso ~ 1:2 50% hydrogenation		[29]
	Ligand C	Rh	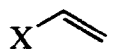 X = OAc, CH_2OAc, *para*-$C_6H_4OCH_3$	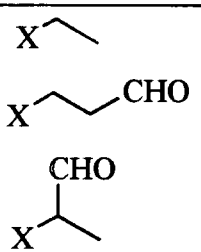	up to 94%	up to 32% ee. n/iso < 1	Pt-based catalysts give much more hydrogenation than Rh-based catalysts	[30]
Coupling	Ligand D	Cu, Zn	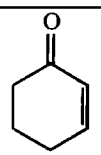 Et_2Zn	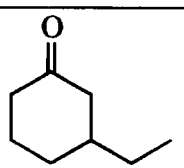	up to 99% in 3 h	up to 90% possible	Yield and ee not as good with acyclic substrates	[31]
	$P(OR)_3$	Pd	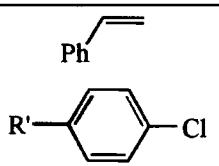 R' = MeO, CF_3	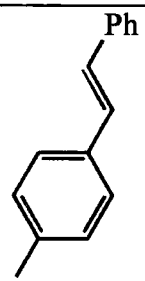	TON up to 31000. Yields can be 100%	-		[32]

Isomerisation	$P(OEt)_3$	Ni	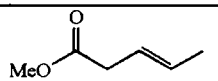	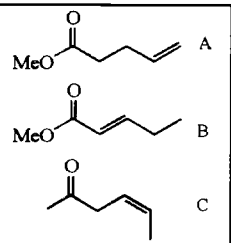	47% in 15 min	Selectivity to product C		[33]
Hydrocyanation	BINAPHOS	Ni, Pd	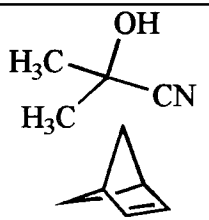	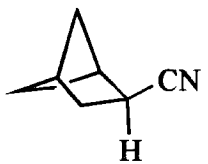	up to 69% (with Ni)	up to 48% (with Pd)	Yield better with Ni, but ee better with Pd	[34]
Telomerisation	$P(OAr)_3$	Pd	butadiene and acetic acid	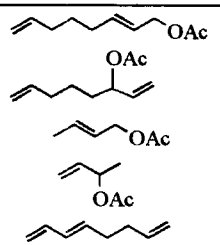	80-100%	selectivity to linear product	Yields best for Ar = (2-phenyl)phenyl or (2-methyl)phenyl	[35]

For coupling reactions, metal complexes containing phosphites were found to make catalysts at least as good as those containing phosphines, but are cheaper and easier to handle [32].

Phosphites have also been used in heterogeneous catalysis to modify the inside of a zeolite pore [36]. Trimethylphosphite was one of a range of phosphorus compounds which were used to reduce the pore size and so increase the selectivity to a linear product.

6.5 Synthesis of Aminophosphine Ligands

The synthesis of aminophosphines has been performed in a similar way for over a century. The reaction of phosphorus trichloride with a secondary amine was found to give aminophosphines, which were characterised by elemental analysis, and by their reactivity with common substrates [37-41]. Substituted phosphorus chlorides such as $PhPCl_2$ and $PhPCl_4$ were found to react with organic amines, particularly aniline and *ortho*-tolylamine to give aminophosphines. The related reactions of phosphorus oxychloride and sulphochloride species were also investigated, and found to yield aminophosphine products. Reactions such as the formation of phosphonium salts by the action of an aryl iodide were also reported. Examples of the type of reaction performed during this era are presented in Scheme 6.6.

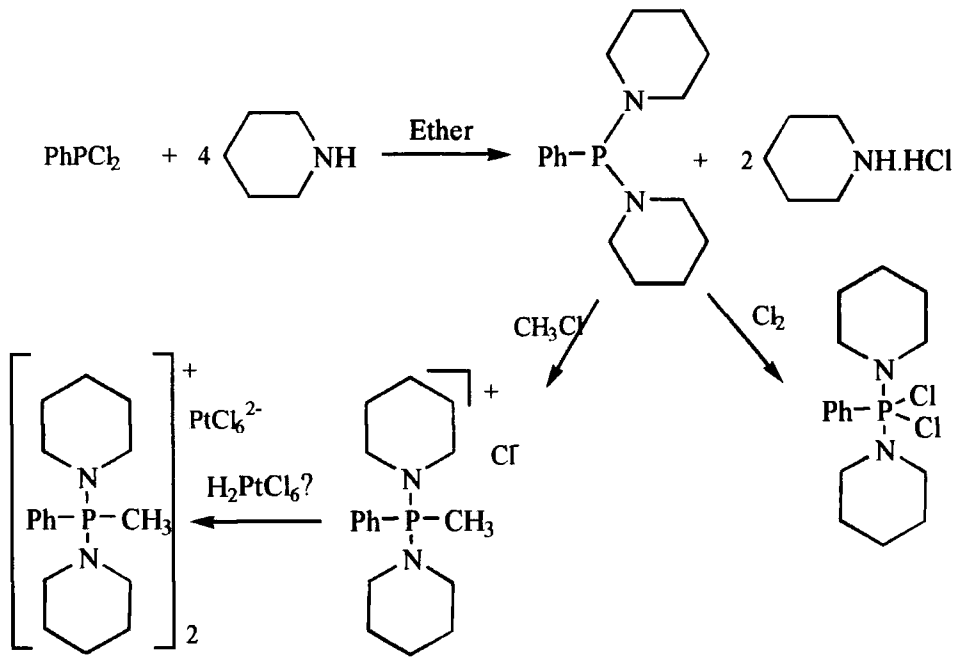

Scheme 6.6: Examples of 19th Century Aminophosphine Chemistry

It was known that the elimination of hydrogen chloride took place during these reactions, and that this was often found as an amine hydrochloride. The phosphines were often reacted with an organic halide to give a phosphonium salt, although this was not necessarily recognised as having the structure given to it today. This was reacted to form the "platinum double salt" which was an ionic compound where the aminophosphonium ion formed the cation to a $PtCl_6^{2-}$ anion, rather than a co-ordination compound.

The use of triethylamine or a related base to eliminate hydrogen chloride from a phosphorus chloride and a nitrogen base is still the main method of synthesis of aminophosphines. It has been put to a great variety of uses, including the synthesis of dendrimers [42], and ligands, as will be discussed below. A related technique is used in the synthesis of cyclophosphazenes and polyphosphazenes [43]. The only other synthetic method of any importance in the synthesis of aminophosphines is lithiation, which uses the reaction of an N-lithiated amine with a phosphorus chloride to give the desired aminophosphine with elimination of lithium chloride. This technique has been used in the synthesis of some silylaminophosphines [44]. Transamination of one aminophosphine, such as $MeP(NEt_2)_2$, with a second amine has led to polymer precursors [45].

The bonding between nitrogen and phosphorus is of interest, and has been the subject of a number of structural and theoretical studies. The structures of tris(morpholino)phosphine and tris(piperidino)phosphine have been determined by x-ray crystallography [46] and the phosphorus - nitrogen bonding examined. There is found to be one sp^3-hybridised nitrogen, which has a P-N bond length longer than the other two in the molecule. The other two nitrogen atoms are more planar, which ties in with them tending towards sp^2 hybridisation, and this in turn implies that the nitrogen lone pair is involved in bonding to phosphorus.

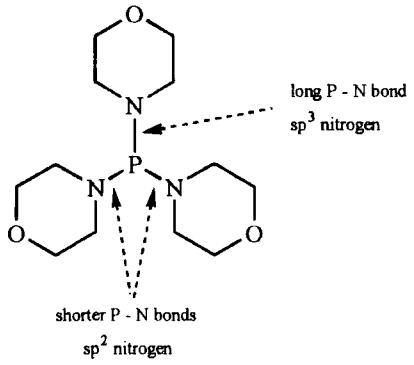

Fig. 6.5: The Structure of Tris(morpholino)Phosphine

In the related compound *trans*-dichloro-P,P'-bis(diphenylphosphino)piperidine) palladium(II) [47], the shortened P - N bond was not thought to be due to extra nitrogen to phosphorus bonding, and the flattening of the piperidine ring was ascribed to the interaction of the nitrogen lone pair with the rest of the ring. The chair geometry preferred by the piperidine substituent disrupts any significant π-bonding between nitrogen and phosphorus. Electrostatic effects and "negative hypoconjugation" (the donation of electron density from a π to a σ^* orbital [48], which shows some analogy with the π-bonding between a metal and a tertiary phosphine ligand [1,48] and leads to a lengthening of the phosphorus - carbon bonds due to donation into the σ^* orbital) have also been cited as the reason for the shortening [49].

A number of different aminophosphines have been used as ligands for transition metals [47, 50-54]. The bonding patterns seen mirror those of tertiary phosphines.

A large number of diphosphines have also been synthesised. The most common aminophosphines to be studied are bis(diphenylphosphino)amines, which are synthesised from chlorodiphenylphosphine and a primary amine. These provide complexes which have a four - membered chelate ring, and their co-ordination chemistry has been investigated with cobalt [55], ruthenium [56] and platinum [57, 58]. They have been found to exhibit both bridging and chelating modes, as has been observed for the carbon containing analogue dppm. A third alternative found has the ligand bound in a monodentate fashion. This is shown in Fig. 6.6.

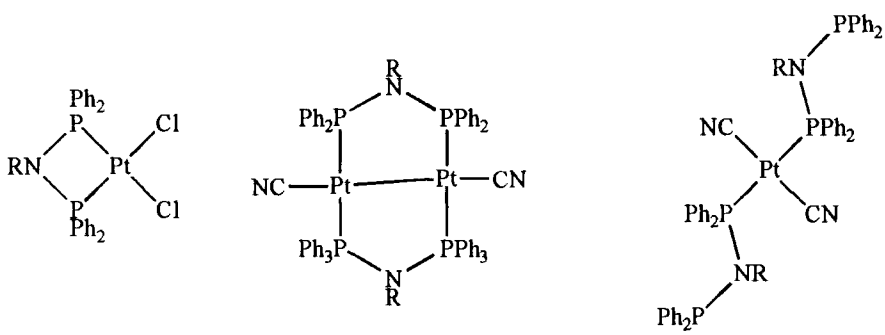

Fig. 6.6: Binding Modes of bis(diphenylphosphino)amines - chelating, bridging and monodentate

One reaction found for dppa but not undergone by dppm is deprotonation. If a complex of dppa is deprotonated by reaction with a strong base, then a negatively-charged ligand results. Reprotonation is also possible by use of an acid such as HBF_4. The nitrogen atom is unreactive as an electron donor, indicating that the lone pair is at least partially distributed into the phosphorus - nitrogen bonds as shown in Scheme 6.7 [58].

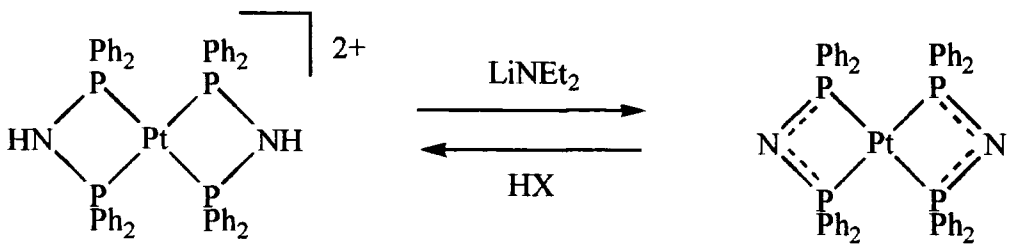

Scheme 6.7: Deprotonation of a dppa Complex

The phosphine oxide and sulphide of dppa and related ligands, formed in analogous ways to those of tertiary phosphines, have also been used as ligands for transition metals, and selective oxidation and protonation has been used to elegantly control their mode of binding [59]. Elimination of HCl by action of base on a platinum dichloride complex yielded a P,O-chelating ligand as shown in Scheme 6.8. This could then be deprotonated in the manner described above.

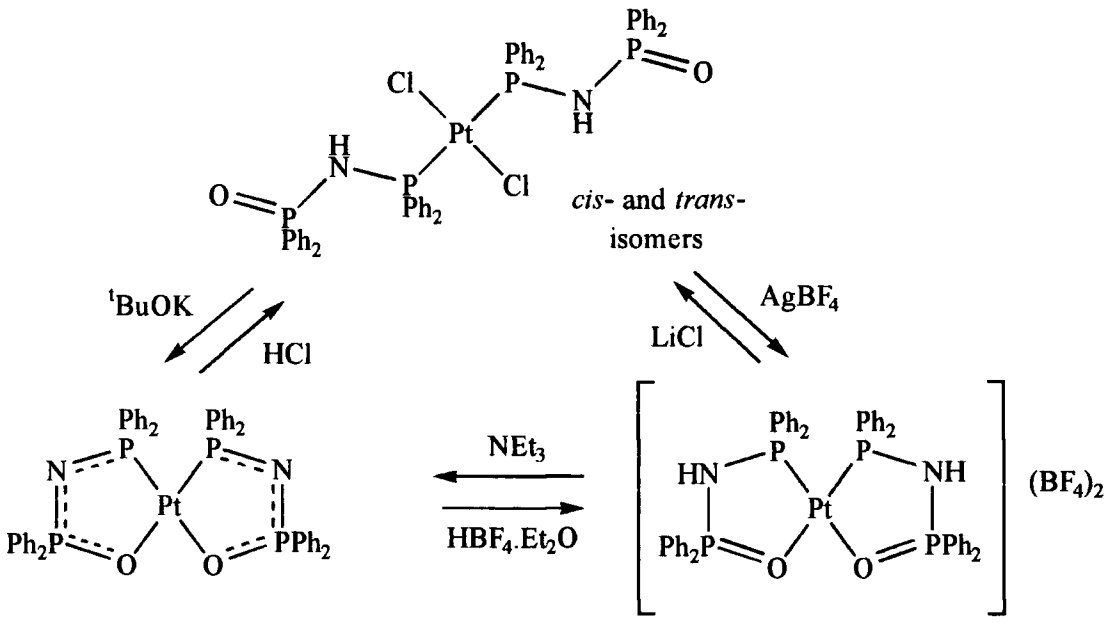

Scheme 6.8: Reactions of dppa monoxide as a ligand

A large number of other chelating aminophosphines have been synthesised and studied, and this includes ligands derived from a whole host of different diamines. The drive for most of the studies is the synthesis of new ligands for catalysis, and the effect of modification of an existing tertiary phosphine ligand by the inclusion of amine functionalities. The reaction of N,N'-dimethylethylenediamine with PCl_3 has been found to give an aminophosphine with all three chlorine atoms replaced [60]. This is shown in Scheme 6.9. Platinum and tungsten complexes of the ligand were also synthesised.

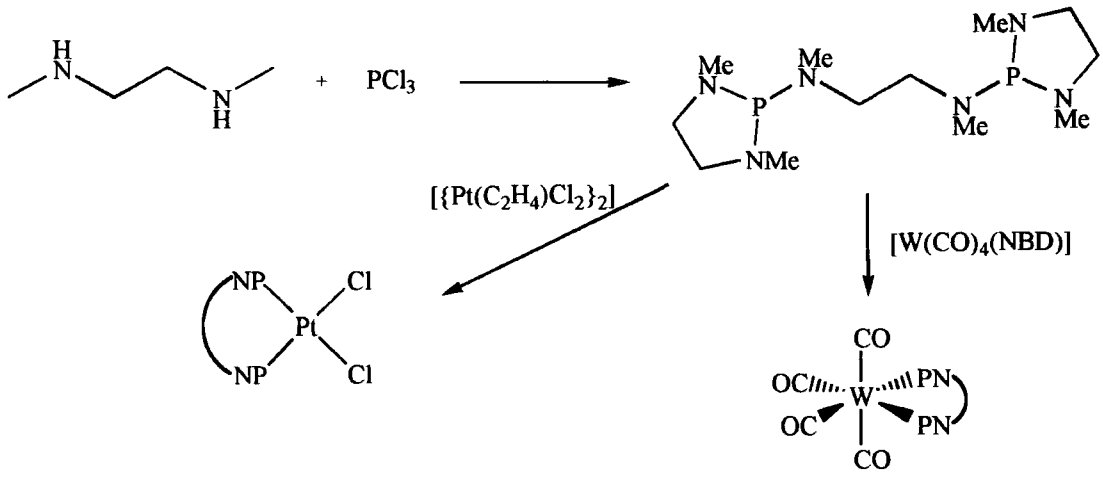

Scheme 6.9: Reaction of PCl_3 with $MeN(H)CH_2CH_2N(H)Me$

Ligands based on aromatic diamines have also been synthesised [61], including one based on the chelating chiral ligand BINAP (2,2'-bis(diphenylphosphino)binaphthyl) [62]. The use of a cyclohexane backbone has also been studied as it is linked to chiral catalysts [63-65]. Other chiral ligands have been prepared by incorporation of a chiral diamine unit into the structure, either by use of an amine containing a chiral centre, such as $H_2NCH(Me)(Ph)$ [65-67] or by using a chiral diamine, such as 2-(anilinomethyl)pyrrolidine [68]. Reaction of 2,6-diaminopyridine with chlorodiphenylphosphine by a lithiation route gave a tridentate ligand with two phosphorus and one nitrogen donor atom [69]. Finally, diaminophosphines containing a urea [70], dimethylethylenediamine [71] or methyl hydrazine [72] backbone were prepared as analogues to the commonly - used chelating diphosphines dppm, dppb and dppe respectively. Complexes of these ligands were made, mostly of the group 10 dichlorides or group 6 carbonyls. Many of the ligands and complexes here were used in catalytic processes, and these are discussed below.

6.6 Uses of Aminophosphine Ligands in Catalysis

Due largely to their ease of synthesis, aminophosphines have found application as ligands for catalysts in homogeneous catalysis. Many of these catalysts have been used for asymmetric catalysis, especially hydrogenation and hydroformylation. The correlation between the selectivity of a rhodium aminophosphine catalyst towards the linear isomer in the hydroformylation reaction and the electron - donating or electron - withdrawing nature of the aminophosphine ligand has been investigated using X-ray photoelectron spectroscopy. This has shown that a more electron -withdrawing ligand gives greater selectivity to the linear product [73]. Donation of electron density from nitrogen to phosphorus was observed in the free ligand, although in a rhodium complex this situation was reversed [74].

Examples of the use of aminophosphines in catalytic processes are given in Table 6.2.

Table 6.2: Catalytic Reactions involving Aminophosphine Ligands

Process	Ligand	Metal	Reagents	Products	Yield	Selectivity	Notes	Ref.
Hydrogenation	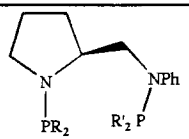 R=Ph, Cpt, Cy	Rh	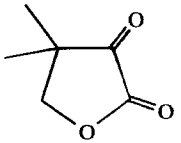	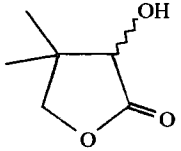	100% conversion in 0.2-48 h	up to 83% ee		[68]
			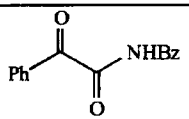	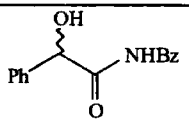	100% conversion in 1.7-28 h	up to 75% ee		[68]
	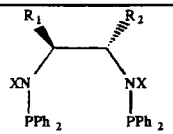 R_1, R_2 = Me, Ph, H, 1,2-cyclohexane X = Me, H	Rh	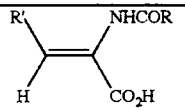 R = Me, Ph R' = H, Ph, ^{i}Pr	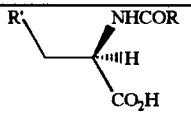	not determined	up to 94% ee	Stereoisomer produced depends on X group	[64]
	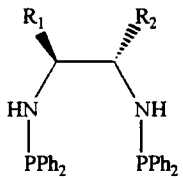 R_1, R_2 = Me, 1,2-cyclohexane	Rh	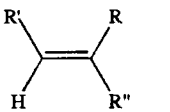 R = H, Me, Ph, CO_2H R' = Me, NHCOMe, CH_2CO_2H R" = CO_2H, Ph	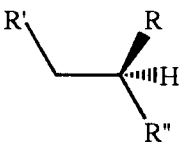	often 100%	up to 85% ee		[63]

Hydrogenation	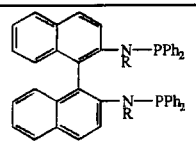 R = H, Me	Rh	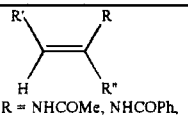 R = NHCOMe, NHCOPh, Me, Ph R' = H, Ph R" = CO_2H, CO_2Me	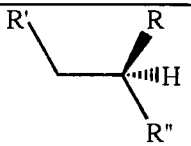	usually 100%	up to 90% ee		[62]
Alkylation	dppmen	Ni	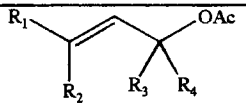 R_1 = H, Me, R R_2, R_3, R_4 = H, Me R = 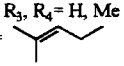	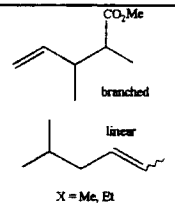 branched linear X = Me, Et	usually 100%	usually to branched product and *cis* isomer	dppmen better than dppb for most substrates.	[69]
	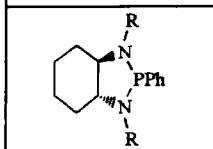 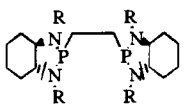 R = Me, H	Pd	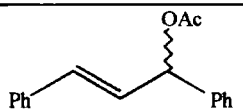 $CH_2(CO_2Me)_2$	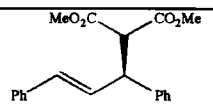	up to 80%	up to 25%		[65]

Aminophosphine ligands have been reported to provide inferior catalysts to aminophosphinephosphinites for hydrogenation [68] and alkylation [69]. However, aminophosphine ligands can be used in catalysis to good effect - with the right combination of catalytic system they can provide good activity and selectivity.

6.7 Chelating Aminophosphinephosphinite Ligands in Catalysis

Aminophosphinephosphinites can be considered as analogues to aminophosphines. They are chelating polyphosphines - usually bidentate although not necessarily so - with one phosphorus atom bound to nitrogen and the other bound to oxygen. They are readily synthesised from aminoalcohols, and since this class of compound contains a number of chiral compounds they find ready application in asymmetric catalysis. The synthesis of these compounds is by the same route described for aminophosphines above; however, since the alcohol and amine functionalities show different reactivities towards the phosphine chloride, it is possible to add the phosphorus groups sequentially, giving a ligand with very different phosphorus donors. An example of this is shown in Scheme 6.10 [75].

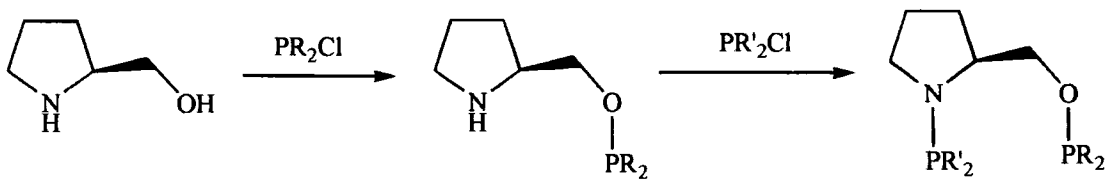

Scheme 6.10: Synthesis of Aminophosphinephosphinite Ligands

Catalysis using these ligands has been more widely studied than using aminophosphine ligands. This may be because they have been reported to give greater activity and enantioselectivity [68]. Examples of their use in catalysis are given in Table 6.3.

The catalysis has been studied only for a few different types of reaction, although many different ligands have been studied. The most studied ligands are based on 2-pyrrolylmethanol (shown in Scheme 6.10), while many other ligands have been based on amino acid precursors [76].

Table 6.3: Examples of Catalytic Reactions Involving Aminophosphinephosphinite Ligands

Process	Metal	Examples of Reagents	Examples of Products	Conversion	Selectivity	Notes	Refs.
Hydrogenation of Alkenes	Rh	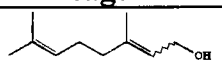	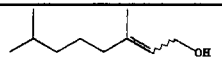	70 - 100% conversion in 8 h.	70-90% to monoalkene. Up to 85% ee.	ee very solvent dependant: benzene > ethanol > THF	[78-83]
		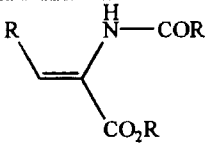	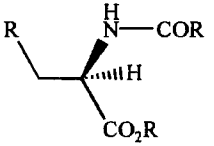	100% in <30 min	up to 92% ee depending on ligand used		
Hydrogenation of Ketones and Keto-Esters	Rh	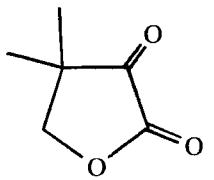	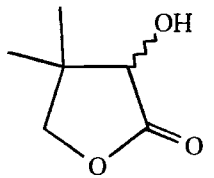	Usually 100% conversion	Up to 95% depending on the ligand used.	Conversion and ee are both dependant on temperature	[23, 75, 80, 84-94]
	Ru	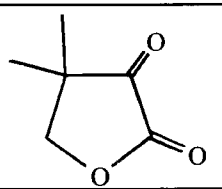	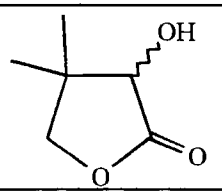	100% conversion in 15-60h	Up to 96% possible	Solvent effects on both ee and conversion	[95,96]

Hydroformylation	Rh	styrene	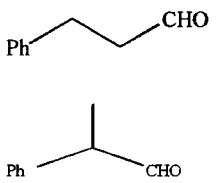	up to 98% at 40°C for 1 - 3 days	Selective to branched product. n/iso ratio typically 1:10, can be 1:44. Up to 30% ee seen.	No hydrogenation to ethylbenzene seen.	[97]
	Pt - Sn	styrene	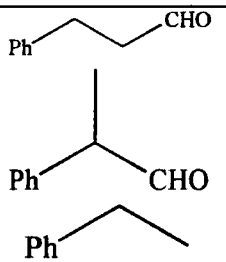	100% conversion possible	~10% hydrogenation seen. n/iso ratio typically 2:1. Up to 60% ee possible		[98, 99]
Reactions of Alkenes	Ni	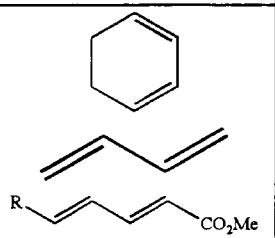	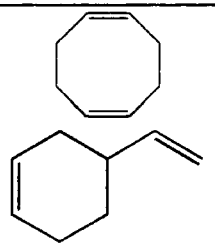	100% conversion possible	Selectivity very dependant on the ligand used	Selectivity to a desired product possible by careful choice of ligand and reagents	[100-102]
Alkylation	Ni	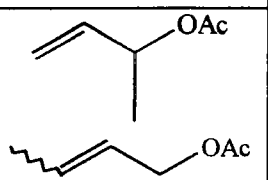	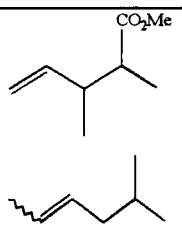	100% conversion in <2 h.	Selective to branched products and *cis*-alkenes	Linear allylic acetates are more reactive than cyclic allylic acetates	[71]

6.8 Summary

Aminophosphines are readily synthesised by reaction of an amine with a chlorophosphine, a reaction which has been used for many years. An alternative route is *via* lithiation. They form complexes with a number of transition metals in the manner seen for hydrocarbon - backbone phosphines, and bidentate aminophosphines will by the same token bridge or chelate according to their geometry. The use of aminophosphine ligands in catalysis has been investigated, especially in asymmetric catalysis, although the use of either phosphite or aminophosphinephosphinite ligands has mostly been preferred. However, given the ease of synthesis and handling, the use of aminophosphine ligand in catalysis shows much potential for investigation and development.

6.9 References

1. R.H. Crabtree, "The Organometallic Chemistry of the Transition Metals", John Wiley and Sons, 1988.
2. C.A. Tolman, *J. Am. Chem. Soc.*, 1970, **92**, 2953-6.
3. C.A. Tolman, *Chem. Rev.*, 1977, **77**, 313-48.
4. M. Hayashi, H. Takezaki, Y. Hashimoto, K. Takaoki and K. Saigo, *Tetrahedron Lett.*, 1998, **39**, 7529-32.
5. L. Malatesta and S. Cenini, "Zerovalent Compounds of Metals", Academic Press, 1974, pp. 69-209.
6. R.C. Weast and M.J. Astle, "Handbook of Chemistry and Physics", 63rd Edn, CRC Press, 1982, p. B-259.
7. D. Evans, J.A. Osborn and G. Wilkinson, *J. Chem. Soc. A*, 1968, 3133-42.
8. D.G. Morrell and P.D. Sherman, jr., United States Patent 4260828 (1981)
9. S.P. Crabtree, Ph.D. Thesis, University of Durham, 1996, pp. 68-80.
10. W.A. Herrmann, C.W. Kohlpainter, R.B. Manetsberger, H. Bahrmann and H. Kottmann, *J. Mol. Catal. A*, 1995, **97**, 65-72.
11. K.G. Allum, R.D. Hancock and M.J. Lawrenson, German Patent 2022710 (1971).
12. R.A. Dubois, P.E. Garrou, K.D. Laurin and H.R. Allcock, *Organometallics*, 1986, **5**, 460-6.
13. A.J. Dennis, G.E. Harrison and J.P. Wyber, United States Patent 4496769 (1985).

14. A.J. Dennis, G.E. Harrison and J.P. Wyber, United States Patent 4567306 (1986).

15. S.N. Poelsma and P.M. Maitlis, *J. Organomet. Chem.*, 1993, **451**, C15-C17.

16. G.J.H. Buisman, E.J. Vas, P.C.J. Kener and P.W.N.M. van Leeuwan, *J. Chem. Soc., Dalt. Trans.*, 1995, 409-17.

17. G. Parnello and J.K. Stille, *J. Am. Chem. Soc.*, 1987, **109**, 7122-7.

18. I. Tóth, T. Kégl, C.J. Elsevier and L. Kollár, *Inorg. Chem.*, 1994, **33**, 5708-12.

19. S. Paganelli, U. Mattedi and A. Scrivanti, *J. Organomet. Chem.*, 1990, **397**, 119-25.

20. D.E.C. Corbridge, "Phosphorus: An Outline of its Chemistry, Biochemistry and Technology", 4th Edn., Elsevier, 1990, pp. 346-54.

21. T.B. Brill and S.J. Landon, *Chem. Rev.*, 1984, **84**, 577-85.

22. C.A. McAuliffe and W. Levason, "Phosphine, Arsine and Stibine Complexes of the Transition Elements", Elsevier Press, 1979, pp. 356-83.

23. C. Hatat, A. Karim, N. Kokel, A. Mortreux and F. Petit, *New J. Chem.*, 1990, **14**, 141-52.

24. K. Nozaki, M. Yasutomi, K. Nakamoto and T. Hiyama, *Polyhedron*, 1998, **17**, 1159-64.

25. K. Nozaki, N. Sato and H. Takaya, *J. Am. Chem. Soc.*, 1995, **117**, 9911-2.

26. S.D. Pastor and S.P. Shum, *Tetrahedron Asymm.*, 1998, **9**, 543-6.

27. Y. Kawayami and K. Yamamoto, *Synlett*, 1995, 1232-4.

28. R.B. Bedford, S. Castillòn, P.A. Chalmer, C. Claver, E. Fernandez and A. Ruiz, *Organometallics*, 1996, **15**, 3990-7.

29. S. Cserépin-Szücs and J. Bakos, *Chem. Commun.*, 1997, 635-6.

30. R. Kadyrov, D. Heller and R. Selke, *Tetrahedron Asymm.*, 1998, **9**, 329-40.

31. A.K.H. Knobel, I.H. Escher and A. Pfalz, *Synlett*, 1997, 1429-31.

32. M. Beller and A. Zapf, *Synlett*, 1998, 792-3.

33. X. Wang and L.K. Woo, *J. Mol. Catal. A*, 1998, **130**, 171-6.

34. T. Horiuchi, E. Shirakawa, K. Nozaki and H. Takaya, *Tetrahedron Asymm.*, 1997, **8**, 57-63.

35. D. Rose and H. Lepper, *J. Organomet. Chem.*, 1973, **49**, 473-6.

36. L.B. Young, S.A. Butter and W.W. Kaeding, *J. Catal.*, 1982, **76**, 418-32.

37. A. Michaelis and G. Schulze, *Berichte*, 1893, **26**, 2937-40.

38. P. Rudert, *Berichte*, 1893, **26**, 565-75.

39. A. Michaelis and K. Luxembourg, *Berichte*, 1895, **28**, 2205-11.

40. A. Michaelis and F. Kuhlmann, *Berichte*, 1895, **28**, 2212-7.

41. A. Michaelis, *Berichte*, 1898, **31**, 1037-47.

42. C. Galliot, D. Prévoté, A.-M. Caminade and J.-P. Majoral, *J. Am. Chem. Soc.*, 1995, **117**, 5470-6.

43. H.R. Allcock, "Phosphorus-Nitrogen Compounds", Academic Press, 1972, pp. 97-133.

44. R. Keat, *J. Chem. Soc. A*, 1970, 1795-9.

45. E.G. Bent, R. Schaeffer, R.C. Haltiwanger and A.D. Norman, *Inorg. Chem.*, 1990, **29**, 2608-13.

46. C. Rømming and J. Songstad, *Acta Chem. Scand. A*, 1978, **32**, 689-99.

47. R.A. Burrow, D.H. Farrar and C.H. Honeyman, *Acta Cryst.*, 1994, **C50**, 681-3.

48. D.G. Gilheany, *Chem. Rev.*, 1994, **94**, 1339-74.

49. N.W. Mitzel, B.A. Smart, K.-H. Dreihäupl, D.W.H. Rankin and H. Schmidbaur, *J. Am. Chem. Soc.*, 1996, **118**, 12673-82.

50. S.M. Socol, R.A. Jacobson and J.G. Verkade, *Inorg. Chem.*, 1984, **23**, 88-94.

51. L.D. Hutchins, R.W. Light and R.T. Paine, *Inorg. Chem.*, 1982, **21**, 266-72.

52. L.D. Hutchins, E.N. Duesler and R.T. Paine, *Organometallics*, 1982, **1**, 1254-6.

53. G. Ewart, A.P. Lane, J. McKechnie and D.S. Payne, *J. Chem. Soc.*, 1964, 1543-7.

54. K.G. Moloy and J.L. Petersen, *J. Am. Chem. Soc.*, 1995, **117**, 7696-7710.

55. Z.-Z. Zhang, A. Yu, H.-P. Xi, R.-J. Wang and H.-G. Wang, *J. Organomet. Chem.*, 1994, **470**, 223-9.

56. M.S. Balakrishna, K. Ramaswamy and R.M. Abhyankar, *J. Organomet. Chem.*, 1998, **560**, 131-6.

57. P. Bhattacharyya, R.N. Sheppard, A.M.Z. Slawin, D.J. Williams and J.D. Woolins, *J. Chem. Soc., Dalt. Trans.*, 1993, 2393-2400.

58. C.S. Browning and D.H. Farrar, *J. Chem. Soc., Dalt. Trans.*, 1995, 521-30.

59. P. Bhattacharyya, A.M.Z. Slawin, M.B. Smith and J.D. Woollins, *Inorg. Chem.*, 1996, **35**, 3675-82.

60. J. Powell, A. Lough and M. Raso, *J. Chem. Soc., Dalt. Trans.*, 1994, 1571-6.

61. T.Q. Ly, A.M.Z. Slawin and J.D. Woollins, *J. Chem. Soc. Dalt., Trans.*, 1997, 1611-6.

62. S. Miyano, M. Nawa, A. Mori and H. Hashimoto, *Bull. Chem. Soc. Jpn.*, 1984, **57**, 2171-6.

63. K.-i. Onuma, T. Ito and A. Nakamara, *Bull. Chem. Soc. Jpn.*, 1980, **53**, 2012-5.

64. K. Kashiwabara, K. Hanaki and J. Fujita, *Bull. Chem. Soc. Jpn.*, 1980, **53**, 2275-80.

65. I.C.F. Vasconcelas, G.K. Anderson, N.P. Rath and C.D. Spilling, *Tetrahedron Asymm.*, 1998, **9**, 927-35.

66. A. Badia, R. Navarro and E.P. Urriolabeitia, *J. Organomet. Chem.*, 1998, **554**, 105-12.

67. R.P.K. Babu, S.S. Krishnamurthy and M. Nethaji, *Tetrahedron Asymm.*, 1995, **6**, 427-38.

68. A. Roucoux, I. Suisse, M. Devocelle, J.-F. Carpentier, F. Agbossou and A. Mortreux, *Tetrahedron Asymm.*, 1996, **7**, 379-82.

69. W. Schirmer, U Flörke and H.-J. Haupt, *Z. anorg. Allg. Chem.*, 1989, **574**, 239-55.

70. P. Bhattacharyya, A.M.Z. Slawin, M.B. Smith and D.J. Williams, *J. Chem. Soc., Dalt. Trans.*, 1996, 3647-51.

71. H. Bricout, J.-F. Carpentier and A. Mortreux, *Tetrahedron Lett.*, 1996, **37**, 6105-8.

72. V.S. Reddy, K.V. Katti and C.L. Barnes, *J. Chem. Soc., Chem. Commun.*, 1995, 31-2.

73. J. Grimblot, J.P. Bonnelle, C. Vaccher, A. Mortreux, F. Petit and G. Peiffer, *J. Mol. Catal.*, 1980, **9**, 357-68.

74. J. Grimblot, J.-P. Bonnelle, A. Mortreux and F. Petit, *Inorg. Chim. Acta*, 1979, **34**, 29-36.

75. F. Agbossou, J.-F. Carpentier, C. Hatat, N. Kokel, A. Mortreux, P. Betz, R. Goddard and C. Krüger, *Organometallics*, 1995, **14**, 2480-9.

76. A. Mortreux, F. Petit, G. Buono and G. Peiffer, *Bull. Chim. Soc. Fr.*, 1987, 631-9.

77. E. Cesarotti, A. Chiesa, G. Giani and A. Sironi, *J. Organomet. Chem.*, 1983, **251**, 79-91.

78. E. Cesarotti, A. Chiesa and G. D'Alfonso, *Tetrahedron Lett.*, 1982, **23**, 2995-6.

79. A. Karim, A. Mortreux and F. Petit, *J. Organomet. Chem.*, 1986, **312**, 375-81.

80. A. Karim, A. Mortreux, F. Petit, G. Buono, G. Peiffer and C. Siv, *J. Organomet. Chem.* 1986, **317**, 93-104.

81. A. Mi, R. Lou, Y. Jiang, J. Deng, Y. Qin, F. Fu, Z. Li, W. Hu and A.S.C. Chan, *Synlett*, 1998, 847-8.

82. D. Heller, R. Kadyrov, M. Michalik, T. Freier, U. Schmidt and H.W. Krause, *Tetrahedron Asymm.*, 1996, **7**, 3025-35.

83. C. Dobler, U. Schmidt, H.W. Krause, H.J. Kreuzfeld and M. Michalik, *Tetrahedron Asymm.*, 1995, **6**, 385-8.

84. A. Roucoux, M. Devocelle, J.-F. Carpentier, F. Agbossou and A. Mortreux, *Synlett*, 1995, 358-60.

85. M. Devocelle, F. Agbossou and A. Mortreux, *Synlett*, 1997, 1306-8.

86. C. Pasquier, S. Naili, L. Pelinski, J. Brocerd, A. Mortreux and F. Agbossou, *Tetrahedron Asymm.*, 1998, **9**, 193-6.

87. M. Ait Ali, S. Allaoud, A. Karim, A. Roucoux and A. Mortreux, *Tetrahedron Asymm.*, 1995, **6**, 369-70.

88. C. Hatat, N. Kokel, A. Mortreux and F. Petit, *Tetrahedron Lett.*, 1990, **31**, 4139-42.

89. J.-F. Carpenter and A. Mortreux, *Tetrahedron Asymm.*, 1997, **8**, 1083-99.

90. A. Roucoux, F. Agbossou, A. Mortreux and F. Petit, *Tetrahedron Asymm.*, 1993, **4**, 2279-82.

91. F. Hapiot, F. Agbossou and A. Mortreux, *Tetrahedron Asymm.*, 1994, **5**, 515-8.

92. C. Hatat, A. Karim, N. Kokel, A. Mortreux and F. Petit, *Tetrahedron Lett.*, 1988, **29**, 3675-8.

93. A. Roucoux, L. Thieffry, J.-F. Carpentier, M. Devocelle, C. Méliet, F. Agbossou, A. Mortreux and A.J. Welch, *Organometallics*, 1996, **15**, 2440-9.

94. J.-F. Carpentier, F. Agbossou and A. Mortreux, *Tetrahedron Asymm.*, 1995, **6**, 39-42.

95. F. Hapiot, F. Agbossou and A. Mortreux, *Tetrahedron Asymm.*, 1995, **6**, 11-4.

96. F. Hapiot, F. Agbossou and A. Mortreux, *Tetrahedron Asymm.*, 1997, **8**, 2881-4.

97. Y. Poltier, A. Mortreux and F. Petit, *J. Organomet. Chem.*, 1989, **370**, 333-42.

98. S. Naili, J.-F. Carpentier, F. Agbossou, A. Mortreux, A. Nowogrcki and J.P. Wignacourt, *Organometallics*, 1995, **14**, 2480-9.

99. S. Mutez, A. Mortreux and F. Petit, *Tetrahedron Lett.*, 1988, **29**, 1911-4.

100. M.A. El Amrani, I. Suisse, N. Knouzi and A. Mortreux, *Tetrahedron Lett.*, 1995, **36**, 5011-14.

101. G. Buono, C. Siv, G. Peiffer, C. Triantaphylides, P. Denis, A. Mortreux and F. Petit, *J. Org. Chem.*, 1985, **50**, 1781-2.

102. I. Suisse, H. Bricout and A. Mortreux, *Tetrahedron Lett.*, 1994, **35**, 413-6.

Chapter Seven : Synthesis and Characterisation of Aminophosphine Ligands and their Complexes

7.1 Introduction

This chapter describes the synthesis and characterisation of a range of new aminophosphine compounds and their palladium and platinum complexes. The aminophosphines (shown in Fig. 7.1) are all based on diamines, and so act as chelating diphosphine ligands.

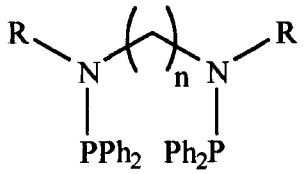

n = 2, R = Me, Ph, ^{i}Pr, ^{t}Bu, -CH_2CH_2-

n = 3, R = Me, ^{i}Pr

Fig. 7.1: Aminophosphine Ligands Synthesised

The two-carbon backbone ligand with R = Me (dppmen) has previously been reported [1], and the catalytic properties of a nickel complex formed in situ from $[Ni(COD)_2]$ and dppmen has been evaluated for the synthesis of vinylcyclohexane from butadiene [1]. Using aminophosphine ligands, such as dppmen, was found to enhance the selectivity to vinylcyclohexane at the expense of other possible products such as cyclooctadiene or divinylcyclobutane, which were produced using ligands such as dppb or PPh_3. Such nickel complexes have also been used in the alkylation of allylic acetates with dimethyl malonate [2]. The catalyst $[Ni(dppmen)_2]$ was found to be superior to $[Ni(dppb)_2]$ for this reaction. Use of the aminophosphine-containing rhodium complexes [(dppmen)Rh(CO)Cl] and [(dpppip)Rh(CO)Cl] in the hydroformylation of 1-hexene gave an increase in the straight-chain to branched ratio of the products compared with complexes containing purely hydrocarbon backbone ligands such as dppp or dppe [3,4]. Some spectroscopic information on the rhodium complexes is reported, but no data regarding the free ligands are presented.

The complexes synthesised in this study are palladium and platinum complexes (Fig. 7.2). Catalytic processes using these complexes are discussed in chapter nine.

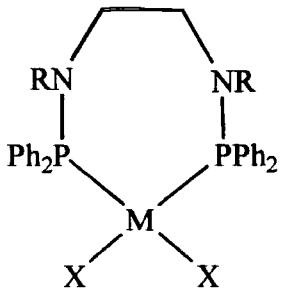

M = Pd, X = Cl, OAc
M = Pt, X = Cl

Fig. 7.2: Metal Complexes Synthesised

7.2 Experimental

7.2.1 Synthesis of Aminophosphine Compounds

7.2.1.1 Synthesis of N,N'-bis(diphenylphosphino)-N,N'-dimethylethylenediamine (dppmen)

Diphenylphosphine chloride (10.0g, 45mmol) was dissolved in dry, degassed toluene (15ml) and the solution degassed. N,N'-dimethylethylenediamine (2.5ml, 24mmol) and triethylamine (6.5ml, 47mmol) were dissolved together in dry, degassed toluene (20ml) and the solution degassed. The amine solution was cooled in an acetone/CO_2 bath and the diphenylphosphine chloride solution added to it by cannula. The reaction was allowed to stir for 30 minutes with the acetone/CO_2 bath in place before being allowed to warm to room temperature. This gave a yellow solution and some white solid. The solution was removed by cannula filter, and the remaining solid washed with five portions of dry, degassed toluene. The washings were combined with the original solution and gave a white solid on standing overnight. (3.1g, 29% yield). ^{31}P nmr: δ_P = 65.0ppm (s, $CDCl_3$). ^1H nmr: δ_H = 7.2-7.3ppm (20H, m, Ph), 3.1ppm (4H, dd, J = 3.9Hz, 2.8Hz, CH_2), 2.4ppm (6H, d, $^3J_{P-H}$ = 5.8Hz, CH_3). ^{13}C nmr: δ_C = 139.5ppm (d, J_{P-C} = 14.3Hz, Ph), 132.2ppm (d, J_{P-C} = 19.8Hz, Ph), 128.5ppm (s, Ph), 128.3ppm (d, J_{P-C} = 5.9Hz, Ph), 55.6ppm (dd, $^2J_{P-C}$ = 22.0Hz, $^3J_{P-C}$ = 6.0Hz, CH_2), 37.5ppm (s, CH_3). IR: The disappearance of ν(N-H) = 3278cm^{-1} (br, neat) from the starting diamine was noted. MS (EI, 1.97x10^4 eV) m/z = 456 (mass ion). Melting point = 117°C.

7.2.1.2 Synthesis of N,N'-bis(diphenylphosphino)-N,N'-diphenylethylenediamine (dpppen)

This compound was synthesised in a manner analogous to that described above for dppmen, giving an off-white solid (1.1g, 8.5% yield). ^{31}P nmr: δ_P = 61.3ppm (s, $CDCl_3$). ^1H nmr: δ_H = 7.2-7.8ppm (m, 20H, P-Ph), 6.6-7.2ppm (m, 10H, N-Ph), 3.2ppm (s, 4H, CH_2). ^{13}C nmr: δ_C = 112-138ppm (m, Ph), 48.1ppm (d, $^2J_{P-C}$ = 4.5Hz, CH_2). IR: The disappearance of ν(N-H) = 3415cm^{-1} (br, solid state) was noted. Melting point = 160°C.

7.2.1.3 Synthesis of N,N'-bis(diphenylphosphino)-N,N'-diisopropylethylenediamine (dppipen)

This compound was synthesised in a manner analogous to that described above for dppmen, giving an off-white solid (0.94g, 11% yield). ^{31}P nmr: δ_P = 46.7ppm (s, $CDCl_3$). ^1H nmr: δ_H = 7.3-7.8ppm (m, 20H, Ph), 2.92ppm (septet, J = 6.4Hz, 2H, CH), 2.65ppm (t, J = 4.5Hz, 4H, CH_2), 0.94ppm (d, J=6.6Hz, 12H, CH_3). ^{13}C nmr: δ_C = 139.3ppm (d, J_{P-C} = 13.9Hz, Ph), 131.0ppm (d, J_{P-C} = 20.0Hz, Ph), 127.0ppm (d, J_{P-C} = 2.4Hz, Ph), 127.0ppm (s, Ph), 50.6ppm (d, J_{P-C} = 20.0Hz, CH_2), 48.2ppm (s, CH), 22.4ppm (d, J_{P-C} = 8.6Hz, CH_3). IR: The disappearance of ν(N-H) = 3249cm^{-1} (br, neat) was noted. MS (CI (positive ion, NH_3), 5.6x10^4 eV): m/z = 513 (M^+). Melting point = 143°C.

7.2.1.4 Synthesis of N,N'-bis(diphenylphosphino)-N,N'-di-*tert*-butylethylenediamine (dpptben)

This compound was synthesised in a manner analogous to that described above for dppmen, giving a white solid (8.6g, 69% yield). ^{31}P nmr: δ_P = 50.7ppm (s, $CDCl_3$). ^1H nmr: δ_H = 7.2 - 7.4ppm (m, 20H, Ph), 2.68ppm (br s, 4H, CH_2), 0.87ppm (s, 18H, CH_3). δ_C = 140.1ppm (d, J_{P-C} = 17.9Hz, Ph), 132.2ppm (d, J_{P-C} = 20.1Hz, Ph), 128.2ppm (d, J_{P-C} = 5.1Hz, Ph), 128.0ppm (s, Ph), 56.3ppm (d, J_{P-C} = 25.2Hz, CH_2), 50.3ppm (d, J_{P-C} = 8.4Hz, CMe_3), 31.3ppm (d, J_{P-C} = 12.4Hz, CH_3). IR: The disappearance of ν(N-H) = 3276cm^{-1} (w, neat) was noted. MS (EI, 1.92x10^5 eV): m/z=540 (M^+); (CI (positive ion, NH_3), 2.97x10^4 eV): m/z = 541 ($(M + H)^+$), 557 ($(M + NH_3)^+$). Melting point =

148°C. A crystal of dpptben suitable for X-ray analysis was grown from a layered toluene - hexane solution and the structure was solved by Dr. A.S. Batsanov. Selected bond lengths and angles are shown in Tables 7.1 and 7.2, and supplementary data can be found in Appendix 7.1.

Table 7.1: Selected Bond Lengths of dpptben

Bond	Length / Å	Bond	Length / Å
P-N	1.710(1)	C(1)-C(1')	1.546(3)
P-C(11)	1.850(2)	C(2)-C(3)	1.532(2)
P-C(21)	1.841(2)	C(2)-C(4)	1.532(2)
N-C(1)	1.488(2)	C(2)-C(5)	1.539(2)
N-C(2)	1.511(2)		

Table 7.2: Selected Bond Angles of dpptben

Bond	Angle / °	Bond	Angle / °
N-P-C(21)	101.37(6)	N-C(2)-C(3)	110.79(11)
N-P-C(11)	110.09(6)	N-C(2)-C(4)	110.54(13)
C(21)-P-C(11)	101.22(7)	N-C(2)-C(5)	109.88(12)
C(1)-N-P	120.05(10)	C(3)-C(2)-C(5)	107.22(13)
C(2)-N-P	116.24(9)	C(4)-C(2)-C(3)	108.44(13)
C(1)-N-C(2)	117.11(11)	C(4)-C(2)-C(5)	109.90(13)
N-C(1)-C(1')	113.3(2)		

Fig. 7.3: The Molecular Structure of N,N'-bis(diphenylphosphino)-N,N'-di-*tert*-butylethylenediamine

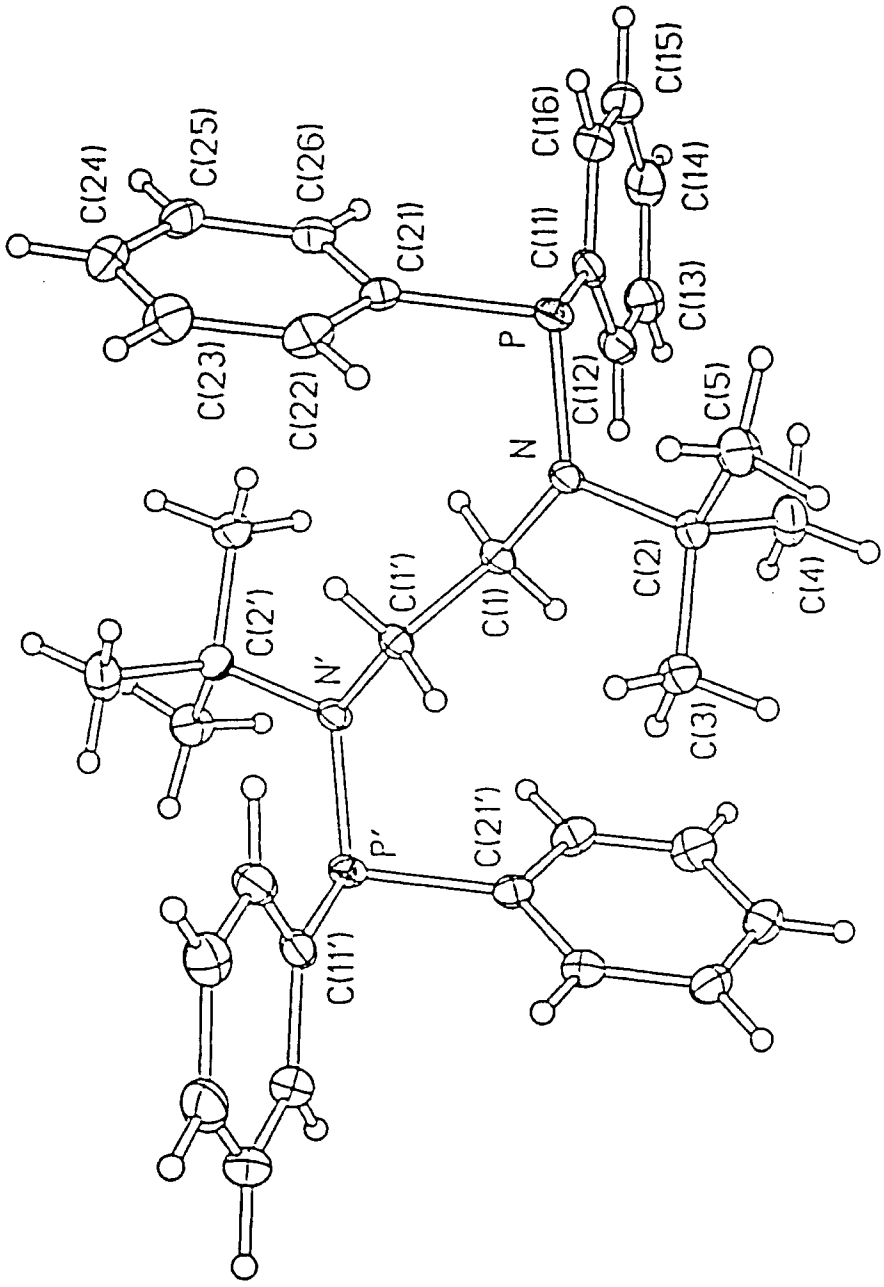

7.2.1.5 Synthesis of N,N'-bis(diphenylphosphino)-N,N'-dimethyl propylenediamine (dppmpn)

This compound was synthesised in a manner analogous to that described above for dppmen. The compound was obtained as a semi-solid. ^{31}P nmr: δ_P = 65.0ppm (s, $CDCl_3$). ^1H nmr: δ_H = 7.2-7.8ppm (m, 20H, Ph), 3.0ppm (m, 4H, NCH_2), 2.4ppm (d, J = 6.0Hz, CH_3), 1.6ppm (m, 2H, CH_2). IR: The disappearance of ν(N-H) = 3284cm^{-1} (w, neat) was noted.

7.2.1.6 Synthesis of N,N'-bis(diphenylphosphino)-N,N'-diisopropyl propylenediamine (dppippn)

This compound was synthesised in a manner analogous to that described above for dppmen. The compound was obtained as a semi-solid. ^{31}P nmr: δ_P = 48.9ppm (s, $CDCl_3$). IR: The disappearance of ν(N-H) = 3262 cm^{-1} (w, neat) was noted.

7.2.1.7 Synthesis of N,N'-bis(diphenylphosphino)piperazine (dpppip)

This compound was synthesised in a manner analogous to that described above for dppmen. The reaction mixture was washed with THF as well as toluene in this case, and the THF solution precipitated a white solid on standing (1.95g, 20.5% yield). Some oxidised material was recovered from the toluene solution. ^{31}P nmr: δ_P = 62.2ppm (s, $CDCl_3$). ^1H nmr: δ_H = 7.25-7.3ppm (m, Ph), 2.8 ppm (s, CH_2). ^{13}C nmr: δ_C = 138.3ppm (d, J_{P-C} = 14.3Hz, Ph), 132.3ppm (d, J_{P-C} = 19.4Hz, Ph), 128.8ppm (s, Ph), 128.4ppm (m, Ph), 51.0ppm (t, J_{P-C} = 10.4Hz, CH_2). IR: The disappearance of ν(N-H) = 3271 cm^{-1} (m, solid state) was noted. MS (EI, 3.7MeV): m/z = 454 (M^+). Elemental analysis: Found C: 73.94%, H: 6.18%, N: 6.19%. $C_{28}H_{28}N_2P_2$ requires C: 74.00%, H: 6.21%, N: 6.16%. Melting point 126°C.

7.2.2 Synthesis of Palladium Dichloride Complexes

7.2.2.1 Synthesis of Dichloro-P,P'-(N,N'-bis(diphenylphosphino)-N,N'-dimethyl ethylenediamine)palladium(II) [(dppmen)$PdCl_2$]

Dichloro-bis(benzonitrile)palladium (0.40g, 1.0mmol) was dissolved in dried, degassed THF (20ml) giving a deep red solution. To this was added a solution of dppmen (0.5g, 1.1mmol) in dried, degassed THF (10ml), immediately giving a green suspension. After stirring overnight the solid was removed by filtration, washed with two small portions of THF and dried in vacuo. The volume of the remaining reaction solution was reduced in vacuo to give a brown residue, which was found to contain mostly benzonitrile by IR (ν(C≡N) = 2227cm^{-1}, lit. value [5] = 2232cm^{-1}) and so was discarded. The green solid product (0.43g, 65% yield) was recrystallised by slow evaporation of a CH_2Cl_2 solution. ^{31}P nmr: δ_P = 78.3ppm (s, $CDCl_3$). ^{1}H nmr: δ_H = 7.4-7.6ppm (m, Ph, 20H), 3.4ppm (t, J = 7.9Hz, 4H, CH_2), 2.5ppm (t, J = 4.1Hz, 6H, CH_3). ^{13}C nmr: δ_C = 133.2ppm (m, Ph), 128.5ppm (m, Ph), 53.2ppm (br s, CH_2), 40.2ppm (s, CH_3). IR (CsI plates, nujol mull): ν(Pd-Cl) = 317(s), 285(s) cm^{-1}, 292(sh) cm^{-1}, ν(Pd - P) = 355(w) cm^{-1}. FAB MS (NOBA matrix): m/z = 634 (M^+), 561-2 ($(M - 2Cl)^+$), 597-9 ($(M - Cl)^+$), 635 ($(M + H)^+$), 657 ($(M + Na)^+$). Melting point: 234°C (dec.). Elemental Analysis: Found C: 52.54%, H: 4.77%, N: 4.51%. $C_{28}H_{32}N_2P_2PdCl_2$ requires C: 53.06%, H: 4.77%, N: 4.42%. A crystal suitable for X-ray diffraction analysis was grown by slow evaporation of a dichloromethane solution, and the structure was solved by Dr. D.S. Yufit. Selected bond lengths and angles are presented in Tables 7.3 and 7.4, and supplementary data can be found in Appendix 7.2.

Table 7.3: Selected Bond Lengths of [(dppmen)$PdCl_2$.CH_2Cl_2]

Bond	Length / Å	Bond	Length / Å
Pd(1)-P(1)	2.2518(7)	P(1)-N(1)	1.655(2)
Pd(1)-P(2)	2.2807(7)	P(1)-C(5)	1.829(3)
Pd(1)-Cl(1)	2.3715(7)	P(1)-C(11)	1.824(3)
Pd(1)-Cl(2)	2.3734(7)	P(2)-N(2)	1.691(2)
N(1)-C(2)	1.467(3)	P(2)-C(17)	1.824(3)
N(1)-C(1)	1.469(3)	P(2)-C(23)	1.828(3)
N(2)-C(3)	1.481(3)	C(2)-C(3)	1.518(4)
N(2)-C(4)	1.474(4)		

Table 7.4: Selected Bond Angles of [(dppmen)$PdCl_2$.CH_2Cl_2]

Bond	Angle / °	Bond	Angle / °
P(1)-Pd(1)-P(2)	94.87(3)	N(1)-P(1)-C(5)	101.06(12)
P(2)-Pd(1)-Cl(1)	85.14(2)	N(1)-P(1)-C(11)	110.27(12)
P(1)-Pd(1)-Cl(2)	88.47(2)	C(11)-P(1)-C(5)	106.58(12)
Cl(1)-Pd(1)-Cl(2)	91.03(2)	N(1)-P(1)-Pd(1)	115.03(8)
P(1)-Pd(1)-Cl(1)	175.93(3)	C(5)-P(1)-Pd(1)	118.75(9)
P(2)-Pd(1)-Cl(2)	172.34(3)	C(11)-P(1)-Pd(1)	104.86(9)
C(1)-N(1)-P(1)	120.7(2)	N(2)-P(2)-C(17)	102.77(12)
C(2)-N(1)-P(1)	122.9(2)	N(2)-P(2)-C(23)	105.38(11)
C(2)-N(1)-C(1)	116.4(2)	C(17)-P(2)-C(23)	108.47(13)
C(3)-N(2)-P(2)	117.0(2)	N(2)-P(2)-Pd(1)	118.47(8)
C(4)-N(2)-P(2)	121.9(2)	C(17)-P(2)-Pd(1)	106.26(9)
C(4)-N(2)-C(3)	109.5(2)	C(23)-P(2)-Pd(1)	114.56(9)
N(1)-C(2)-C(3)	111.4(2)	N(2)-C(3)-C(2)	113.0(2)

Fig. 7.4: Molecular Structure of Dichloro-P,P'-(N,N'-bis(diphenylphosphino)-N,N'-dimethylethylenediamine)palladium(II) as its Dichloromethane Solvate

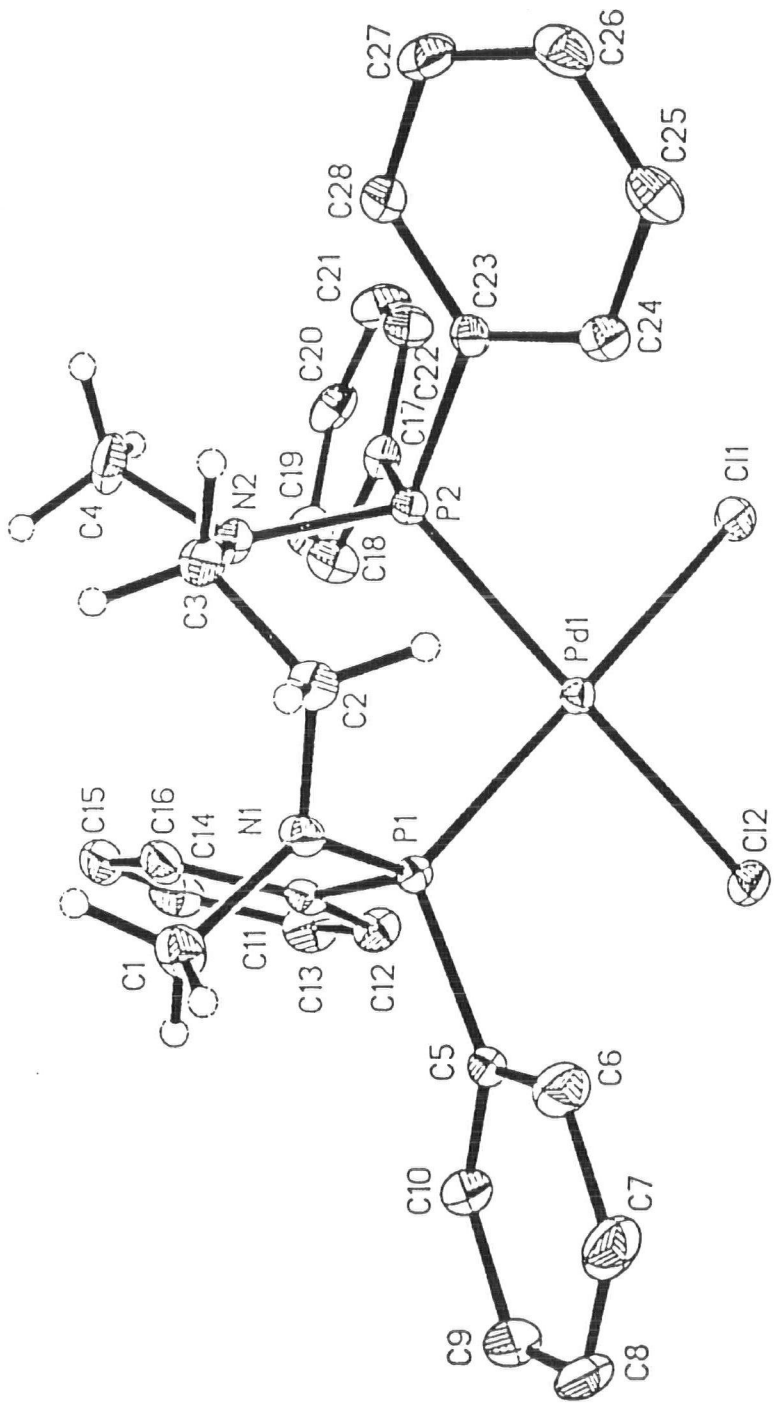

7.2.2.2 Synthesis of Dichloro-P,P'-(N,N'-bis(diphenylphosphino)-N,N'-diphenyl ethylenediamine)palladium(II) [(dpppen)$PdCl_2$]

[$(PhCN)_2PdCl_2$] (0.33g, 0.86mmol) was dissolved in dry, degassed THF (25ml) and added to a suspension of dpppen (0.51g, 0.88mmol) in THF (25ml). After an hour a bright yellow suspension had formed. The reaction mixture was stirred overnight. Yellow solid (0.21g, 33.3% yield) was isolated from the reaction by filtration and was washed with two portions of THF. The washings were combined with the reaction mixture and their volume reduced by two-thirds, yielding further yellow solid which was separated by filtration and combined with the original sample. The complex was recrystallised by the slow evaporation of a chloroform solution. ^{31}P nmr: δ_P = 87.6ppm (s, $CDCl_3$). ^{1}H nmr: δ_H = 8.1ppm (m, 8H, P-Ph), 7.4ppm (m, 12H, P-Ph), 6.9ppm (m, 6H, N-Ph), 6.6ppm (m, 4H, N-Ph), 3.88ppm (t, J = 5.9Hz, 4H, CH_2). ^{13}C nmr: δ_C = 145.8ppm (m, Ph), 135.2ppm (t, J = 6.0Hz, Ph), 131.8ppm (s, Ph), 128.8ppm (s, Ph), 128.2ppm (m, Ph), 128.0ppm (m, Ph), 125.8ppm (s, Ph), 53.9ppm (s, CH_2). IR (CsI plates, nujol mull): ν(Pd-Cl) = 311(s), 289(s) cm^{-1}, ν(Pd-P) = 374(vw) cm^{-1}. FAB MS (NOBA matrix) m/z = 721 ($(M - Cl)^+$), 685-6 ($(M - 2Cl)^+$). Melting point: 190°C (dec.). Elemental analysis for [(dpppen)$PdCl_2$.1.15$CHCl_3$]: Found C: 52.49, H: 3.97, N: 3.13%. $C_{39.15}H_{35.15}N_2P_2PdCl_{5.45}$ requires C: 52.52, H: 3.96, N: 3.13%. A crystal suitable for X-ray diffraction analysis was grown by the slow evaporation of a chloroform solution, and its structure was determined by Mr. Simon Borwick. Selected bond length and angle data are presented in Tables 7.5 and 7.6, and full data can be found in Appendix 7.3.

Table 7.5: Selected Bond Distances for [(dpppen)$PdCl_2$.$CHCl_3$]

Bond	Length / Å	Bond	Length / Å
Pd(1)-P(2)	2.262(1)	P(1)-N(1)	1.692(3)
Pd(1)-P(2)	2.288(1)	P(2)-N(2)	1.681(3)
Pd(1)-Cl(1)	2.369(1)	P(1)-C(1A)	1.821(4)
Pd(1)-Cl(2)	2.368(1)	P(1)-C(1B)	1.829(4)
N(1)-C(1)	1.488(4)	P(2)-C(1E)	1.840(4)
N(2)-C(2)	1.479(4)	P(2)-C(1F)	1.809(4)
N(1)-C(1C)	1.435(4)	C(1)-C(2)	1.509(5)
N(2)-C(1D)	1.438(4)		

Table 7.6: Selected Bond Angles of [(dpppen)$PdCl_2$.$CHCl_3$]

Bond	Angle / °	Bond	Angle / °
P(1)-Pd(1)-P(2)	98.19(3)	N(1)-P(1)-C(1A)	101.7(2)
P(1)-Pd(1)-Cl(1)	94.94(3)	N(1)-P(1)-C(1B)	102.2(2)
P(2)-Pd(1)-Cl(2)	88.32(3)	C(1A)-P(1)-C(1B)	108.8(2)
Cl(1)-Pd(1)-Cl(2)	88.87(3)	N(1)-P(1)-Pd(1)	123.33(11)
C(1)-N(1)-P(1)	120.1(2)	C(1A)-P(1)-Pd(1)	109.90(12)
C(1)-N(1)-C(1C)	116.0(3)	C(1B)-P(1)-Pd(1)	109.94(12)
C(1C)-N(1)-P(1)	123.8(2)	N(2)-P(2)-C(1F)	105.0(2)
C(2)-N(2)-P(2)	113.6(2)	N(2)-P(2)-C(1E)	101.6(2)
C(2)-N(2)-C(1D)	117.1(3)	C(1E)-P(2)-C(1F)	106.3(2)
C(1D)-N(2)-P(2)	129.3(2)	N(2)-P(2)-Pd(1)	116.51(11)
N(1)-C(1)-C(2)	112.1(3)	C(1E)-P(2)-Pd(1)	112.02(12)
C(1)-C(2)-N(2)	111.0(3)	C(1F)-P(2)-Pd(1)	114.18(12)

Fig. 7.5: Molecular Structure of Dichloro-P,P'-(N,N'-bis(diphenylphosphino)-N,N'-diphenylethylenediamine)palladium(II) as its Chloroform Solvate

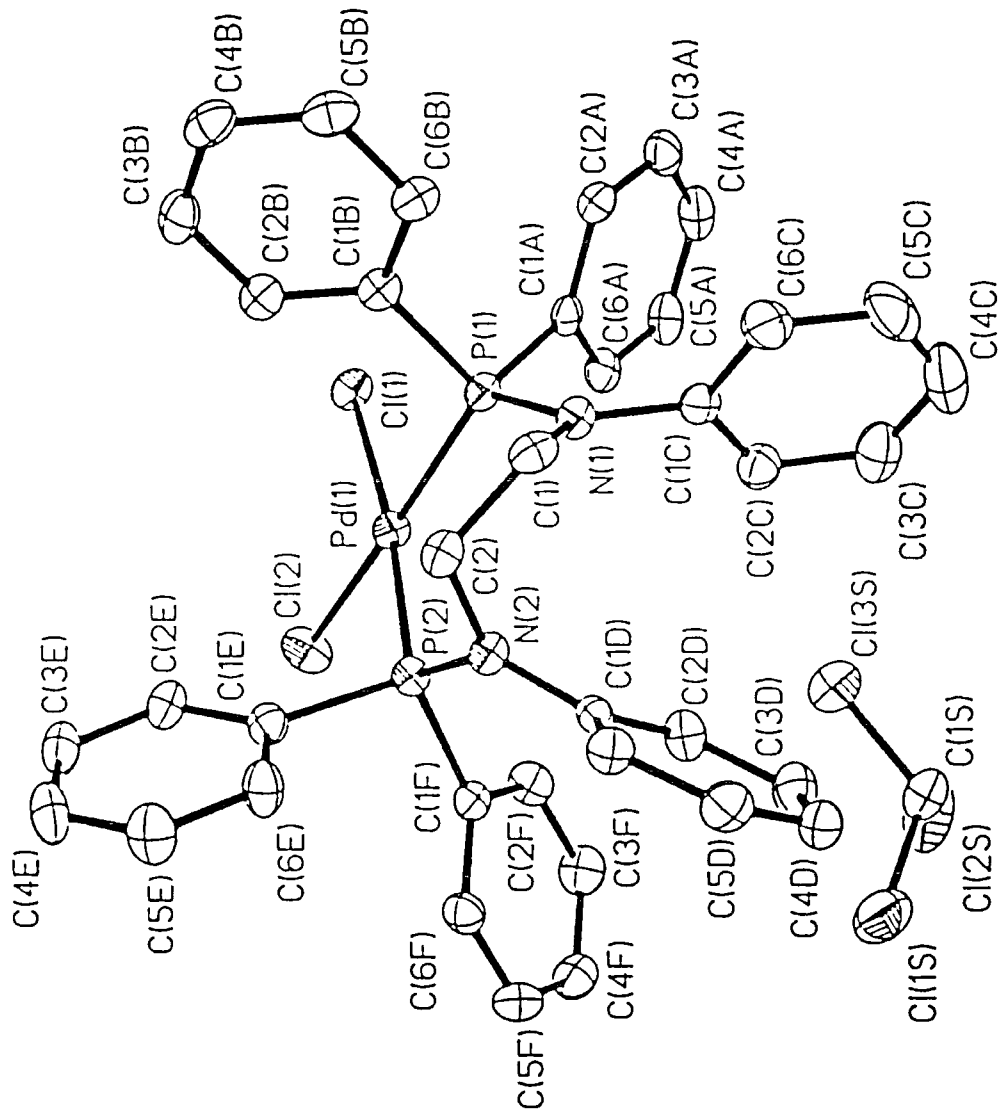

7.2.2.3 Synthesis of Dichloro-P,P'-(N,N'-bis(diphenylphosphino)-N,N'-diisopropylethylenediamine)palladium(II) [(dppipen)$PdCl_2$]

[$(PhCN)_2PdCl_2$] (0.2g, 0.52mmol) was dissolved in dry, degassed THF (10ml) to give a deep red solution. To this was added a solution of dppipen (0.3g, 0.59mmol) in dry, degassed THF (10ml). On addition the deep red solution gradually lightened to yellow and within ten minutes a yellow precipitate had formed. The reaction was allowed to stir overnight, giving a yellow precipitate and a yellow solution. The volume of the solution was reduced to aid precipitation and the solid (0.21g, 58% yield) separated by filtration. It was recrystallised by the slow evaporation of a chloroform solution. ^{31}P nmr: δ_P = 82.9ppm (s, $CDCl_3$). ^1H nmr: δ_H =7.3-7.7ppm (m, 20H, Ar), 3.45ppm (m, 6H, CH_2 and CH), 0.87ppm (d, J = 6.6Hz, 12H, CH_3). ^{13}C nmr: δ_C = 133.1ppm (t, J = 5.7Hz, Ph), 131.1ppm (s, Ph), 128.2ppm (t, J_{P-C} = 5.6Hz, Ph), 51.3ppm (t, J_{P-C} = 2.3Hz, CH), 44.6ppm (t, J_{P-C} = 6.8Hz, CH_2), 21.1ppm (s, CH_3). IR (CsI plates, nujol mull): ν(Pd - Cl) = 312(s), 293 (vs) cm^{-1}, ν(Pd - P) = 329(w) cm^{-1}. FAB MS (NOBA matrix): m/z = 655 ($(M - Cl)^+$), 617-8 ($(M - 2Cl)^+$). Melting point: 178°C (dec.). Elemental analysis for [(dppipen)$PdCl_2$.0.18$CHCl_3$]: Found C: 54.34, H: 5.55, N: 4.06%. $C_{32.18}H_{38.18}N_2P_2PdCl_{2.54}$ requires C: 54.33, H: 5.41, N: 3.94%.

7.2.2.4 Synthesis of Dichloro-P,P'-(N,N'-bis(diphenylphosphino)-N,N'-di-*tert*-butylethylenediamine)palladium(II) [(dpptben)$PdCl_2$]

[$(PhCN)_2PdCl_2$] (0.36g, 0.94mmol) was dissolved in dry, degassed THF (10ml) to give a deep red solution. To this was added a solution of dpptben (0.52g, 0.96mmol) in dry, degassed THF (15ml). This gave a yellow-orange solution, which was allowed to stir overnight, giving a yellow precipitate which was separated by filtration. Further yellow solid was obtained from the solution. The two portions of solid were combined, washed with THF and dried in vacuo (Yield 0.27g, 40%). The solid was recrystallised by slow evaporation of a chloroform solution. ^{31}P nmr: δ_P = 76.8ppm. ^1H nmr: δ_H = 7.8ppm (m, 8H, Ph), 7.3-7.5ppm (m, 12H, Ph), 3.84ppm (t, J = 9.6Hz, 4H, CH_2), 1.09ppm (s, 18H, CH_3). ^{13}C nmr: δ_C = 133.6ppm (t, J_{P-C} = 5.9Hz, Ph), 131.1ppm (s, Ph), 128.0ppm (t, J_{P-C} = 5.7Hz), 62.7ppm (t, J_{P-C} = 3.8Hz, CMe_3), 50.9ppm (t, $^2J_{P-C}$ = 8.3Hz, CH_2), 31.0ppm (s, CH_3). IR (CsI plates, nujol mull): ν(Pd - Cl) = 306(s), 289(s) cm^{-1}.

FAB MS (NOBA matrix) m/z = 645-7 ($(M - 2Cl)^+$), 681-3 ($(M - Cl)^+$). Melting point: 184°C (dec.). Elemental analysis for [(dpptben)$PdCl_2$.1.15$CHCl_3$]: Found C: 49.43, H: 5.17, N: 3.28%. $C_{35.15}H_{43.15}N_2P_2PdCl_{5.45}$ requires C: 49.36, H: 5.09, N: 3.28%. A crystal suitable for X-ray diffraction analysis was grown by slow evaporation of a tetrahydrofuran solution, and the structure was solved by Mr. Michael Leech. Selected bond lengths and angles are shown in Tables 7.7 and 7.8, and a full set of supplementary data can be found in Appendix 7.4.

Table 7.7: Selected Bond Lengths of [(dpptben)$PdCl_2$.2THF]

Bond	Length / Å	Bond	Length / Å
Pd(1)-P(1)	2.2904(7)	P(1)-N(1)	1.698(3)
Pd(1)-P(2)	2.2758(8)	P(2)-N(2)	1.676(3)
Pd(1)-Cl(1)	2.3504(7)	N(1)-C(1)	1.554(4)
Pd(1)-Cl(2)	2.3653(8)	N(1)-C(2)	1.491(4)
C(2)-C(3)	1.520(4)	N(2)-C(3)	1.482(4)
C(1)-C(5)	1.530(5)	N(2)-C(4)	1.533(4)
C(1)-C(6)	1.525(5)	C(4)-C(8)	1.526(5)
C(1)-C(7)	1.542(4)	C(4)-C(9)	1.527(5)
C(4)-C(10)	1.529(5)		

Table 7.8: Selected Bond Angles of [(dpptben)$PdCl_2$.2THF]

Bond	Angle / °	Bond	Angle / °
P(1)-Pd(1)-P(2)	98.54(3)	Pd(1)-P(1)-N(1)	120.03(9)
P(1)-Pd(1)-Cl(2)	83.62(3)	Pd(1)-P(1)-C(17)	101.4(1)
P(2)-Pd(1)-Cl(1)	89.31(3)	N(1)-P(1)-C(17)	108.45(13)
Cl(1)-Pd(1)-Cl(2)	87.95(3)	Pd(1)-P(1)-C(11)	110.5(1)
P(1)-Pd(1)-Cl(1)	169.93(3)	N(1)-P(1)-C(11)	105.82(13)
P(2)-Pd(1)-Cl(2)	173.79(3)	C(17)-P(1)-C(11)	110.47(14)
Pd(1)-P(2)-C(23)	113.39(12)	P(1)-N(1)-C(1)	127.8(2)
Pd(1)-P(2)-C(29)	103.57(11)	P(1)-N(1)-C(2)	111.91(19)
C(23)-P(2)-C(29)	106.02(17)	C(1)-N(1)-C(2)	109.3(2)
Pd(1)-P(2)-N(2)	115.5(1)	P(2)-N(2)-C(3)	115.3(2)
C(23)-P(2)-N(2)	106.94(15)	P(2)-N(2)-C(4)	127.3(2)
C(29)-P(2)-N(2)	111.04(14)	C(3)-N(2)-C(4)	114.9(2)

N(1)-C(2)-C(3)	118.7(2)	N(2)-C(3)-C(2)	115.4(2)
N(1)-C(1)-C(5)	106.9(3)	N(2)-C(4)-C(8)	109.0(3)
N(1)-C(1)-C(6)	115.0(3)	N(2)-C(4)-C(9)	111.7(3)
N(1)-C(1)-C(7)	110.9(2)	N(2)-C(4)-C(10)	110.6(3)
C(5)-C(1)-C(6)	106.7(3)	C(8)-C(4)-C(9)	107.4(3)
C(5)-C(1)-C(7)	109.9(3)	C(8)-C(4)-C(10)	109.4(3)
C(6)-C(1)-C(7)	107.3(3)	C(9)-C(4)-C(10)	108.7(3)

Fig. 7.6: Molecular Structure of Dichloro-P,P'-(N,N'-bis(diphenylphosphino)-N,N'-di-*tert*-butylethylenediamine)palladium(II) as its Bis(tetrahydrofuran) Solvate

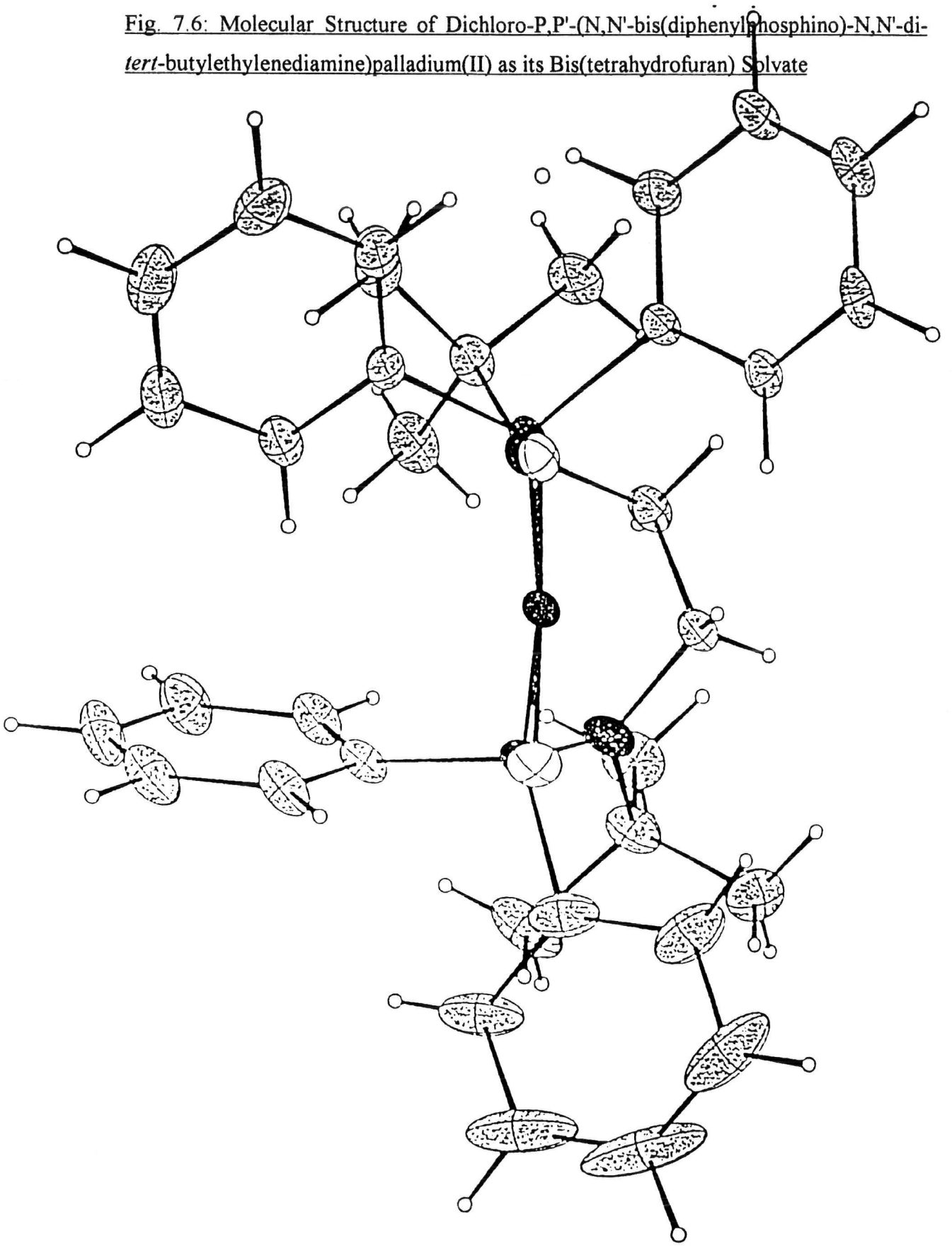

7.2.2.5 Synthesis of Dichloro-P,P'-(N,N'-bis(diphenylphosphino)-N,N'-dimethyl propylenediamine)palladium (II) [(dppmpn)$PdCl_2$]

This complex was synthesised in a manner analogous to that described for [(dppmen)$PdCl_2$] above, giving a yellow solid (0.33g, 48% yield) which was recrystallised by slow evaporation of a chloroform solution. ^{31}P nmr: δ_P = 90.9ppm (s, $CDCl_3$). ^1H nmr: δ_H = 8.0-8.1ppm (m, 8H, Ph), 7.5ppm (m, 12H, Ph), 2.91ppm (s, 4H, NCH_2), 2.41ppm (s, 6H, CH_3), 1.75ppm (s, 2H, CH_2). ^{13}C nmr: δ_C = 134.6ppm (t, J_{P-C} = 23.4Hz, Ph), 131.4ppm (s, Ph), 128.4ppm (t, J_{P-C} = 21.8Hz), 52.8ppm (s, NCH_2), 37.1ppm (s, CH_3), 24.9ppm (m, CH_2). IR (CsI plates, nujol mull): ν(Pd - Cl) = 309(m), 285(vs) cm^{-1}. FAB MS (NOBA matrix) m/z = 576 ($(M - 2Cl)^+$), 611-3 ($(M - Cl)^+$), 648 (M^+), 671 ($(M + Na)^+$). Melting point: 197°C (dec.). Elemental analysis for [(dppmpn)$PdCl_2$.0.65$CHCl_3$]: Found C: 49.00, H: 4.47, N: 3.80%. $C_{29.65}H_{32.65}N_2P_2PdCl_{3.95}$ requires C: 49.09, H: 4.54, N: 3.86%. A crystal suitable for X-ray analysis was grown by the slow evaporation of a chloroform solution, and its structure was determined by Dr. D.S. Yufit. Selected bond length and angle data are presented in Tables 7.9 and 7.10, and full data can be found in Appendix 7.5.

Table 7.9: Selected Bond Lengths of [(dppmpn)$PdCl_2$]

Bond	Length / Å	Bond	Length / Å
Pd(1) - P(1)	2.2593(9)	P(1) - N(1)	1.683(2)
Pd(1) - P(2)	2.2693(8)	P(1) - C(6)	1.812(3)
Pd(1) - Cl(1)	2.3757(9)	P(1) - C(12)	1.839(3)
Pd(1) - Cl(2)	2.3861(8)	P(2) - N(2)	1.670(2)
N(1) - C(1)	1.474(4)	P(2) - C(18)	1.835(3)
N(1) - C(2)	1.477(4)	P(2) - C(24)	1.828(3)
N(2) - C(4)	1.471(4)	C(2) - C(3)	1.526(4)
N(2) - C(5)	1.470(4)	C(3) - C(4)	1.530(4)

Table 7.10: Selected Bond Angles for [(dppmpn)$PdCl_2$]

Bond	Angle / °	Bond	Angle / °
P(1) - Pd - P(2)	99.74(3)	N(1) - P(1) - C(6)	102.83(13)
P(1) - Pd - Cl(2)	84.88(3)	N(1) - P(1) - C(12)	104.28(13)
P(2) - Pd - Cl(1)	86.73(3)	C(6) - P(1) - C(12)	109.06(14)
Cl(1) - Pd(1) - Cl(2)	90.19(3)	N(1) - P(1) - Pd(1)	109.11(9)
C(1) - N(1) - P(1)	122.7(2)	C(6) - P(1) - Pd(1)	111.57(10)
C(2) - N(1) - P(1)	115.7(2)	C(12) - P(1) - Pd(1)	109.38(10)
C(1) - N(1) - C(2)	113.0(3)	N(2) - P(2) - C(18)	100.67(13)
C(4) - N(2) - P(2)	124.5(2)	N(2) - P(2) - C(24)	102.57(13)
C(5) - N(2) - P(2)	120.4(2)	C(18) - P(2) - C(24)	110.45(13)
C(4) - N(2) - C(5)	114.5(2)	N(2) - P(2) - Pd(1)	124.92(10)
N(1) - C(2) - C(3)	113.0(3)	C(18) - P(2) - Pd(1)	107.51(10)
C(2) - C(3) - C(4)	112.9(3)	C(24) - P(2) - Pd(1)	110.02(10)
C(3) - C(4) - N(2)	115.3(3)		

Fig. 7.7: The Molecular Structure of Dichloro-P,P'-(N,N'-bis(diphenylphosphino)-N,N'-dimethylpropylenediamine)palladium(II)

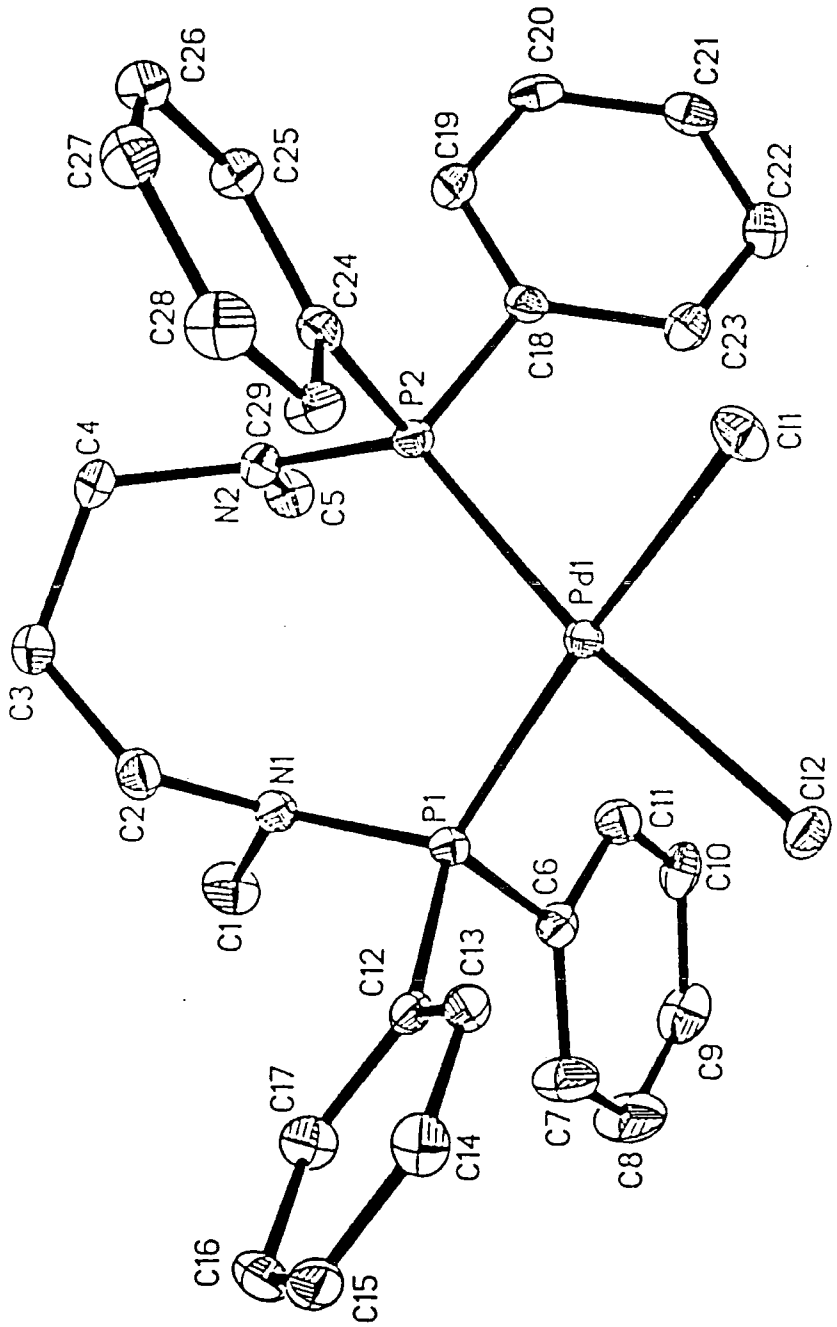

7.2.2.6 Attempted Synthesis of Dichloro-P,P'-(N,N'-bis(diphenylphosphino)-N,N'-diisopropylpropylenediamine)palladium(II) [(dppippn)$PdCl_2$]

[$(PhCN)_2PdCl_2$] (0.22g, 0.57mmol) was dissolved in 20 ml dry, degassed THF to give a deep red solution. To this was added a solution containing an excess of dppippn (0.98g, 1.86mmol) in dry, degassed THF (10ml). The colour changed immediately to deep orange, but no precipitate formed. The reaction was allowed to stir overnight. The solvent was removed slowly in vacuo to promote precipitation; however, only palladium black was seen. ^{31}P nmr: δ_P = 86.6ppm (s, THF) - major peak. ^1H nmr of impure sample: δ_H = 7.4-8.0ppm (Ph), 3.3ppm (br, NCH_2), 1.41ppm (d, J = 6.4Hz, CH_2), 0.87ppm (d, J = 6.6Hz, CH_3).

7.2.2.7 Synthesis of Dichloro-P,P'-(N,N'-bis(diphenylphosphino)piperazine) palladium(II) [(dpppip)$PdCl_2$]

To a solution of [$(PhCN)_2PdCl_2$] (0.34g, 0.89mmol) in dry, degassed THF (30ml) was added a solution of dpppip (0.42g, 0.93mmol) also in dry, degassed THF (10ml). This caused an immediate colour change from red to yellow. On stirring overnight, a yellow solid precipitated, which was separated from the pale yellow solution by filtration and dried in vacuo (0.48g, 86% yield). ^{31}P nmr: δ_P = 104.1ppm (s, $CDCl_3$). ^1H nmr: δ_H = 8.4ppm, 7.4-7.6ppm (2m, 20H, Ph), 1.5ppm (s, 8H, CH_2). IR: ν(Pd - Cl) = 358(vs) cm^{-1}. FAB MS (NOBA matrix): m/z = 560 ($(M - 2Cl)^+$), 597 ($(M - Cl)^+$), 655 ($(M + Na)^+$). Melting point: 182°C (dec.). Elemental analysis: Found C: 53.30%, H: 4.48%, N: 4.51%. $C_{28}H_{28}N_2P_2PdCl_2$ requires C: 53.23%, H: 4.47%, N: 4.43%.

7.2.2.8 Synthesis of Diacetato-P,P'-(N,N'-bis(diphenylphosphino)-N,N'-dimethylethylenediamine)palladium(II) [(dppmen)$Pd(OAc)_2$]

A solution of dppmen (0.63g, 1.4 mmol) in dried, degassed THF (20ml) was added to a solution of palladium acetate (0.30g, 1.3 mmol) in dried, degassed THF (20ml). This caused the colour of the solution to change from yellow/brown to deep red. The addition of a small amount of dried, degassed hexane caused the precipitation of a red solid. This proved to be difficult to characterise by nmr or infrared spectroscopy, mass spectrometry or elemental analysis. However, a crystal suitable for X-ray analysis

was grown from a THF solution, and its structure solved by Mr. Angus Mackinnon. Selected bond length and angle data are shown in Tables 7.11 and 7.12, and full supplementary data are given in Appendix 7.6.

Table 7.11: Selected Bond Length Data of [(dppmen)Pd(OCOCH$_3$)$_2$]

Bond	Length / Å	Bond	Length / Å
Pd(1)-O(8)	2.088(3)	P(2)-N(3)	1.654(4)
Pd(1)-O(12)	2.091(3)	P(2)-C(16)	1.824(5)
Pd(1)-P(2)	2.2348(13)	P(2)-C(22)	1.826(5)
Pd(1)-P(7)	2.2494(15)	P(7)-N(6)	1.691(4)
O(8)-C(9)	1.275(6)	P(7)-C(28)	1.820(4)
O(12)-C(13)	1.285(5)	P(7)-C(34)	1.811(5)
C(4)-N(3)	1.460(6)	C(9)-O(10)	1.222(6)
C(40)-N(3)	1.471(6)	C(13)-O(15)	1.236(6)
C(5)-N(6)	1.485(6)	C(9)-C(11)	1.513(7)
C(41)-N(6)	1.468(6)	C(13)-C(14)	1.528(7)
C(4)-C(5)	1.515(6)		

Table 7.12: Selected Bond Angles of [(dppmen)Pd(OCOCH$_3$)$_2$]

Bond	Angle / °	Bond	Angle / °
P(2)-Pd(1)-P(7)	95.65(5)	C(4)-N(3)-C(40)	116.2(4)
P(2)-Pd(1)-O(8)	88.70(10)	C(4)-N(3)-P(2)	121.5(3)
O(8)-Pd(1)-O(12)	90.37(13)	P(2)-N(3)-C(40)	112.3(3)
O(12)-Pd(1)-P(7)	84.82(10)	C(5)-N(6)-C(41)	107.7(4)
N(6)-C(5)-C(4)	115.4(4)	C(5)-N(6)-P(7)	118.5(3)
N(3)-C(4)-C(5)	114.2(4)	P(7)-N(6)-C(41)	117.9(3)
N(3)-P(2)-Pd(1)	114.9(2)	N(6)-P(7)-Pd(1)	120.21(14)
C(22)-P(2)-Pd(1)	107.7(2)	C(28)-P(7)-Pd(1)	104.8(2)
C(16)-P(2)-Pd(1)	113.9(2)	C(34)-P(7)-Pd(1)	112.0(2)
N(3)-P(2)-C(16)	103.8(2)	N(6)-P(7)-C(28)	103.7(2)
N(3)-P(2)-C(22)	109.9(2)	N(6)-P(7)-C(34)	107.5(2)
C(16)-P(2)-C(22)	106.3(2)	C(28)-P(7)-C(34)	107.7(2)
Pd(1)-O(8)-C(9)	112.1(3)	Pd(1)-O(12)-C(13)	122.4(3)

O(8)-C(9)-C(11)	114.6(5)	O(12)-C(13)-O(15)	122.3(4)
O(8)-C(9)-O(10)	124.7(5)	O(12)-C(13)-C(14)	118.6(4)
C(11)-C(9)-O(10)	120.7(5)	C(14)-C(13)-O(15)	119.1(4)

Fig. 7.8: Molecular Structure of O,O'-diacetato-P,P'-(N,N'-bis(diphenylphosphino)-N,N'-dimethylethylenediamine)palladium(II)

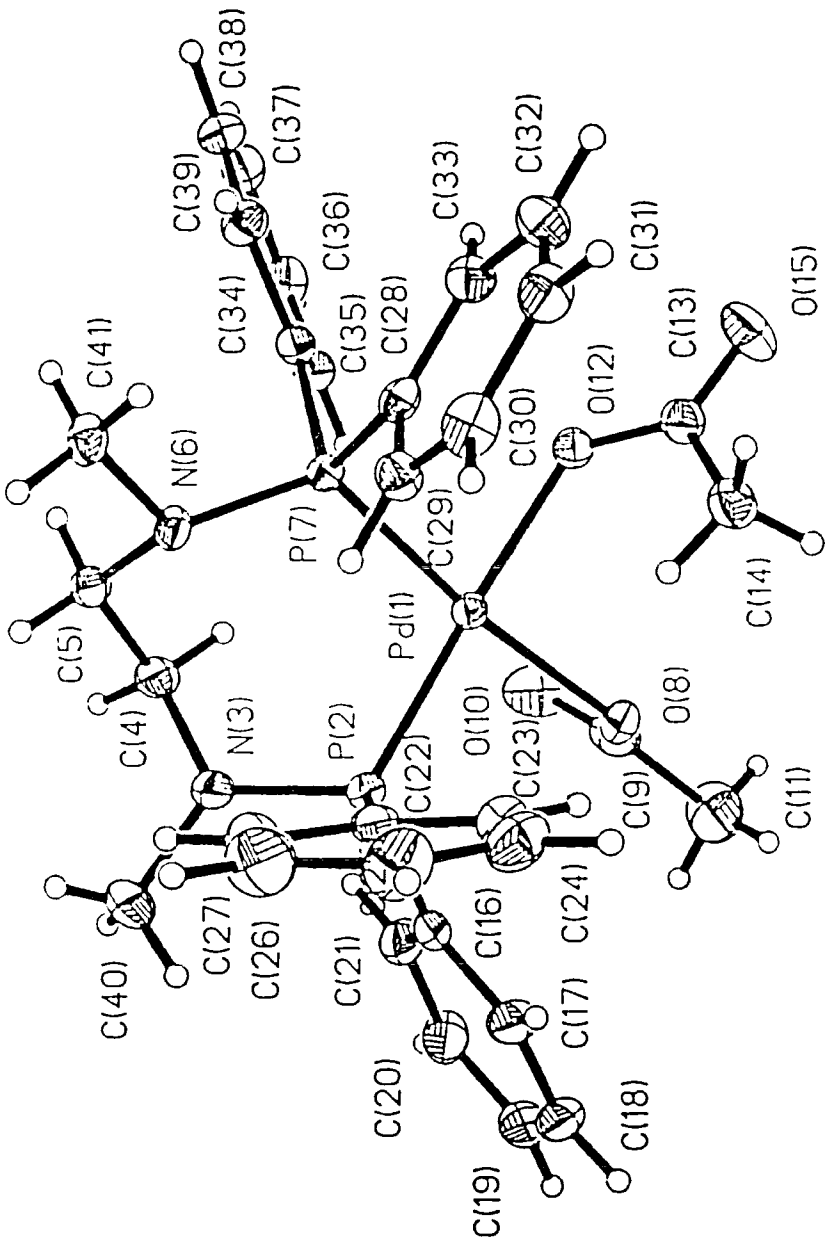

7.2.3 Synthesis of Platinum Complexes

7.2.3.1 Synthesis of Dichloro-P,P'-(N,N'-bis(diphenylphosphino)-N,N'-dimethyl ethylenediamine)platinum(II) [(dppmen)$PtCl_2$]

A solution of dppmen (0.51g, 1.12mmol) in dry degassed THF (15ml) was added to a suspension of [$(PhCN)_2PtCl_2$] (0.50g, 1.06mmol) in dry, degassed THF (15ml) by stirring. Within a few minutes the colour had lightened to pale yellow. After being allowed to stir overnight, a cream-coloured solid had precipitated and was separated by filtration. The yellow solution contained predominantly benzonitrile (along with THF solvent) and was discarded. The solid was washed with two small portions of dry, degassed THF and dried in vacuo. Yield 0.48g (59%). ^{31}P nmr: δ_P = 55.2ppm (t, $^1J_{Pt\text{-}P}$ = 4022Hz, $CDCl_3$). ^1H nmr: δ_H = 7.3-7.5ppm (m, 20H, Ph), 3.4ppm (dt, J = 45.2Hz, J = 15Hz, 4H, CH_2), 2.5ppm (dt, J = 45.2Hz, J = 7.5Hz, 6H, CH_3). ^{13}C nmr: δ_C = 128 - 133ppm (m, Ph), 52.5ppm (s, CH_2), 39.6ppm (d, $^2J_{P\text{-}C}$ = 8Hz, CH_3). IR (CsI plates, nujol mull): ν(Pt - Cl): 317(s), 290(s) cm^{-1}. FAB MS (NOBA matrix) m/z = 650-1 ($(M - 2Cl)^+$), 687 ($(M - Cl)^+$), 722 (M^+), 745 ($(M + Na)^+$). Melting point: 286°C (dec.). Elemental analysis: Found C: 46.20%, H: 4.14%, N: 3.97%. $C_{28}H_{30}N_2P_2PtCl_2$ requires C: 46.55%, H: 4.19%, N: 3.88%. A crystal suitable for X-ray diffraction analysis was grown by slow evaporation of a dichloromethane solution, and its structure was solved by Dr. JingWen Yao. Selected bond lengths and angles are given in Tables 7.13 and 7.14, and full supplementary data is in Appendix 7.7.

Table 7.13: Selected Bond Lengths of [(dppmen)$PtCl_2.CH_2Cl_2$]

Bond	Length / Å	Bond	Length / Å
Pt(1)-P(1)	2.2498(7)	P(1)-N(1)	1.693(2)
Pt(1)-P(2)	2.2302(6)	P(1)-C(11)	1.823(3)
Pt(1)-Cl(1)	2.3707(6)	P(1)-C(21)	1.824(3)
Pt(1)-Cl(2)	2.3674(7)	P(2)-N(2)	1.649(2)
N(1)-C(1)	1.473(3)	P(2)-C(31)	1.825(3)
N(1)-C(01)	1.476(3)	P(2)-C(41)	1.813(3)
N(2)-C(2)	1.463(3)	C(1)-C(2)	1.519(4)
N(2)-C(02)	1.468(3)		

Table 7.14: Selected Bond Angles of [(dppmen)$PtCl_2.CH_2Cl_2$]

Bond	Angle / °	Bond	Angle / °
P(1)-Pt(1)-P(2)	95.46(2)	N(1)-P(1)-C(11)	102.6(1)
P(1)-Pt(1)-Cl(1)	85.97(2)	N(1)-P(1)-C(21)	105.0(1)
P(2)-Pt(1)-Cl(2)	89.60(2)	C(11)-P(1)-C(21)	108.5(1)
Cl(1)-Pt(1)-Cl(2)	88.54(2)	N(1)-P(1)-Pt(1)	117.8(1)
P(1)-Pt(1)-Cl(2)	171.95(2)	C(11)-P(1)-Pt(1)	107.1(1)
P(2)-Pt(1)-Cl(1)	175.70(2)	C(21)-P(1)-Pt(1)	114.8(1)
C(1)-N(1)-C(01)	109.6(2)	N(2)-P(2)-C(41)	109.9(1)
C(1)-N(1)-P(1)	117.1(2)	N(2)-P(2)-C(31)	101.1(1)
C(01)-N(1)-P(1)	121.2(2)	C(41)-P(2)-C(31)	106.4(1)
C(2)-N(2)-C(02)	116.6(2)	N(2)-P(2)-Pt(1)	115.1(1)
C(2)-N(2)-P(2)	122.8(2)	C(41)-P(2)-Pt(1)	106.1(1)
C(02)-N(2)-P(2)	120.5(2)	C(31)-P(2)-Pt(1)	117.9(1)
N(1)-C(1)-C(2)	112.9(2)	N(2)-C(2)-C(1)	111.4(2)

Fig. 7.9: Molecular Structure of Dichloro-P,P'-(N,N'-bis(diphenylphosphino)-N,N'-dimethylethylenediamine)platinum(II) as its Dichloromethane Solvate

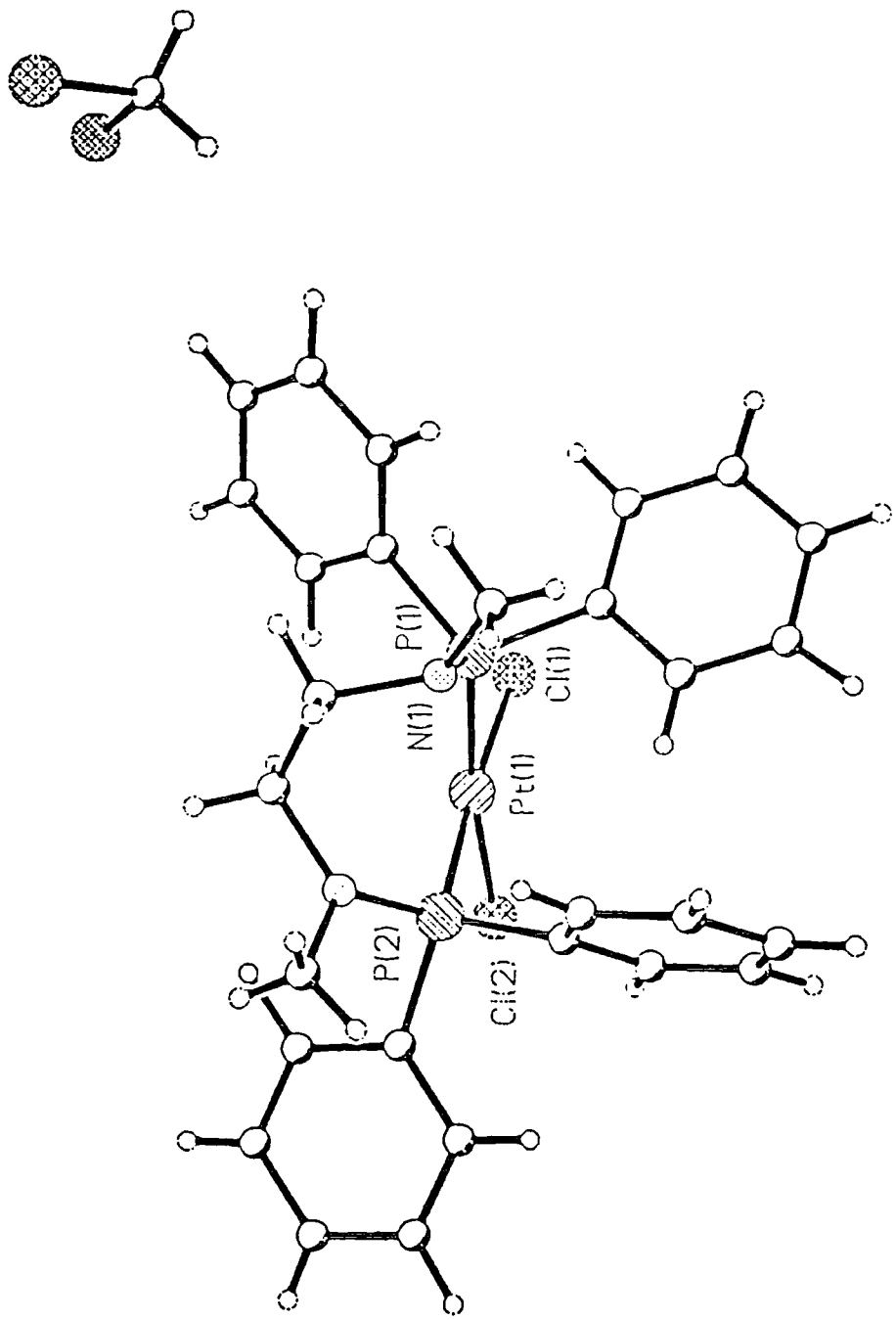

7.2.3.2 Synthesis of Dichloro-P,P'-(N,N'-bis(diphenylphosphino)-N,N'-diphenyl ethylenediamine)platinum(II) [(dpppen)$PtCl_2$]

A solution of dpppen (0.25g, 0.43mmol) in dry, degassed toluene was added to a suspension of [$(PhCN)_2PtCl_2$] (0.20g, 0.42mmol) in dry, degassed toluene (15ml). This caused a slight lightening of the colour of the solution. The mixture was allowed to stir overnight before being heated briefly to reflux and cooled to room temperature. A small amount of a beige precipitate was separated by filtration, washed with a small (10ml) portion of diethyl ether and dried in vacuo (Yield 0.21g, 59%). The solid produced was recrystallised by slow evaporation of a dichloromethane solution. ^{31}P nmr: δ_P = 61.7ppm (t, $^1J_{Pt-P}$ = 4206Hz, $CDCl_3$). ^1H nmr: δ_H = 8.1ppm, 7.4ppm (2 m, 20H, P-Ph), 6.9ppm, 6.7ppm (2 m, 10H, N-Ph), 3.77ppm (d, J = 11.6Hz, 4H, CH_2). ^{13}C nmr: δ_C = 145.6ppm (s, P-Ph), 135.4ppm (m, P- Ph), 131.7ppm (s, P-Ph), 131.5ppm (s, P-Ph), 130.0ppm (s, N-Ph), 128.6ppm (m, N-Ph), 128.0ppm (m, N-Ph), 125.7ppm (s, N-Ph), 53.6ppm (s, CH_2). IR (CsI plates, nujol mull): ν(Pt - Cl) = 315(m), 288(m) cm^{-1}. FAB MS (NOBA matrix) m/z = 774-5 ($(M - 2Cl)^+$), 811 ($(M - Cl)^+$), 846 (M^+), 869 ($(M + Na)^+$). Melting point: 227°C (dec.). Elemental analysis for [(dpppen)$PtCl_2$.1.6CH_2Cl_2]: Found C: 48.29, H: 3.81, N: 3.08%. $C_{39.6}H_{37.2}N_2P_2PtCl_{5.2}$ requires C: 48.41, H: 3.82, N: 2.85%.

7.2.3.3 Synthesis of Dichloro-P,P'-(N,N'-bis(diphenylphosphino)-N,N'-diisopropylethylenediamine)platinum(II) [(dppipen)$PtCl_2$]

A solution of dppipen (0.25g, 0.49mmol) in dry, degassed THF was added to a suspension of [$(PhCN)_2PtCl_2$] (0.20g, 0.42mmol) in dry, degassed THF (10ml) to give a yellow solution. The colour of the solution lightened immediately and it became more clear; however, within ten minutes there was a precipitate forming. After stirring overnight, an off-white solid was present in a pale green solution. The solid was separated by filtration and dried briefly in vacuo. The solution was shown to contain a small amount of the platinum product (by ^{31}P nmr) but was discarded as it was shown by IR to contain largely benzonitrile. This gave an isolated yield of 0.18g (55%) of off-white solid, which could be recrystallised by the slow evaporation of a dichloromethane solution. ^{31}P nmr: δ_P = 59.8ppm (t, $^1J_{Pt-P}$ = 4030Hz, $CDCl_3$). ^1H nmr: δ_H = 7.3-7.7ppm (m, 20H, Ph), 3.46ppm (d, J = 17.6Hz, 4H, CH_2), 1.59ppm (s, 2H, CH), 0.86ppm (d, J =

6.4Hz, 12H, CH_3). ^{13}C nmr: δ_C = 133.3ppm (m, Ph), 131.1ppm (s, Ph), 128.1ppm (m, Ph), 50.9ppm (t, J_{P-C} = 13.7Hz, CH_2), 44.2ppm (m, CH), 21.2ppm (s, CH_3). FAB MS (NOBA matrix): m/z = 706-7 ($(M - 2Cl)^+$), 743 ($(M - Cl)^+$), 777-8 (M^+). Melting point: 258°C (dec.). Elemental analysis for [(dppipen)$PtCl_2$.0.3CH_2Cl_2]: Found C: 48.15, H: 4.95, N: 3.61%. $C_{32.3}H_{38.6}N_2P_2PtCl_{2.6}$ requires C: 48.25, H: 4.84, N: 3.48%.

7.2.3.4 Synthesis of Dichloro-P,P'-(N,N'-bis(diphenylphosphino)-N,N'-di-*tert*-butylethylenediamine)platinum(II) [(dpptben)$PtCl_2$]

A solution of dpptben (0.51g, 0.94mmol) in dry, degassed THF (15ml) was added to a suspension of [$(PhCN)_2PtCl_2$] (0.41g, 0.87mmol) in dry, degassed THF (15ml). This resulted in a slight darkening of the solution. After stirring overnight, an off-white solid in an opaque solution was produced. The THF was removed in vacuo and the remaining solid was washed with four small portions of diethylether and dried in vacuo, giving an off white solid (0.25g, 35.7% yield). The solid was recrystallised by slow evaporation of a dichloromethane solution. ^{31}P nmr: δ_P = 54.5ppm (t, $^1J_{Pt-P}$ = 4141Hz, $CDCl_3$). ^1H nmr: δ_H = 7.7ppm (m, 8H, Ph), 7.3ppm (m, 12H, Ph), 3.87ppm (d, J = 18.2Hz, 4H, CH_2), 1.08ppm (s, 18H, CH_3). ^{13}C nmr: δ_C = 133.9ppm (m, Ph), 130.9ppm (s, Ph), 127.7ppm (m, Ph), 61.9ppm (d, J_{P-C} = 7.5Hz, CMe_3), 50.4ppm (m, CH_2), 31.2ppm (s, CH_3). IR: ν(Pt - Cl) = 312(s), 288(s) cm^{-1}. FAB MS (NOBA matrix): m/z = 734-5 ($(M - 2Cl)^+$), 771 ($(M - Cl)^+$). Melting point: 288°C (dec.). Elemental analysis: C: 50.52%, H: 5.36%, N: 3.53%. $C_{34}H_{42}N_2P_2PtCl_2$ requires C: 50.63%, H: 5.36%, N: 3.53%.

7.2.3.5 Synthesis of Dichloro-P,P'-(N,N'-bis(diphenylphosphino)-N,N'-dimethyl propylenediamine)platinum(II) [(dppmpn)$PtCl_2$]

This complex was synthesised in a similar fashion to that described above, and gave an off-white solid (0.28g, 36% yield). The solid was recrystallised by the slow evaporation of a dichloromethane solution. ^{31}P nmr: δ_P = 65.0ppm (t, $^1J_{Pt-P}$ = 4174Hz, $CDCl_3$). ^1H nmr: δ_H = 8.0ppm (m, 8H, Ph), 7.5ppm (m, 12H, Ph), 3.02ppm (br s, 4H, N-CH_2), 2.44ppm (d, J = 10.2Hz, 6H, CH_3). ^{13}C nmr: δ_C = 134.7ppm (m, Ph), 131.4ppm (s, Ph), 128.3ppm (m, Ph), 128.1ppm (s, Ph), 52.8ppm (br s, CH_2), 36.9ppm (s, CH_3). IR (CsI plates, nujol mull): 309(s), 286(s) cm^{-1}. FAB MS (NOBA matrix): m/z = 664-5

$((M - 2Cl)^+)$, 700 $((M - Cl)^+)$, 736 (M^+), 759 $((M + Na)^+)$. Melting point: 256°C (dec.). Elemental analysis for $[(dppmpn)PtCl_2.0.75CH_2Cl_2]$: Found C: 44.71, H: 4.12, N: 3.08%. $C_{29.75}H_{33.5}N_2P_2PtCl_{3.5}$ requires C: 44.65, H: 4.22, N: 3.50%.

7.2.3.6 Synthesis of Dichloro-P,P'-(N,N'-bis(diphenylphosphino)-N,N'-diisopropylpropylenediamine)platinum(II) [(dppippn)PtCl$_2$]

A solution of dppippn (0.32g, 0.61mmol) in dry, degassed THF (10ml) was added to a suspension of $[(PhCN)_2PtCl_2]$ (0.20g, 0.42mmol) in dry, degassed THF (10ml). Initially, this caused the solution to clear, but within ten minutes precipitation started. The solution was allowed to stir overnight, giving a white solid in a pale green solution, which was cooled in an ice-bath to aid precipitation before the solid was separated by filtration. The white solid was dried briefly in vacuo (Yield 0.14g, 42%), and was recrystallised by slow evaporation of a chloroform solution. ^{31}P nmr: δ_P = 62.2ppm (t, $^1J_{Pt-P}$ = 4155Hz, $CDCl_3$). ^1H nmr: δ_H = 7.9ppm (m, 8H, Ph), 7.4ppm (m, 12H, Ph), 3.3ppm (m, 4H, NCH_2), 1.71ppm (br s, 2H, CH_2), 1.39ppm (s, 2H, CH), 0.81ppm (d, J = 6.6Hz, CH_3). ^{13}C nmr: δ_C = 137ppm (s, Ph), 136.8ppm (m, Ph), 133.9ppm (s, Ph), 131.1ppm (m, Ph), 53.8ppm (s, NCH_2), 44.8ppm (s, CH_2), 25.3ppm (s, CH_3), 22.3ppm (s, CH). FAB MS (NOBA matrix): m/z = 720-1 $((M - 2Cl)^+)$, 757 $((M - Cl)^+)$, 791-2 (M^+), 815 $((M + Na)^+)$. Melting point: 208°C (dec.). Elemental analysis for $[(dppippn)PtCl_2.0.17CHCl_3]$: Found C: 48.53, H: 5.38, N: 3.95%. $C_{33.17}H_{40.17}N_2P_2PtCl_{2.51}$ requires C: 49.00, H: 4.98, N: 3.45%.

7.2.3.7 Synthesis of Dichloro-P,P'-(N,N'-bis(diphenylphosphino)piperazine) platinum(II) [(dpppip)PtCl$_2$]

A solution of dpppip (0.4g, 0.88mmol) in dry degassed THF (10ml) was added to a suspension of $[(PhCN)_2PtCl_2]$ (0.4g, 0.85mmol) in dry, degassed THF (25ml). An immediate lightening of the solution was observed, followed by the precipitation of a light green-yellow solid. The reaction mixture was left to stir overnight, after which time the green-yellow precipitate was separated by filtration. This gave a yield of 0.55g (90%). ^{31}P nmr: δ_P = 74.7ppm (t, $^1J_{Pt-P}$ = 4037Hz, $CDCl_3$). ^1H nmr: δ_H = 8.4ppm (m, 8H, Ph), 7.4-7.6ppm (m, 12H, Ph), 3.0ppm (br m, 8H, CH_2). ^{13}C nmr: δ_C = 134.5ppm (m, Ph), 131.7ppm (s, Ph), 128.1ppm (s, Ph), 127.3ppm (m, Ph), 42.2ppm (s, CH_2). IR

(CsI plates, nujol mull): ν(Pt - Cl) = 342(s) cm^{-1}. FAB MS (NOBA matrix): m/z = 649 ($(M - 2Cl)^+$), 685 ($(M - Cl)^+$), 719-20 (M^+). Melting point: 245°C (dec.). Elemental analysis: Found C: 46.44, H: 3.98, N: 3.81%. $C_{28}H_{28}N_2P_2PtCl_2$ requires C: 46.68, H: 3.92, N: 3.89%.

7.3 Discussion

7.3.1 Synthesis of Aminophosphines

In this work, a number of new chelating aminophosphine compounds have been synthesised. The method used (shown in Scheme 7.1) is identical to one cited in the literature [1], and is one which has been widely applied to making a range of heteroatom-containing phosphine ligands [6]. It was first used in the late nineteenth century to make a variety of mono-, bis- and tris-aminophosphines [7]. The addition of chlorodiphenylphosphine to an amine in the presence of triethylamine causes the precipitation of a large amount of white triethylamine hydrochloride. After removal by filtration, the product is then precipitated from the toluene solution. For some reactions the product precipitates from the reaction mixture with the triethylamine hydrochloride, in which case it can be separated by extraction with tetrahydrofuran. All the aminophosphines have been isolated as white or off-white solids.

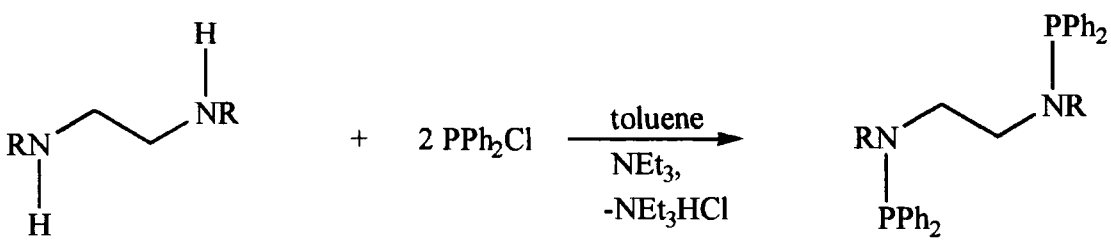

Scheme 7.1: Synthesis of Aminophosphine Compounds

A range of aminophosphines of this type, differing in the group at nitrogen and also in the backbone, have been prepared by this method.

The effect of the presence of an NR group on the phosphorus atom is of interest. ^{31}P nmr data for these compounds shows notable differences from other compounds with other atoms adjacent to phosphorus, and are summarised in Table 7.13.

Table 7.13: ^{31}P nmr Data for Aminophosphines and Related Compounds

Compound	^{31}P nmr Chemical Shift / ppm
Ph_2P-OMe [8]	115.6
Ph_2P-OBu [8]	111.1
dppmen	65.0
dppmpn	65.0
dpppip	62.2
dpppen	61.3
dpptben	50.9
dppippn	48.9
dppipen	46.7
Ph_2P-SEt [9]	26.5
Ph_2P-PPh_2 [10]	-15
Ph_2P-$(CH_2)_4$-PPh_2	-17

^{31}P nmr chemical shifts are seen to increase when going across a row in the Periodic Table (carbon to nitrogen to oxygen) and decrease when going down a group in the Periodic Table (nitrogen to phosphorus; oxygen to sulphur) in terms of the atom adjacent to phosphorus. This is due to changes in electronegativity, which affects the electron density at the phosphorus atom and hence its chemical shift. The compounds synthesised here fit this pattern, and are also in the range in which other aminophosphines are found. Some typical values are given in Table 7.16. Changing the other (organic) groups at phosphorus will also affect the value of the chemical shift. This is illustrated by the final entries in Table 7.14.

Table 7.14: ^{31}P nmr Data for Aminophosphines

Compound	^{31}P nmr Chemical Shift / ppm
Ph_2P-N(Me)-PPh_2 [12]	72.8
Ph_2P-N(Et)-PPh_2 [13]	61
$(Ph_2P)_2$NCH(Me)(Ph) [14]	52.2
Ph_2P-NMe_2 [13]	63.9
Me_2P-NMe_2 [13]	39

The ^{1}H and ^{13}C nmr spectra of the aminophosphines have also been investigated. In the ^{1}H spectrum, the backbone (CH_2) protons are generally seen at approximately 3ppm, with phenyl ring protons between 7.5ppm and 8ppm. Protons on the organic groups at nitrogen tend to come at lower frequency than the backbone protons, typically between 0.8 and 1.5ppm. The exception to this is dpppen, where the phenyl ring protons are seen between 6.6 and 7.2ppm. In ^{13}C nmr spectra, the carbons of the phenyl rings are seen between 125ppm and 140ppm, with backbone carbons at 45 - 55ppm. Carbons of aliphatic groups at nitrogen are again seen at lower frequency with respect to the backbone carbons. In dpppen, the phenyl ring carbons in the phenyl rings attached to nitrogen are seen between 112 and 138ppm, and are not easily distinguished from the phenyl ring carbons of phenyl rings attached to phosphorus. Coupling of hydrogen and carbon to phosphorus is observed, and was used to aid assignation in some cases.

The molecular structure of one of these compounds (dpptben) has been determined. It was found to have a centre of symmetry, and consequently the phosphorus atoms are equivalent. This is shown also to be true in solution by the solution-state ^{31}P nmr spectrum, which shows one phosphorus environment (a singlet). The bonding between phosphorus and nitrogen is especially interesting. The bond length is found to be 1.710(1)Å, which is significantly shorter than the 1.77Å quoted for the P-N single bond [15], and is due to more than σ-bonding between phosphorus and nitrogen, implying the involvement of the nitrogen lone pair. The π-bonding component manifests itself as a shorter P-N bond, and a more planar nitrogen. The latter can be quantified by consideration of the sum of angles at nitrogen. For a planar nitrogen these will be 360°, whilst for a pyramidal nitrogen centre the sum of angles will be closer to 330°. As the lone pair becomes more involved in P-N bonding, the nitrogen will tend more towards planarity. Examples of phosphorus - nitrogen bonding are given in Table 7.15. Compounds with three P-N bonds per phosphorus, such as $P(NMe_3)$, have been found to possess two different types of phosphorus - nitrogen bond: two 'short' bonds with almost planar (sp^2 hybridised) nitrogen atoms, and one 'long' one with a pyramidal (sp^3 hybridised) nitrogen atom. This is reflected in the data in the Table.

Table 7.15: Structural Data on Compounds Containing P-N Bonding

Compound	P-N Bond Length / Å	Sum of Angles at Nitrogen / °
dpptben	1.710(1)	353.4(1)
$F_2P\text{-}NMe_2$* [14]	1.628	360.0
$P(NMe_2)_3$ [15]	1.687(3)	355.9(3)
	1.731(3)	337.6(3)
$H_2C{=}P(NMe_2)_3$ [15]	1.666(4) / 1.669(4)	355.6(4) / 351.1(4)
	1.698(4)	337.3(4)
$(O(CH_2CH_2)_2N)_3P$ [17]	1.691(3) / 1.696(3)	353.2(3) / 350.5(3)
	1.726(3)	337.6(3)
$(CH_2(CH_2CH_2)_2N)_3P$ [17]	1.692(3) / 1.705(3)	359.8(3) / 350.1(3)
	1.727(3)	339.3(3)

A comparison of dpptben to other compounds in Table 7.15 would suggest that the nitrogen lone pair in dpptben is also involved in extra π-bonding to phosphorus. The phosphorus - nitrogen distance is comparable to others, such as tris(piperidino)phosphine [17], where π-bonding is seen, and the sum of angles at nitrogen tends towards 360° rather than 330°.

The length of the nitrogen - phosphorus bond is slightly longer than most aminophosphines, as shown in Table 7.15. This long bond length could be caused by steric interactions with the bulky *tert*-butyl group at nitrogen. The ready bonding of aminophosphine ligands to transition metals indicates that the phosphorus lone pair cannot be significantly involved in additional bonding to nitrogen. The carbon - phosphorus - nitrogen and carbon - phosphorus - carbon bond angles are smaller than would be expected for a tetrahedral geometry, and indeed the tetrahedron at phosphorus is a little elongated by reducing these angles. This is a consequence of the phosphorus lone pair repelling the bonding electrons more strongly than would a bonded pair of electrons. The phenyl rings at phosphorus are arranged so as to minimise steric and electronic interactions with each other. The sum of the angles at the phosphorus atom in dpptben is 312.7°, which is slightly greater than expected for a tertiary phosphine, which is usually in the range 295-310° [17], although bulky phosphines such as tris(*tert*-butyl)phosphine have been known [18] to deviate from this range of values. The

* The esd values determined for this compound were not given.

presence of *tert*-butyl groups in dpptben, despite being somewhat removed from the phosphorus centre, could give rise to this small deviation.

7.3.2 Synthesis of Metal Complexes

7.3.2.1 Synthesis of Palladium Complexes

Palladium dichloride complexes of the ligands described above were synthesised by reaction of dichlorobis(benzonitrile)palladium(II) with the appropriate ligand in tetrahydrofuran or toluene. Dissolving this yellow palladium complex in THF gives a deep red solution, thought to be $[(THF)_2PdCl_2]$. Addition of the ligand, also in THF or toluene gives an immediate precipitate, which is yellow or yellow-green, and reaction is complete after stirring at room temperature overnight. The complex is isolated by filtration, followed by washing with THF and drying in vacuo. The by-product, benzonitrile, and excess aminophosphine are removed by this washing. Yields of the palladium complexes are in the range 33 - 86%. Some yields are low, but often further product was identified or isolated from the washings. This second crop, however, tended to contain high proportions of benzonitrile, identified by its infra-red spectrum [5], and so was not used. The complexes were sparingly soluble or insoluble in many solvents, but were soluble in chlorinated solvents such as dichloromethane or chloroform. The exception to this was $[(dpppip)PdCl_2]$ which is only sparingly soluble in chloroform or dichloromethane, but dissolves readily in N,N-dimethylformamide.

The complexes were initially characterised by ^{31}P nmr spectroscopy. All the complexes gave a singlet between δ_P = 76.8ppm and 90.9ppm, the exception being $[(dpppip)PdCl_2]$ which has δ_P = 104.1ppm. Table 7.16 summarises this data. Although palladium has an isotope which is nmr active (^{105}Pd: I = 5/2, 22.2% natural abundance [19]), its large nuclear spin quantum number and low abundance mean that coupling is not observed.

Table 7.16 ^{31}P nmr Data of Aminophosphine Ligands and their Palladium Dichloride Complexes

Ligand	δ_P[(Ligand)$PdCl_2$] / ppm	δ_P (Ligand) / ppm	Difference / ppm
dppmen	78.3	65.0	+13.3
dpppen	87.6	61.3	+26.3
dppipen	82.9	46.7	+36.2
dpptben	76.8	50.9	+25.9
dppmpn	88.8	65.0	+23.8
dppippn	86.6	48.9	+37.7
dpppip	104.1	62.2	+41.9
$(Ph_2PNH)_2CO$ [20]	62.9	25.1	+37.5
$(Ph_2P)_2NCH(Me)(Ph)$ [14]	33.3	52.2	-18.9

It is seen from these data that the change in chemical shift on complexation lies in the range +13 to +42 ppm. The trend appears to be generally that ligands with more bulky substituents (^{i}Pr, ^{t}Bu) have a greater change on complexation than those with smaller substituents (Me). This may relate to either an increased value for the complex, or a decreased value for the free ligand, though, except for dpppip, the complexes have more consistent values than do the free ligands. [(dpppip)$PdCl_2$] has the greatest change in chemical shift on complexation. This could be related to the change in conformation that must take place on complexation. In the free ligand, the piperazine backbone must be a chair form to minimise interactions between 1,3-diaxial substituents [40]. However, in the complex, both phosphorus atoms will be pointing towards the metal, and so the backbone must now be in a boat form, as shown in Fig. 7.9. This would increase ring strain in the system as the piperazine ring tries to minimise interactions, and could influence the phosphorus chemical shift of the complex.

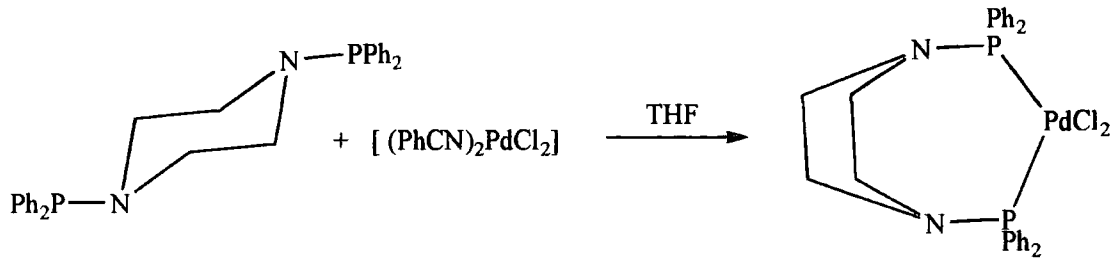

Fig. 7.9: Complexation of dpppip

Another possibility is that the ligand is bridging between two palladium centres (Fig 7.10), although this is unlikely for the corresponding platinum dichloride complex (see section 7.3.3) as the platinum - phosphorus coupling constant ($^1J_{Pt-P}$ = 4037Hz) is too large for a complex with *trans* phosphorus atoms [21], which would be the product of a bridging diphosphine. To reinforce this, the coupling constant is of a similar magnitude to [(dppmen)$PtCl_2$] ($^1J_{Pt-P}$ = 4022Hz) which has been shown to contain a chelating diphosphine by crystal structure analysis. However, consideration of the metal - chlorine stretching frequencies as follows shows that, in the solid state, a polymeric structure is preferred. For palladium dichloride complexes, a single absorption at ca. 350cm^{-1} is indicative of a *trans* - dichloride whilst two resonances between 330 and 280cm^{-1} are characteristic for a *cis* - dichloride [41]. The latter pattern is seen for all the palladium dichloride complexes synthesised here with the exception of [(dpppip)$PdCl_2$] which I conclude is a *trans* - dichloride in the solid state. The polymeric structure is also suggested by elemental analysis, which confirms a 1:1 ratio of ligand to metal. In the solution state, however, the palladium and platinum dichloride complexes of dpppip are both *cis* - dichlorides as seen by the ^{31}P nmr shift and coupling constant. This change in structure on dissolution is responsible for the insolubility reported above.

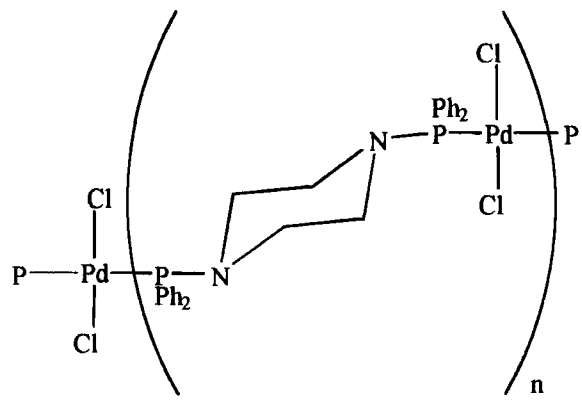

Fig. 7.10: Bridging Mode of dpppip

The data in Table 7.16 regarding $(Ph_2P)_2NCH(Me)(Ph)$ are different to those for the ligands reported in this work. The ^{31}P nmr chemical shift of the free ligand, δ_P = 52.2ppm, is within the range of other aminophosphines, but the low shift for the palladium complex (33.3ppm) and the decrease on complexation are contrary to the other data. This is due to the four-membered chelate ring, which has been found to move the ^{31}P nmr chemical shift to low frequency [22].

It has been shown that it is possible to draw a linear relationship between the ^{31}P nmr chemical shift of a tertiary phosphine ligand and its change on co-ordination to a metal [23]. This is also affected by a factor known as the chelate chemical shift, which depends on the size of the chelate ring. For compounds with the same chelate ring size, however, this term can be considered a constant. The relationship is $\Delta = A\delta_F + B$, where Δ is the change in chemical shift on co-ordination, δ_F is the chemical shift of the free phosphine and A and B are constants. It is constant B which will incorporate the chelate chemical shift term. Knowledge of these constants will enable the prediction of the chemical shifts of the complexes of phosphines whose own chemical shift (δ_F) is known. Due to the effect of chelate ring size, the compounds synthesised were divided into two groups - those with seven-membered chelate rings, and those with eight-membered chelate rings. For the former compounds, the values of A and B are -0.93 and 77.7ppm respectively. The only compound not to fit this relationship is dpppip, which lies above the line. This could be due to the boat-form backbone which will affect the ring geometry and hence deviate from a "true" seven-membered chelate ring geometry by the introduction of extra strain. If the compounds with eight membered chelate rings are added to the data, then the values of A and B are now -0.89 and 77.1ppm respectively. This shows that the difference in chelate chemical shift for a seven- and an eight-membered ring is small. As the origin of the chelate chemical shift can be explained in terms of ring strain effects [22] it may well be that these larger rings are not strained to the extent of, for example, a four- or five-membered ring. This is why dpppip deviates from the relationship - the cyclohexane-boat backbone enforces restraints on the geometry of the chelate ring.

The ^1H and ^{13}C nmr spectra were also investigated. These showed many features in common with the spectra of the related ligand. Problems were encountered regarding solubility of complexes; the ^{13}C spectrum of $[(dpppip)PdCl_2]$ was not obtained for this reason.

Four of the palladium dichloride complexes, [(dppmen)$PdCl_2$], [(dpppen)$PdCl_2$], [(dpptben)$PdCl_2$] and [(dppmpn)$PdCl_2$], have been characterised by crystal structure analysis. The structures are similar in that they all possess *cis* geometry as would be expected for a diphosphine ligand. The geometry at palladium is square planar, with the sum of the angles at palladium being between 359° and 361°, indicating only a very small deviation from true square planarity. The exception to this is [(dppmpn)$PdCl_2$], which has the sum of angles at palladium being 361.5°. The two P - Pd - P - N units are planar, as shown in Fig. 7.11, a feature not found for the other compounds. It is possible that this planarity is favoured at the expense of the planarity of Cl - Pd - P units. The phosphorus - palladium - phosphorus angle (the "bite angle") is always the largest angle, the others tending to be less than 90° to compensate.

Fig. 7.11: Planarity of N-P-Pd-P-N Units in [(dppmpn)$PdCl_2$]

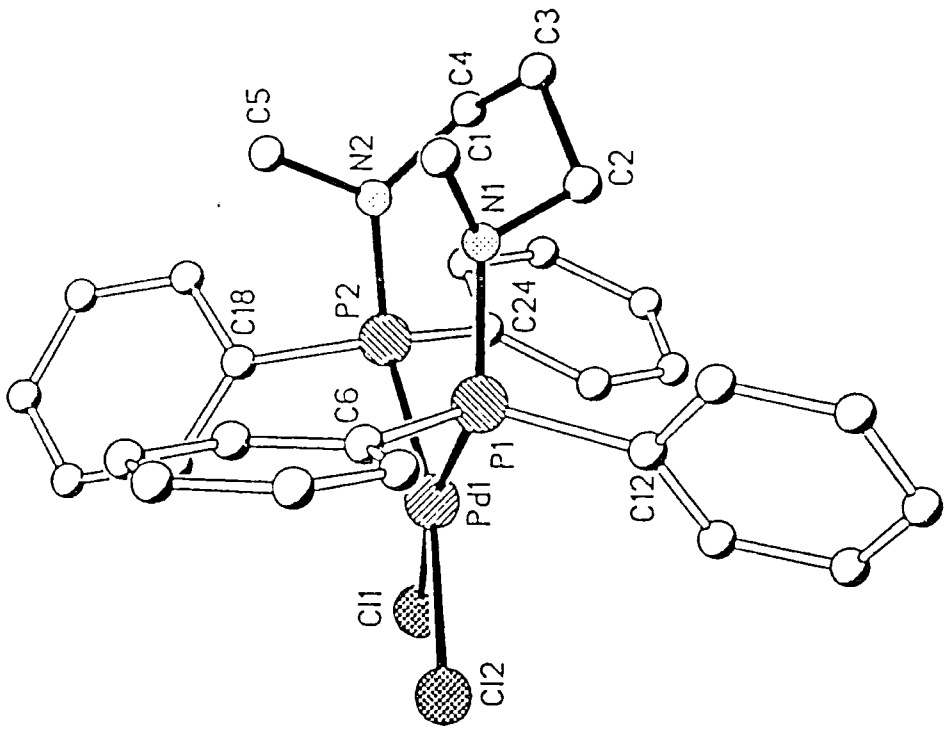

The structure of [(dppmen)$PdCl_2$] (Fig. 7.4) has two inequivalent phosphorus atoms. One is part of a planar N-P-Pd-P unit, whilst the other N-P-Pd-P system is bent. The planarity is caused by π-bonding from nitrogen to phosphorus, which is more for the planar P-N-Pd-P unit. This is reflected in the shorter phosphorus - nitrogen bond length and more planar nitrogen atom. It is interesting to note that the phosphorus atoms are equivalent in solution, the ^{31}P nmr spectrum of the complex being a singlet. The difference in P - N bonding does not affect the lengths of the Pd - Cl bonds. At 2.3715Å and 2.3734Å, they can be considered to be the same. However, a disparity is seen in the palladium - phosphorus bond lengths - a shorter P - N bond leads to a shorter P - Pd bond. This could be because the extra bonding to phosphorus leads to it becoming relatively electron rich, and thus a better donor to the metal. The phosphorus atom with the shorter P - Pd bond has greater N - P - C and C - P - C angles, due to steric interactions with both the metal and the methyl group on the nitrogen. The methyl groups are pointing in the same general direction, although the configuration of the backbone means that they are separated enough to be allowed to do this. The nitrogen lone pairs also appear to be pointing towards each other. As they are involved in bonding to phosphorus as discussed above, their electron density will be greatly reduced and the resulting electronic interactions will be small. The complex is crystallised with a molecule of dichloromethane which has no effect on the geometry of the complex.

The structure of [(dpptben)$PdCl_2$] (Fig. 7.6) is in many ways similar to that of [(dppmen)$PdCl_2$] described above. I ascribe the changes to the introduction of sterically-demanding *tert*-butyl ligands, which affect the geometry of the rest of the complex. Again there are two different phosphorus environments in the molecule, with the shorter P - N bond being longer than its counterpart in [(dppmen)$PdCl_2$]. The same trends regarding the lengths of P - N and P - Pd bonds are evident, but here the Pd - Cl bond distances are not the same, and the bond *trans* to the shorter P - Pd bond is the longer Pd - Cl bond. This would tie in with the *trans* influence [28] as seen in square planar metal complexes, where the length of a metal ligand bond is affected by the ligand *trans* to it - the same metal d orbitals are being used for bonding in both cases. In the case of [(dpptben)$PdCl_2$], it is possible that differences in the phosphorus environment on one side of the palladium atom are giving rise to differences in palladium - chlorine bonding on the other side of the palladium atom. Both the phenyl rings and the *tert*-butyl groups are arranged to minimise interactions with each other. The *tert*-butyl groups are

arranged in a similar fashion to the methyl groups in [(dppmen)$PdCl_2$], but again the backbone is oriented such that they do not approach too closely. The lone pairs are also pointing towards each other, but again depletion of electron density may lessen their interaction significantly. The complex is co-crystallised with two molecules of tetrahydrofuran. The effect of this is to introduce a small amount of disorder involving one of the phenyl rings.

In [(dpppen)$PdCl_2$], the complex geometry (Fig. 7.5) is affected by the π-systems in the extra phenyl rings. This makes both nitrogen atoms planar, and the difference between the P - N distances decreases considerably. The phosphorus - palladium distances show the same trend as the other complexes, but the palladium - chlorine bonds are identical in length. The six phenyl rings are arranged so as to minimise steric and electronic interactions with each other. The rings bound to the nitrogen atoms are oriented at approximately 45° to the C - N - P plane. The molecule is co-crystallised with a molecule of chloroform, but this has no great effect on the complex geometry.

The structure of [(dppmpn)$PdCl_2$] (Figs. 7.7 and 7.11) is slightly different to the complexes discussed above in having a planar P - N - Pd - P - N unit, as mentioned above. The bite angle of the ligand is 99.74°, which is bigger than all the two-carbon backboned complexes, despite the methyl substituents at nitrogen being less sterically demanding than, for example, *tert*-butyl. This is a consequence of the extra CH_2 unit in the backbone, which allows this different geometry. The lengths of the phosphorus - nitrogen bonds and the palladium - phosphorus distances are both similar. The palladium - chlorine distances are the same, as has been seen for the other complexes. The orientation of the methyl groups is to point away from each other, minimising any steric interactions. This is in contrast to the structure of [(dppmen)$PdCl_2$], for example, and again is a consequence of the longer, more flexible backbone.

Features of interest in these [$(N_2P_2)PdCl_2$]-type complexes include the bonding between phosphorus and nitrogen, and the bite angle at palladium. These data, plus some literature compounds for comparison, are given in Table 7.17.

Table 7.17: Geometry at Palladium for some Palladium Dichloride Complexes

Complex	Pd-P distance / Å	Pd-Cl distance / Å	P-Pd-P Angle / °
[(dppmen)$PdCl_2$]	2.2518(7)	2.3715(7)	94.87(3)
	2.2807(7)	2.3734(7)	
[(dpppen)$PdCl_2$]	2.262(1)	2.369(1)	98.19(3)
	2.288(1)	2.368(1)	
[(dpptben)$PdCl_2$]	2.2758(8)	2.3653(8)	98.54(3)
	2.2904(7)	2.3504(7)	
[(dppmpn)$PdCl_2$]	2.2593(9)	2.3757(9)	99.74(3)
	2.2693(8)	2.3861(8)	
trans-[$(C_5H_{10}NPPh_2)_2PdCl_2$] [24]	2.324(2)	2.289(2)	-
[$((Ph_2P)_2NCH(Me)(Ph))PdCl_2$] [14]	2.212(2)	2.376(3)	71.5(1)
	2.211(3)	2.365(3)	
[$(CO(NHPPh_2)_2)PdCl_2$] [20]	2.200(3)	2.359(3)	91.4(1)
	2.216(2)	2.340(2)	

As Table 7.17 shows, the geometries about palladium in [(dppmen)$PdCl_2$], [(dpppen)$PdCl_2$], [(dpptben)$PdCl_2$] and [(dppmpn)$PdCl_2$] are similar to other [(aminophosphine)$PdCl_2$] complexes reported in the literature. The bite angles (P-Pd-P angles) for [(dpptben)$PdCl_2$] and [(dpppen)$PdCl_2$] are a little greater than that of [(dppmen)$PdCl_2$]. This is due to the additional steric bulk provided by the *tert*-butyl or phenyl groups, which have the effect of widening the P-Pd-P angle at the expense of the other angles at palladium. However, [(dppmpn)$PdCl_2$] has the widest bite angle of those complexes studied as it has a longer backbone. The complex [$((Ph_2P)_2NCH(Me)(Ph)PdCl_2$] [14] has a much smaller bite angle than the other complexes in Table 7.17. This is due to it having a much smaller (four-membered) chelate ring.

Table 7.18: Phosphorus - Nitrogen Bonding Features in some [(Aminophosphine)$PdCl_2$] Complexes

Complex	P-N distance / Å	Sum of Angles at Nitrogen / °
[(dppmen)$PdCl_2$]	1.655(2)	360.0(2)
	1.691(2)	348.4(2)
[(dpppen)$PdCl_2$]	1.692(3)	359.9(3)
	1.681(3)	360.0(3)
[(dpptben)$PdCl_2$]	1.676(3)	357.5(2)
	1.698(3)	349.0(2)
[(dppmpn)$PdCl_2$]	1.683(2)	351.4(3)
	1.670(2)	359.4(2)
trans-[($C_5H_{10}NPPh_2$)$PdCl_2$] [24]	1.727(6)	349.6(9)
[((Ph_2P)$_2$NCH(Me)(Ph))$PdCl_2$] [14]	1.700(7)	360(6)
	1.718(7)	
[(CO(NHPPh_2)$_2$)$PdCl_2$] [20]	1.680(7)	not determined
	1.687(8)	

The phosphorus - nitrogen distances in [(dppmen)$PdCl_2$], [(dpppen)$PdCl_2$], [(dpptben)$PdCl_2$] and [(dppmpn)$PdCl_2$] are similar to those in the other aminophosphine complexes. The P-N bonds in the literature compounds cited all have bond orders greater than one, as they are all shorter than the P-N single bond (1.77Å [15]). This is linked with π-bonding interactions from the nitrogen lone pair to phosphorus.

As the molecular structures of the free ligand dpptben and its complex [(dpptben)$PdCl_2$] have both been solved, it is of interest to compare them.

Table 7.19: A Comparison of dpptben and [(dpptben)$PdCl_2$]

	dpptben	[(dpptben)$PdCl_2$]
P-N distance / Å	1.710(1)	1.698(3)
		1.676(3)
Sum of Angles at Nitrogen / °	353.4(1)	349.0(2)
		357.5(2)
Sum of non-metal Angles at Phosphorus / °	312.7(7)	324.0(2)
		324.7(2)
Backbone Carbon - Nitrogen distance / Å	1.488(2)	1.491(4)
		1.482(4)
Backbone Carbon - Carbon distance / Å	1.546(3)	1.520(4)

As Table 7.19 shows, there are a number of changes to the dpptben ligand on complexation. Possibly the most striking change is to the phosphorus - nitrogen bonds, which shorten notably. This may be because the phenyl groups are moved away from the tert-butyl group by complexation, allowing for a shorter P - N bond, or that chelation decreases the electron density at phosphorus, encouraging donation from the nitrogen lone pair. The two nitrogen atoms cease to be equivalent, one becoming almost planar, and the other is more pyramidal. The sum of C-P-C and C-P-N angles at phosphorus become larger, because lone pair-bonded pair repulsions are greater than bonded pair-bonded pair repulsions and the phosphorus lone pair is now used in bonding to palladium. The backbone contracts slightly to compensate for the complexing of the phosphorus atoms. This is seen mostly in the C - C bond. The backbone itself exhibits a motif seen in all these structures, whereby it stands above the metal, and does not possess a plane of symmetry. One Cl-Pd-P-N unit is almost planar, whilst on the other side of the molecule, the Cl-Pd-P unit is planar, but the nitrogen is above and behind the phosphorus. This is the more planar nitrogen.

The molecular structure of [(dppmen)$Pd(OAc)_2$] has also been solved. It is similar in structure to [(dppmen)$PdCl_2$] discussed above, to which it is compared in Table 7.20. The palladium - oxygen bond lengths are the same with the acetate groups pointing away from each other (up and down relative to the P - Pd - P plane) to minimise steric

and electronic interactions. However, the square planar arrangement around palladium is not distorted.

Table 7.20: Structural Comparison of [(dppmen)$PdCl_2$] and [(dppmen)$Pd(OAc)_2$]

	[(dppmen)$PdCl_2$]	[(dppmen)$Pd(OAc)_2$]
Pd - P distances / Å	2.2518(7)	2.2348(13)
	2.2807(7)	2.2494(15)
P - N distances / Å	1.655(2)	1.654(4)
	1.691(2)	1.691(4)
N - C (backbone) distances / Å	1.467(3)	1.485(6)
	1.481(3)	1.460(6)
N - C (methyl) distances / Å	1.469(3)	1.468(6)
	1.474(4)	1.471(6)
C - C (backbone) distance / Å	1.518(4)	1.515(6)
P - Pd - P angle / °	94.87(3)	95.65(5)
Sum of angles at Nitrogen / °	348.4(2)	344.1(4)
	360.0(2)	360.0(4)
Sum of C-P-C and C-P-N	317.9(1)	318.9(2)
angles at Phosphorus / °	316.7(1)	320.0(2)
Sum of angles at Palladium / °	359.5(3)	359.5(1)

As seen in Table 7.20, the structures of the two complexes are very similar. The only notable differences are in (*i*) the palladium to phosphorus distances, which are slightly shorter for the acetate complex, and in (*ii*) the bite angle is slightly wider for the acetate complex. The bond length difference is due to the different σ-donor properties of the acetate and chloride ligands, which affect the lengths of the metal - phosphorus bonds opposite (the *trans* influence [39]).

7.3.2.2 Synthesis of Platinum Complexes

The platinum dichloride complexes were synthesised in a manner analogous to the palladium dichloride complexes described above; that is, the reaction of an aminophosphine with $[(PhCN)_2PtCl_2]$ in THF or toluene solvent. The reaction mixture was stirred overnight and the complex precipitated as a white or off-white solid. This could be separated by filtration and the by-product, benzonitrile, and any excess ligand removed by THF washing. The complexes are largely insoluble in ethers or toluene, but soluble in chlorinated solvents such as dichloromethane or chloroform.

The metal - chlorine stretching frequencies of the complexes were measured. Again all the complexes showed signals characteristic of a *cis* - dichloride, with the exception of $[(dpppip)PtCl_2]$ which is a *trans* - dichloride in the solid state. The structure is thought to be analogous to that of the palladium complex.

The ^{31}P nmr spectra of the complexes were investigated, the chemical shifts falling in the range 55 - 75ppm and the $^1J_{Pt\text{-}P}$ coupling constants in the range 4020 - 4206Hz. These data are given in Table 7.21.

Table 7.21: ^{31}P nmr Data for $[(Phosphine)PtCl_2]$ Complexes

Complex	Chemical Shift / ppm	Coupling Constant / Hz
$[(dppmen)PtCl_2]$	55.2	4022
$[(dpppen)PtCl_2]$	61.7	4206
$[(dppipen)PtCl_2]$	59.8	4030
$[(dpptben)PtCl_2]$	54.5	4141
$[(dppmpn)PtCl_2]$	65.0	4174
$[(dppippn)PtCl_2]$	62.2	4155
$[(dpppip)PtCl_2]$	74.7	4037
$[(dppa)PtCl_2]$ [25]	-5.2	3130
$[(dppma)PtCl_2]$ [25]	15.6	3300
cis-$[(PPh_3)_2PtCl_2]$ [26]	13.9	3681
trans-$[(PPh_3)PtCl_2]$ [26]	22.0	2605
$[(dppe)PtCl_2]$ [26]	43.8	3600

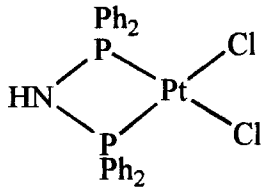

[(dppa)$PtCl_2$]

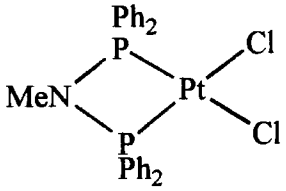

[(dppma)$PtCl_2$]

Fig 7.12: Structures of [(dppa)$PtCl_2$] and [(dppma)$PtCl_2$]

The values of the chemical shift of the [$(N_2P_2)PtCl_2$] complexes are different from those of [(dppa)$PtCl_2$] and [(dppma)$PtCl_2$], due to a chelate ring size effect as a four membered ring lowers the value of the chemical shift [22].

The magnitude of a coupling constant depends on a number of factors, as has been determined quantitatively by Pople and Santry [27], and has led to the magnitude of a ^{195}Pt - ^{31}P coupling constant being expressed as follows [28]:

$$J_{Pt\text{-}P} \propto \gamma_P\gamma_{Pt} \cdot (\Delta E^{-1}) \cdot \alpha_{Pt}^2\alpha_P^2 \cdot |\Psi_{Pt(6s)}(0)|^2|\Psi_{P(3s)}(0)|^2$$

where γ_P and γ_{Pt} are the magnetogyric ratios for phosphorus and platinum respectively, and will be constant for a range of related Pt - P complexes; ΔE is related to the nuclear excitation energy [28] and is constant for a series of similar compounds; α is the s-character of the hybrid orbital used in bonding by the given atom; and $\Psi(0)$ is the s-electron density at the parent nucleus. Thus, only these last two terms influence the size of the Pt - P coupling constant. In practice, this means that factors such as the geometry of the complex [28,29] and the nature of the ligand *trans* to the phosphorus atom (the *trans* influence [30]) affect the coupling constant. The coupling constants for the complexes synthesised here are all larger than those observed for a hydrocarbon-backboned [(diphosphine)$PtCl_2$] complex, which tend [26,29] to have coupling constants of the order of 2500Hz for a *trans* complex and 3500Hz for a *cis* complex. This increase in coupling constant in aminophosphine complexes compared with hydrocarbon-backboned phosphine complexes could be due to the additional bonding between nitrogen and phosphorus, which would increase the electron density at phosphorus. The large values of $^1J_{Pt\text{-}P}$ could also be a chelate ring size effect, the larger seven-membered chelate ring of dppb having greater values of $^1J_{Pt\text{-}P}$ than equivalent complexes of dppe [22]. The order of $^1J_{Pt\text{-}P}$ coupling constants observed is

$[(dpppen)PtCl_2]$ > $[(dppmpn)PtCl_2]$, $[(dppippn)PtCl_2]$, $[(dpptben)PtCl_2]$ > $[(dpppip)PtCl_2]$, $[(dppipen)PtCl_2]$, $[(dppmen)PtCl_2]$

The high coupling constant for the dpppen complex must be due to the presence of the phenyl group at nitrogen since other features of the complex are the same. None of the other compounds have π-electrons in the backbone, and this may lead to an enhancement of N-P bonding, and therefore a more electron-rich phosphorus. For the complexes containing dppmpn and dppippn, coupling constants are equivalent (the difference is 19Hz), and greater than for the complexes of their two-carbon backbone counterparts dppmen and dppipen respectively. This implies that the greater conformational freedom of complexes containing the longer backbone ligands gives increased electron density at phosphorus by strengthening of the phosphorus - nitrogen bond. The constraints on the geometry of the complex of a two-carbon backboned ligand must therefore restrict the phosphorus - nitrogen bond from its ideal position. The coupling constant of $[(dpptben)PtCl_2]$ is of the same size as for $[(dppmpn)PtCl_2]$ and $[(dppippn)PtCl_2]$, which is a consequence of the electron donating properties of the *tert*-butyl group, which increases the electron density at phosphorus and so the phosphorus - platinum coupling constant as well.

As for the palladium dichloride complexes above, a straight line results when the chemical shift of a free aminophosphine ligand is plotted against the change in this value on complexation for the platinum dichloride complexes synthesised, and relates to the relationship $\Delta = A\delta_F + B$, where Δ is the difference between the ^{31}P nmr chemical shifts of the free and complexed ligand, δ_F is the shift of the free ligand and A and B are constants. This gives values of A = -1.02 and B = 58.3ppm. Again, the data for the three-carbon backbone ligands does not fit the relationship, nor does the data for dpppip, for the reasons discussed above.

The ^1H and ^{13}C spectra of these complexes were also examined. As in the case of the palladium complexes, spectra resembled those of the relevant ligand. Some coupling to ^{195}Pt was seen, but this was often difficult to assign with certainty due to the low abundance of nmr-active ^{195}Pt and the presence of other couplings, for example phosphorus to carbon or hydrogen to hydrogen.

The complex [(dppmen)$PtCl_2$] has been characterised by crystal structure analysis. As for the related palladium complexes, the phosphorus atoms are inequivalent in the solid state, although ^{31}P nmr shows only one phosphorus environment in solution due to fluxional changes of the compound. The phosphorus - nitrogen bond lengths are inequivalent in the solid state, with the shorter bond being to the more planar (more sp^2 hybridised) nitrogen atom, which has the greatest degree of nitrogen lone pair π-bonding. The phosphorus forming the shorter P - N bond also forms the shorter of the two P - Pt bonds, but the Pt - Cl bonds are almost the same length. As seen for the palladium complexes of this ligand, the methyl and phenyl groups are arranged to minimise unfavourable interactions. The methyl groups point in the same direction, but the backbone is configured to ensure that they do not approach too closely. The complex is co-crystallised with one molecule of dichloromethane, which has no effect on the complex geometry. Features of interest of this and related complexes are shown in Table 7.22.

Table 7.22: Geometry at Platinum in [(Phosphine)$PtCl_2$] Complexes

Complex	P-Pt distance / Å	Pt-Cl distance / Å	P-Pt-P Angle / °
[(dppmen)$PtCl_2$]	2.2302(6)	2.3674(7)	95.46(2)
	2.2498(7)	2.3707(6)	
[L'$PtCl_2$] [31]	2.230(3)	2.378(3)	98.0(1)
	2.228(3)	2.365(3)	
cis-[($PPh_2Me)_2PtCl_2$]	2.2480(17)	2.3504(16)	99.43(6)
[34]	2.2495(16)	2.3491(18)	
[(dppe)$PtCl_2$] [35]	2.230(2)	2.355(2)	86.82(9)
	2.224(3)	2.355(2)	
[(dppp)$PtCl_2$] [36]	2.2325(8)	2.3687(8)	91.63(3)
	2.2317(8)	2.3559(8)	
[((-)-DIOP)$PtCl_2$]	2.246(8) / 2.258(8)	2.324(8) / 2.339(8)	97.6(3)
[37,38]	2.24(5) / 2.27(5)	2.34(5) / 2.32(5)	97(5)
	2.22(5) / 2.28(5)	2.34(5) / 2.36(5)	96(5)

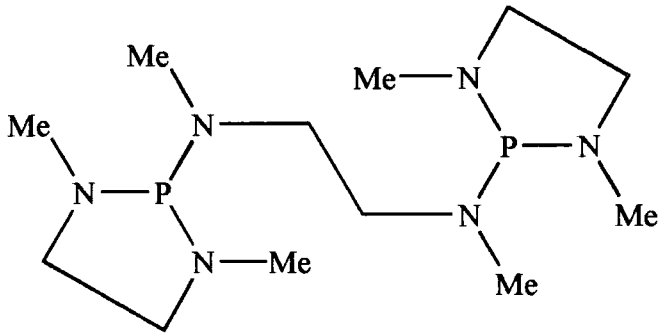

Fig. 7.13: Structure of ligand denoted L' (from ref. 31)

The ligand L' makes an interesting comparison to dppmen as they both have a seven-membered chelate ring, and both contain phosphorus-nitrogen bonding. Details are given in Table 7.23.

Table 7.23: Phosphorus - Nitrogen Bonding in (Diaminodiphosphine)$PtCl_2$ Complexes

Complex	P-N Distances / Å	Sum of Angles at Nitrogen / °
[(dppmen)$PtCl_2$]	1.693(2)	347.9(2)
	1.649(2)	359.9(2)
[L'$PtCl_2$] [26]	1.663(11) (ring)	358.4(11) (ring)
	1.680(11) (ring)	351.2(11) (ring)
	1.685(11) (ring)	354.9(11) (ring)
	1.662(10) (ring)	355.8(11) (ring)
	1.686(8) (backbone)	346.1(10) (backbone)
	1.654(12) (backbone)	359.7(10) (backbone)

The P - N bonding in the backbone is similar in the two compounds; the bond order in all the phosphorus - nitrogen bonds is greater than one as the bond length is shorter than 1.77Å [15]. The shapes of the backbones of both compounds have the same distinctive motif as seen in the palladium complexes discussed earlier. This leads to the sums of angles about the backbone nitrogens being very similar.

It is also interesting to compare the structure of [(dppmen)$PtCl_2$] with that of [(dppmen)$PdCl_2$] discussed earlier. Relevant data are given in Table 7.24.

Table 7.24: Structural Comparison of [(dppmen)$PdCl_2$] and [(dppmen)$PtCl_2$]

	[(dppmen)$PdCl_2$]	[(dppmen)$PtCl_2$]
P-N distance / Å	1.655(2)	1.649(2)
	1.691(2)	1.693(2)
P-M distance / Å	2.2518(7)	2.2302(6)
	2.2807(7)	2.2498(7)
M-Cl distance / Å	2.3715(7)	2.3674(7)
	2.3734(7)	2.3707(6)
P-M-P Angle / °	94.87(3)	95.46(2)
Cl-M-Cl Angle / °	91.03(2)	88.54(2)
Sum of Angles at	360.0(2)	359.9(2)
Nitrogen / °	348.4(2)	347.9(2)

The great similarity in the structures of these compounds is evident from the data in Table 7.24. The phosphorus - nitrogen bonding, indicated once again by the sum of angles at nitrogen and the P - N bond distance, is the same in both complexes. The bite angle is slightly greater at platinum than palladium, with a corresponding decrease in the Cl - M - Cl bond angle. The diameter of the Pd^{2+} and Pt^{2+} ions differ by only 0.2Å [33] due to the lanthanide contraction [35]. This being the only difference in the two compounds, they are structurally very similar.

7.4 Conclusions

In this chapter the synthesis and characterisation of new aminophosphines based on a diamine backbone is reported. These compounds are new, apart from dppmen and dpppip which have previously been mentioned in the literature. The molecular structure of one of these compounds, dpptben, has been determined and the phosphorus - nitrogen bonds found to have bond order between one and two. This effect, assigned to π - bonding between phosphorus and nitrogen involving the nitrogen lone pair, is supported by the geometry at the nitrogen atoms tending towards planarity. These features have been recorded for a number of similar compounds.

Palladium and platinum complexes of the aminophosphines have also been synthesised and characterised. These are believed to be the first palladium and platinum complexes reported for these ligands. Six of these complexes have been

crystallographically characterised, allowing their structures to be discussed in terms of structural and nmr information. The phosphorus - nitrogen bonds are found to be shorter than a single bond, and the planarity of the nitrogen atom suggests that the nitrogen lone pair is involved in bonding to phosphorus. This is in agreement with previously published results. The structure of a palladium diacetate complex, [(dppmen)Pd$(OAc)_2$], has also been determined, and is similar to the related dichloride complex. This is of interest as the diacetate complexes have direct relevance to catalysis.

The change in bonding which is seen to occur when replacing CH_2 in chelating diphosphines with NR affects the ligand properties of phosphorus to transition metals, and investigations of the reactivity, properties and catalysis of chelating aminophosphines and their complexes are reported in the next chapters.

7.5 References

1. I. Suisse, H. Bricout and A. Mortreux, *Tetrahedron Lett.*, 1994, **35**, 413-6.
2. H. Bricout, J.-F. Carpentier and A. Mortreux, *Tetrahedron Lett.*, 1996, **37**, 6105-8.
3. J. Grimblot, J.P. Bonnelle, A. Mortreux and F. Petit, *Inorg. Chim. Acta.*, 1979, **34**, 29-36.
4. J. Grimblot, J.P. Bonnelle, C. Vaccher, A. Mortreux, F. Petit and G. Pfeiffer, *J. Mol. Catal.*, 1980, **9**, 357-68.
5. C.J. Pouchert, "The Aldrich Library of Infra-Red Spectra", Edition III, Aldritch Chemical Company, 1981, p. 1128.
6. For example: (a) K.-i. Onuma, T. Ito and A. Nakamura, *Bull. Chem. Soc. Jpn.*, 1980, **53**, 2012-5; (b) E. Cesarotti, A. Chiesa, G. Ciani and A. Sironi, *J. Organomet. Chem.*, 1983, **251**, 79-91.
7. For example: (a) A. Michaelis and K. Luxembourg, *Berichte*, 1895, **28**, 2205-11; (b) A. Michaelis, *Berichte*, 1898, **31**, 1037-47.
8. V. Mark, C. Duncan, M. Crutchfield and J. van Wazer, "Topics in Phosphorus Chemistry", Vol. 5, John Wiley, New York, 1967, cited in "^{31}P NMR Data of Three Co-ordinate Phosphorus Compounds Containing Bonds to Chalcogenides (O, S, Se, Te) but no Bonds to Halogen", A.W.G. Platt and S.G. Kleeman, Chapter 4, "Handbook of Phosphorus-31 Nuclear Magnetic Resonance Data", J.C. Tebby (ed), CRC Press, 1991, p.85.

9. E.A. Krasil'nikova, *Russ. Chem. Rev.*, 1977, **46**, 861, cited in "^{31}P NMR Data of Three Co-ordinate Phosphorus Compounds Containing Bonds to Chalcogenides (O, S, Se, Te) but no Bonds to Halogen", A.W.G. Platt and S.G. Kleeman, Chapter 4, "Handbook of Phosphorus-31 Nuclear Magnetic Resonance Data", J.C. Tebby (ed), CRC Press, 1991, p.85.
10. A. Hinke and W. Kuchen, *Chem. Ber.*, 1983, **116**, 3003-10.
11. (a) D. Rehder and A. Keçeci, *Inorg. Chim. Acta*, 1985, **103**, 173-7. (b) H.G. Horn and K. Summer, *Spectrochim. Acta, Part A*, 1971, **27**, 1049-54.
12. I.J. Colquhoun and W. McFarlane, *J. Chem. Soc., Dalt. Trans.*, 1977, 1674-9.
13. V. Mark, C. Duncan, M. Crutchfield and J. van Wazer, "Topics in Phosphorus Chemistry", Vol. 5, John Wiley, New York, 1967, cited in "^{31}P NMR Data of Three Co-ordinate Phosphorus Compounds Containing Bonds to Group V Elements (N, P, As, Sb) but no Bonds to Halogens nor Chalcogenides", Y. Leroux, R. Burgada, S.G. Kleeman and E. Fluck, Chapter 5, "Handbook of Phosphorus-31 Nuclear Magnetic Resonance Data", J.C. Tebby (ed), CRC Press, 1991, p.107.
14. R.P.K. Babu, S.S. Krishnamurphy and M. Nethaji, *Tetrahedron Asymm.*, 1995, **6**, 427-38.
15. N.N. Greenwood and A. Earnshaw, "Chemistry of the Elements", Pergamon Press, 1984, p.620.
16. N.W. Mitzel, B.A. Smart, K.-H. Dreihäupl, D.W.H. Rankin and H. Schmidbaur, *J. Am. Chem. Soc.*, 1996, **118**, 12673-82.
17. C. Rømming and J. Songstad, *Acta Chem. Scand.*, 1978, **32**, 689-99.
18. M.-C. Labarre and M. Hausard, *J. Mol. Struct.*, 1975, **26**, 17, quoted in ref. 17.
19. R.C. Weast and M.S. Astle, "CRC Handbook of Chemistry and Physics", 63rd Edn., 1982-3, pB-280.
20. P. Bhattacharyya, A.M.Z. Slawin, M.B. Smith, D.J. Williams and J.D. Woolins, *J. Chem. Soc., Dalt. Trans.*, 1996, 3647-51.
21. P.S. Pregosin and R.W. Kunz, "^{31}P and ^{13}C NMR of Transition Metal Phosphine Complexes", vol. 16, "NMR Basic Principles and Progress", P. Diehl, E. Fluck, R. Kosfeld (eds), Springer-Verlag, 1979, pp. 43-4.
22. P.E. Garrou, *Chem. Rev.*, 1981, **81**, 229-66.
23. B.E. Mann, C. Masters and B.L. Shaw, *J. Chem. Soc. A*, 1971, 1104-6.
24. R.A. Burrow, D.H. Farrar and C.H. Honeyman, *Acta. Cryst.*, 1994, **C50**, 681-3.
25. C.S. Browning and D.H. Farrar, *J. Chem. Soc. Dalt. Trans.*, 1995, 521-30.

26. M. Gómez, G. Muller, D. Sainz, J. Sales and X. Solans, *Organometallics*, 1991, **10**, 4036-45.

27. J.A. Pople and D.P. Santry, *Mol. Phys.*, 1964, **8**, 1-18.

28. A. Pidcock, R.E. Richards and L.M. Venanzi, *J. Chem. Soc. A.*, 1966, 1707-10.

29. S.O. Grim, R.L. Keiter and W. McFarlane, *Inorg. Chem.*, 1967, **6**, 1133-7.

30. N.N. Greenwood and A. Earnshaw, "Chemistry of the Elements", Pergamon Press, 1984, pp 1352-3.

31. J. Powell, A. Lough and M. Raso, *J. Chem. Soc., Dalt. Trans.*, 1994, 1571-6. L' is the ligand shown in Fig. 7.13.

32. G.K. Anderson, H.C. Clark, J.A. Davies, G. Ferguson and M. Parvez, *J. Crystallogr. Spectrosc. Res.*, 1982, **12**, 449-58.

33. The ionic radii are: Pd^{2+}: 0.50Å, Pt^{2+}: 0.52Å. J.G. Stark and H.G. Wallace, "Chemistry Data Book", Second Edition in SI, John Murray Publishers, 1992, p29.

34. H. Kin-Chee, G.M. McLaughlin, M. McPartlin and G.B. Robertson, *Acta Cryst.*, 1982, **B38**, 421-5.

35. L.M. Engelhard, J.M. Patrick, C.L. Raston, P. Twiss and A.H. White, *Aust. J. Chem.*, 1984, **37**, 2193-2200.

36. G.B. Robertson and W.A. Wickramasinghe, *Acta Cryst.*, 1987, **C43**, 1694-7.

37. C. Ganter, A.G. Orpen, P. Bergamini and E. Costa, *Acta Cryst.*, 1994, **C50**, 507-10.

38. V. Gramlich and G. Consiglio, *Helv. Chim. Acta*, 1979, **62**, 1016-24.

39. R.H. Crabtree, "The Organometallic Chemistry of the Transition Metals", John Wiley and Sons, 1988, pp. 5-7.

40. J. McMurry, "Organic Chemistry", Brooks/Cole Publishing, 1992, pp. 118-132.

41. D.M. Adams, "Metal - Ligand and Related Vibrations", Edward Arnold (Publishers), 1967, pp. 51, 74-5.

Chapter Eight: Reactivity Studies of Aminophosphine Ligands and their Complexes

8.1 Introduction

The aim of the work reported in this chapter was to investigate the general reactivity of the ligands synthesised and their reactivity relative to each other. Processes such as oxidation and hydrolysis, which relate to the decomposition of these ligands, and their reactions with transition metal complexes relevant to catalysis, are discussed. Relative rates of co-ordination are determined for manganese and palladium complexes.

8.1.1 Investigation of the Co-ordination of Different Ligands

This was done using two methods. The first is the competition reaction of an aminophosphine - palladium dichloride complex with a free phosphine or aminophosphine ligand [1]. The reaction was followed by ^{31}P nmr - two new species were detected if displacement had occurred. An example is given in Scheme 8.1. The data in the Scheme refer to ^{31}P nmr peaks.

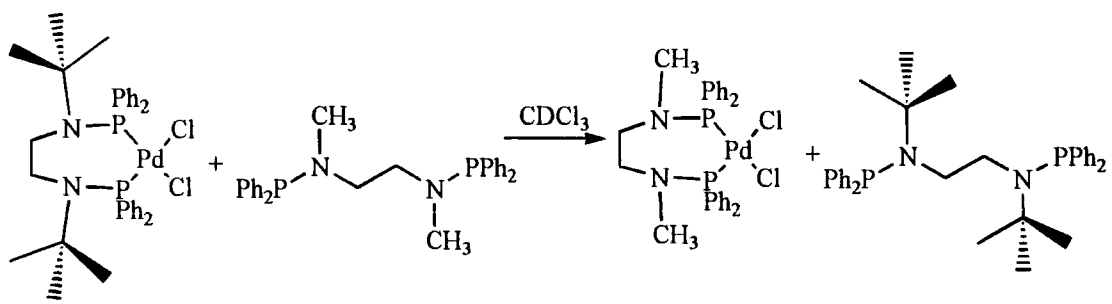

[(dpptben)PdCl$_2$]	dppmen	[(dppmen)PdCl$_2$]	dpptben
76.8 ppm	65.0ppm	78.3ppm	50.7ppm

Scheme 8.1 Reaction of [(dpptben)PdCl$_2$] with dppmen

The incoming ligand is taken to be a better donor to palladium dichloride than the ligand which is displaced.

Angelici and co-workers [2] determined a method of following the rate of substitution of a manganese pentacarbonyl bromide complex by a ligand L, by following the decrease in concentration of $[Mn(CO)_5Br]$ by infra-red spectroscopy.

Scheme 8.2: Substitution of a Carbonyl Ligand at Manganese Pentacarbonyl Bromide

The reaction shown in Scheme 8.2 is a second order reaction, the rate being dependant on the concentration both of the ligand and of manganese pentacarbonyl bromide. It has often been studied using a great excess of ligand [2], giving pseudo-first order conditions as the concentration of the ligand may be considered to be constant.

8.1.2 Determination of Ligand Donor Properties

Related to this is a method of determining the donor properties of a ligand derived from the work of Tolman [3,4]. The carbonyl stretching frequencies of nickel tetracarbonyl, $[Ni(CO)_4]$, are shifted when a monodentate ligand is co-ordinated to the metal, displacing one of the carbonyl ligands. The new value of the carbonyl stretching frequency is indicative of the relative electron donor or acceptor properties of the ligand. The same theory has been applied to the less toxic manganese pentacarbonyl bromide system [2,5-9]. Most of the data in the literature concern monodentate ligands, especially phosphines and amines, although some work has been done using bidentate ligands [10].

Both pieces of work define a factor, χ, based on the difference between the A_1 stretching frequency of a reference compound (Tolman [3] chose $[(PBu_3)Ni(CO)_3]$ as PBu_3 was the most basic phosphine he studied) and that of the substituted compound $[(LNi(CO)_3)]$. Tolman defined this factor as the difference in the A_1 stretching frequency per substituent on phosphorus, and used this information to derive a factor that could be used to predict the stretching frequencies of nickel tricarbonyl complexes of ligands such as PPh_2Me (Equation 8.1):

$$\nu_{CO}(A_1, [(PPh_2Me)Ni(CO)_3]) = \nu_{CO}(A_1, [(PBu_3)Ni(CO)_3]) + 2\chi(Ph) + \chi(Me) \quad [8.1]$$

A similar equation is derived for manganese pentacarbonyl bromide complexes [10], where χ^{Mn} represents the difference between the A_1 stretching frequency in, for example, $[(PPh_3)Mn(CO)_4Br]$ and $[LMn(CO)_4Br]$, where L is the ligand under investigation:

$$\nu_{CO}(A_1, [LMn(CO)_5Br]) = \nu_{CO}(A_1, [(PPh_3)Mn(CO)_4Br]) + \chi^{Mn} \quad [8.2]$$

In both cases, the factor χ is representative of the electronic properties of a particular ligand or substituent.

Due to the toxicity of $[Ni(CO)_4]$, the $[Mn(CO)_5Br]$ system was used in this study. The symmetry considerations of the various manganese species obtainable by reaction with a diphosphine ligand are given in Table 8.1 [11].

Table 8.1: Manganese Carbonyl Compounds and their IR Spectra

Species	Point Group	IR Spectrum
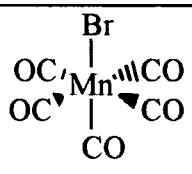 $[Mn(CO)_5Br]$	C_{4v}	3 bands $2A_1 + E$ (also B_1)[†]
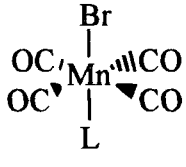 *trans*-$[LMn(CO)_4Br]$	C_{4v}	3 bands $A_1 + B_1 + E$
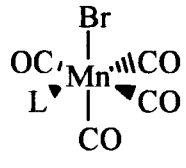 *cis*-$[LMn(CO)_4Br]$	C_s	4 bands 2A' + 2A"
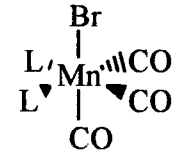 *fac*-$[L_2Mn(CO)_3Br]$	C_s	3 bands 2A' + A"
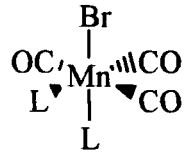 *cis,mer*-$[L_2Mn(CO)_5Br]$	C_s	3 bands 2A' + A"

8.2 Experimental

8.2.1 Reactions of Aminophosphine Ligands with $[Mn(CO)_5Br]$

Two different types of experiment were carried out with each ligand. The first was at room temperature, and used dichloromethane as the solvent, whilst the second was at 60°C (reflux temperature) in chloroform. The aim of the first set of experiments was to determine the rate of reaction of the ligand with the metal, whilst the second set were performed to investigate the final products of this reaction.

[†] The B_1 stretch is symmetry forbidden but can be seen as a weak band in some cases.

8.2.1.1 Reactions at Room Temperature in CH_2Cl_2

A solution of aminophosphine ligand in CH_2Cl_2 was degassed by nitrogen bubbling. The flask was placed in a waterbath, and its temperature noted. After ca. 5 minutes' bubbling, $[Mn(CO)_5Br]$ was added in one portion, dissolving easily to give a yellow or orange solution. Nitrogen bubbling was continued throughout the experiment to remove dissolved carbon monoxide and so prevent any back-reaction being significant. Samples of the solution were taken at regular intervals, and the solution IR spectrum measured between $1800cm^{-1}$ and $2200cm^{-1}$. When enough data points had been taken to determine the rate, or when the starting material had been consumed, monitoring was stopped. Details of individual reactions are given in Table 8.2 and Appendix 8.1.

Table 8.2: Parameters of Reactions Carried Out at Room Temperature

Ligand	Amount of Ligand / mmol	Amount of $[Mn(CO)_5Br]$ / mmol	Volume of CH_2Cl_2 / ml	Waterbath Temperature / °C
dppb	0.33	0.36	30	‡
dppmen	0.13	0.29	15	6.5
dpppen	0.17	0.25	15	18
dppipen	0.16	0.18	15	16
dpptben	0.33	0.36	30	13
dppmpn	1.06§	0.36	30	13.5
dppippn	0.42§	0.36	30	14
dpppip	0.33	0.36	30	13

‡ No waterbath was used in this experiment.
§ This compound was used in an impure state so a greater amount was added.

8.2.1.2 Reactions in Refluxing $CHCl_3$

Portions of aminophosphine ligand and of $[Mn(CO)_5Br]$ were dissolved together in chloroform, and the solution degassed by nitrogen bubbling. The mixture was then heated to the reflux temperature, and the IR spectrum monitored at regular intervals until reaction was complete. Details of these experiments are given in Table 8.3 and Appendix 8.1.

Table 8.3: Parameters of Reactions Carried Out in Refluxing $CHCl_3$

Ligand	Amount of Ligand / mmol	Amount of $[Mn(CO)_5Br]$ / mmol	Volume of $CHCl_3$ / ml
dppb	2.42	0.25	35
dppmen	0.04	0.04	20
dpppen	0.03	0.04	20
dppipen	0.06	0.04	20
dpptben	0.78	0.07	20
dppmpn	2.26	0.22	35
dppippn	0.38	0.11	20
dpppip	0.09	0.07	20

8.2.1.3 Decomposition of $[(L_2)Mn(CO)_3Br]$ Complexes: the Crystal Structure of N,N'-di-*tert*-butylethylenediammonium hydrohalide dihydrate

On standing for a few days, a number of the manganese pentacarbonyl bromide - aminophosphine reaction solutions became clear, and deposited a white solid. In the case of the reaction of dpptben with $[Mn(CO)_5Br]$, this yielded colourless crystals suitable for X-ray diffraction. The structure of the compound was determined by Dr. A.S. Batsanov, and found to be N,N'-di-*tert*-butylethylenediammonium dihalide dihydrate, with the halide ions being chloride or bromide in the ratio 4:1. The structure is shown in Fig. 8.1. Selected bond lengths and angles are given in Tables 8.4 and 8.5, and full structural data is in Appendix 8.2.

Table 8.4: Selected Bond Lengths of N,N'-di-*tert*-butylethylenediammonium dihalide dihydrate

Bond	Length / Å	Bond	Length / Å
N - C(1)	1.489(2)	C(1) - C(1')	1.525(2)
N - C(2)	1.527(2)	C(2) - C(3)	1527(2)
C(2) - C(4)	1.521(2)	C(2) - C(5)	1.525(2)

Table 8.5: Selected Bond Angles of N,N'-di-*tert*-butylethylenediammonium dihalide dihydrate

Bond	Angle / °	Bond	Angle / °
N - C(1) - C(1')	108.90(12)	C(1) - N - C(2)	117.66(10)
C(3) - C(2) - N	105.05(11)	C(4) - C(2) - N	108.73(12)
C(5) - C(2) - N	108.54(11)		

Fig. 8.1: The Molecular Structure of N,N'-di-*tert*-butylethylenediammonium dihalide dihydrate (halide is chloride or bromide in a 4:1 ratio)

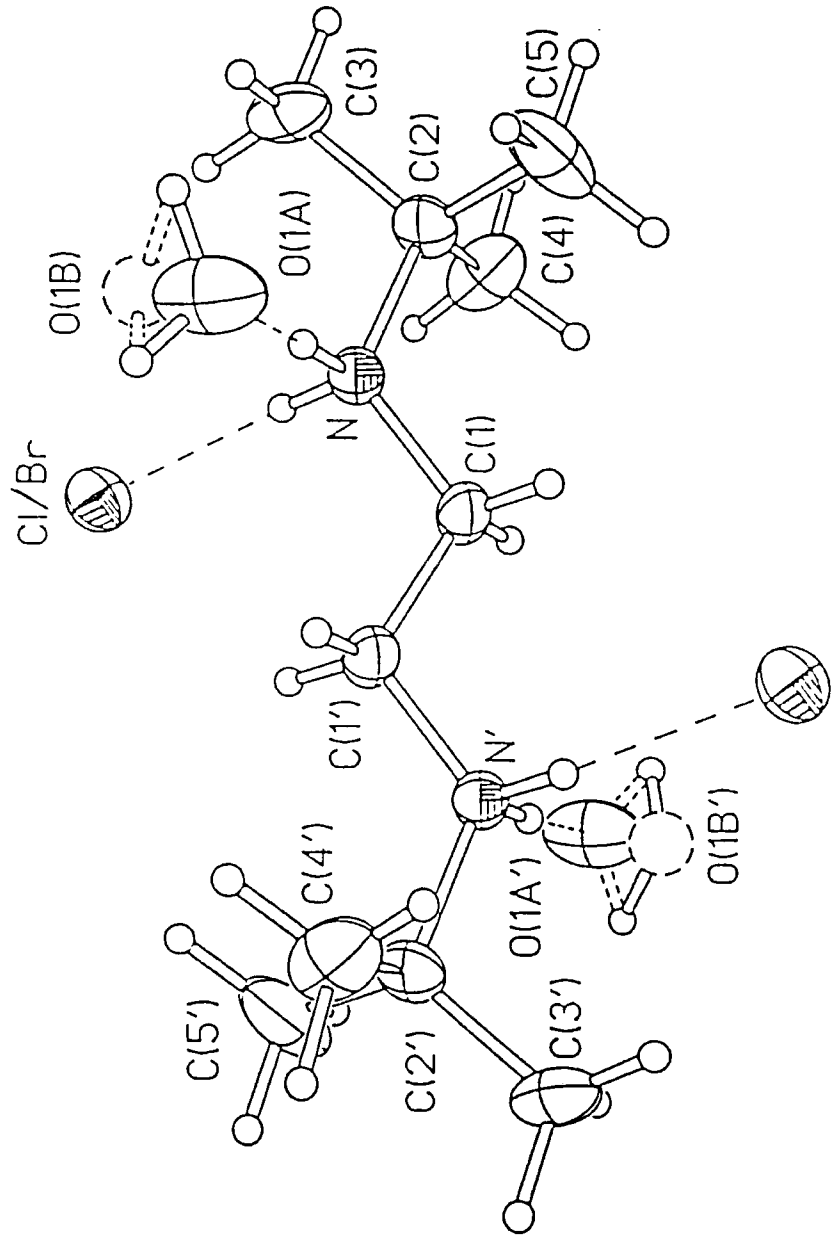

8.2.2 Competitive Reactions of [(diaminodiphosphine)$PdCl_2$] Complexes

In a typical procedure, a [(diaminodiphosphine)$PdCl_2$] complex was dissolved in 1 - 2ml dry, degassed $CDCl_3$ and its ^{31}P nmr spectrum noted. A portion of a different phosphine ligand was added, and the ^{31}P nmr spectrum run again, the solution being monitored over 12 - 18 hours. Details of experiments undertaken are given in Table 8.9. The results are presented in section 8.3.2.

8.2.3 Decomposition of a Palladium Dichloride Complex: The Crystal Structure of Dichloro-N,N'-(*trans*-N,N'-bis(benzyl)cyclohexane-1,2-diamine)palladium(II)

The ligand *trans*-N,N'-(phenylphosphino)-N,N'-bisbenzylcyclohexane-1,2-diamine (see Fig. 8.2) was synthesised by reaction of dichlorophenylphosphine ($PhPCl_2$) and *trans*-N,N'-bis(benzyl)cyclohexane-1,2-diamine. The latter was synthesised by a literature procedure [12]. The crude phosphine was reacted with bis(benzonitrile)palladium dichloride, [$(PhCN)_2PdCl_2$], and crystals of a product were obtained by evaporation of a diethylether solution over several weeks. The structure of the compound was determined by Dr. C.W. Lehmann as that of dichloro-N,N'-(*trans*-N,N'-bis(benzyl)cyclohexane-1,2-diamine)palladium(II), as shown in Fig. 8.3. Selected bond lengths and angles are shown in Tables 8.6 and 8.7, and further structural data are presented in Appendix 8.3.

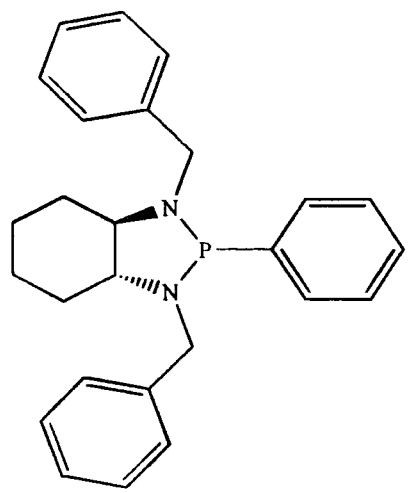

Fig 8.3: *trans*-N,N'-(phenylphosphino)-N,N'-bis(benzyl)cyclohexane-1,2-diamine

Table 8.6: Selected Bond Lengths of Dichloro-N,N'-(*trans*-N,N'-bis(benzyl)cyclohexane-1,2-diamine)palladium(II)

Bond	Length / Å	Bond	Length / Å
Pd(1) - N(1)	2.069(5)	Pd(1) - Cl(1)	2.322(2)
Pd(1) - N(2)	2.075(5)	Pd(1) - Cl(2)	2.314(2)
N(1) - C(1)	1.501(7)	N(1) - C(10)	1.490(8)
N(2) - C(6)	1.499(8)	N(2) - C(20)	1.500(8)
C(1) - C(6)	1.537(8)		

Table 8.7: Selected Bond Angles of Dichloro-N,N'-(*trans*-N,N'-bis(benzyl)cyclohexane-1,2-diamine)palladium(II)

Bond	Angle / °	Bond	Angle / °
N(2) - Pd(1) - N(1)	83.2(2)	N(1) - Pd(1) - Cl(2)	93.61(14)
N(2) - Pd(1) - Cl(1)	94.39(14)	Cl(1) - Pd(1) - Cl(2)	88.86(6)
C(10) - N(1) - C(1)	114.3(5)	C(6) - N(2) - C(20)	113.5(5)
C(10) - N(1) - Pd(1)	120.5(4)	C(20) - N(2) - Pd(1)	120.3(4)
C(1) - N(1) - Pd(1)	109.3(4)	C(6) - N(2) - Pd(1)	108.0(4)
N(1) - C(1) - C(6)	106.9(4)	N(2) - C(6) - C(1)	106.5(5)
N(1) - C(1) - C(6) -N(2)	55.9(6)		

Fig 8.4: The Molecular Structure of Dichloro-N,N'-(*trans*-N,N'-bis(benzyl)cyclohexane-1,2-diamine)palladium(II)

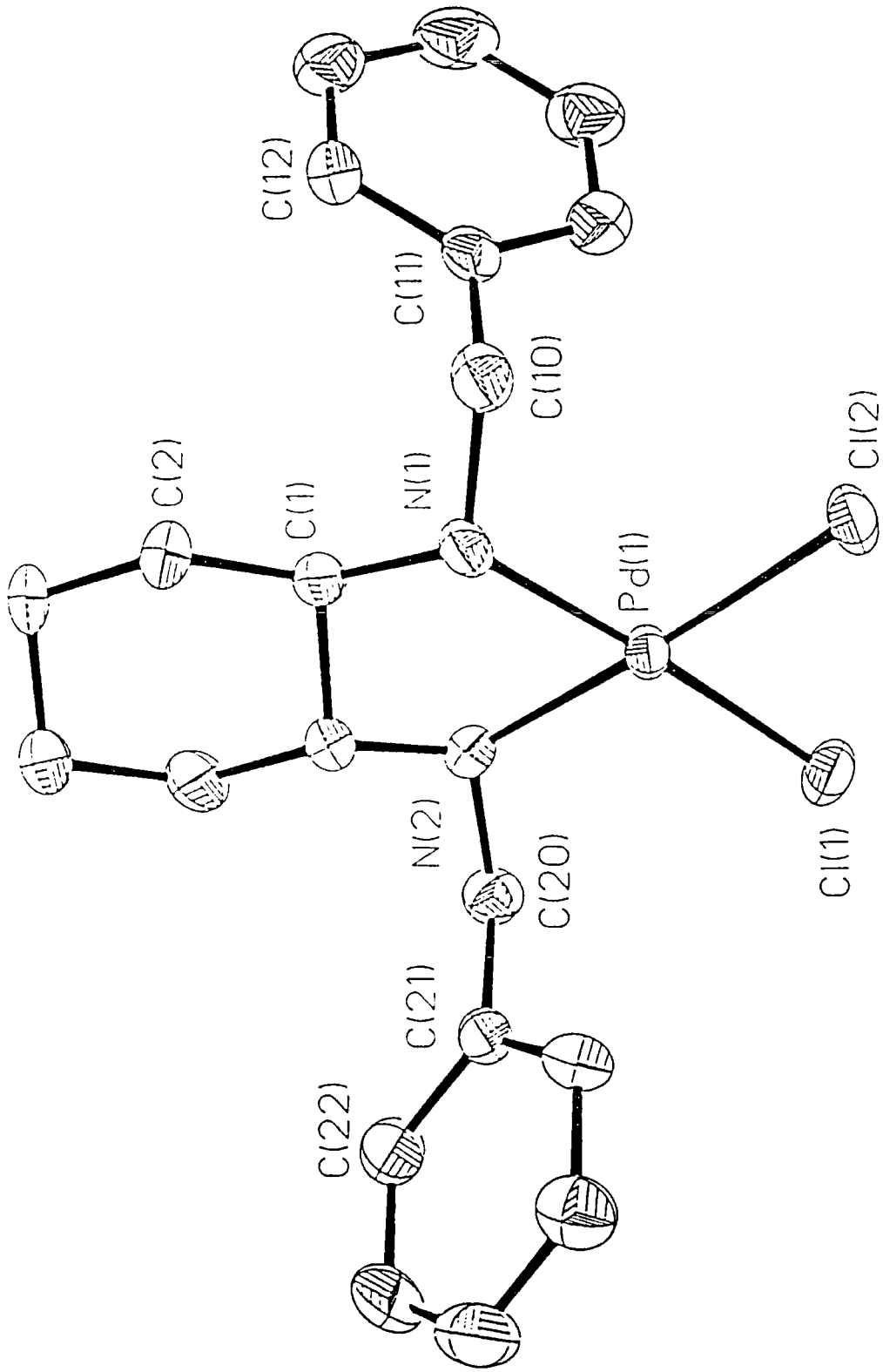

8.2.4 Reaction of [(dpptben)$PtCl_2$] with PPh_3

A portion of [(dpptben)$PtCl_2$] (0.01g, 1.2 x 10^{-5} mol) was dissolved in dry, degassed $CDCl_3$ (2ml). ^{31}P nmr: δ_P = 52.5ppm (t, J_{Pt-P} = 4139Hz). To this was added triphenylphosphine (0.06g, 2.3 x 10^{-4} mol). ^{31}P nmr showed no sign of reaction, even after standing for 72 hours.

8.2.5 Reaction with Non-Metal Reagents

8.2.5.1 Reaction of dpptben with air

To investigate the decomposition of the ligand dpptben, a portion (0.31g, 5.7x10^{-4} mol) was dissolved in toluene which was dry but not degassed. After leaving to stand overnight the solution had darkened, and after a few days a white precipitate had formed, which was separated from the solution by filtration. The white solid gave the following spectrum in $CDCl_3$: ^{31}P nmr: δ_P = 32.3 (s). ^1H nmr: δ_H = 7.3 - 7.7ppm (m, Ph), 3.1ppm (m, 4H, CH_2), 0.8ppm (s, 18H, CH_3). The solution remaining after filtration showed many peaks in the ^{31}P nmr spectrum, at δ_P = 54.0ppm (s), 50.7ppm (s, dpptben), 46.0ppm (s), 29.2ppm (s), 28.2ppm (s), 16.7ppm (s), 14.9ppm (s).

8.2.5.2 Reaction of dpptben with sulphur

To a solution of dpptben (0.01g, 1.9 x 10^{-5} mol) in $CDCl_3$ (2ml) was added a small portion of elemental sulphur (0.03g, 9.4 x 10^{-4} mol). This changed the ^{31}P nmr signal from 50.7ppm (s, dpptben) to 65.3ppm (s).

8.2.5.3 Reaction of dpptben with water

A portion of dpptben (0.15g, 2.8 x 10^{-4} mol) was dissolved in dry, degassed CH_2Cl_2 (15ml). To this was added degassed water (15ml), forming a clear two-layered mixture. This could be emulsified by vigorous stirring. A small amount of white precipitate was seen. The reaction mixture was allowed to stir for several days, and the ^{31}P nmr spectrum monitored. The spectrum showed peaks at δ_P = 53.8ppm (s), 49.8ppm (s), 48.5ppm (s), 32.4ppm (s, largest peak), 21.6ppm (s). The disappearance of the free

ligand peak at δ_P = 50.7ppm was also noted. In the (CH_2Cl_2 solution) IR spectrum, a broad peak was seen at 3200-3400cm^{-1}, though no detail was visible underneath it.

8.2.5.4 Reaction of dpptben with Ethyl Iodide

To a suspension of dpptben (0.3g, 5.6 x 10^{-4} mol) in dry, degassed diethyl ether (15ml) was added a degassed solution of ethyl iodide (0.35g, 2.2 x 10^{-3} mol) in diethyl ether (15 ml). This gave also a white suspension. After stirring overnight, a white precipitate had settled, which was found to be dpptben (δ_P = 50.7ppm) and decomposition product (δ_P = 32.3ppm) by ^{31}P nmr.

8.2.5.5 Reaction of dpppip with HBF_4

A portion of dpppip (0.02g, 4.4 x 10^{-5} mol) was dissolved in diethyl ether (2 ml) and its ^{31}P nmr spectrum run (δ_P = 63.5ppm). HBF_4 . Me_2O (1ml, 0.010 mol) was added in one portion and the ^{31}P nmr spectrum (δ_P = 67.0ppm (s), 59.0ppm (s), 46.6ppm (s), 36.2ppm (s), 34.0ppm (s), 25.8ppm (s, br), 3.7ppm (s), -19.6ppm (s)), ^{1}H nmr spectrum (δ_H = 9.6ppm (s), 9.1ppm (s, br), 8.2ppm (s, br), 7.6-7.9ppm (m, Ar), 6.9ppm (s), 3.9ppm (q), 3.7ppm (s), 1.3ppm (t)) and solid-state infrared spectrum (ν(NH) = 3152, 3222 cm^{-1}) followed.

8.2.5.6 Reaction of [(dpppip)$PdCl_2$] with HBF_4

A portion of [(dpppip)$PdCl_2$] (0.01g, 1.6 x 10^{-5} mol) was suspended in HBF_4 . Me_2O, and the ^{31}P nmr of the sample was followed, despite the complex being largely insoluble. This meant that the peaks seen were invariably small and broad. δ_P = 160.2ppm (s), 148.9ppm (s), 89.1ppm (s), 81.2ppm (s), 69.9ppm (s), 59.0ppm (s), 48.2ppm (s). The signal due to [(dpppip)$PdCl_2$] at δ_P = 104.1ppm (s) was found to disappear. ^{1}H nmr showed broad peaks at δ_H = 10.5ppm (s), 9.2ppm (s), 7.3ppm (m, Ph), 3.7ppm (s), 3.5ppm (s).

8.3 Results

8.3.1 Reactions with $[Mn(CO)_5Br]$

8.3.1.1 Characterisation of Complexes Formed

The IR spectra of the complexes of aminophosphines and $[Mn(CO)_5Br]$ formed in solution were assigned by comparison with data for complexes reported in the literature, most notably *cis*-$[(PPh_3)Mn(CO)_4Br]$ and *mer*-$[(PPh_3)_2Mn(CO)_3Br]$ [13].

Table 8.8: Characterisation of [(diaminodiphosphine)$Mn(CO)_xBr$] Complexes by IR Spectroscopy

Ligand	*cis*-$[LMn(CO)_4Br]$	*fac*-$[(L_2)Mn(CO)_3Br]$	*mer*-$[(L_2)Mn(CO)_3Br]$
dppb	2090 (s) 2023 (vs) 2006 (vs) 1956 (vs)	2029 (vs) 1961 (s) 1919 (s)	**
dppmen	2090 (m) 2023 (s) 2005 (vs) 1960 (s)	2029 (vs) 1962 (s) 1920 (s)	2048 (w) 1960 (vs) 1924 (m, br)
dpppen	2091 (w) 2021 (s) 2008 (s) 1959 (m)	2028 (vs) 1958 (s) 1919 (s)	2045 (w, br) 1960 (vs) 1920 (m)
dppipen	2089 (w) 2024 (m) 2006 (m) 1957 (m)	2028 (vs) 1961 (s) 1919 (s)	2049 (w) 1960 (vs) 1924 (m, br)

** This species was not observed.

dpptben	2091 (w) 2017 (s) 2008 (s) 1962 (m)	2027 (s) ††	2045 (w) 1960 (vs) 1920 (m)
dppmpn	2090 (s) 2020 (vs) 2005 (vs) 1960 (vs)	2026 (vs) 1956 (s) 1918 (s)	**
dppippn	2089 (w) 2021 (s) 2008 (s) 1960 (s)	**	2045 (w) 1960 (vs) 1920 (m)
dpppip	2091 (s) 2023 (vs) 2005 (vs) 1961 (vs)	**	2042 (w) 1954 (vs) 1916 (m)

8.3.1.2 Rates of Complexation Reactions

The information presented here refers to the reaction of $[Mn(CO)_5Br]$ with a chelating diaminodiphosphine ligand. The disappearance of $[Mn(CO)_5Br]$ was followed by following the area of the E band at $2052cm^{-1}$ [13]. The concentration of the ligand was not followed, and a great excess was not used, making the accurate determination of rate constants impossible. However, the relative rates of the reactions have been compared by inspection of a plot of the concentration of manganese pentacarbonyl bromide against time, and been found to fall into three groups:

dppmpn, dppb, dppmen, dpppip > dpppen, dppipen, dppippn >> dpptben

The shapes of these plots were different for different ligands, either straight lines or curved. The significance of this is not fully understood.

†† Other peaks were not identified due to a mixture of isomers being present.

8.3.2 Competitive Reactions of Diaminodiphosphine Palladium Dichloride Complexes

Table 8.9: Results of Competitive Reactions of Palladium Dichloride Complexes

Starting Materials (δ_P / ppm)	Amount Used / mmol	Spectrum (δ_P / ppm)	Assignment	Exchange ?
[(dpptben)$PdCl_2$] (74.8)	0.01	50.7	dpptben	Yes
		-21.5 (br)		
dppm (-23) [14]	0.08	-23.4 (br)	dppm	
[(dpptben)$PdCl_2$] (74.8)	0.01	56.8	[(dppe)$PdCl_2$] [1,15,16]	Yes
dppe (-13) [14]	0.10	50.7	dpptben	
		-11.5	dppe	
[(dpptben)$PdCl_2$] (74.8)	0.01	50.7	dpptben	Yes
		-0.7 (br)		
dppp (-17) [15,17,18]	0.12	-16.5	dppp	
[(dpptben)$PdCl_2$] (74.8)	0.03	50.7	dpptben	Yes
		-15.0 (br)	dppb	
dppb (-16) [15,18,19]	0.14			
[(dpptben)$PdCl_2$] (74.8)	0.03	50.7	dpptben	Yes
		24.4	[$(PPh_3)_2PdCl_2$] [1]	
PPh_3 (-4.7) [14]	0.19	-4.3	PPh_3	
[(dpptben)$PdCl_2$] (74.8)	0.01	104.1	[(dpppip)$PdCl_2$]	Yes
		63.5	dpppip	
dpppip (63.5)	0.13	50.7	dpptben	
[(dpppip)$PdCl_2$] (104.1)	0.02	104.1	[(dpppip)$PdCl_2$]	No
		-4.7	PPh_3	
PPh_3 (-4.7)	0.23			

[(dpptben)$PdCl_2$]	0.01	80.9	[(dppipen)$PdCl_2$]	Yes
(74.8)		50.7	dpptben	
dppipen (47.1)	0.10	47.1	dppipen	
[(dppipen)$PdCl_2$]	0.01	80.9	[(dppipen)$PdCl_2$]	No
(80.9)		-4.7	PPh_3	
PPh_3 (-4.7)	0.46			
[(dpptben)$PdCl_2$]	0.01	85.6	[(dpppen)$PdCl_2$]	Yes
(74.8)		62.3	dpppen	
dpppen (62.3)	0.03	50.7	dpptben	
[(dpppen)$PdCl_2$]	0.01	85.6	[(dpppen)$PdCl_2$]	No
(85.6)		-4.3	PPh_3	
PPh_3 (-4.7)	0.31			
[(dpptben)$PdCl_2$]	0.01	79.5	[(dppmen)$PdCl_2$]	Yes
(74.8)		65.9	dppmen	
dppmen (65.9)	0.11	50.7	dpptben	
[(dppmen)$PdCl_2$]	0.02	79.5	[(dppmen)$PdCl_2$]	No
(79.5)		-4.3	PPh_3	
PPh_3 (-4.7)	0.34			
[(dppipen)$PdCl_2$]	0.03	80.9	[(dppipen)$PdCl_2$]	No
(80.9)		62.3	dpppen	
dpppen (62.3)	0.05			
[(dppmen)$PdCl_2$]	0.02	79.4	[(dppmen)$PdCl_2$]	Yes, to an
(79.4)		65.9	dppmen	extent
dpppip (63.5)	0.13	63.5	dpppip	
[(dpppen)$PdCl_2$]	0.03	79.4	[(dppmen)$PdCl_2$]	Yes
(85.5)		65.9	dppmen	
dppmen (65.9)	0.11	62.3	dpppen	
[(dpppip)$PdCl_2$]	0.02	88.8	[(dppmpn)$PdCl_2$]	Yes
(104.1)		81.3	further reaction	
dppmpn (65.1)	0.13	65.1	dppmpn	
		63.4	dpppip	

[(dppipen)$PdCl_2$]	0.02	82.7	[(dppipen)$PdCl_2$]	Yes
(82.9)		80.8	[(dppippn)$PdCl_2$]	
dppippn (48.9)	0.19	46.8	dppipen	
[(dppippn)$PdCl_2$]	0.02	80.8	[(dppippn)$PdCl_2$]?	No
(80.8)		62.3	dpppen	
dpppen (62.3)	0.02			
[(dppmpn)$PdCl_2$]	0.02	65.2	dppmpn	Yes
(88.8)		-14.1 (br)	[(dppb)$PdCl_2$]	
dppb (-16)	0.09		exchanging with	
			dppb	
[(dppmen)$PdCl_2$]	0.02	82.8 (small)	[(dppippn)$PdCl_2$]	Small
(79.4)		79.4	[(dppmen)$PdCl_2$]	amount of
dppippn (46.8)	0.04	65.9 (small)	dppmen	exchange.
		46.8	dppippn	

Some of the peaks relating to dppb, dppp, dppe and dppm were broad, and this made them difficult to assign with certainty. Sometimes a peak appeared at a value between that of the free ligand and its complex, indicative of exchange processes between the ligand and its complex.

The results shown in Table 8.9 give the following order of ligand strength:

dppmpn > dpppip > dppmen > dppippn > dppipen > dpppen > PPh_3 > dpptben

It would also appear that dpppip, dppmen and dppippn have similar binding properties, since only a limited amount of exchange is seen in these cases.

8.3.3 Reaction with Non - Metal Systems

Table 8.11 Reaction of Aminophosphine Ligands with Non-Metals

Starting Materials (δ_P / ppm)	Products (δ_P / ppm)	Assignment	Results
dpptben (50.7) air	solid: 32.3 solution: many peaks	phosphine dioxide	Oxidation occurs giving a solid. Other decomposition products in solution
dpptben (50.7) sulphur	65.3	phosphine disulphide	Oxidation occurs.
dpptben (50.7) water	53.8 49.8 48.5 32.4 21.6	phosphine dioxide	Decomposition.
dpptben (50.7) ethyl iodide	50.7 32.4	dpptben phosphine dioxide	No reaction with ethyl iodide.
dpppip (63.5) HBF_4	67.0 59.0 46.6 36.2 34.0 25.8 (br) 3.7 -19.6	Disappearance of dpppip noted.	Reaction gives many products.
$[(dpppip)PdCl_2]$ (104.1) HBF_4	160.2 148.9 89.1 81.2 69.9 59.0 48.2	Disappearance of $[(dpppip)PdCl_2]$ noted.	Reaction to give many products.

8.4 Discussion

8.4.1 Reactions with $[Mn(CO)_5Br]$

Reactions of aminophosphines with $[Mn(CO)_5Br]$ were investigated as described above. Products corresponding to mono- and di-substitution were identified by solution IR spectra. When the solution was heated, the rate of reaction was much greater, and the di-substituted product was seen. The facial isomer was seen to form first in most cases, followed by isomerisation to the meridianal isomer. This relieves the steric interaction between the large bromine atom and one end of the ligand. However, the initial substitutions were usually *cis* to the bromine atom, as these are the most labile carbonyl groups [2]. This is a demonstration of kinetic (facial) and thermodynamic (meridianal) products being formed under different conditions. The reactions are shown in Scheme 8.3. It is possible that a *fac*-isomer could be formed by two bridging ligands as shown in Fig. 8.4, but this is disfavoured compared to chelation for a dilute solution (the concentration of $[Mn(CO)_5Br]$ is typically 0.01-0.02 mol dm^{-3} here) since it is more likely that the end of a free ligand will meet the manganese centre to which the other end is joined, rather than a second molecule. Also, some of the sterically bulky ligands used in this work may form a *trans,mer*-isomer, also shown in Fig. 8.4, but this is not likely for the reasons outlined above.

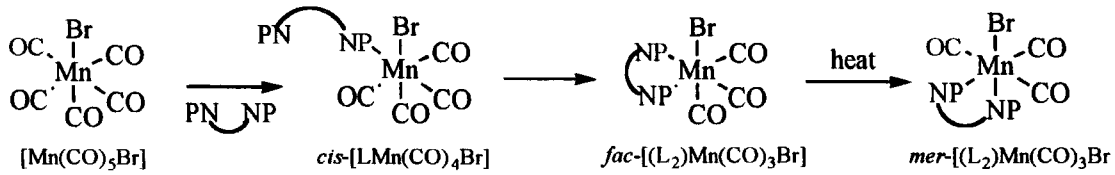

Scheme 8.3: Reactions of Chelating Aminophosphine Ligands with $[Mn(CO)_5Br]$ in solution

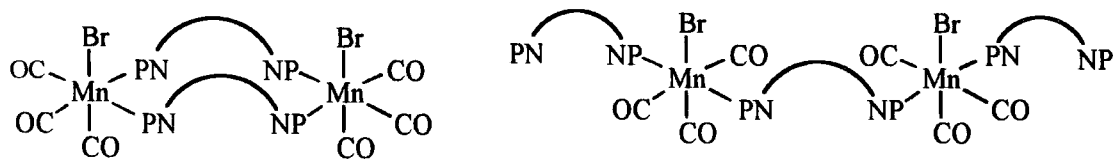

Fig. 8.5: Bridging Isomers of *fac*-$[L_2Mn(CO)_3Br]$ (left) and *trans,mer*-$[L_2Mn(CO)_3Br]$ (right)

The assignments of particular bands in the IR spectra of these compounds are given in Appendix 8.1. Often, the presence of more than one species in solution made

the assignment difficult, and broad peaks were indicative of two peaks with similar frequencies. This is indicated in the Tables. Attempts were made to follow these reactions by ^{31}P nmr spectroscopy, but broad peaks made assignment difficult. The broadness could be caused by coupling to ^{55}Mn (I = 5/2, natural abundance = 100% [20]), exchange, paramagnetic impurities or decomposition.

On standing for a few days, the solutions containing these products decomposed, turning from their initial yellow colour to colourless. A colourless solid was deposited in all cases. In the case of dpptben, the crystal structure of the solid was determined and found to be N,N'-di-*tert*-butylethylenediammonium dihalide, with chloride and bromide ions in the ratio 4:1. This means that the decomposition of these compounds can involve cleavage of the nitrogen-phosphorus bond. Attempts were made to investigate these solutions by ^{31}P nmr, but broad peaks made this difficult. Hydrolysis of the phosphorus - nitrogen bond is suggested by the presence of two water molecules in the crystal structure. The presence of bromide ions in the crystal indicates decomposition of the manganese - bromine bond, whilst the chloride ions have come from the solvent, which was either chloroform or dichloromethane. Chloroform has been found to react with oxygen in the presence of light to give $Cl_2C=O$ (phosgene), chlorine and hydrogen chloride [21]. It is possible that one of these compounds is responsible for the decomposition of the complex.

8.4.1.1 Kinetic Study

The reaction of $[Mn(CO)_5Br]$ with chelating diaminodiphosphine ligands was studied in dichloromethane solution at room temperature, giving the relative order of reaction rate shown:

dppmpn, dppb, dppmen, dpppip > dpppen, dppipen, dppippn >> dpptben

The order of reaction rate found in these experiments was essentially based on the steric requirements of the ligand used, and mirrors the order observed in the competitive reactions of palladium dichloride complexes. The rate of reaction of dpptben is the

lowest of all the diaminodiphosphine ligands studied which is thought to be a reflection of the extreme bulk of the *tert*-butyl group.

8.4.1.2 Determination of Electronic Parameters

Attempts were made to calculate the variation in the donor - acceptor properties of the ligands studied by comparison of the A_1 stretching frequency of the tetracarbonyl complex [$LMn(CO)_4Br$]. However, the differences in these were very small, less than the resolution of the spectrometer. This means that any conclusions drawn on this basis would be insignificant. Elsewhere a range of $15cm^{-1}$ has been reported for a series of phosphorus donor ligands [10]. For example, [$(PPh_3)Mn(CO)_4Br$] has ν(CO, E) = $2091cm^{-1}$ whilst [$(L_2)Mn(CO)_4Br$] has ν(CO, E) = $2107cm^{-1}$ where the ligand L_2 is 1,2-bis(dichlorophosphino)ethane [10].

It appears possible that the donation of electron density from the lone pair on nitrogen to the phosphorus - nitrogen bond compensates for any electron withdrawal from phosphorus due to the electronegativity of nitrogen, and the net effect is similar to that of a methylene group. This means that changing the group at nitrogen has little effect on the electronic properties of the ligand. The ligand dppa has been reported to be a more electron withdrawing ligand than hydrocarbon-backboned ligands such as dppp and dppe [22].

8.4.2 Competitive Reactions of Diaminodiphosphine Ligands with Diaminodiphosphine Palladium Dichloride Complexes

The reaction of a phosphine or diaminodiphosphine ligand with the palladium dichloride complex of a different diaminodiphosphine was studied to investigate the comparative binding ability of the diaminodiphosphine ligands synthesised. This led to the following order of ligand ability:

dppmpn > dpppip > dppmen > dppippn > dppipen > dpppen > PPh_3 > dpptben

The ligand dpptben was also displaced by dppm, dppe, dppp and dppb. The general trend is that less bulky ligands, such as dppmen, bind in preference to more

sterically demanding ligands, for example dpptben. The steric demands of bulky ligands can make their complexes unstable to reaction with a less bulky ligand. It is noted that less bulky ligands react more quickly with $[Mn(CO)_5Br]$ than their bulkier counterparts, as discussed above. Differences in the two sets of results are ascribed to differences in the nature of the metal centre, such as electron donor - acceptor properties or steric requirements.

A second factor which affects the binding ability is the size and nature of the backbone. The three-carbon backboned ligands dppmpn and dppippn both bind in preference to their two-carbon backboned analogues dppmen and dppipen respectively. The increased conformational flexibility and so decreased activation energy of binding of the longer backbone is responsible for the preferential co-ordination. A measure of this is that dppippn, a bulky ligand, will displace dpppen. The ligand dpppip preferably forms a *trans*-isomer due to the inflexibility of its backbone, and this precipitates from solution. The precipitation could be responsible for its strong co-ordination as the reaction would no longer be an equilibrium process.

It is interesting to observe that dpptben is replaced at palladium by triphenylphosphine. This is unusual in that the chelate effect gives a significant enhancement in the binding of bidentate over monodentate ligands [23]. The ligand exchange is a reflection of the large steric bulk of the dpptben ligand, and so in turn of the *tert*-butyl group. None of the other ligands investigated were displaced by PPh_3, nor was dpptben when co-ordinated to platinum. This is a consequence of the greater lability of palladium over platinum complexes. It has been observed that dppa co-ordinates to $[Pt(COD)Cl_2]$ in preference to dppm [24]. This effect was ascribed to dppa forming stronger bonds to the metal.

8.4.3 Reaction with Non-Metal Reagents

8.4.3.1 Reaction with Air

The reaction of a toluene solution of dpptben yielded a white solid, which was shown to have one ^{31}P nmr signal at δ_P = 32.3ppm ($CDCl_3$ solution), and is assigned to the phosphine dioxide shown in Fig. 8.5. This is in good agreement with data for the aminophosphine oxide $Ph_2P(O)NMe_2$, which has δ_P = 29.5ppm [25]. The slight difference is due to the difference in organic groups at nitrogen.

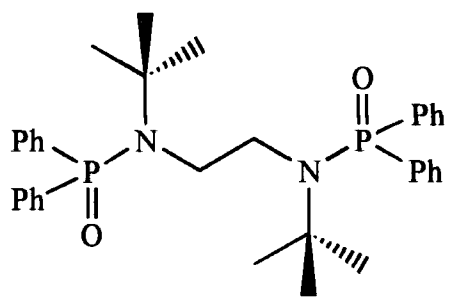

Fig. 8.6: Phosphine Dioxide of dpptben

Analysis of the filtrate by ^{31}P nmr showed the presence of small quantities of other phosphorus - containing materials, which were not characterised, indicating that many different decomposition products are formed.

8.4.3.2 Reaction with Elemental Sulphur

Reaction of dpptben with elemental sulphur in deuterochloroform solution gave a species with δ_P = 65.3ppm (s) as the only peak in the ^{31}P nmr spectrum. This signal is assigned to the disulphide, shown in Fig. 8.6. As there is only one peak, the monosulphide, which would show two peaks, is eliminated as a possibility. Comparison with literature data for other aminophosphines is presented in Table 8.10. The difference between the free aminophosphine chemical shift and that of the disulphide for dpptben is in the range of the other compounds in the Table, supporting this assignment.

Table 8.10: Comparison of ^{31}P nmr Data for Aminophosphines and Aminophosphine Sulphides

Aminophosphine (δ_P / ppm)	Aminophosphine Sulphide (δ_P / ppm)	δ_P(Aminophosphine Sulphide) - δ_P(Aminophosphine)/ppm
dpptben (50.7)	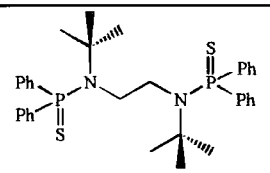 (65.3)	14.6
dppa (41.3 [26])	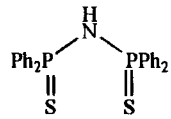 (55.2 [27])	13.9
Ph_2PNMe_2 (63.9 [28])	$Ph_2P(S)NMe_2$ (70.9 [29])	7.0

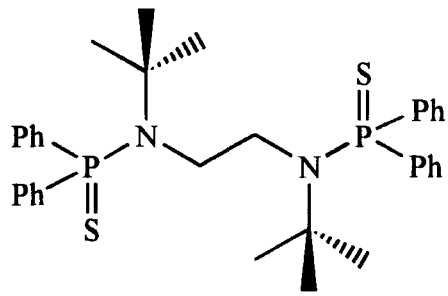

Fig. 8.7: Phosphine Disulphide of dpptben

8.4.3.3 Reaction with Water

Over a period of a few days, a dichloromethane solution of dpptben was seen to react with water, producing numerous products, including the phosphine dioxide. The other products, present in small amounts, were not identified. However, the disappearance of the peak due to the starting material confirms the moisture-sensitive nature of the ligand.

8.4.3.4 Reaction with Ethyl Iodide

There was no reaction between dpptben and ethyl iodide. This was disappointing, as tertiary phosphines will typically react with alkyl iodides to give four co-ordinate phosphonium salts such as $[Ph_2P(Et)NMe_2]I$ (δ_P = 50.0ppm [30]). However, it is possible that either the steric bulk of dpptben disfavours reaction with an alkyl iodide, or that the phosphorus lone pair of electrons is involved in bonding within the molecule, and so is not available for further bonding. However, since aminophosphine dioxides and disulphides can be synthesised, as shown above, reaction with the phosphorus lone pair must be possible.

8.4.3.5 Reaction with HBF_4

HBF_4 is an acid with an essentially non co-ordinating anion. Reactions of iminophosphine complexes with acids have been investigated [27], and protonation at nitrogen is found to be possible for the anionic ligand, as shown in Scheme 8.4.

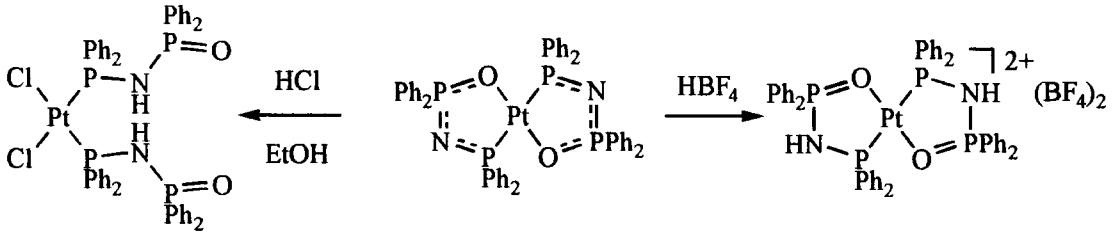

Scheme 8.4: Reactions of $[(dppa)_2Pt]^{2+}$

It is interesting to note that a second protonation at nitrogen to form a quaternary centre was not observed. This is doubtless due to the delocalisation of the nitrogen lone pair through bonding to phosphorus, as illustrated by the crystal structure of dpptben (chapter seven).

The reaction of dpppip with HBF_4 gave a number of products, in contrast to the reactions shown in Scheme 8.4, which gave a single product. It is possible that protonation occurred at phosphorus, since a ^{31}P nmr chemical shift was observed at δ_P = -19.6ppm (s). The literature compound $[Ph_2PH_2](SO_3F)$ has been shown to have δ_P = -21.2ppm [30].

8.4.4 Decomposition Reactions

Decomposition of a diaminophosphine palladium complex and a diaminodiphosphine manganese complex has been found to occur on standing. In both cases cleavage of the nitrogen - phosphorus bond has been observed, giving a free amine or ammonium salt. The decomposition products are characterised by crystal structure analysis; however, the other products were not identified.

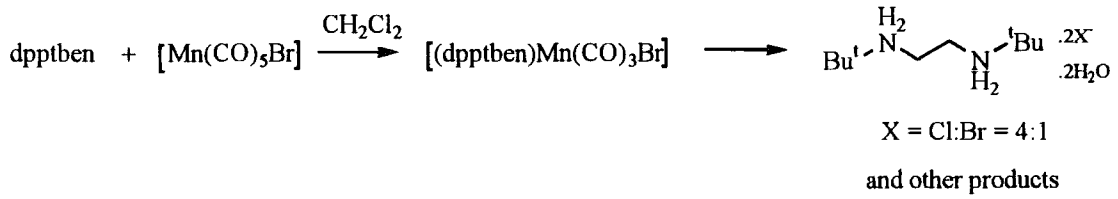

Scheme 8.5: Decomposition of [Mn(dpptben)(CO)$_3$Br]

The presence of the halide counterions to the ammonium salt indicate decomposition of the solvent and also of the manganese - bromine bond has occurred. The presence of two molecules of water in the structure suggests that hydrolysis may be a mechanism for this decomposition.

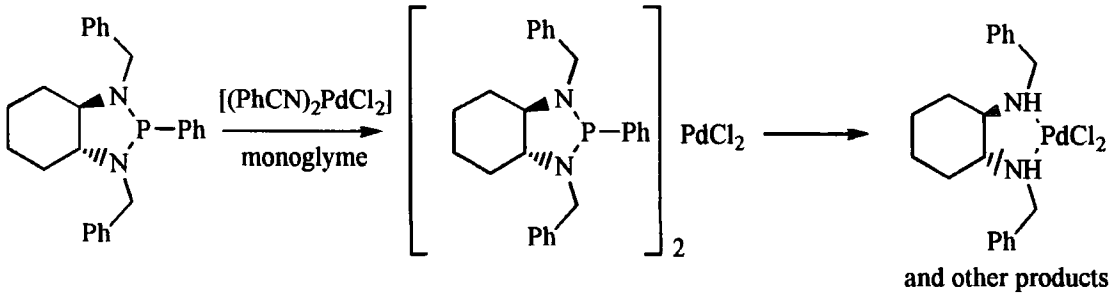

Scheme 8.6: Decomposition of Dichloro-N,N'-(*trans*-N,N'-bis(benzyl) cyclohexanediamine)palladium(II)

Again, nitrogen - phosphorus bond fission is seen, and the resulting amine, *trans*-N,N'-bis(benzyl)cyclohexane-1,2-diamine, has co-ordinated to the metal. The phosphorus - containing products were not characterised.

8.5 Summary

The reactions of aminophosphine ligands with $[Mn(CO)_5Br]$ have been investigated. Complexes containing the ligands in a monodentate and bidentate fashion have been observed, and the gradual reaction from *cis*-tetracarbonyl to *fac*-tricarbonyl to *mer*-tricarbonyl has been followed by infrared methods. The latter correspond to kinetic and thermodynamic products respectively. The reason for the isomerisation is thought to be steric interactions with the bromine atom since it does not occur for the less sterically demanding ligands dppb or dppmpn.

It was hoped to be able to calculate a relative electronic order by consideration of the A_1 band of the tetracarbonyl product. However, due to the small range of values of the E symmetry carbonyl stretching band seen this was not possible, which implies an electronic similarity between a CH_2 and an NR group. An example of this is that $[(dppb)Mn(CO)_4Br]$ has $\nu(CO, A_1) = 2090\ cm^{-1}$, whilst the range of complexes $[(diaminodiphosphine)Mn(CO)_4Br]$ have $\nu(CO, A_1) = 2089 - 2091\ cm^{-1}$.

The kinetics of the reactions of these ligands with $[Mn(CO)_5Br]$ was also investigated, giving the following order of reaction rate:

dppmpn, dppb, dppmen, dpppip > dpppen, dppipen, dppippn >> dpptben

The rate of reaction was dependant largely on steric factors, and mirrors the order seen for the competitive reactions of palladium dichloride complexes, which was found to be:

dppmpn > dpppip > dppmen > dppippn > dppipen > dpppen > PPh_3 > dpptben

which is based on the steric bulk of the ligands. Again dpptben was seen to be the weakest ligand, and was even displaced by PPh_3. This was not observed to be the case at a platinum dichloride centre, due to the greater stability of platinum complexes.

The aminophosphine ligands have been found to be vulnerable to attack by air and moisture. The diphosphine dioxide of dpptben was identified by ^{31}P and ^{1}H nmr.

Reactivity with sulphur was also observed, forming the diphosphine disulphide. Reaction with the non-coordinating acid HBF_4 with either co-ordinated or free dpppip gave many products. No reactivity occurred towards ethyl iodide.

Two new crystal structures, of N,N'-(*trans*-N,N'-bis(benzyl)cyclohexane-1,2-diamine)palladium(II) and of N,N'-di-*tert*-butylethylenediammonium dihalide dihydrate (halide = chloride or bromide in a 4:1 ratio) are reported. These compounds were both formed by decomposition of an aminophosphine metal complex.

8.6 References

1. G.S. Robertson, Ph.D. Thesis, University of Durham, 1997.
3. C.A. Tolman, *J. Am. Chem. Soc.*, 1970, **92**, 2953-6.
4. C.A. Tolman, *Chem. Rev*, 1977, 77, 313-48.
5. R.J. Angelici, F. Basolo and A.J. Poë, *Nature*, 1962, 993-4.
2. R.J. Angelici and F. Basolo, *J. Am. Chem. Soc.*, 1962, **84**, 2495-9.
6. R.J. Angelici and F. Basolo, *Inorg. Chem.*, 1963, **2**, 728-31.
7. R.J. Angelici, *J. Inorg. Nucl. Chem.*, 1966, **28**, 2627-35.
8. R.J. Angelici, F. Basolo and A.J. Poë, *J. Am. Chem. Soc.*, 1963, **85**, 2215-9.
9. R.J. Angelici, *Organomet. Chem. Rev.*, 1968, **3**, 173-226.
10. P.W. Tidswell, Ph.D. Thesis, University of Durham, 1993.
11. M. Kilner, Ph.D. Thesis, University of Nottingham, 1963, pp.84-103.
12. S.E. Denmark, J. Stadler, R.L. Dorow and J.-H. Kim, *J. Org. Chem.*, 1991, **56**, 5063-79.
13. D.M. Adams, "Metal - Ligand and Related Vibrations", Edward Arnold Publishers, 1967, Chapter 3, pp. 84-181.
14. L. Maier, "Primary, Secondary and Tertiary Phosphines", in "Organic Phosphorus Compounds", Vol. 1, G.M. Kosalopoff and L. Maier (eds), J. Wiley and Sons, 1972, p. 106, quoted in ref. 31, p.153.
15. G.T.L. Broadwood-Strong, P.A. Chaloner and P.B. Hitchcock, *Polyhedron*, 1993, **12**, 721-30.
16. D.L. Oliver and G.K. Anderson, *Polyhedron*, 1992, **11**, 2145-20.
17. I.J. Colquhoun and W. McFarlane, *J. Chem. Soc., Dalt. Trans.*, 1982, 1915, quoted in ref. 31, p.153.

18. H.G. Horn and K. Summer, *Spectrochim. Acta, Part A*, 1971, **27**, 1049-54.

19. D. Rehder and A. Keçeci, *Inorg. Chim. Acta*, 1985, **103**, 173-7.

20. R.C. Weast and M.J. Astle, "Handbook of Chemistry and Physics", 3rd Edn., CRC Press, 1982, p. B-263.

21. W.L.F. Armarego and D.D. Perrin, "Purification of Laboratory Chemicals", 4th Edn, Butterworth - Heinemann, 1997, p. 143.

22. Z.-Z. Zhang, A. Yu, H.-P. Xi, R.-J. Wang and H.-G. Wang, *J. Organomet. Chem.*,1994, **470**, 223-9.

23. N.N. Greenwood and A. Earnshaw, "Chemistry of the Elements", Pergamon Press, 1984, pp. 1066-8.

24. C.S. Browning and D.H. Farrar, *J. Chem. Soc., Dalt. Trans.*, 1995, 521-30.

25. A. Schmidpeter and H. Brecht, *Z. Naturforsch*, 1969, **B24**, 179, quoted in ref. 31, p. 356.

26. (a) A. Schmidpeter and J. Ebeling, *Chem. Ber.*, 1968, **101**, 815. (b) A. Schmidpeter and H. Groeger, *Z. Anorg. Allg. Chem.*, 1966, **345**, 106. Both quoted in ref. 31, p. 363.

27. P. Bhattacharyya, A.M.Z. Slawin, M.B. Smith and J.D. Woollins, *Inorg. Chem.*, 1996, **35**, 3675-82.

28. M.M. Crutchfield, C.H. Dungan, J.H. Letcher, V. Mark and J.R. van Wazer, "P^{31} Nuclear Magnetic Resonance", in "Topics in Phosphorus Chemistry", Vol. 5, Wiley Interscience, 1967, quoted in ref. 31, p. 107.

29. A. Schmidpeter and H. Brecht, *Z. Naturforsch*, 1969, **B24**, 179, quoted in ref. 31, p. 363.

30. A. Schmidpeter and H. Brecht, *Z. Naturforsch*, 1969, **B24**, 179, quoted in ref. 31, p. 204.

31. J.C. Tebby (ed), "Handbook of Phosphorus-31 Nuclear Magnetic Resonance Data", CRC Press, 1991.

Chapter Nine: Catalytic Reactions involving Aminophosphine Ligands

9.1 Introduction

This chapter describes the investigation of the catalytic properties of the aminophosphine ligands synthesised in this work, together with their palladium and platinum complexes. Two different reactions were studied, and in each case the findings using the new ligands were compared to a standard system. The reactions investigated were hydroformylation of styrene to give phenylpropanal isomers and methoxycarbonylation of ethene to give methyl propanoate, polyketone polymer or both.

9.1.1 Hydroformylation

Hydroformylation [1] is used industrially in the production of aldehydes [2]. It is an efficient process, and uses cheap and readily-available feedstocks - hydrogen, carbon monoxide and alkenes.

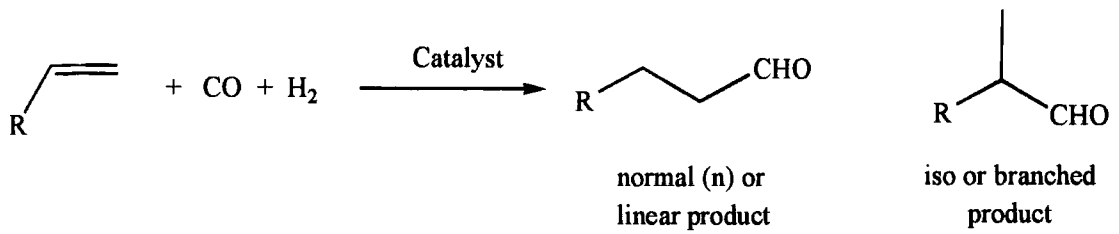

Scheme 9.1: Hydroformylation

The aldehydes produced are rarely used directly, and typically they are instead reduced to the corresponding alcohol [3]. These are widely used, for example as solvents [4] and as starting materials for a wide range of different materials [5]. Hydroformylation of longer chain alkenes produces aldehydes which are reduced to give alcohols for use in detergents. A second method of producing longer chain alcohols is using the aldol condensation [6]. Alcohols such as 2-ethylhexanol originate from the

hydroformylation of propene to butanal [7] and are used as surfactants and fuel additives.

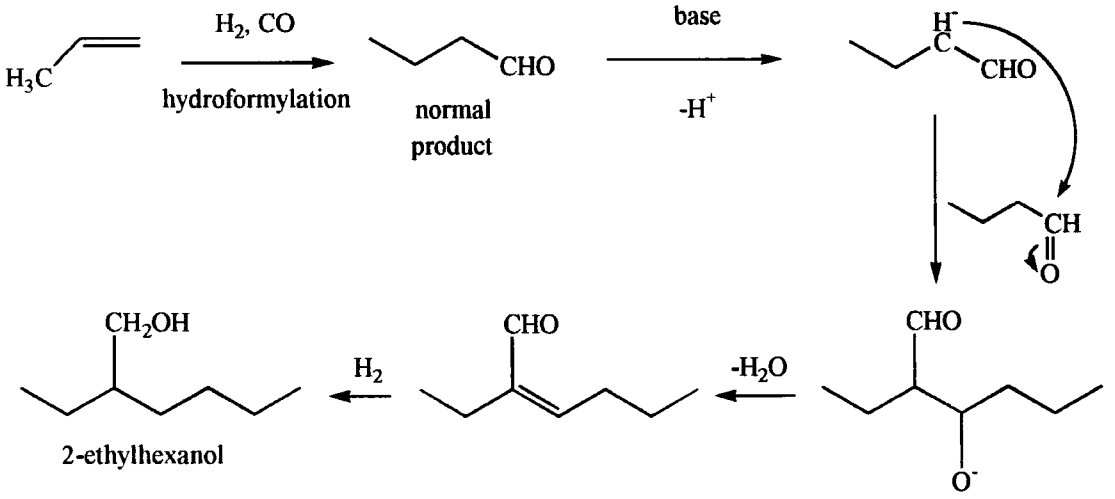

Scheme 9.2: Using The Aldol Reaction to form 2-ethylhexanol

It is also possible to hydroformylate functionalised alkenes, leading to speciality chemicals or pharmaceuticals [8].

The hydroformylation reaction was discovered in 1930 [9], and was commercialised by Otto Roelen [10] in 1943. For many years it was known as the Roelen reaction. The initial work used a heterogeneous catalyst system containing cobalt which was being investigated as a catalyst for Fischer-Tropsch reactions. Many systems were investigated for activity, and early developments lead to a homogeneous catalyst system based on cobalt carbonyl systems [11]. These were active at high pressures (200-400 bar) and temperatures (150°C). The low selectivity of the system to the desired normal product could be improved by the addition of electron-donating ligands such as tertiary phosphines or phosphites [12]. However, the maximum ratio of linear to branched products (the "n to iso ratio") achieved was still in the region of seven to one.

A major breakthrough was made by Osborn, Wilkinson and co-workers in discovering and developing a rhodium-catalysed technology based on triphenylphosphine complexes [13]. This operates at lower pressures and temperatures than the cobalt system, and some compounds are even active at room temperature and pressure [14]. Selectivity to the normal product is also improved to greater than ninety

percent. Most industrial processes now use this technology, or a similar system based on iridium [15].

The mechanism of the reaction has been extensively studied, and is believed to involve rhodium hydride and acyl complexes [16].

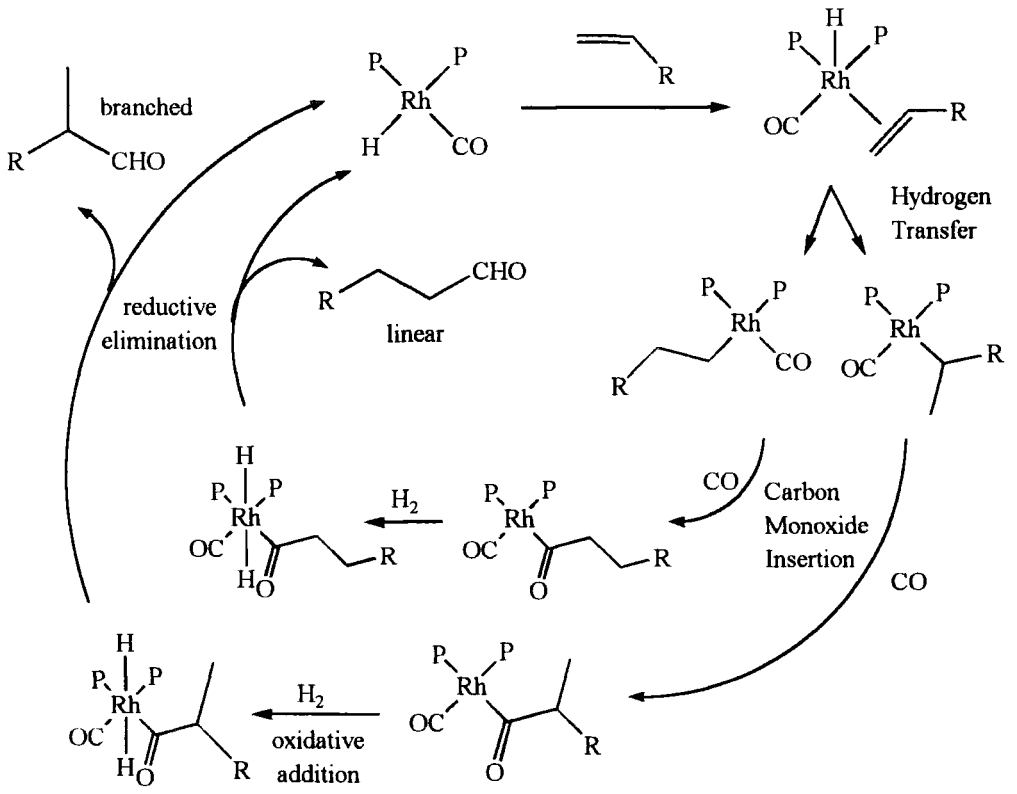

Scheme 9.3: Mechanism of Formation of Linear and Branched Products during Hydroformylation

Changing the nature of the phosphorus ligands can affect the activity and selectivity of the system [17,18].

A growing part of this area of catalysis is asymmetric hydroformylation. Reaction of an alkene to give the branched product produces a chiral carbon and therefore two enantiomers. For example, in the hydroformylation of 1-butene:

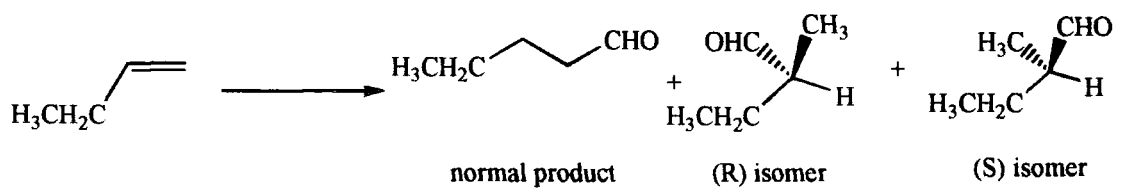

Scheme 9.4: Hydroformylation of 1-butene

The creation of a new chiral centre has found applications in the synthesis of pharmaceuticals and natural products [8]. This means that the reaction has been extensively studied, and it has been found to be possible to obtain enantiomeric excesses (ee) of 80 - 90%.

Asymmetric hydroformylation has been undertaken using the rhodium-catalysed system, but employing chiral diphosphine ligands to favour the production of one enantiomer over the other [19]. Examples of these ligands are DIOP and CHIRAPHOS.

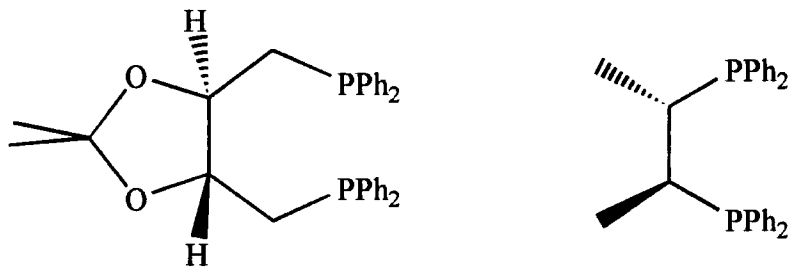

DIOP CHIRAPHOS

Fig. 9.1: Chiral Diphosphine Ligands

A second type of catalytic system is based on a platinum dichloride complex activated by tin dichloride [20, 21]. The activity is based on the formation of anionic $SnCl_3^-$ ligands. These allow the co-ordination of two-electron donor reagent molecules such as alkenes and carbon monoxide, as shown in Scheme 9.5, but it is not thought that this is the basis of the catalytic activity seen [20]. Pt^{II} can be oxidised to Pt^{IV} in a manner analogous to Rh^{I} being oxidised to Rh^{III}, and it may also be reduced to Pt^{O}. This redox behaviour is thought to be central to the activity of successful hydroformylation catalysts.

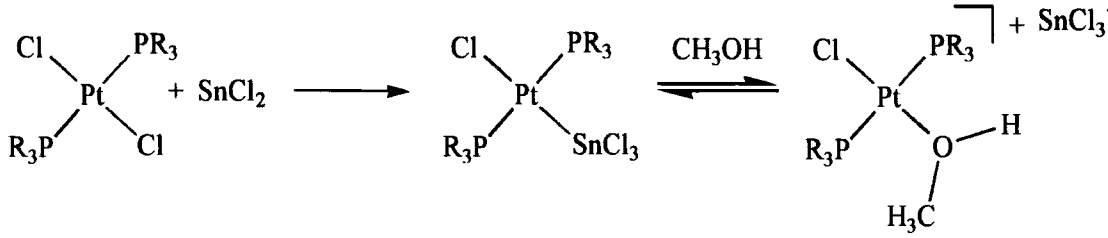

Scheme 9.5: Activation of Platinum Dichloride Complexes with Tin Dichloride

Aminophosphinephosphinite platinum dichloride complexes have been evaluated for activity in the asymmetric hydroformylation of styrene [22]. These complexes use ligands such as those shown in Fig. 9.2.

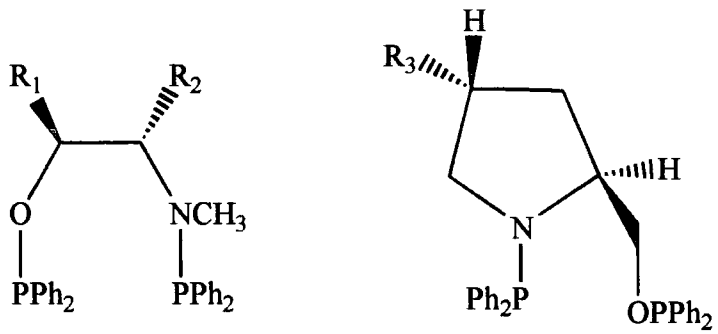

Fig. 9.2 : Aminophosphinephosphinite Ligands

The activity of these catalysts is significantly lower than that of [((-)-DIOP)$PtCl_2$] - $SnCl_2$, for which conversions between 20% and 80% were recorded for a reaction time of four hours. However, the enantiomeric excesses seen were much greater - up to thirty percent in favour of the (S) isomer. The enantiomeric excess obtained was found to be greater at higher partial pressures of hydrogen and could be increased to 48%.

9.1.2 Methoxycarbonylation

Methoxycarbonylation concerns the reaction of alkenes and carbon monoxide in the presence of methanol. There are two possible product types - esters, specifically methyl esters such as methyl propanoate when methanol is used, and polyketone, the alternating copolymer of carbon monoxide and an alkene. Which product is formed depends on the catalyst used.

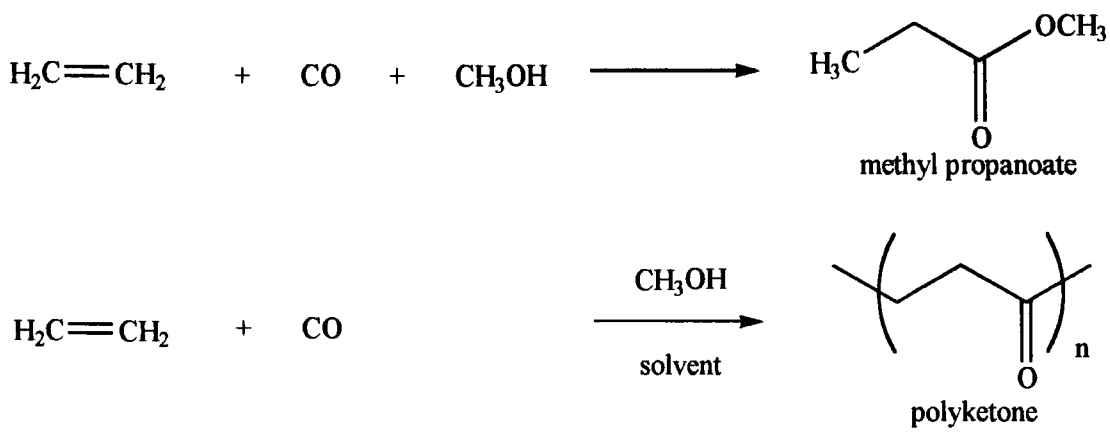

Scheme 9.6: Reactions of Carbon Monoxide and Alkenes

The esters produced find a number of commercial applications such as flavourings in foodstuffs or as solvents. Polyketone is a polymer new to the marketplace, but is noted for being made from cheap, readily available reagents and, being perfectly alternating, possesses the well defined properties of a regular polymer. As the carbonyl group is a reactive entity, polyketone could be the starting point for a range of functionalised polymers.

The reaction of carbon monoxide with alkenes dates back to work in the 1950s. The reaction of ethene and carbon monoxide in the presence of water and cobalt or nickel carbonyl was found to yield carboxylic acids [23]. Carbon dioxide was added to suppress the water - gas shift reaction. When ethene was used as the feedstock, the product was propanoic acid; when the feed was changed to propene, the products were butanoic acid and 2-methylpropanoic acid in the ratio 2:1. It was also reported that metals other than cobalt were inactive if the catalyst was a metal propanoate, and that CO_2 concentration should be kept to a minimum to avoid carbonate formation [24]. A related process was reported to make diethyl ketone (3-pentanone) [25], and another development used active carbon as a co-catalyst [26]. Reppe and Magin reported the formation of polyketones [27], as well as other ketonic compounds such as 3-pentanone, 3,6-octanedione, 3,6,9-undecanetrione and higher oligomers, using nickel cyanide complexes as catalysts. Rhodium [28] catalysts were also reported as active. Compounds such as $[(PBu_3)PdCl_2]_2$ and $[(PBu_3)_2PdCl_2]$ gave the first palladium catalysts for polyketone formation [29], and palladium cyanides [31,32], tetrakis(triphenylphosphine)palladium [32] and arylphosphine palladium chloride [33] complexes were evaluated soon after. This paved the way for modern systems, which are based on either nickel or palladium. A breakthrough in the utility of the reaction was made by Drent and co-workers [34] when they found that a catalytic system based on dppp (1,3-bis(diphenylphosphino)propane), palladium acetate and *para*-toluenesulphonic acid selectively produces polyketone. Recently, palladium catalysts have been used in molten salt media in the hydroesterification of styrene, giving 2-arylpropionic esters which are used in anti-inflammatory medicines [35]. It has also been shown to be possible to make esters using methyl methanoate (methyl formate) as starting material in place of carbon monoxide and methanol. This employs homogeneous ruthenium or iridium complexes as catalysts [36].

Two different mechanisms have been proposed for manufacture of these compounds [37]. One is based on palladium methoxycarbonyl compounds and the other on hydride compounds. It has been shown that the routes operate independently [38].

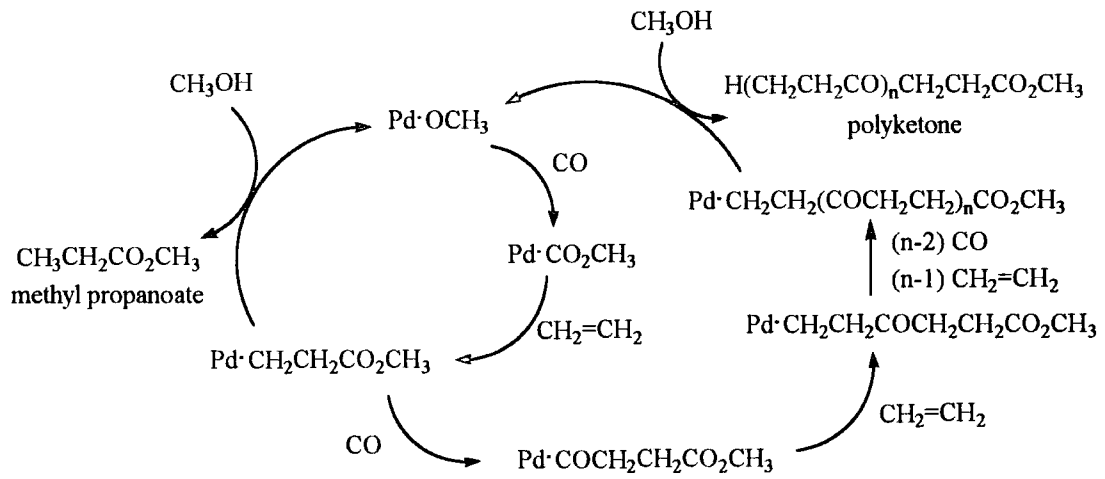

Scheme 9.7: "Methoxy Cycle" for Palladium-catalysed Carbonylation of Alkenes

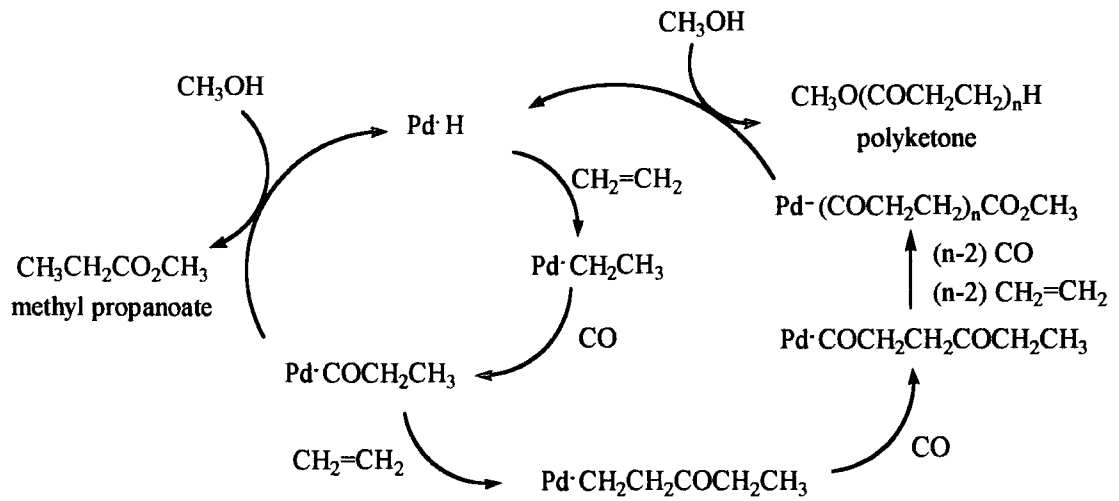

Scheme 9.8: "Hydride Cycle" for Palladium-catalysed Carbonylation of Alkenes

The relative probability of forming a molecule of methyl propanoate or propagating the chain of a molecule of polyketone depends on the likelihood of a methanol molecule attacking the palladium acyl compound compared with the insertion of an alkene molecule. This is dependant on the nature of the catalyst, and can also be influenced by reaction conditions such as the concentration of alkene. By considering this kind of mechanism it can be seen that methyl propanoate is a polyketone molecule with n = 1.

Table 9.1: Carbonyl Compounds formed by the reaction of CO and ethene

Number of alkene insertions	Formula	Name
1	$CH_3CH_2CO_2CH_3$	Methyl Propanoate
2	$H(CH_2CH_2CO)_2OCH_3$	Oligomer
3	$H(CH_2CH_2CO)_3OCH_3$	Oligomer
10	$H(CH_2CH_2CO)_{10}OCH_3$	Oligomer
n	$H(CH_2CH_2CO)_nOCH_3$	Polyketone

A polyketone molecule can have different endgroups, either ethyl or ester, and these can be identified by ^{13}C NMR.

It is seen from the mechanisms given in Schemes 9.7 and 9.8 that the polymer has a perfectly alternating structure; that is, there are no double insertions of either alkene or carbon monoxide. This happens for two reasons: firstly, the insertion of carbon monoxide into a metal acyl bond has not been observed since the CO-CO fragment is unstable with respect to a free carbon monoxide molecule. This means that ethene will always insert into the palladium - acyl bond. Secondly, insertion of an alkene is very slow with respect to insertion of carbon monoxide into a palladium - alkyl bond, and so carbon monoxide will always insert into a palladium alkyl bond. This gives rise to the perfectly alternating structure [39] which can be seen as only two signals in ^{13}C nmr, except for small signals due to the endgroups as mentioned above.

9.2 Experimental

9.2.1 Hydroformylation using [(diaminodiphosphine)$PtCl_2$] - $SnCl_2$ Catalysts

The procedure used in these experiments mirrors that used by Mutez *et al* [17]. Tin (II) chloride (0.07g, 0.35mmol, 3 equivalents to Pt) and [(aminophosphine)$PtCl_2$] (0.12mmol) were charged into the glass liner of a 150ml stainless steel autoclave. To this was added styrene (2ml, 17mmol, 150 equivalents to Pt) with its inhibitor removed [40] and toluene (30ml, 280mmol) which was the solvent. The autoclave was then sealed and flushed once with nitrogen, before being pressurised to 130 bar with a 1:1 mixture of hydrogen and carbon monoxide. The reaction was heated to 80°C for four

hours with stirring, and then cooled to room temperature. The autoclave was then depressurised and flushed three times with nitrogen to remove traces of carbon monoxide. The liquid products were taken from the autoclave and a portion vacuum distilled to give a sample suitable for GC and GC-MS analysis. Details of the products found are given in Table 9.2.

Table 9.2: Products Resulting from Hydroformylation Reactions

Ligand Used	Solution Colour	Solid Colour
none	pale yellow, almost clear	black
dppmen	yellow	black
dpppen	dark yellow	black
dppipen	yellow	brown
dpptben	yellow - orange	brown
dppmpn	orange	brown
dppippn	pale yellow	some white and some black
dpppip	pale yellow	grey - brown

The products were characterised by GC and GC-MS using standard samples of the compounds and by the mass spectra of the products. The response factors of the different components were determined by analysing samples of known concentration, and plotting lines of best fit by the least squares method [41] from the following equation:

$$\frac{\text{mass of product}}{\text{mass of toluene}} \times \text{Response Factor} = \frac{\text{Peak Area of Product}}{\text{Peak Area of Toluene}}$$

This gave response factors of 0.96 ± 0.04, 0.79 ± 0.04 and 0.482 ± 0.007 for ethylbenzene, 2-phenylpropanal and 3-phenylpropanal respectively.

9.2.2 NMR Scale Reactions of [(diaminodiphosphine)$PtCl_2$] Complexes with Tin (II) Chloride

In a typical procedure, 0.01g of an aminophosphine platinum dichloride complex was dissolved in $CDCl_3$ (2 ml), and its ^{31}P nmr spectrum run. To the sample was added $SnCl_2.2H_2O$ (0.01g, 4.4×10^{-5} mol), and the ^{31}P nmr spectrum run again. Details of the different experiments are given in Table 9.3.

Table 9.3: Reactions of [(Aminophosphine)$PtCl_2$] Complexes with $SnCl_2$

Ligand Used	Description of Product	^{31}P nmr	Assignment
dppmen	White Solid	δ_P = 56.1ppm (s) δ_P = 78.9ppm (s)	Starting Material Product
dpppen	Bright Orange Precipitate	δ_P = 59.7ppm J_{Pt-P} = 4218Hz	Starting Material
dpptben	Yellow Solution and Yellow Solid	δ_P = 44.7ppm J_{Pt-P} = 4160Hz δ_P = 68.4ppm J_{Pt-P} = 3505Hz δ_P = 50.7ppm (s)	Starting Material? Product Free dpptben
dppmpn	Yellow Solution and Yellow Solid	δ_P = 62.9ppm (s)	Starting Material
dppippn	Yellow Solid and Pale Green Solution	δ_P = 62.2ppm J_{Pt-P} = 4169Hz δ_P = 101.9ppm J_{Pt-P} = 3109Hz	Starting Material Product
dpppip	Orange Solid and Colourless Solution	δ_P = 75.8ppm (s)	Product

9.2.3 Methoxycarbonylation Using Diphosphine - Palladium Acetate Catalysts

The procedure used for these reactions mirrors that of Drent *et al* [34]. A portion of an aminophosphine ligand (0.15mmol, 1.5 equivalents to Pd) was charged into the glass liner of a stainless steel autoclave. The pot was flushed with a stream of nitrogen gas, then dry, degassed methanol (50ml, 1.2 mol), palladium acetate (0.022g, 0.1mmol) and *para*-toluenesulphonic acid (0.34g, 2mmol, 20 equivalents to Pd) were added in that order. The order of addition was found to be critical: without the ligand being present, the *para*-toluenesulphonic acid would decompose the palladium acetate to palladium black within minutes. Once the additions were complete, the autoclave was sealed and flushed with three portions of nitrogen to remove traces of oxygen. It was pressurised with 23 bars each of carbon monoxide and ethene, with the ethene being added first to aid its dissolution. The reaction mixture was heated, with stirring, to 115°C for four hours and allowed to cool to room temperature. The autoclave was then depressurised and flushed with three portions of nitrogen to remove any traces of carbon monoxide. The products were separated by filtration: the solid products were analysed by solid - state infrared spectroscopy (polyketone has ν(CO) = 1690cm^{-1}[42], esters have ν(CO) ca. 1740cm^{-1} depending on their structure [43], oligomers have ν(CO) = 1700-15 cm^{-1} [28,39]) and a portion of the liquid products were vacuum distilled before being analysed by GC and GC-MS. These products were determined by calibration of the GC with known standards, and by identification of the mass spectra produced by the GC-MS. Descriptions of the products are given in Table 9.4. The response factor of methyl propanoate was determined by determining the peak areas of samples of known concentration, and plotting a line of best fit to determine the response factor, using the equation:

$$\frac{\text{Peak Area of Methyl Propanoate}}{\text{Total Peak Area of Solution}} = \text{Response Factor} \times \frac{\text{Mass of Methyl Propanoate}}{\text{Total Solution Mass}}$$

This gave a value of 0.79 ± 0.05 for the response factor of methyl propanoate.

Table 9.4: Products of Methoxycarbonylation Reactions

Ligand Used	Solution Colour	Solid Colour and IR Spectrum (ν(CO)/cm^{-1})
dppb	dark brown	brown ν(CO) = 1692(vs) cm^{-1}
dppmen	orange	black ν(CO) = 1719(m, br) cm^{-1}
dpppen	dark orange	black ν(CO) = 1689(vs) cm^{-1}
dppipen	orange	black ν(CO) = 1688(w) cm^{-1}
dpptben	dark brown	brown ν(CO) = 1692(vs) cm^{-1}
dppmpn	brown	black ν(CO) = 1689(m) cm^{-1}
dppippn	orange	black ν(CO) = 1689(s) cm^{-1}
dpppip	dark orange	brown ν(CO) = 1692 (vs) cm^{-1}

9.3 Results

9.3.1 Hydroformylation using [(diaminodiphosphine)$PtCl_2$] - $SnCl_2$ Catalysts

Three products were found to be made using the aminophosphine - containing platinum dichloride catalysts. These were 2-phenylpropanal and 3-phenylpropanal from hydroformylation, and ethylbenzene from hydrogenation of styrene. The results of these experiments are given in Table 9.5.

Table 9.5: Performance of Platinum Complexes in the Hydroformylation of Styrene

Ligand Used	2 - phenyl propanal / mmol	3 - phenyl propanal / mmol	Ethylbenzene / mmol	Conversion of Styrene / %	Turnover Number / mol products per mol Pt	Turnover Frequency / mol product per mol Pt per hr	Selectivity to Hydroformylation / %	n / iso ratio
none	-	-	-	-				
dppmen	0.52	trace	0.66	6.92	9.8	2.5	44.2	'zero'
dpppen	1.01	0.02	1.27	13.58	19.2	4.8	44.9	0.028 (1:35½)
dppipen	0.42	0.04	0.53	5.81	8.2	2.1	46.5	0.098 (1:10)
dpptben	-	-	-	-				
dppmpn	-	-	-	-				
dppippn	-	-	-	-				
dpppip	-	-	-	-				

9.3.2 Methoxycarbonylation using Diphosphine - Palladium Acetate Catalysts

The reaction of ethene and carbon monoxide in the presence of aminophosphine ligands and palladium acetate gave a number of different products. Their distribution is shown in Table 9.6. A key to the products formed is in Fig. 9.3.

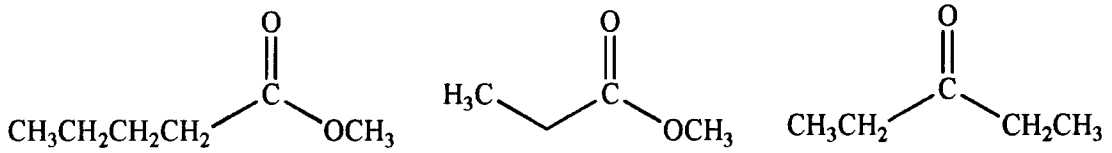

Methyl Pentanoate (Methyl Valerate)

Methyl Propanoate (Methyl Propionate)

3 - Pentanone (Diethyl Ketone)

Fig. 9.3: Products of the Methoxycarbonylation of Ethene

Table 9.6: Performance of Palladium Acetate - Aminophosphine Systems in Methoxycarbonylation Reactions

Ligand Used	Polyketone observed?	Methyl Propanoate Produced / mmol	Methanol Conversion / %	Turnover Number / mol product per mol catalyst	Turnover Frequency / mol product per mol catalyst per hour	Other Products Observed
dppb	Yes	17.1	1.4	1710	428	3-Pentanone
dppmen	Yes	4.7	0.4	471	118	Methyl Pentanoate one unidentified product
dpppen	Yes	-				-
dppipen	Yes	-				-
dpptben	Yes	1.5	0.1	146	37	-
dppmpn	Yes	trace				-
dppippn	Yes	-				-
dpppip	Yes	-				-

9.4 Discussion

9.4.1 Hydroformylation using [(diaminodiphosphine)$PtCl_2$] - $SnCl_2$ Catalysts

Of the complexes investigated in the hydroformylation reaction, only three were active: [(dppmen)$PtCl_2$], [(dpppen)$PtCl_2$] and [(dppipen)$PtCl_2$]. The other complexes were inactive, possibly because their steric bulk inhibited the co-ordination of styrene. If the reaction was repeated with a less sterically-demanding alkene, for example ethene, it is possible that other complexes may show activity. Another reason for inactivity could be insolubility, as has been seen for complexes in nmr - scale reactions. Often no ^{195}Pt - ^{31}P satellites, or even no signal for the product, could be seen due to the insolubility of the reaction products. This could be overcome by using a different solvent, such as DMF which has been shown to dissolve [(dpppip)$PdCl_2$] easily. However, this is a co-ordinating solvent, and as such would compete with reagents for active sites at the metal centre.

The reaction of $SnCl_2$ with phosphine platinum dichloride complexes has been shown to give both mono-substituted and di-substituted complexes [45]. The effect on the ^{31}P nmr spectrum is to increase the chemical shift slightly, and to decrease the ^{195}Pt - ^{31}P coupling constant markedly [46]. For example, the reaction of [(DIOP)$PtCl_2$] or [$(PEt_3)_2PtCl_2$] with $SnCl_2$ is shown in Table 9.7.

Table 9.7: Reaction of [(DIOP)$PtCl_2$] with $SnCl_2$

Complex	δ_P / ppm	J_{Pt-P} / Hz
(DIOP)$PtCl_2$	-1.4	3517
(DIOP)$PtCl(SnCl_3)$	8.9ppm (P *trans* to $SnCl_3$)	3510
	-0.8ppm (P *trans* to Cl)	2852
cis-$(PEt_3)_2PtCl_2$	9.3	3518
trans-$(PEt_3)PtCl_2$	12.2	2397
trans-$(PEt_3)_2Pt(SnCl_3)Cl$	13.6	2042
trans-$(PEt_3)_2Pt(SnCl_3)_2$	8.4	1873

Coupling of phosphorus to the three nmr-active tin nuclei (^{117}Sn, I = ½, natural abundance 7.7%; ^{119}Sn, I = ½, natural abundance = 8.6%, ^{115}Sn, I = ½, natural

abundance =0.4% [47]) is possible, although in practice coupling to the latter isotope are generally not observed due to its low abundance. The reaction of *cis*-[(phosphine)$_2$PtCl$_2$] complexes with SnCl$_2$ has been studied by ^{31}P nmr. The structure of the products was elucidated using the coupling of phosphorus to platinum and tin nuclei [46]. However, the low solubility of the complexes described here made the splittings difficult to resolve. The coupling constants reported were determined at low temperatures (-50°C), and it is possible that at room temperature fluxionality is a problem.

The complex [(dpppen)PtCl$_2$] gives a considerably more active catalyst than the other two complexes that show activity. It is also interesting to note that it has the greatest platinum - phosphorus coupling constant. This is usually indicative of an electron-withdrawing ligand - for example, the complex *cis*-[(P(OPh)$_3$)$_2$PtCl$_2$] has a coupling constant of 5793Hz [48], whereas *cis*-[(PMePh$_2$)$_2$PtCl$_2$] has $J_{Pt\text{-}P}$ = 3616Hz [49]. The implication, therefore, is that the high coupling constant in [(dpppen)PtCl$_2$] can be ascribed to the electron withdrawing effect of a phenyl group and so this could be related to its catalytic activity - an electron deficient metal centre would encourage the co-ordination of electron-rich substrates such as alkenes. However, [(dppmen)PtCl$_2$] and [(dppipen)PtCl$_2$] have the lowest coupling constants of the series, so other factors must also play a part.

Other complexes have been investigated for the platinum dichloride - tin dichloride catalysed hydroformylation of styrene. The complex [(DIOP)PtCl$_2$] has been found to give high conversions in short times, with some selectivity to the linear isomer [22, 49]. This comparison is presented in Table 9.8.

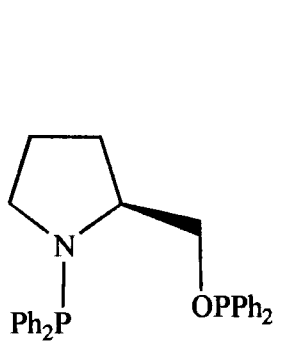

(S)-ProNOP

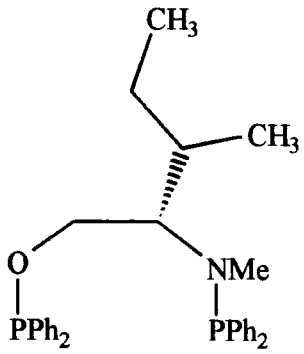

(S)-LeuNOP

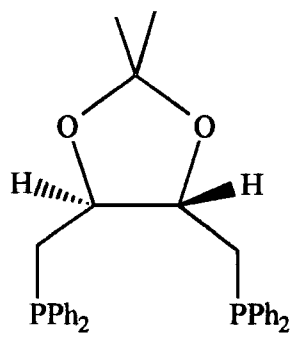

(R,R)-DIOP

Fig. 9.4: Chiral Ligands used for Asymmetric Hydroformylation

Table 9.8: Literature Values for Platinum - Tin Catalysed Hydroformylation of Styrene

Complex / mmol $SnCl_2$ used	Conditions (Styrene Concentration, Temperature, Gases, Pressure)	Styrene Conversion / % Reaction Time	Selectivity to Hydrogenation / %	Selectivity to Hydroformylation / %	n / iso ratio
[(dppmen)$PtCl_2$] 0.12 mmol 3 eq. $SnCl_2$	17 mmol Styrene 80°C 1:1 H_2 / CO 130 bar gas pressure	6.92 4 hours	55.8	44.2	'zero'
[(dpppen)$PtCl_2$] 0.12 mmol 3 eq. $SnCl_2$	17 mmol Styrene 80°C 1:1 H_2 / CO 130 bar gas pressure	13.58 4 hours	55.1	44.9	1 : 35.5 0.0282
[(dppipen)$PtCl_2$] 0.12 mmol 3 eq. $SnCl_2$	17 mmol Styrene 80°C 1 : 1 H_2 / CO 130 bar gas pressure	5.81 4 hours	53.5	46.5	1 : 10 0.098
[((-)-DIOP)$PtCl_2$] [50] 5 eq. $SnCl_2$	100°C 1 : 1 H_2 / CO 245 bar gas pressure	~100 1 hour	not reported	not reported	53 : 47 1.13
[(DIOP)$PtCl_2$] [22] 0.087mmol 2.5 eq. $SnCl_2$	90°C 1 : 1 H_2 / CO 100 atm. Gas pressure	100 5 hours	22	78	1 : 0.45 2.2

[((R,R)-DIOP)$PtCl_2$] [22] 0.07 mmol 3 eq. $SnCl_2$	80°C 1 : 1 H_2 / CO 130 bar gas pressure	100 20 minutes	14.5	85.5	1:1.54 0.64
[(ProNOP)$PtCl_2$] [22] 0.07 mmol 3 eq. $SnCl_2$	80°C 1 : 1 H_2 / CO 130 bar gas pressure	99 100 minutes	5.5	94.5	1 : 1.54 0.64
[((S)-LeuNOP)$PtCl_2$] [22] 0.07 mmol 3 eq. $SnCl_2$	80°C 1 : 1 H_2 / CO 130 bar gas pressure	85 4 hours	4	96	1: 1.04 0.96

Given the conversions and reaction rates reported in Table 9.6, it is reasonable to conclude that the complexes reported in this work provide relatively inactive catalysts. Complexes containing the ligand DIOP have a much greater activity than dppmen, dpppen or dppipen. This is due to electronic factors - it has been seen that dppb is a better donor (to palladium) than any of the aminophosphine ligands reported here (chapter eight). This could influence the rate of co-ordination of a reagent, or the stability of a particular intermediate, and hence give more effective catalysis. The aminophosphinephosphinite-containing complexes have similar electronic properties but are significantly less sterically demanding than most of the ligands prepared here. This leads to greater activity.

Catalysts prepared in this work have greater activity for hydrogenation of styrene to ethylbenzene than for hydroformylation. This is a reflection of the relative probability of CO insertion against H_2 co-ordination of an alkyl-platinum intermediate, as shown in Scheme 9.9. This can also be controlled by the influence of the ligand on the properties of the metal complex, as well as by reaction conditions, such as the partial pressures of carbon monoxide and hydrogen. It is possible that these compounds could be used in the absence of carbon monoxide as hydrogenation catalysts.

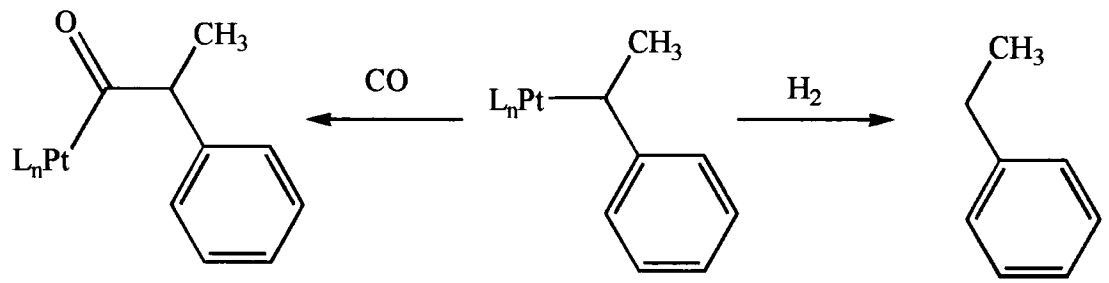

Scheme 9.9: Competitive Reactions at Platinum during Hydroformylation of Styrene

The area where dppmen, dppipen and dpppen ligands give better catalysts than others described in Table 9.6 is in the n/iso ratio. All three ligands give catalysts which are selective to the branched isomer – [(dpppen)$PtCl_2$] gives greater than 97% selectivity to this isomer. This would be of application in asymmetric hydroformylation, as it is the branched isomer which contains the chiral centre. Small changes in structure could produce chiral analogues, and some examples of this are shown in Fig. 9.5.

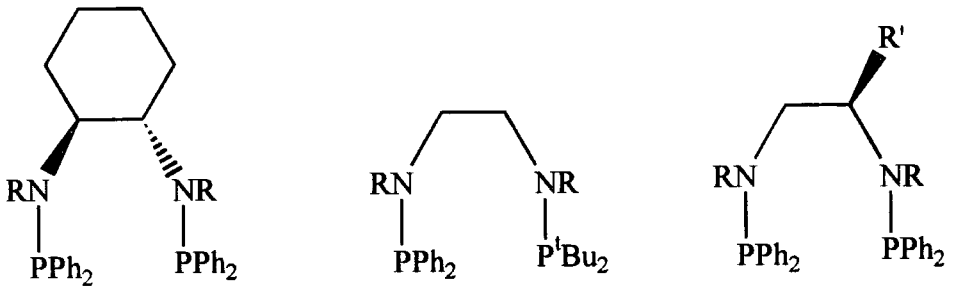

Fig. 9.5: Chiral Ligands based on Aminophosphines Reported in This Work

It may be possible to optimise the reaction conditions to minimise the hydrogenation activity, and so increase selectivity to hydroformylation. It may also be possible to increase activity as described above.

9.4.2 Methoxycarbonylation using Diphosphine - Palladium Acetate Catalysts

All the catalytic systems evaluated for reactions of carbon monoxide and ethene in the presence of methanol were slightly active, as a small amount of polyketone was formed in every case. However, this was never enough to analyse thoroughly. The production of methyl propanoate was also seen in the case of dppb, dppmen, dppmpn and dpptben ligands. Extremely active catalysis has been seen using dppb [34], with a reported reaction rate of 2300g of polyketone per gram of palladium per hour (or 4374 moles of product per mole of palladium per hour). Under the reaction conditions used here, that would have yielded 98g! Clearly the system used does not give as great activity as those reported, nor the selectivity to polymer production. The same study also found that changing the ligand has a great effect on the yield and quality of polymer produced, or whether esters are seen.

In the reaction using dpptben, both polyketone and methyl propanoate were produced. As has been seen in ^{31}P nmr-scale reactions, dpptben is easily replaced at a metal centre, and co-ordinates only weakly (chapter eight). This could lead to an increase in reactivity by allowing reagents to co-ordinate to the metal centre more easily. It is possible that the other ligands, whilst co-ordinated in a bidentate fashion are too sterically demanding to allow co-ordination. The ligands dppb, dppmpn and dppmen are amongst the least sterically hindered of those studied, and other successful catalysts contain planar ligands such as 2,2'-bipyridine [51] or 1,10-phenanthroline [52]. However, recent studies using the ligand 1,8-bis(diphenylphosphino)naphthalene [53],

which is also a planar ligand, showed poor activity. This implies that other factors influence the reactivity.

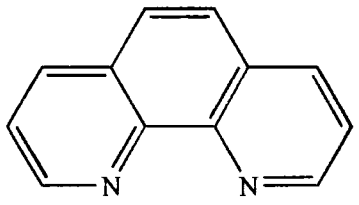

1,10-phenanthroline
(phen)

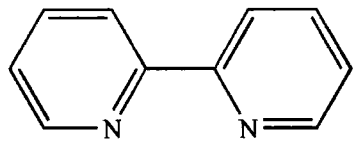

2,2'-bipyridine
(bipy)

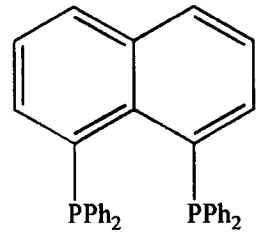

1,8-bis(diphenylphosphino)
naphthalene (dppn)

Fig. 9.6: Ligands used for Methoxycarbonylation Reactions

If the aminophosphine ligands studied are electron withdrawing ligands, they should encourage the co-ordination of ethene to the metal centre. However, it is also possible that this intermediate is too stable to quickly form a metal alkyl complex, which means that catalysis is slow or even stops. This would reinforce the observation of only small amounts of palladium black in the reactions from catalyst decomposition.

9.5 Conclusions

The catalytic reactions of alkenes with carbon monoxide with or without hydrogen present have been studied using platinum and palladium catalysts respectively. Catalytic activity has been poor in both cases, although in the case of hydroformylation high selectivity to branched products is seen. This encourages the investigation of chiral variants of these ligands, as it is the branched isomer that carries the chiral carbon. The platinum complexes studied have been found to react with tin dichloride, presumably to give complexes containing the trichlorostannate ligand ($SnCl_3^-$).

This is believed to be the first time that aminophosphine ligands have been used to catalyse reactions of alkenes with carbon monoxide and alcohol. Catalysis is seen for all the compounds, although yields of polymer products are exceedingly low. Four of the catalyst systems give esters as products, although the aminophosphine systems are less active than one containing dppb.

The steric bulk and insolubility of these compounds is thought to be responsible for their relative inactivity, but this could be modified by changes in the starting materials used in the synthesis or catalytic procedure.

9.6 References

1. H.M. Colquhoun, D.J. Thompson and M.V. Twigg, "Carbonylation - Direct Synthesis of Carbonyl Compounds", Plenum Press, 1991, pp. 60-68.
2. R. Fowler, British Patent 1387657 (1975).
3. M.W. Bradley, A.G. Hiles and J.W. Kippax, United States Patent 4451677 (1984).
4. N. Harris, A.J. Dennis and G.E. Harrison, United States Patent 4503275 (1985).
5. *Chemical Economics Handbook*, February 1995.
6. J.E. McMurry, "Organic Chemistry", 3rd Edn., Brooks/Cole Publishers, 1992 pp. 882-3.
7. M. Polievka, *Ropa Uhlie*, 1973, **15**, 366-72. *Chem. Abs.*, 1973, **79**, 125500*a*.
8. G.D. Cuny and S.L. Buchwald, *Synlett*, 1995, 519-22.
9. D.F. Smith, C.O. Hawk and P.L. Golden, *J. Am. Chem. Soc.*, 1930, **52**, 3221.
10. O. Roelen, United States Patent 2327066 (1943). *Chem. Abs.*, 1944, **38**, 550*l*.
11. I. Wender, R. Levine and M. Orchin, *J. Am. Chem. Soc.*, 1950, **72**, 4375.
12. L.H. Slaugh, Belgian Patent 621662 (1963).
13. D. Evans, J.A. Osborn and G. Wilkinson, *J. Chem. Soc. A*, 1968, 3133.
14. C.K. Brown and G. Wilkinson, *Tetrahedron Lett.*, 1969, 1725.
15. For example: (a) H.B. Tinker and A.J. Solodar, United States Patent 4268688 (1981). (b) H.R. Menapace, United States Patent 4484006 (1984).
16. G. Yagupsky, C.K. Brown and G. Wilkinson, *J. Chem. Soc. A*, 1970, 1392.
17. K.L. Olivier and F.B. Booth, *Amer. Chem. Soc. Div. Petrol. Chem. Prepr.*, 1969, **14**, A7-A11. *Chem. Abs.*, 1971, **75**, 5160*k*.
18. W. Kniese, H.J. Nienburg and R. Fischer, *J. Organomet. Chem.*, 1969, **17**, 133-41.
19. G.J.H. Buisman, E.J. Vas, P.C.J. Kamer and P.W.N.M. van Leeumen, *J. Chem. Soc., Dalt. Trans.*, 1995, 409.
20. G. Cavinato and L. Torciolo, *J. Organomet. Chem.*, 1983, **241**, 275-9.
21. C.-Y. Hsu and M. Orchin, *J. Am. Chem. Soc.*, 1975, **97**, 3553.
22. S. Mutez, A. Mortreux and F. Petit, *Tetrahedron Lett.*, 1988, 1911-4.

23. W.F. Gresham and R.E. Brooks, United States Patent 2448368 (1948). *Chem. Abs.*, 1949, **48**, 669*g*.

24. D.G. Hedburg, Jr., United States Patent 2510105 (1950). *Chem. Abs.*, 1950, **44**, 7344*i*.

25. W.F. Gresham, R.E. Brooks and W.E. Grigsby, United States Patent 2473995 (1949). *Chem. Abs.*, 1950, **44**, 1130*a*. W.F. Gresham, R.E. Brooks and W.E. Grisby, British Patent 638917 (1950). *Chem. Abs.*, 1950, **44**, 7344*i*.

26. A.T. Larson, United States Patent 2448375 (1948). *Chem. Abs.*, 1949, **43**, 670*i*.

27. W. Reppe and A. Magin, United States Patent 2577208 (1951). *Chem. Abs.*, 1952, **46**, 6143*b*.

28. Y. Iwashita and M. Sakuraba, *Tetrahedron Lett.*, 1971, 2409-12.

29. A. Gough, British Patent 1081304 (1967). *Chem. Abs.*, 1967, **67**, 100569*u*.

30. D.M. Fenton, United States Patent 3530109 (1970). *Chem. Abs.*, 1970, **73**, 11046*w*.

31. K. Nozaki, United States Patent 3835123 (1974). *Chem. Abs.*, 1975, **83**, 132273*q*.

32. K. Nozaki, United States Patent 3689460 (1972). *Chem. Abs.*, 1972, **77**, 152860*h*.

33. K. Nozaki, United States Patent 3694412 (1972). *Chem. Abs.*, 1972, **77**, 165324*m*.

34. E. Drent, J.A.M. van Broekhoven and M.J. Doyle, *J. Organomet. Chem.*, 1991, **417**, 235-51.

35. D. Zim, R.F. de Souza, J. Dupont and A.L. Monteiro, *Tetrahedron Lett.*, 1998, **39**, 7071-4.

36. M. Röper, *Erdöl und Kohle - Erdgas - Petrochemie vereinigt mit Brennstoff-Chemie*, 1984, **37**, 506-11.

37. E. Drent and P.H.M. Budzelaar, *Chem. Rev.*, 1996, **96**, 663-81.

38. M.A. Zuideveld, P.C.J. Kamer, P.W.N.M. van Leeuwen, P.A.A. Klusener, H.A. Stil and C.F. Roobeek, *J. Am. Chem. Soc.*, 1998, **120**, 7977-8.

39. T.-W. Lai and A. Sen, *Organometallics*, 1984, **3**, 866-70.

40. W.L.F. Armarego and D.D. Perrin, "Purification of Laboratory Chemicals", 4th Edn., Butterworth-Heinemann, 1996, p. 326.

41. H.D. Young, "Statistical Treatment of Experimental Data", McGraw-Hill, 1962, pp.115-23 & 145-6.

42. A. Sen and Z. Jiang, *Macromolecules*, 1993, **26**, 911-5. The figure quoted is for poly-(1-oxo-2-phenylpropane), i.e. the copolymer of styrene and carbon monoxide.

43. R.M. Silverstein, G.C. Bassler, T.C. Morrill, "Spectrometric Identification of Organic Compounds", John Wiley and Sons, 1963, pp. 121-3, 167.

44. S. Mutez, A. Mortreux and F. Petit, *Tetrahedron Lett.*, 1989, 5759 - 62.

45. F.R. Hartley (ed), "Chemistry of the Platinum Group Metals: Recent Developments", Elsevier, 1991, pp. 384-5.

46. P.S. Pregosin and S.N. Sze, *Helv. Chim. Acta*, 1979, **61**, 1848-55.

47. R.C. Weast and M.J. Astle (eds), "Handbook of Chemistry and Physics", 3rd Edn., CRC Press, 1982, p. B-285.

48. N. Ahmed, E.W. Ainscough, T.A. James and S.D. Robinson, *J. Chem. Soc., Dalt. Trans.*, 1973, 1148-50.

49. S.O. Grim, R.L. Keiter and W. McFarlane, *Inorg. Chem.*, 1967, **6**, 1133-7.

50. G. Consiglio and P. Pino, *Helv. Chim. Acta*, 1976, **59**, 642-5.

51. (a) A.W. De Jong and J.J. Keijsper, European Patent Application EP 486103 (1992). *Chem. Abs.*, 1992, **117**, 172290*b*. (b) Japanese Patent JP 62131025 [87131025] (1987). *Chem. Abs.*, 1988, **108**, 6617*b*.

52. M. Barsacchi, G. Consiglio, L. Medici, G. Petrucci and U.W. Suter, *Angew. Chem. Intl. Edn. Engl.*, 1991, **30**, 989-991.

53. G.S. Robertson, Ph.D. Thesis, University of Durham, 1997.

Chapter Ten: Summary of Aminophosphine Studies

The synthesis, structure and reactivity of some novel chelating aminophosphines have been investigated in this work. The ligands have been synthesised in good or moderate yield from a substituted diamine by the action of chlorodiphenylphosphine. The diaminodiphosphines were complexed to palladium and platinum by reaction with the relevant $[(PhCN)_2MCl_2]$ complex. Spectroscopic data is reported for these compounds. Reaction of the diaminodiphosphine ligands with $[Mn(CO)_5Br]$ gave manganese complexes $[LMn(CO)_4Br]$ and $[L_2Mn(CO)_3Br]$, which contain monodentate and chelating bidentate diaminodiphosphines respectively, and were identified by their infrared spectra. A summary of these reactions is shown in Scheme 10.1.

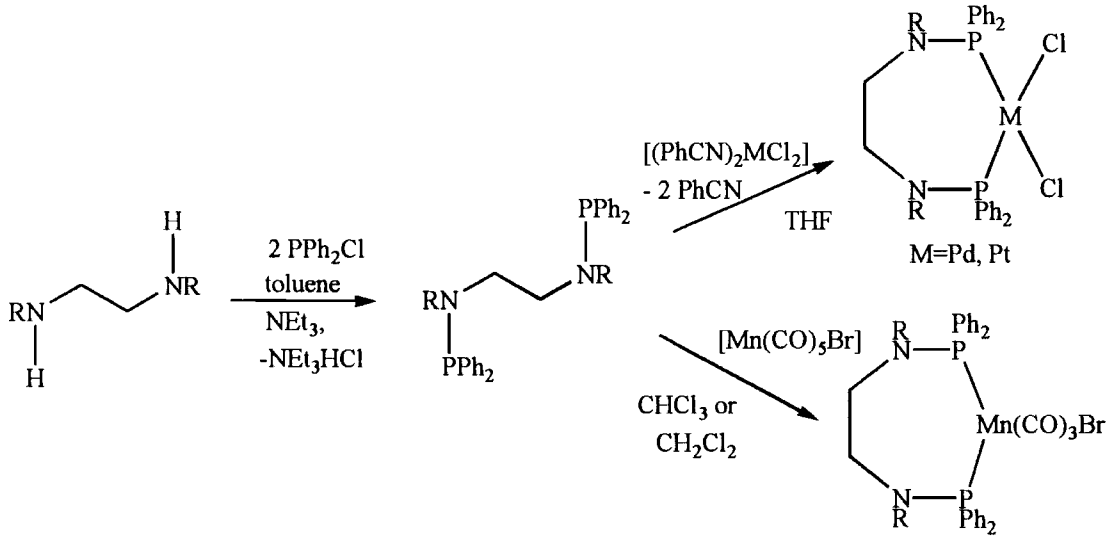

Scheme 10.1: Synthesis of Aminophosphine Ligands and their Complexes

^{31}P nmr spectroscopy has been used to identify the effect of chelation on these ligands. The relationship between the chemical shift of the ligand and its change on complexation [1] is linear for two-carbon backbone ligands (dppmen, dpppen, dppipen and dpptben) with respect to both palladium and platinum dichloride complexes. Three-carbon backbone ligands show a small deviation from this relationship, which is a consequence of the slight amount of strain inherent in seven- and eight-membered chelate rings. The properties of the ligand dpppip deviated from those of the other ligands which is ascribed to restrictions on its geometry imposed by the cyclohexane ring structure of the piperazine ring.

Another anomaly relating to this ligand was detected while using IR to investigate the metal-chlorine stretching frequencies of palladium and platinum complexes. This showed that in the solid state both [(dpppip)$PdCl_2$] and [(dpppip)$PtCl_2$] have *trans* geometry at the metal centre. This is in contrast to the other aminophosphines, which show the *cis* geometry expected of a chelating ligand. In solution, all the complexes are thought to contain *cis* phosphorus atoms, as their ^{31}P nmr spectra show similar chemical shifts, the value of the platinum - phosphorus coupling constant is of a large enough magnitude to imply a *cis* geometry, and some complexes have been crystallographically characterised. The solid state structure of [(dpppip)$PdCl_2$] and [(dpppip)$PtCl_2$] is thought to be polymeric, with each ligand bridging two metal centres. This allows the piperazine backbone to retain the preferred chair geometry.

The solid state structures of one of the ligands, five palladium complexes and one platinum complex have been determined by X-ray crystallography. This has allowed the bonding within these compounds to be explored. Of particular interest is the bonding between phosphorus and nitrogen. In the compounds reported here, the bond length is shortened compared with a single bond and the nitrogen atom is more sp^2 - hybridised (planar) than expected, which implies that the nitrogen lone pair is delocalised into the phosphorus - nitrogen bond. The length of a phosphorus - nitrogen single bond with no extra π-bonding is 1.77Å [6], whereas the phosphorus - nitrogen bond length in dpptben was found to be 1.71Å and those in palladium and platinum complexes were in the range 1.65-1.70Å. The sum of angles at nitrogen was found to be 353.4° for dpptben, and between 344.1° and 360.0° for the palladium and platinum complexes. In these complexes, there is typically one sp^2 - hybridised nitrogen, and one sp^3 - hybridised nitrogen, leading to two different phosphorus - nitrogen bond lengths. This is a feature which has been seen in related compounds [2]. However, ^{31}P nmr shows that in solution the phosphorus atoms are equivalent. The metal - chlorine distances are equivalent in most of these complexes, and no obvious relationship with the phosphorus - nitrogen distance is seen.

The reactivity of these ligands has been assessed in both qualitative and quantitative terms. Following a literature method [3], the rate constant for the

displacement of a carbonyl ligand from $[Mn(CO)_5Br]$ by one of these aminophosphines has been determined. The order of binding has been found to be

dppmpn > dppb > dppmen > dpppip > dpppen > dppipen > dppippn >> dpptben

which reflects the steric size of the incoming ligand. It is interesting that dpppip binds more slowly than dppmen as there are structural similarities between the two ligands. This is a reflection of the restriction of the conformations available to dpppip due to its two backbones. The ligand dpptben reacts very much more slowly that any of the other ligands, a consequence of the large steric bulk of the *tert*-butyl group, and of the ligand in general.

The complexes formed in reactions between aminophosphine ligands and $[Mn(CO)_5Br]$ were identified by solution state IR spectroscopy. In all cases, the initial product was the *cis*-substituted tetracarbonyl derivative (displacement of one carbonyl ligand), which then reacted further to give a disubstituted tricarbonyl derivative, seen in two isomeric forms. This is shown in Scheme 10.2.

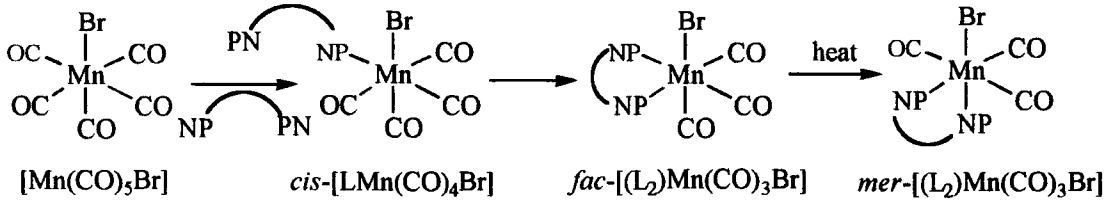

$[Mn(CO)_5Br]$ *cis*-$[LMn(CO)_4Br]$ *fac*-$[(L_2)Mn(CO)_3Br]$ *mer*-$[(L_2)Mn(CO)_3Br]$

Scheme 10.2: Reactions of Aminophosphine Ligands with $[Mn(CO)_5Br]$

For the majority of the ligands investigated, the initial disubstituted product was the *fac*-isomer, which corresponds with reports that the carbonyl ligands *cis* to the bromine atom are the most labile [3]. Heating the solution slowly converts this to the *mer*-isomer. This is thought to be due to steric interactions with the large bromine atom, since the isomerisation was not seen for dppb or dppmpn, which are the least sterically demanding of the ligands studied. This is an example of kinetic (*fac*-isomer) and thermodynamic (*mer*-isomer) products being formed.

Many of the reaction solutions were found to decompose on standing for a few days, giving a clear solution and colourless solid. One decomposition product from the

reaction of dpptben with $[Mn(CO)_5Br]$ in chloroform solvent was characterised by X-ray crystallography as $[^tBuN(H)_2CH_2CH_2N(H)_2{}^tBu]X_2 \cdot 2H_2O$, where X represents a halide ion which is chloride or bromide in a 4:1 ratio. This implicates reaction with the solvent as a possible decomposition mechanism for these compounds.

The relative binding strength of these ligands was determined separately by following the reaction of an aminophosphine palladium dichloride complex with a second aminophosphine ligand by ^{31}P nmr. Displacement could be seen be the appearance of a new complex and ligand peak, or the disappearance of the starting materials. This approach gave the following order of binding:

dppmpn > dpppip > dppmen > dppippn > dppipen > dpppen > PPh_3 > dpptben

Again this is largely a reflection of steric parameters of the ligands. Differences between this order and the one shown above for $Mn(CO)_5Br$ are assigned to the different steric requirements of the manganese and palladium systems. With palladium, binding appears to be more effective with a three-carbon backbone ligand than a two-carbon backbone ligand. An example of this is the displacement of dppipen by dppippn. The extra flexibility afforded to dppippn by its longer backbone, and the range of conformations available as a consequence could be responsible. It is interesting to note that dpptben is replaced by PPh_3, as the displacement of a chelating ligand by a monodentate ligand is most unusual, and a reflection of the size of dpptben. The common chelating diphosphines (dppm, dppe, dppp, dppb) also displaced dpptben from its palladium dichloride complex.

The decomposition of an aminophosphine palladium dichloride complex has been found to yield a diamine palladium dichloride complex, and the latter has been characterised by X-ray crystallography. Cleavage of the phosphorus - nitrogen bond is therefore one decomposition pathway available to these complexes.

The reaction of dpptben with air has been found to give the diphosphine dioxide, and with sulphur gives the diphosphine disulphide. Both reactions involve oxidation at phosphorus. Reaction with water has also been detected. These results confirm the air- and moisture - sensitivity of the uncomplexed ligands in solution.

Two catalytic reactions have been performed using these ligands. The first is hydroformylation, using an [(aminophosphine)$PtCl_2$] - $SnCl_2$ catalyst system. Activity for hydroformylation was detected using dppmen, dpppen and dppipen as ligands. The conversions were low, and the selectivity to hydroformylation poor, with an equal amount of hydrogenation product seen. However, the n to iso ratio of the hydroformylation product was extremely selective in favour of the branched isomer, which suggests that chiral variants of these ligands might be effective asymmetric catalysts, since it is the branched isomer that contains the chiral carbon. The results were compared to published work [4], and the activity and selectivity to hydroformylation found here are not nearly as good, though selectivity in the present work favours the alternative isomer. The low activity seen here is thought to relate to the insolubility of the complexes. The reaction of an aminophosphine platinum complex with tin dichloride has been studied separately, and the products found to be largely insoluble. The generation of complexes containing the trichlorostannate ligand ($SnCl_3^-$) by reaction of [(diaminodiphosphine)$PdCl_2$] complexes with $SnCl_2$ was detected in a separate ^{31}P nmr study.

The second reaction studied was the reaction of ethene with carbon monoxide in the presence of methanol. The products of this reaction would either be polyketone polymer, or esters such as methyl propanoate. When the reaction is performed using dppb as the ligand, despite reports of great activity and selectivity to polymer products [5] the activity was found to be low and selectivity was to ester products instead. All the aminophosphine ligands studied gave slightly active catalysts, a trace amount of polyketone being clearly identified in each case by its solid state IR spectrum. Catalysts containing dppmen, dpptben and dppmpn gave ester products in addition to the polyketone. The relatively low activity of aminophosphine-containing catalysts has been ascribed to the steric bulk of the ligands, hindering the co-ordination of reactant molecules.

In conclusion, diaminodiphosphines are ligands with an interesting co-ordination chemistry, which can be tuned by changing the steric requirements of the backbone. Reactions giving a range of metal complexes have been investigated, some of which give

active catalysts. Although their catalytic performance is generally poor, there are features which could be changed to improve their efficiency.

References

1. P.E. Garrou, *Chem. Rev.*, 1981, **81**, 229-66.
2. C. Rømming and J. Songstad, *Acta. Chem. Scand. A*, 1978, **32**, 689-99.
3. R.J. Angelici and F. Basalo, *J. Am. Chem. Soc.*, 1962, **84**, 2495.
4. S. Mutez, A. Mortreaux and F. Petit, *Tetrahedron Lett.*, 1988, **29**, 1911-4.
5. E. Drent, J.A.M. van Broekhoven and M.J. Doyle, *J. Organomet. Chem.*, 1991, **417**, 235-51.
6. N.N. Greenwood and A. Earnshaw, "Chemistry of the Elements", Pergamon Press, 1984, pp.620-33.